SYNTHESIS, PHYSICOCHEMICAL AND BIOCHEMICAL PROPERTIES OF C3'-MODIFIED 2',5'-LINKED OLIGONUCLEOTIDES

Kazim Ally Agha

Department of Chemistry
McGill University
Montreal, Canada

A thesis submitted to the Faculty of
Graduate Studies and Research
in partial fulfillment of the requirements of the degree of
Doctor of Philosophy

Your file Votre référence
ISBN: 0-612-98190-8
Our file Notre référence
ISBN: 0-612-98190-8

Dedicated to

My parents:

Shama and Raza Ally Agha

My brothers:

Muhammed and Hassan Ally Agha

& My family:

Batul, Musa and Faiza Kazim

ABSTRACT

Oligoribonucleotides comprising of 2',5'-linked internucleotide linkages are known to bind selectively to RNA over DNA. The ability to bind to RNA renders them suitable as probes for many biological applications, such as 'antisense technology'. Little is known about the effect of sugar structure (and conformation) on the binding properties of 2',5'-linked oligonucleotides. To get insight into the role of sugar conformation, 2',5'-linked oligonucleotides modified at the C3'-position of the furanose ring were synthesized *via* solid phase synthesis and their binding to complementary single stranded DNA and RNA was studied. Their application as antisense oligonucleotides was also evaluated.

The first analogue studied was the C3'-epimer of 2',5'-linked ribonucleic acids (2',5'-RNA), that is, an oligonucleotide in which the ribofuranose sugar is replaced by xylofuranose (2',5'-XNA). This was followed by the synthesis and analysis of the C3'-fluorinated xylofuranose analogue (2',5'-FXNA). The sugar conformation in these oligonucleotides are believed to have a very high population of the C3'-*endo* ('extended') conformation. Consistent with this notion, CD structural studies indicated that 2'5,'-linked XNA and FXNA show structural similarities to the 'extended' C2'-*endo* form of DNA. We found that both 2',5'-XNA and 2',5'-FXNA bound weakly to complementary single stranded DNA and RNA. Neither of the xylooligomers resulted in RNaseH activated degradation of RNA.

The last modified oligonucleotide to be studied was the C3'-fluorinated-2',5'-linked ribonucleic acids (2',5'-FRNA), which has a compact C2'-*endo* sugar conformation. In contrast to 2',5'-FXNA, 2'5,'-FRNA bound strongly to complementary oligonucleotides and showed structural similarities to RNA (CD spectroscopy). Our studies showed that it did not cause RNase H based degradation of RNA.

These studies are consistent with the notion that the effect of sugar conformation in 2',5'-oligonucleotides is opposite to that of 3',5'-oligonucleotides. In other words, a C3'-*endo* sugar conformation in 2',5'-oligomers renders the oligonucleotide as 'extended' and

portrays itself equivalent to the 'extended' DNA conformation (which has C2'-*endo* conformation), whereas a C2'-*endo* 2',5'-oligonucleotide adopts a 'compact' conformation that is equivalent to that seen in 3',5'-oligonucleotides adopting the C3'-*endo* pucker (e.g. RNA).

RESUME

Les oligoribonucléotides liés par des liaisons inter-nucléotides en position 2' et 5' sont connus pour s'hybrider sélectivement à un brin d'ARN ou d'ADN. Leur capacité à se lier ainsi à l'ARN les rend potentiellement intéressants pour de multiples applications biologiques, telle que la technologie 'antisens'. La structure (et la conformation du sucre) est connue pour avoir un effet sur les propriétés de liaison des oligonucléotides liés en 2', 5'. Afin de mieux comprendre le rôle de la conformation du sucre, des oligonucléotides liés en 2', 5' et modifiés au niveau du C3' du furanose, ont été synthétisés en phase solide puis leur capacité à se lier de façon complémentaire à un seul brin d'ARN et d'ADN a été étudiée. De même leur application en tant qu'oligonucléotides antisens a été évaluée.

Le premier analogue étudié, est l'épimère en C3' des acides ribonucléiques liés en 2', 5' (2', 5'-ARA) qui est un oligonucléotide dont le ribofuranose est remplacé par un xylofuranose (2', 5'-XNA). Par la suite, un analogue fluoré en C3' du xylofuranose a été synthétisé et analysé. Les conformations prédominantes du sucre en lui-même, semblent exister majoritairement sous la forme C3'-endo ('étendue'). Confortant cette notion, des études structurales CD montrent que les XNA 2', 5' et les FXNA ont des similitudes structurales à la forme C2'-endo étirée de l'ADN. Nous avons découvert que le 2', 5'-XNA ainsi que le 2', 5'-FXNA s'associent faiblement à un mono brin d'ADN ou d'ARN et qu'aucun de ces xylo-oligomères ne permet d'activer l'ARNase H, enzyme responsable de la dégradation de l'ARN.

Le dernier oligonucléotide modifié que nous avons étudié est l'acide ribonucléique fluoré en C3' et lié en 2', 5', qui est caractérisé par sa conformation du sucre en C2'-endo. Contrairement au 2', 5'-FXNA, le 2', 5'-FRNA se lie fortement aux oligonucléotides complémentaires et possède des similitudes structurales avec l'ARN (spectroscopie CD). Mais nos études montrent qu'il ne permet pas la dégradation de l'ARN par l'intermédiaire de l'ARNase H.

Ces études réalisées confirment que l'effet de la conformation des sucres des oligonucléotides liés en 2', 5' est à l'opposé de celui des oligonucléotides en 3', 5'. Autrement dit, une conformation C3'-endo du sucre dans les oligomères 2', 5' conduit à des oligonucléotides de forme allongée similaire à celle de l'ADN (qui possède une conformation C2'-endo); alors que l'oligonucléotide 2', 5' en C2'-endo adopte une conformation plus compacte comme celle observée pour les oligonucléotides 3', 5' adoptant la forme C3'-endo (ex : ARN). Enfin, l'inaptitude de tous ces oligonucléotides modifiés à activer l'ARNase H responsable de la dégradation de l'ARN, est expliquée par les différences structurales de ces hybrides avec celles des substrats naturels ADN : ARN.

ACKNOWLEDGMENTS

I would like to thank my PhD. supervisor Dr. Masad J. Damha for the opportunity to conduct research in his laboratory. His enthusiasm led this work from one modification to another. I would especially like to acknowledge him for his 'human touch' which many lack. I am also grateful to him for the proof-reading of this thesis.

I would like express my gratitude to the Department of Chemistry at McGill University, FCAR and NSERC for teaching assistantships, the opportunity to study there and for fellowships.

I appreciate all the efforts of Renee Charron, Chantal Marotte, Sandra Aerssen and Carol Brown.

I am indebted to Drs. F. Sauriol and Zhicheng (Paul) Xia for all their help with the NMR instrument, Dr. J. Turnbull for use of the CD instrument, Mr. Nadeem Saade for running the mass spectra of sugars and nucleosides and Mrs. Antisar Hlil for MALDI-TOF-MS.

Thanks to Sebastien Robidoux, Christopher Wilds, Anne Noronha, Robert Donga, Mohamed Elzagheid, Kyung L. Min, Annie Galarneau, Zhicheng (Paul) Xia, Sandra Carriero, Ulhas Bhatt and Hasan Bazzi for their friendship. Your presence made the difficult times disappear faster and the memorable times even better. Chris, Anne and Robert-thanks for proof-reading this thesis. Mohamed, our discussions on chemistry over coffee was something I looked forward to every day. Min and Annie, thanks for showing me how to perform the enzyme assays. Sandra, thanks for explaining how the gene-machine worked. Ulhas, every time your name is mentioned, it reminds me of our first cricket match against Pakistan; and playing tennis against you was always a great joy. Thank you for showing me how to use the NMR spectrometer, again and again. Hasan, time with you was always fun and I hope to see you again. Benedicte Patureau: thank you for the translation of the abstract.

To my Batul and Musa, my dearest daughter and son, whose eyes, look, hugs and kisses could change my night into day, anytime; who made me look at life from a global perspective-Thank you!

To Faiza, my loving wife, no words can express my gratitude to you. For your patience, constant support and for keeping up with me-Thank you!

To Muhammed and Hassan, my brothers, my best of friends: thanks. Muhammed thanks for letting me borrow your laptop and keeping it for so long, without it, writing this thesis would have been difficult. Hassan, thanks for your constant push and all the brotherly advice.

To Amma and Agha, Thank you!

Kazim Ally Agha

TABLE OF CONTENTS

ABBREVIATIONS AND SYMBOLS

A	adenosine
Å	angstrom
A_{260}	UV absorbance at 260nm
Ac_2O	acetic anhydride
Ac	acetyl
ACN	acetonitrile
AcOH	glacial acetic acid
AIDS	acquired immune deficiency syndrome
AON	antisense oligonucleotide(s)
APS	ammonium persulphate
br	broad
bp	base pairs
B	base
BIS	N,N'-methylene-bis(acrylamide)
Bn	benzyl
BPB	bromophenol blue
Bz	benzoyl
C	Celsius
CEO-	2-cyanoethoxy (β-cyanoethyl)
COSY	correlated spectroscopy
CPG	controlled pore glass
Cyt	cytosine
d	doublet
DAST	diethylaminosulfur trifluoride
DCE	1,2-dichloroethane
DCM	dichloromethane
dd	doublet of doublets.
ddd	doublet of doublet of doublets
DEC	1-(3-dimethylaminopropyl)-3-ethylcarbodiimide hydrochloride
DIPEA	N,N-diisopropylethylamine
DMAP	N,N-dimethyl-4-aminopyridine
DMF	N,N-dimethylformamide
DMSO	dimethylsulfoxide
DMT	dimethoxytrityl
DNA	2'-deoxyribonucleic acid
DTT	dithiothreitol
ds	double stranded
E.coli	*Escherichia coli*
EDTA	disodium ethylenediaminetetraacetate dehydrate
e.g.	for example
EtOH	ethanol
EtOAc	ethyl acetate
eq	equivalent(s)
FAB-MS	fast atom bombardment mass spectrometry

G	guanosine
g	gram(s)
Glu	glutamic acid
Gua	guanine
HBr	hydrobromic acid
HCl	hydrochloric acid
HIV-1	human immunodeficiency virus type 1
HPLC	high pressure (performance) liquid chromatography
h	hours
%H	percent hyperchromicity
HMDS	1,1,1,3,3,3-hexamethyldisilazane
Hz	Hertz
i.e.	that is
i-Bu	isobutyryl
J	coupling constant
λ	wavelength
LCAA-CPG	long chain alkyamine controlled pore glass
M	molar
m	multiplet
MALDI-TOF	matrix assisted laser desorption/ionization time of flight
max	maximum
m/c	mass to charge ratio
Me	methyl
MeOH	methanol
min	minute(s)
mL	milliliter
mg	milligram
mM	millimolar
μM	micromolar
MMT	monomethoxyltrityl
mol	mole
mRNA	messenger RNA
MS	mass spectroscopy
MW	molecular weight
N	northern
$NaBH_4$	sodium borohydride
NBA	4-nitrobenzyl alcohol
nm	nanometer
NMR	nuclear magnetic resonance spectroscopy
NOE	nuclear overhauser effect
NOESY	nuclear overhauser and exchange spectroscopy
OD	optical density
ODN	oligodeoxynucleotides
PAGE	polyacrylamide gel electrophoresis
PCC	pyridinium chlorochromate
ppm	parts per million

pre	precursor
Pu	purine
Py	pyrimidine
q	quartet
®	registered trademark
R_f	(TLC mobility) retardation factor
RNA	ribonucleic acid
RNase	ribonuclease
rRNA	ribosomal RNA
RT	reverse transcriptase
rt	room temperature
s	singlet (NMR)
S	southern
ss	single stranded
SEC	size exclusion chromatography
sec	second
T	thymidine
t	tertiary, triplet (NMR)
TBDMS	*t*-butyldimethylsilyl
TBAF	tetrabutylammonium fluoride
TBE	TRIS/boric acid/EDTA buffer
TCA	trichloroacetic acid
TEA	triethylamine
TEMED	N,N,N',N'-tetramethylethylenediamine
Thy	thymine
THF	tetrahydrofuran
TLC	thin layer chromatography
T_m	thermal melt transition temperature (melting temperature)
TM	trademark
TMS-Cl	trimethylsilyl chloride
TREATHF	triethylamine-tris(hydrogen fluoride)
TRIS	2-amino-2-(hydroxylmethyl)-1,2-propanediol
tRNA	transfer RNA
U	Uridine
Ura	uracil
UV	ultraviolet
UV-VIS	ultraviolet-visible
v/v	volume to volume
vs	versus
WC	Watson Crick
w/v	weight to volume
XC	xylene cyanol
2',5'-FRNA	2',5'-linked-3'-deoxy-3'-fluoro-ribonucleic acid(s)
2',5'-FXNA	2',5'-linked-3'-deoxy-3'-fluoro-xylonucleic acid(s)
2',5'-XNA	2',5'-linked-xylonucleic acid(s)

LIST OF FIGURES

LIST OF TABLES

The Psalm of Life (Henry W. Longfellow)

Tell me not, in mournful numbers,
Life is but an empty dream!
For the soul is dead that slumbers,
And things are not what they seem.

Life is real! Life is earnest!
And the grave is not its goal;
Dust thou art, to dust returnest,
Was not spoken of the soul.

Not enjoyment, and not sorrow,
Is our destined end or way,
But to act, that each tomorrow
Find us farther than today.

Art is long, and Time is fleeting,
And our hearts, though stout and brave,
Still, like muffled drums, are beating,
Funeral marches to the grave.

In the world's broad field of battle,
In the bivouac of Life,
Be not dumb, driven cattle!
Be a hero in the strife!

Trust no Future, howe'er pleasant!
Let the dead Past bury its dead!
Act,~act in the living present!
Heart within, and God o'erhead!

Lives of great men all remind us
We can make our lives sublime,
And, departing leave behind us
Footprints on the sands of time;

Footprints, that perhaps another,
Sailing o'er life's solemn main,
A forlorn and shipwrecked brother,
Seeing, shall take heart again.

Let us, then be up and doing,
With a heart for any fate;
Still achieving, still pursuing,
Learn to labor and to wait.

CHAPTER 1

INTRODUCTION

1.1 IMPORTANCE OF NUCLEIC ACIDS[1-5]

Nucleic acids existing in the cell are of two types: deoxyribonucleic acid (DNA) and ribonucleic acid (RNA). DNA is the "storehouse" of genetic information, its pivotal role. It also functions as a template for RNA synthesis, in copying of cells, as a scaffold for the organization of proteins and regulating gene expression. Therefore it is involved in all aspects of a cell: metabolism, reproduction and biosynthesis.

RNA is the carrier of genetic information in organisms and also plays a major role in gene expression. There are three major types of RNAs involved in gene expression: messenger RNA (mRNA), transfer RNA (tRNA) and ribosomal RNA (rRNA). The significance of RNA has further increased lately, with the discovery of naturally catalytic RNA (ribozymes)[6] and involvement of RNA in gene silencing (antisense RNA and RNA interference).[5] From an evolutionary perspective, the existence of ribozymes points to the fact, that RNA and not DNA, was the initial genetic material. However DNA is more stable than RNA, due to the absence of a hydroxyl group. Therefore, DNA is more suited for conservation of genetic information and likely evolved from RNA.

The importance of nucleic acids is self evident and this has attracted scientists from different backgrounds. Francis Crick, one of the scientists who elucidated the structure of DNA and received a Nobel prize for it, was a physicist.[7] This work has been marked as the end of classical biology and the birth of molecular biology.

Since then, the field of nucleic acids has grown exponentially and continues to do so. It is self evident that most of the development in this field would have medicinal

significance. Scientists have looked at DNA and analogues as a diagnostic tool[8] for different diseases, and with the completion of sequencing of the human genome, along with constant development in sequencing methodologies, significant expansion in this field is expected. DNA analogues as therapeutic agents (antisense and antigene therapy)[5] are also being developed. Although this field is relatively new, dating back only to the late 1970s, about a dozen oligonucleotides are in clinical trials.[9] Other interesting areas related to nucleic acids include: molecules that bind to DNA, like chromomycin;[10] DNA as a molecular scaffold,[11,12] a ligand,[13] a catalyst[14] and as a computer[15].

The field of nucleic acids is not limited to these areas, and development in it is limited only by the imagination of one's mind. As more is learnt about the structure and behavior of these biopolymers, significant advancement will be made in their application.

1.2 NUCLEIC ACID STRUCTURE[1,16,17]

The primary structure of DNA and RNA consists of three parts: a heterocyclic base and a ribofuranose sugar linked by a phosphate backbone (**Figure 1.1**). The heterocyclic bases are purines (adenine and guanine) and pyrimidines (cytosine, thymine and uracil). Thymine is present in DNA and replaced by uracil in RNA. Although there are other kinds of bases, especially in tRNA, those mentioned are the most common. The bases are attached to the C1' position of the pentose (furanose) sugar; the purines form the glycosidic bond from the N9 position and the pyrimidines from the N1 position. The nomenclature is such that a number with " ' " (pronounced as 'prime') refers to the sugar position, while those without are for the base. The bases are present in a β configuration, *i.e.*, on the same face as C5' of the sugar ring. In general, the bases occur in an *anti*

conformation, allowing hydrogen bond formation with another base; where adenine base pairs with thymine (uracil in RNA) and guanine base pairs with cytosine. In an oligonucleotide, the base pairs stack over each other (π-π interaction) further stabilizing the secondary structure.

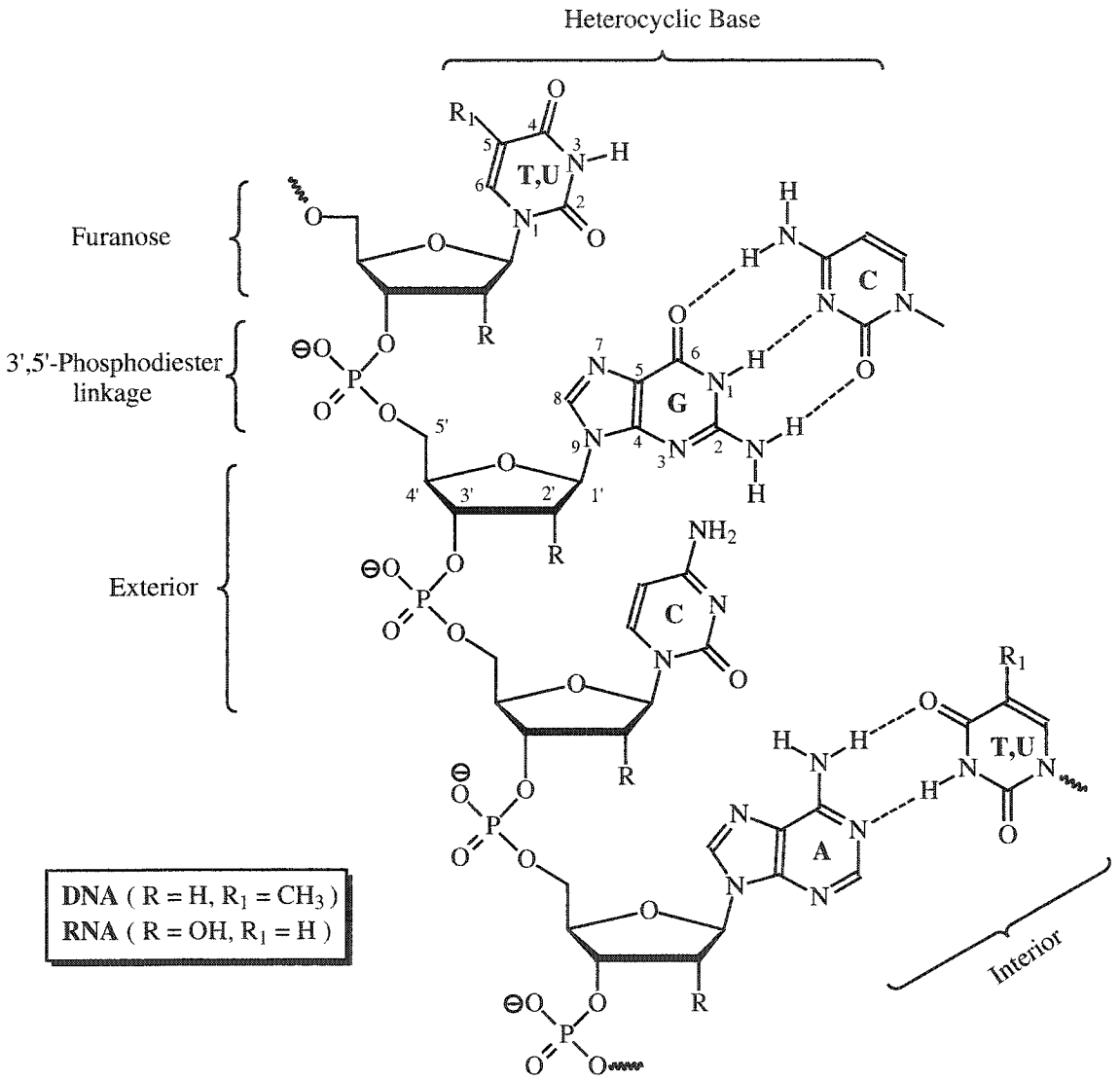

Figure 1.1: Primary structure of deoxyribonucleic acid (DNA) and ribonucleic acid (RNA) with Watson-Crick hydrogen bonding between complementary bases. The numbering of the bases and sugar is shown.

The ribofuranose sugar is found in both DNA and RNA, the difference being the absence of a 2'-OH group in DNA (2'-deoxyribonucleic acid). This seemingly small change has a major impact on the structure, function and stability of these molecules. The sugar is not flat but puckered; where generally C1'-O4'-C4' define the plane with C2' and C3' being out of plane (**Figure 1.2a**). The sugar conformation with C2' being on the same side as C5' is known as C2'-*endo*, C3'-*exo* or S (southern) conformation, and with C3' being on the same side as C5' is known as C3'-*endo*, C2'-*exo* or N (northern) conformation. The conformation of sugar affects the helical structure of the oligonucleotide. The N and S nomenclature has been adopted from the NMR studies done on cyclopentane. It is a coincidence that the pathway C4'-C3'-C2'-C1' formed by the C3'-*endo* and C2'-*endo* puckers resembles the letters N and S (**Figure 1.2a**). Other conformations are also possible, such as O4' *endo* or E (eastern). In fact most of the conformations lie somewhere between the northern and southern conformation, lying towards the eastern side; the western conformation is forbidden due to steric effects.

The conformation adopted by a sugar depends upon a number of factors, such as the anomeric effect, gauche effect and steric interactions. Under physiological conditions, DNA predominantly exists in the C2'-*endo* conformation while RNA exists solely in the C3'-*endo* conformation. Interestingly, the conformation predominantly adopted by a nucleoside is not always present in an oligonucleotide. NMR studies[16] on a monomeric unit of ribo-adenosine shows that it predominantly exists in the C2'-*endo* form, while in an oligonucleotide double helix the steric hindrance by the 2'-OH prevents it from adopting this conformation.

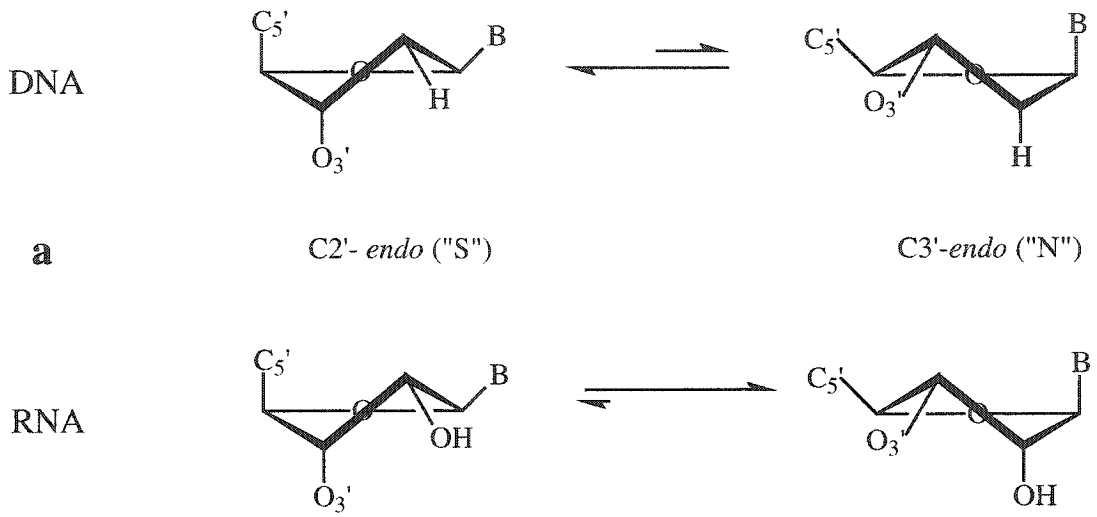

Figure 1.2: (a) Sugar conformations in DNA and RNA. (b) Double helical structure of RNA and DNA. RNA predominantly exists in the A-form, while DNA exists in both A- and B-forms depending upon humidity. Under physiological conditions, DNA duplexes exist in the B-form.

Oligonucleotides are connected by a phosphate backbone, which connect the 3'-oxygen to the 5'-oxygen of the monomeric units. This gives an oligonucleotide polarity, defined by the directionality from the 5'-OH to the 3'-OH.

For DNA, at high humidity (and low salt concentration) the preferred conformation is called "B form"; a clean X-ray diffraction pattern of it was first observed by Maurice Wilkins.[18] Rosalind Franklin showed that DNA was dimorphic[19] and that another form, called "A form", existed at low humidity and high salt concentration (**Figure 1.2b**).

Under physiological conditions, DNA exists in the B-form while RNA predominantly adopts the A-form. Both the A- and B-form exist as an anti-parallel right handed helix. Some differences include the number of base pairs per helical turn (10 vs. 11 in B and A forms, respectively), the bases being perpendicular to the helical axis in B form and slightly tilted in the A form. An extremely important difference lies in the sugar conformation of the two forms; in the A-form the sugars adopt the C3'-*endo* conformation whereas in the B-form the conformation is C2'-*endo*. Also distinctly visible in the different forms are two grooves, which can act as possible hydrogen bond acceptors and donors. The major groove of A-DNA is narrow and deep, while in B-DNA it is wide and deeper. The minor groove of A-DNA is broad and shallow, whereas in B-DNA, it is deep and narrow.

There are other forms adopted by double helices depending upon strand composition (e.g., a hybrid of DNA and RNA), salt concentration and base sequence.

1.3 REGULATION OF GENE EXPRESSION-"THE ANTISENSE STRATEGY"

The flow of genetic information starts from DNA and ends with protein synthesis, with RNA as the intermediary between the two, acting as the information-carrier for the type of protein to be synthesized.

RNA synthesis is initiated by transcription. The transcription initiation complex is composed of proteins that recognize and bind to a specific sequence of DNA. The duplex DNA is unwound and RNA polymerase transcribes the single stranded DNA into a single stranded precursor-mRNA. Normally during transcription the 5'-end of the pre-mRNA is 'capped' by adding a methyl-guanosine and subsequent methylation of one or two sugar residues of the adjacent nucleotides, leading to stabilization of the pre-mRNA. A stretch of nucleotides are also present between the capping site and the initiation site which are believed to play a key role in regulating mRNA half-life. Similarly the 3'-end of the pre-mRNA is composed of several hundred nucleotides beyond the translation-termination site which also plays an important role in determining RNA half-life. Usually most pre-mRNA are poly-adenylated which stabilizes the RNA and assists in transportation of the mature RNA into the cytoplasm.

The pre-mRNA is composed of exons and introns (intervening sequences). These intervening sequences are excised and mature RNA is 'spliced' together by host of enzymes and small molecular weight RNAs which make up the 'Splicesome' machinery. The mature RNA (mRNA) is then transported to the cytoplasm where it undergoes 'translation' and proteins are produced. The half life of the mRNA is highly regulated and varies significantly from a few minutes to many hours.[2]

In 1978, Zamecnik and Stephenson were the first to demonstrate the potential of oligonucleotides as chemotherapeutic agents.[20,21] Their approach was quite novel, using oligonucleotides to target mRNA to inhibit gene expression (as opposed to using small molecules to target proteins). The term 'Antisense' was coined to describe oligonucleotides that bind to the 'sense' mRNA in an anti-parallel, sequence specific manner via Watson-Crick hydrogen bonding (**Figure 1.3**). The antisense oligonucleotides have the advantage of greater specificity and efficacies over traditional drugs. Statistically, a 17-mer oligonucleotide base sequence occurs just once in the base sequence of the human genome and antisense oligonucleotides would bind specifically to them due to base sequence specificity. Also following translation, an mRNA can lead to production of a large number of proteins and the traditional drugs that bind to these proteins would be required in an equally large quantity. Relative to the proteins, the quantity of mRNA present is quite low and therefore a much smaller quantity of an equally efficacious drug would be required.

Antisense oligonucleotides can lead to inhibition of gene expression by 'translational arrest' or degradation of the mRNA by activation of RNA cleaving enzymes such as RNase H. In the former mode of action, an antisense oligonucleotide strongly associates to the untranslated region of the mRNA and prevents translation. It has been shown that antisense oligonucleotides acting via 'translational arrest' are readily unwound by the ribosome and do not block mRNA translation when targeted within the coding region.[22,24] Nevertheless a high affinity antisense oligonucleotide can overcome the unwinding activity of the initiation complex when targeted upstream to the coding region.[22,24]

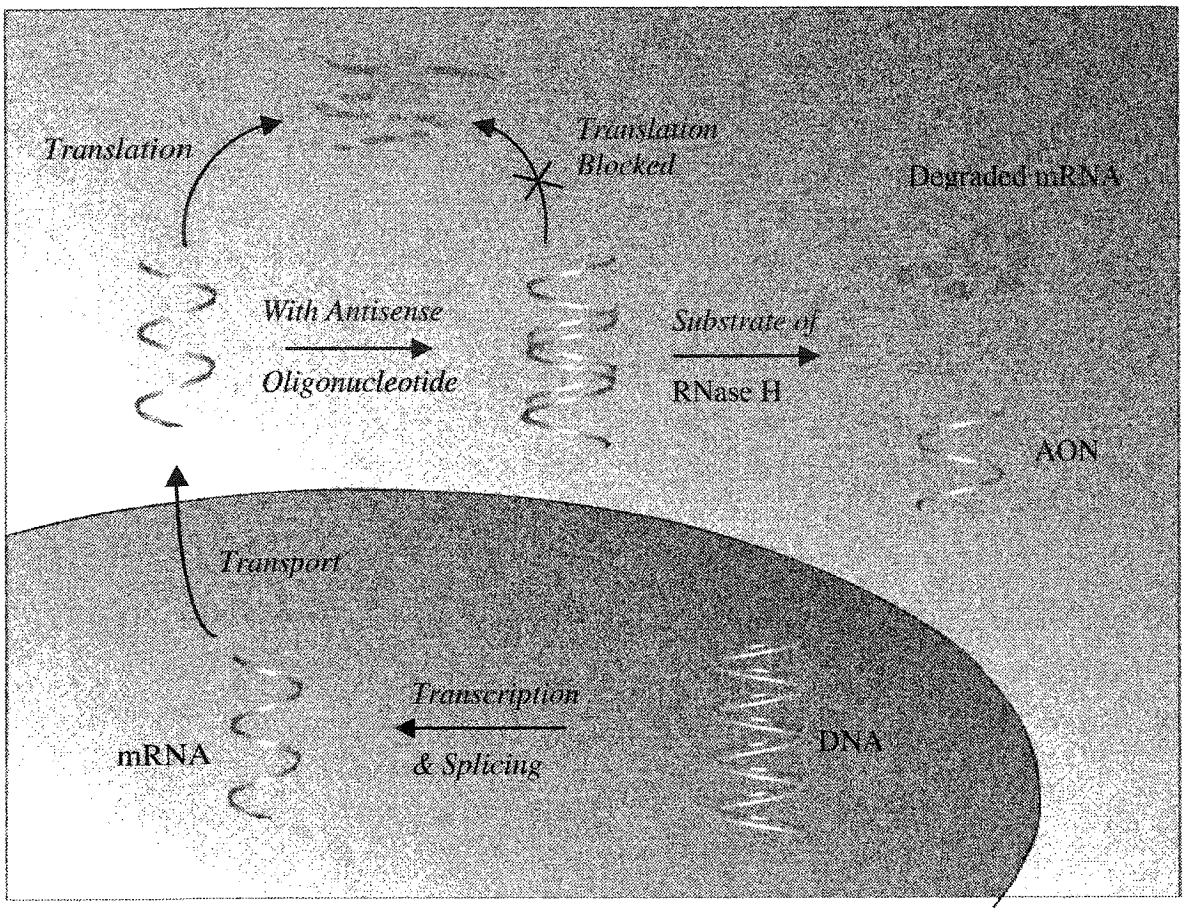

Figure 1.3: Inhibition of gene expression by the antisense strategy.

An alternative mode of action is by activation of RNA cleaving enzymes, such as RNase H and RNase L. RNase H is an ubiquitous enzyme that cleaves the RNA strand of a RNA:DNA hybrid duplex.[24] If the antisense oligonucleotide is structurally similar to DNA, or the AON:RNA duplex adopts a structure that resembles the DNA:RNA duplex transition state within RNase H, then the RNA strand is cleaved. Thus an antisense oligonucleotide that can activate RNase H can act catalytically and 'knock out' several copies of the mRNA and be several orders of magnitude more potent that AONs acting via translational arrest. Another advantage of these AONs is that unlike sterically blocking AONs (translational arrest mechanism) they can be targeted to the coding region

of the mRNA. Examples of AONs acting via the two mechanistic routes are discussed later in this section.

A second class of enzyme activating antisense oligonucleotides are the 2',5'-linked adenylate-antisense chimera, that lead to mRNA degradation, by activation of other cellular enzymes like RNase L.[25-32] Within biological systems, 2',5'-adenylates leads to interferon based induction of RNase L, an ubiquitous enzyme in mammalian cells, as a defense response against viral infection.[33,34] There are three essential components in this system:[35] 2',5'-A synthetase, the enzyme responsible for 2',5'-adenylate synthesis from ATP; the latent 2',5'-A-dependent ribonuclease (RNase L); and 2',5'-phosphodiesterase which degrades 2',5'-A to AMP and ATP. The 2',5'-A-antisense chimeras consists of a 2',5'-linked tetra-adenylate (2',5'-A) linked to an antisense oligonucleotide via a flexible alkyl linker. The antisense oligonucleotide sequence binds to the mRNA selectively and the 2',5'-adenylate portion induces RNase L leading to the localized RNA degradation of the RNA:AON duplex.[28,31]

Thus the 'antisense strategy' poses a very attractive route for gene silencing and treatment of diseases. It offers a binding motif to which the oligonucleotide drug can have target affinity, with a much higher order of magnitude than traditional drugs. Theoretically, it is also possible to develop an antisense drug for any known disease as long as its genomic sequence is known.

Interest in this field has grown exponentially as evident from the large number of research publications, review articles and books that have been published since 1978. A detailed description of this field is beyond the scope of this thesis and the reader is referred to some excellent review articles[36-46] and books[47-51] on this area.

A large number of modified oligonucleotides have been synthesized and tested for their ability to act as antisense oligonucleotides.[5,40,42,52-55] Some of the criteria and desired properties of these oligonucleotides are: (i) Stability to nucleases: all therapeutic oligos must be reasonably stable to enzymatic degradation. Native oligonucleotides are not suitable as they are rapidly hydrolyzed by extra and intracellular nucleases, especially 3'-exonucleases present in the serum. (ii) Strong affinity, specificity and selectivity towards the target RNA sequence: the AON:RNA-target duplex should be sufficiently stable under physiological conditions. The base sequence leads to the specificity of the oligonucleotide drug and should target only the desired RNA over other sites of interaction. (iii) Permeability through the cell membrane. (iv) Activation of enzymes that would lead to selective degradation of the RNA strand of an AON:RNA heteroduplex.

In general, most, if not all, backbone modified oligonucleotides are more stable to nuclease digestion than the natural phosphodiester linkage. Among the modified oligonucleotides synthesized and studied are the so-called 'first generation' antisense oligonucleotides, in which the phosphodiester linkage has been replaced with an alternative moiety. Examples[5] of these include phosphorothioates, boranophosphates, phosphorodithioates, phosphoramidates and methylphosphonates, to name a few. Among these only the first three are able to activate RNase H based degradation of RNA. The phosphorothioates were the first modified oligonucleotides to obtain US Food and Drug Administration (FDA) approval. The drug formivisren (Vitravene)™ is a product of ISIS pharmaceuticals (Carlsbad, California) and is used for the treatment of cytomegalovirus (CMV) retinitis in patients with a suppressed autoimmune system (like

AIDS). Efficient cellular uptake is still a major obstacle for these oligonucleotides and different strategies for delivery have been researched, such as use of cationic liposomes,[56] microinjection, [57] scrape loading[58] and conjugation to small peptides.[59] In order to aid in cellular uptake, neutral oligonucleotide backbones have also been synthesized, however, it is unknown whether such backbones assist in traversing the cellular membrane. A major destabilizing force in oligonucleotide duplexes is the electrostatic repulsion and this is reduced by synthesizing neutral and positively charged backbones.

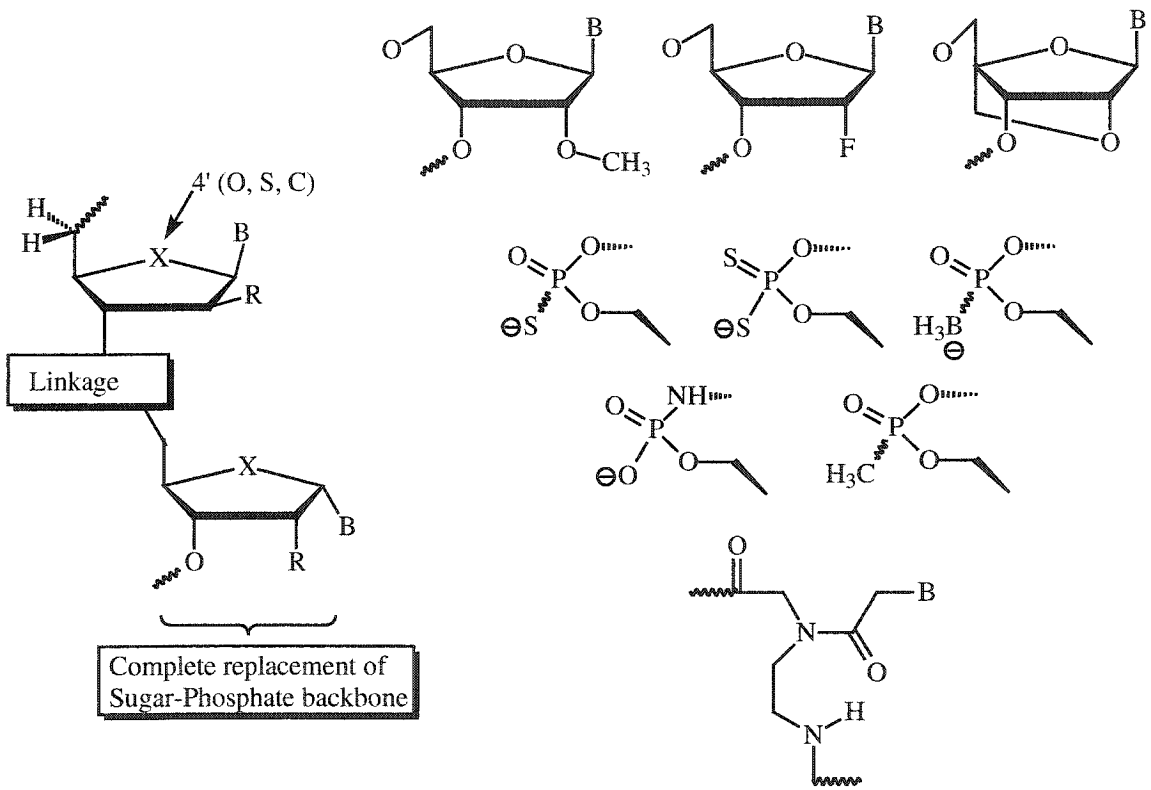

Figure 1.4: Examples of modified oligonucleotides. The sites of modification are the sugars, phosphate backbones, heterocyclic bases or complete replacement of the sugar phosphate backbone.

The other sites of modification within an oligonucleotide, are the sugar and heterocyclic base. Amendment of the heterocyclic bases is usually kept to a minimal, in-order to prevent any possible negative impact upon their hydrogen bonding and base

stacking ability, both of which are important for binding and duplex formation. It has been observed that C-5 modification (methyl and propynyl addition)[60-62] of pyrimidines generally results in an improvement of the desired properties.

Sugar modifications are another area of significant interest. Sugar modifications that favour a C3'-*endo* or northern (*N*) conformation, typically found in RNA, tend to form the most stable duplexes.[63,64] As eluded to earlier, the presence of a 2'-hydroxyl drives the sugar equilibrium within oligonucleotides to the C3'-*endo* pucker. This is attributed to a combination of *gauche* interaction between 2'-OH and 4'-O (ring oxygen) and anomeric effect between O4' and the heterocyclic base (when in the pseudoaxial position). In DNA the *gauche effect* between O3' and O4' results in a C2'-*endo* sugar conformation. By modifying the sugar with electronegative substituents at the C2' and C3' position the overall conformation of the sugar can be molded to yield oligonucleotides that bind with high affinity.[65,66] Examples of sugar modified oligonucleotides are shown in **Figure 1.4**. The arabinofuranosyl and 2'-fluoro-arabinofuranosyl oligonucleotides, developed in our laboratory, were the first sugar modified antisense oligonucleotides that led to RNA degradation by activation of RNase H. As seen, examples also exist where the sugar moiety has been completely replaced, like in peptide nucleic acids (PNA).[5]

Duplex formation leads to a large loss of entropy due to restriction of the translational, vibrational and rotational energy. The pre-organization of an oligonucleotide in the proper conformation is highly beneficial as it reduces the loss of high entropic cost upon hybridisation. For example the locking of the sugar in a defined conformation pre-organizes the oligonucleotide prior to hybridization, energetically

assisting the antisense oligonucleotide for duplex formation.[64] Another factor, often overlooked, is the degree of hydration of an oligonucleotide duplex and it is desired that any oligonucleotide duplex formed be properly hydrated.[67]

All these factors should be kept in mind when designing novel antisense oligonucleotides.

1.4 2',5'-LINKED OLIGONUCLEOTIDES

A very interesting backbone modification is the change in linkage position from C3' (as found in DNA and RNA) to C2' (**Figure 1.5**). This leads to an increase in the number of bonds between O5' and phosphorus from six to seven. As described below, such a change results in antisense oligonucleotides with very unique physiochemical and biological properties. Throughout this thesis the native oligonucleotides with 3',5'-linkage are referred to as either DNA or RNA, while backbone modified oligonucleotides are described in a manner that would reflect their linkage, such as 2',5'-RNA (2',5'-linked ribonucleic acids).

2',5'-RNA occurs naturally in a number of different cells and tissues but to a much lower extent, e.g., 2',5'-linked riboadenylates have been found in L1210 cells and human lymphocytes.[69] Torrence *et al.* have shown that these oligonucleotides may also be involved in cell growth, cell differentiation and in mediating antiviral effects of interferon.[70] They have explored the latter method by utilizing the 2',5'-oligoadenylate system for RNA degradation.[71,72] In interferon treated cells, several new proteins are synthesized including 2',5'-synthetase which catalyzes the formation of 2',5'-oligoadenylates from ATP. This catalysis is induced by dsRNA, formed as an

intermediate in viral replication. The 2',5'-riboadenylates activates the latent enzyme, RNase L, leading to degradation of mRNA.[32,73] In order to generate a higher degree of selective degradation, 2',5'-oligonucleotides have been conjugated to RNA which is complementary to its target sequence.

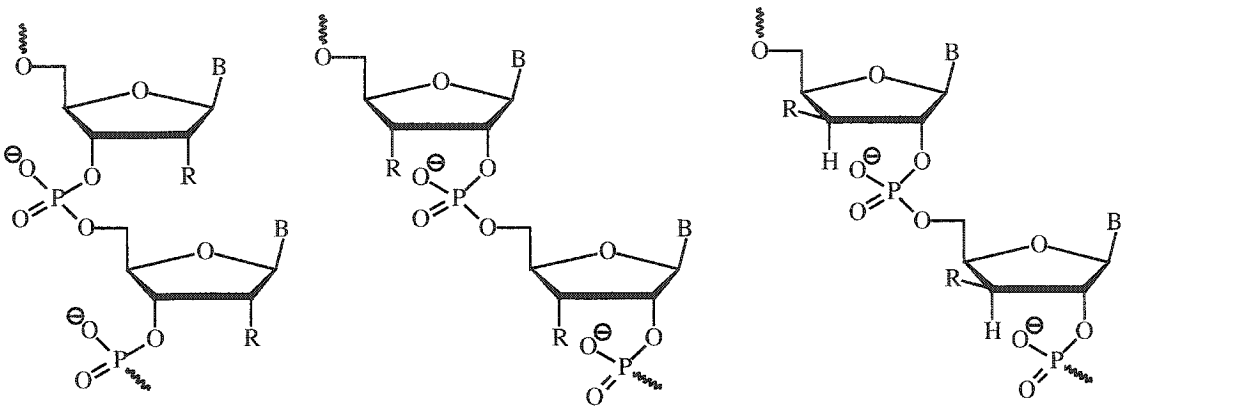

R	
OH	3',5'-RNA
H	3',5'-DNA

R	
OH	2',5'-RNA
F	2',5'-Ribo-Fluoro nucleic acids (2',5'-FRNA)

R	
OH	Xylonucleic acids (2',5'-XNA)
F	Xylo-fluoro nucleic acids (2',5'-FXNA)

Figure 1.5: Comparison of the primary structure of 3',5' and 2',5'-linked oligonucleotides. 2',5'-XNA, 2',5'-FXNA and 2',5'-FRNA are the subject of study of this PhD. thesis.

For many years, scientists have wondered why nature chose 3',5'-linked ribose (and 2'-deoxyribose) as the backbone of RNA and DNA over 2',5'-linked sugar?.[74-77] In this respect, it is interesting to note that in the presence of divalent metal ion and uranyl-ion catalysts, 2',5'-RNA is preferentially formed from activated mononucleotides.[78-81] 2',5'-RNA is also predominantly produced from 3',5'-RNA template mediated oligomerization.[82] However, in the presence of clay mineral catalyst the oligomerization of activated nucleotides results in formation of 3',5'-oligonucleotides.[83,85] Thus, the formation of both 2',5' and 3',5'-linkages were possible during evolution and nature likely chose the 3',5'-linkage due to the desired properties required for the sustenance of

life. The initial belief for selecting 3',5' over 2',5' linkages was that the latter could not support Watson-Crick base pairing.[86-88] However, subsequent binding studies of 2',5'-linked oligonucleotides clearly established that these molecules support duplex and triplex formation.[74,89-96] Therefore, other factors must be responsible for nature's choice of 3',5'-linked oligonucleotides.

The binding studies mentioned above clearly point to the unique behavior of 2',5'-linked oligonucleotides. Our laboratory was the first to report that 2',5'-RNA binds selectively to RNA over single stranded DNA.[97,98] This was later corroborated by others and shown to be a general property of 2',5'-linked oligonucleotides.[99-101] Also hybrid duplexes formed between 2',5'-RNA and RNA are less stable than a pure RNA duplex. The 2',5'-linked oligonucleotide:RNA duplexes have also been tested for RNA degradation by RNase H, and though the duplex binds to RNase H, no degradation of RNA was observed.[96,101,102] Although none of the 2',5'-modified oligonucleotides synthesized to date elicit RNase H activity, their ability to bind to RNA and to resist degradation by nuclease enzymes, make them attractive antisense constructs.

Relatively little is known about the structure of 2',5'-oligomers and the duplexes formed by them. Early work and conclusions were derived from the circular dichroism (CD) studies. Recent molecular modeling and NMR studies have shown that 2',5'-RNA and 2',5'-DNA adopt the C2'-*endo* and C3'-*endo* sugar conformations, respectively. This exactly contrasts what is found in 3',5'-linked oligonucleotides.[93,95,104] During the course of this thesis work, Yathindra *et al.* reported an elegant study pointing to the relationship between sugar and backbone conformation of 2',5'-linked and 3',5'-linked oligonucleotides.[77] They reasoned that the structure of oligonucleotides can be reviewed

as having either an '*extended*' or '*compact*' conformation depending upon the distance between intra-strand phosphate groups (P-P) (**Figure 1.6**). They also pointed out that such conformations were intimately related to the sugar pucker form. Thus the C3'-*endo* sugar conformation of 2',5'-linked oligonucleotides would yield an 'extended' conformation that was equivalent to the C2'-*endo* conformation of 3',5'-linked oligonucleotides. In other words, in order to create a 2',5'-linked oligonucleotide equivalent in structure to a particular 3',5'-nucleic acid, the sugar must undergo a conformational switch. Another consequence of moving the linkage from C3' to C2', as stated by Yathindra, "is a mandatory displacement of the Watson-Crick base pairs from the helical axis, which is due to a direct consequence of the lateral shift of the sugar-phosphate backbone from the periphery towards the interior of the helix".

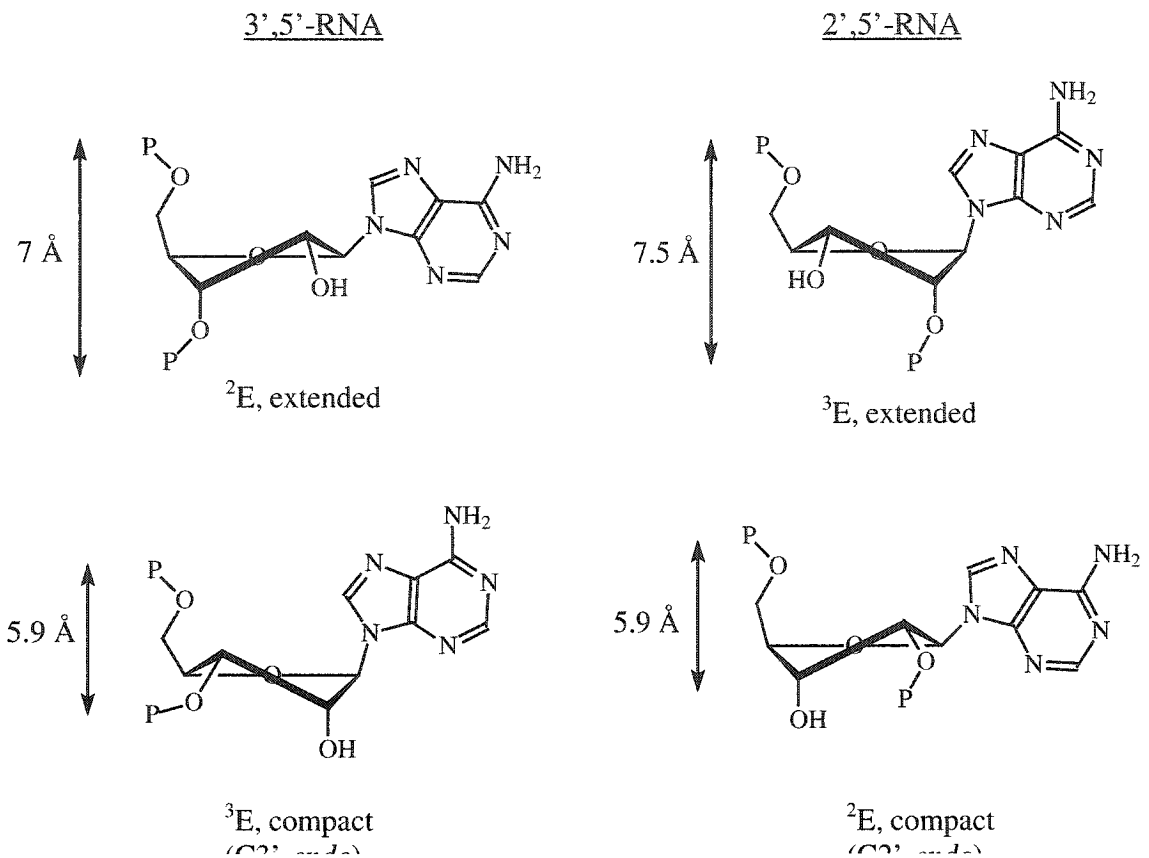

Figure 1.6: Comparison of the sugar and backbone conformations of 3',5' and 2',5'-oligonucleotides.

1.5 TECHNIQUES UTILIZED IN SURVEYING NUCLEIC ACIDS

A wide array of techniques are employed in studying nucleic acid structure. Those most used during the course of this study are discussed below.

1.5.1 Ultraviolet (UV) Spectroscopy

Nucleic acids contain chromophoric heterocyclic purine and pyrimidine bases with UV λ_{max} absorption generally centered around 260 nm. The wavelength maximum for an oligonucleotide is dependent upon a number of factors, such as base composition, base-base interactions and the pH of the solution. The extinction coefficient of purines is

higher than those of the pyrimidines, and in general, oligonucleotides with greater purine content have a higher extinction coefficient.[16]

Interestingly, the absorption of an oligonucleotide is lower than what would be predicted based upon summation of the extinction coefficients of the individual nucleotides. This reduction in absorption arises due to dipole-dipole interactions of the bases when they stack and is referred to as 'hypochromicity'. The same is true when one compares the absorption of a nucleic acid duplex vs. those of the individual strands. Thus at lower temperatures, the ordered structures like duplexes, have a lower absorption than at higher temperatures. The study of the absorbance of the oligonucleotide versus temperature is known as a "melting temperature or T_m" experiment. The increase in absorbance as the duplex dissociates into single strands is referred to as "hyperchromicity" (H). Its magnitude reflects the degree of base stacking, and therefore is more pronounced in ordered structures like duplexes and triplexes and is generally reported as a percentage according to the formula

$$\Delta H\% = [\ (A_f - A_i) / A_f\ ] \times 100$$

where A_i = absorbance at initial temperature, A_f = absorbance at final temperature.

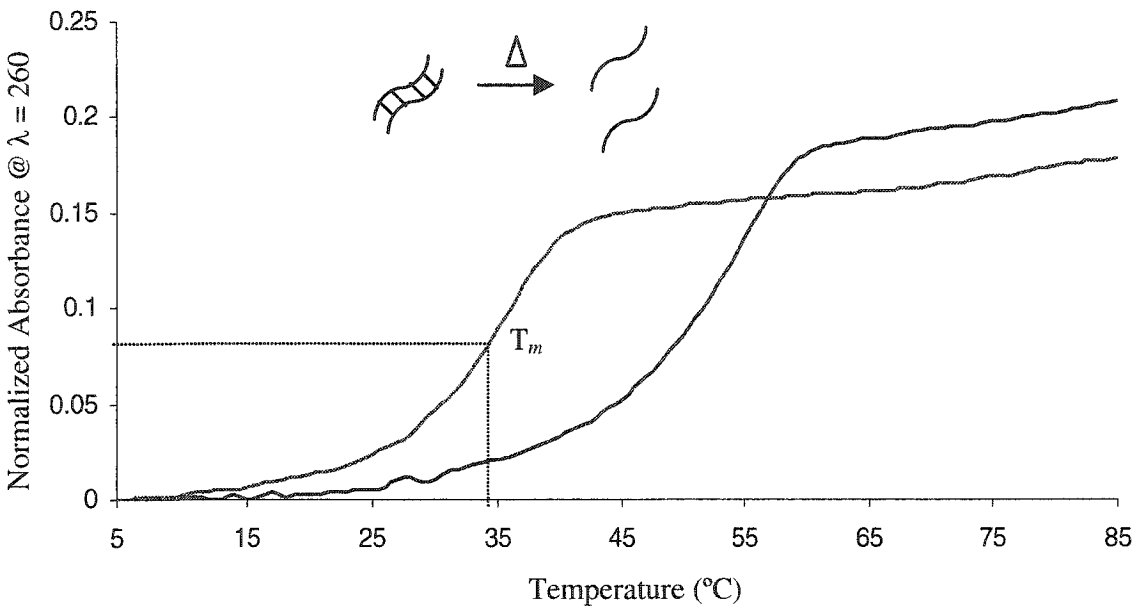

Figure 1.7: A representative melting curve ('T_m') of an oligonucleotide duplex. At low temperature the base stacking leads to a reduction in UV absorbance which is lost upon heating and leads to an increase in the absorbance value.

Duplexes that 'melt' at higher temperature have a stronger association to their complementary oligonucleotides relative to those with a lower T_m. The T_m value is taken as the mid-point of the sigmoidal melting curve or by taking the first derivative of the melting curve (T_m=the inflection point). A representative melting curve of an oligonucleotide duplex is shown in **Figure 1.7**.

1.5.2 Circular Dichroism (CD) Spectroscopy[105-108]

Another powerful technique for studying nucleic acids is circular dichroism spectroscopy, as it provides insight into the helical conformation of oligonucleotides. CD measures the wavelength dependence of the ability of an optically active chromophore to differentially absorb left and right circularly polarized light. The heterocyclic bases in nucleic acids have a plane of symmetry and therefore are not intrinsically optically active.

However, the sugar moiety is asymmetric and since the bases are attached to the 1'-carbon of the sugars, the sugars can induce a CD in the absorption bands of the chromophoric bases.

The advantage of CD spectroscopy over other techniques (e.g. NMR) in studying nucleic acid structure, is the small quantity of sample required (μM versus mM sample concentration). However NMR is an absolute method whereas CD is used as a qualitative tool, *i.e.*, the CD spectra for a modified oligonucleotide is compared to the CD "signatures" of an oligonucleotide of established structure and inferences are drawn about the structure of the modified oligonucleotide by comparing two spectra.

1.5.3 Electrophoresis[1, 108]

The transport of charged molecules like DNA through a medium (solvent or porous gels) under the influence of an electric field is known as electrophoresis. The medium generally utilized to study long fragments of nucleic acids is agarose, whereas polyacrylamide is generally used to analyze and purify small to medium size (2-100nt) oligonucleotides. The size of the pores in the gel can be controlled by the amount of cross-linking agent. The mobility of the oligonucleotide is based on the charge, size and shape of the oligonucleotide, with the smaller oligomers generally moving faster than the longer ones. The gels can be prepared in either denaturing conditions (with added urea) or under native conditions. The denaturing gels are used for purification and identification purposes and the native gels are utilized to study nucleic acid interaction. Following gel electrophoresis, the oligonucleotide is visualized by either UV shadowing

or staining with a dye. Most of the oligonucleotides prepared in this study were purified by polyacrylamide gel electrophoresis.

1.6 PROJECT OBJECTIVES

In RNA and DNA the sugar units are linked by a 3',5'-phosphate backbone. In DNA duplexes the sugar prefers a C2'-*endo* conformation and in RNA the predominant conformation is C3'-*endo*, leading to B and A-form duplexes respectively.[16] The role of such sugar conformations is not well understood in 2',5'-oligonucleotides. The focus of this thesis was to investigate the effect of sugar conformation on the physicochemical and biological properties of 2',5'-linked oligonucleotides.

Our method of study will involve hybridization and structural studies on 2',5'-oligonucleotides bearing modifications at the C3'-position. As a first step, the impact of C3'-stereochemistry on hybridization will be investigated by synthesizing 2',5'-xylooligonucleotides. The required monomers will first be synthesized and then appropriately protected making them amenable to solid phase oligonucleotide synthesis. Following deprotection and purification, binding and structural studies will be performed by melting temperature UV measurements (T_m) and circular dichroism spectroscopy, respectively.

The first oligonucleotide analogue to be prepared and studied will be the 2',5'-linked β-D-xylo-furanose nucleic acids (2',5'-XNA) (**Figure 1.5**) and are discussed in **Chapter II**. These are the 3'-epimer of 2',5'-RNA and adopt predominantly the C3'-*endo* conformation. In principle, 2',5'-XNA, like 2',5'-RNA, could have been chosen as genetic material (*i.e.*, they are interesting from an etiological perspective) and therefore

physicochemical data of these compounds may provide new insight as to why nature chose 3',5'-nucleic acids. The effect of attaching fluorine at the C3'-position was also of interest and therefore "second generation" xylo-nucleic acids were developed. The first one considered was 2',5'-linked 3'-deoxy-3'-fluoro- β-D-xylo-furanosyl-nucleic acids (2',5'-FXNA) and is examined in **Chapter III**. Since the sugar conformation of 2',5'-FXNA is expected to be similar to that of 2',5'-XNA, the effect of sterics and/or hydrogen bonding on sugar pucker could be evaluated. Finally, in **Chapter IV**, we investigate the antisense properties of 2',5'-linked 3'-deoxy-3'-fluoro-β-D-ribo-furanosyl-nucleic acids (2',5'-FRNA) for the first time.

CHAPTER II

SYNTHESIS, PHYSICOCHEMICAL AND BIOCHEMICAL PROPERTIES OF XYLONUCLEOSIDES AND OLIGONUCLEOTIDES

2.1 INTRODUCTION

Nucleosides derived from the sugar D-xylose (xylonucleosides) are the C3'-epimer of the naturally occurring ribonucleosides (**Figure 2.1**). This stereochemical modification significantly alters their biological properties and, in fact, xylonucleosides are known to exhibit high antitumor and antiviral activities.[109,110] The most prominent among them is 9-(β-D-xylofuranosyl)adenine (XyloA), the antitumor activity for which was first reported by LePage and Ellis[111,112] and later by others[113-6] along with its antiviral properties.[117,118] The antiproliferative properties of XyloA are amplified by inhibition of adenosine deaminase,[113,119-122] which also links XyloA to its inhibitory effects on various metabolic reactions.[109,111,112,115,121-131]

Xylonucleosides represent attractive synthons and have been used for the synthesis of valuable antivirals like 3'-deoxy-3'-azidothymidine (AZT), 2',3'-didehydro-3'-deoxythymidine (D4T) and their derivatives.[132-141] Both AZT and D4T are known to be effective against the human immunodeficiency virus (HIV) and in the treatment of acquired immunodeficiency syndrome (AIDS).[132]

Early reports on the synthesis of pyrimidine xylonucleosides involved coupling of a mercuric derivative of thymine to a peracylated halo generated sugar.[145] Of the purine nucleosides, xyloadenosine was the first to be synthesized by Baker and Hewson.[146]

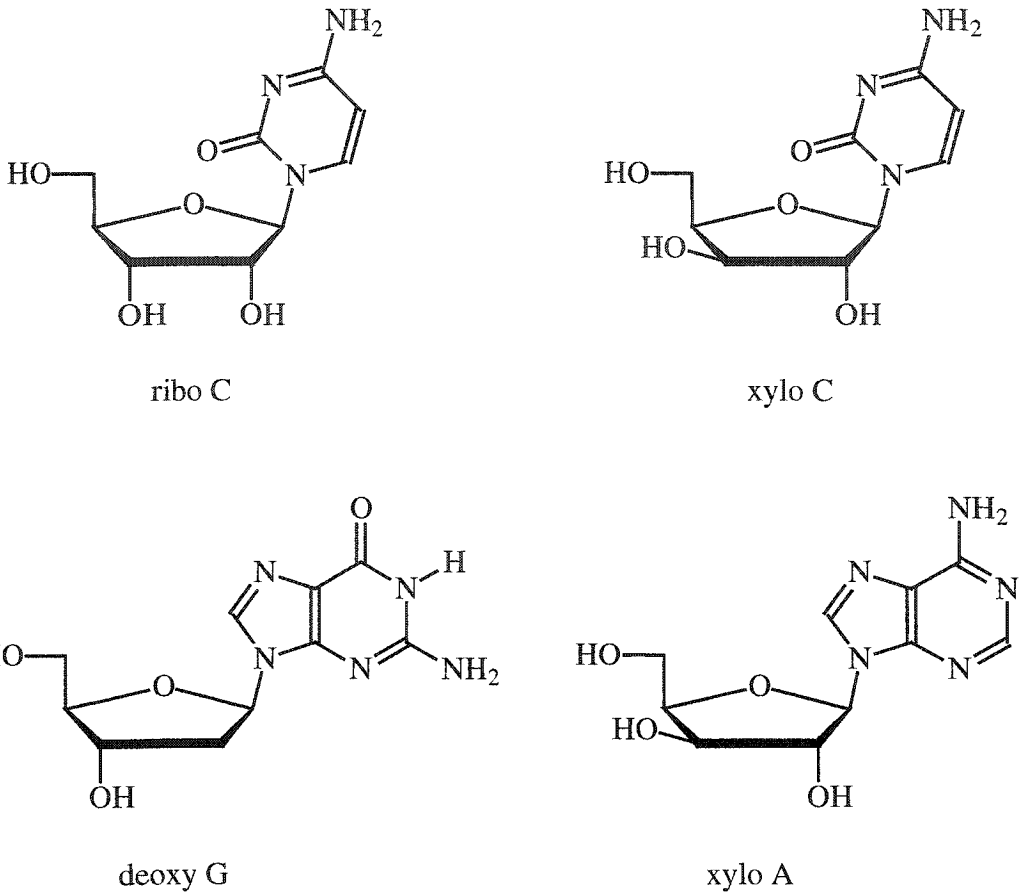

Figure 2.1: Structural comparison of xylonucleosides to natural nucleosides.

Other routes have also appeared starting from the ribonucleoside. These involve either the oxidation-reduction[147-149] of the C3'-hydroxyl group or hydrolytic cleavage of a 2',3' ribo-epoxide moiety (**Figure 2.2**).[150] However, these routes suffer from several drawbacks. For example, the oxidation-reduction route of C3'-OH requires tedious chromatographic separation of mixtures of the C2' and C3'-protected nucleosides and the purification problem occurs again in the separation of the α and β reduction products.

Therefore the coupling of a silylated base to an appropriate peracylated sugar seems to be a more desirable route to the nucleoside. One possible way, known as the silyl-Hilbert Johnson procedure[151] employs Friedel-Crafts reagents as coupling catalysts.

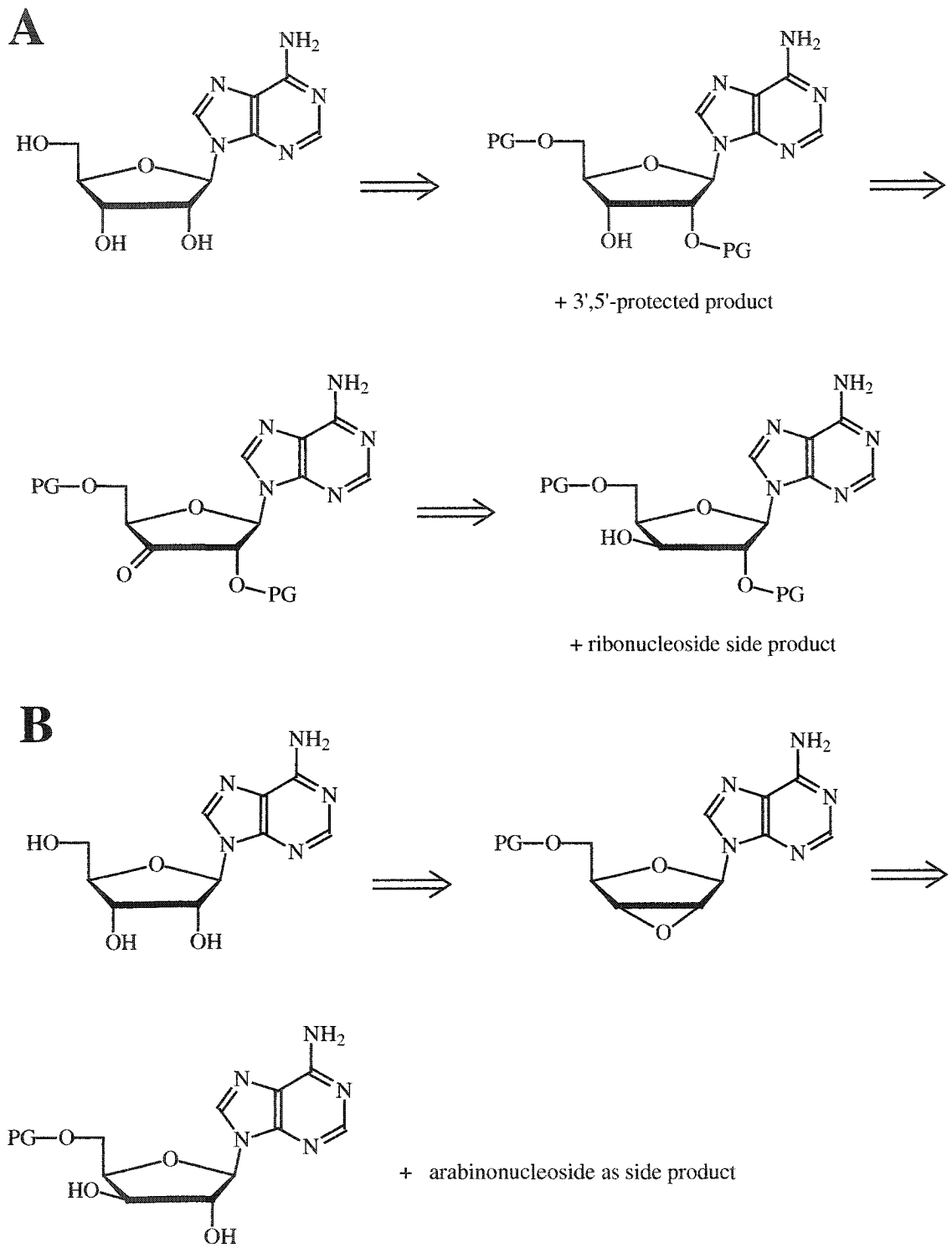

Figure 2.2 a & b: Synthetic routes to xylonucleosides. PG = protecting groups.

This was further improved by Vorbrüggen *et al.*,[152-155] so that the final synthesis could be carried out in a single pot (**Figure 2.3**). Indeed xylonucleosides have been synthesized on many occasions via Vorbrüggen coupling.[136,138,141,156-161] The advantage of such procedure is the predominant formation of the desired β-nucleoside due to neighbouring group participation of the 2'-acyloxy group during the glycosylation reaction. Therefore sugars having a 2'-acyloxy group on the α face (like ribose and xylose furanose) would lead to a β configured base, while those having a participating 2'-acyloxy group on the β-face (like arabinose and lyxose furanose) would lead to the base coupling in an α configuration (Baker's rule).[162]

The synthesis of 5-methyl-xylouridine (xyloU$^{5\text{-Me}}$) is well documented and attainable in good yields; however problems exist in the coupling of the purines to the sugar as well as in the use of 1,2,3,5-tetra-O-acetyl-xylofuranose. Gosselin *et al.* have reported that this sugar, which is obtained as a syrup, is consistently contaminated with the pyranose and hexaacetylated forms and is difficult to purify on a preparative scale.[160] This problem can be avoided by use of the benzoylated form of the sugar.

As to the problem for formation of purine xylonucleosides, there are reports[156,158,163-166] indicating that the coupling of the silylated purines to the peracylated xylofuranose sugar led to mixtures of α and β anomers, as well as N-9 and N-7 regioisomers, which are extremely difficult to separate. Formation of the α anomers is probably due to the possible 1,3 and 1,5-acyloxy group participation in the formation of the acyloxonium ion, as suggested by Paulsen *et al.*[167] This problem was averted and the procedure of coupling adenine to a sugar was simplified by Saneyoshi *et al.*,[168,169] who showed that coupling an unprotected adenine and 6-substituted purine to peracylated or

perbenzoylated ribofuranose and xylofuranose sugars in the presence of a Friedel-Crafts catalyst (such as $SnCl_4$), lead to the exclusive formation of the N-9 β nucleoside. Interestingly, coupling an unprotected cytosine base to a protected xylofuranose via Saneyoshi coupling has also been shown to take place cleanly with formation of only the N-1 nucleoside.[160]

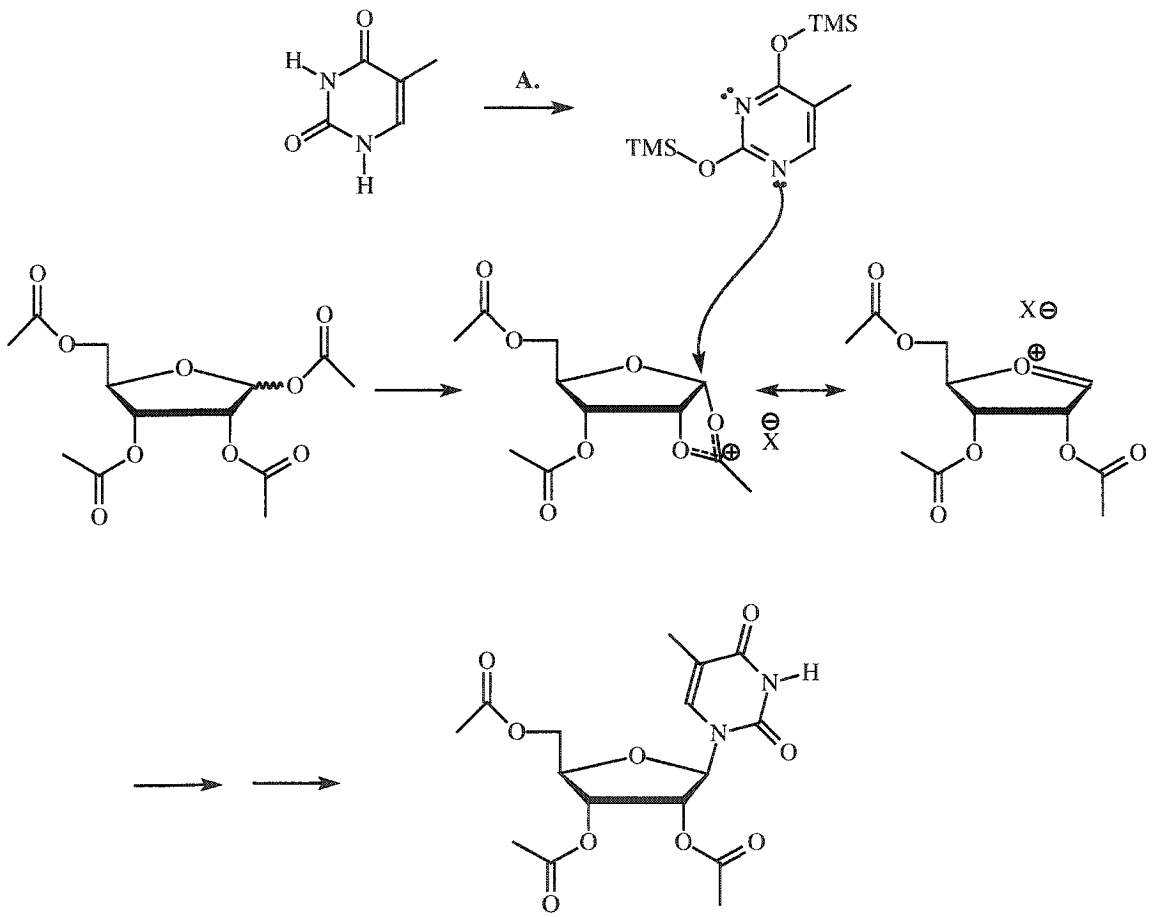

Figure 2.3: Vorbrüggen reaction mechanism for the stereoselective synthesis of nucleosides. **A.** Silylating reagent (e.g., TMS-Cl, HMDS); X = Lewis acid catalyst.

Although the Vorbrüggen and Saneyoshi coupling procedures made matters easier, the problem of coupling a guanine base to a sugar still persisted, due to the formation of N-7/N-9 isomeric mixtures of nucleosides. The N-9 isomer is

thermodynamically more stable[169] and can be obtained by fortuitous crystallization of the N-9/N-7 mixture after Vorbrüggen coupling. However, Garner *et al.*[170] developed, for the first time, conditions that led to the formation of either the N-9 or the N-7 isomer. They showed that under kinetic conditions (using $SnCl_4$ in acetonitrile at room temperature) the N^2-acetylguanine coupled to form predominantly the N-7 isomer, while under thermodynamic conditions (trimethylsilyl triflate in dichloroethane under reflux) led to an isomeric ratio of 8:1 in favour of the N-9 isomer. They also showed that the presence of a 2'-O-benzoyl group instead of a 2'-O-acetyl protecting group improved the N9/N7 ratio due to the greater stabilization of the ionic aryloxonium intermediate formed. Recently Robins *et al.*[161,171] showed that a N^2-acetyl-6-O-diphenylcarbamoylguanine could be used under similar conditions as those described by Garner *et al.* to selectively obtain the N-9 isomer with no detectable amount of the N-7 isomer. This procedure was also used by them for the synthesis of the guanine xylonucleoside.[161]

Although the synthesis of xylonucleosides has previously been established, very little work has been done on the incorporation of xylonucleosides into 2',5'-linked oligonucleotides. Imbach *et al.* were the first to synthesize[159,172] 2',5'-linked xyloadenylic acid (up to tetramers) via solution-phase phosphotriester methodologies. Their objective was to study the interferon induced degradation of RNA via activation of RNase L and the stability of the 2',5'-oligomers with regard to 2',5'-phosphodiesterase activity (PDE).[173] They also showed that xylonucleosides can be incorporated into oligonucleotides by the enzyme T4 RNA ligase[174] and that xylonucleoside analogs inhibit the replication of herpes simplex virus I and II.[175] These compounds displayed strong resistance towards degradation by 2',5'-PDE,[173] cell free extract[176] and homogenous

poly(A) specific 2',3'-exo-ribonuclease,[177] all desirable properties in oligonucleotides being developed for therapeutic applications.

NMR spectroscopic studies of 2',5'-xyloadenylic acids have revealed that the furanose sugar and N-glycosidic bonds adopt primarily the C3'-*endo* (Northern, $^3T_2$) and anti conformations, respectively (**Figure 2.4**).[178] The same features have been observed for the xyloadenosine nucleoside.[179-181] However, slight differences were noted between the riboA and xyloA nucleosides, both in terms of sugar pucker (C3'-*endo*-C4'-*exo versus* C3'-*endo*-C2'-*exo*) and rotamer populations about the C4'-C5' bond. For the pyrimidines, X-ray crystallography and NMR studies showed that xylouridine exists predominantly in a C3'-envelope (^3E) or a Northern ($^3T_2$) conformation depending upon pH and temperature.[182]

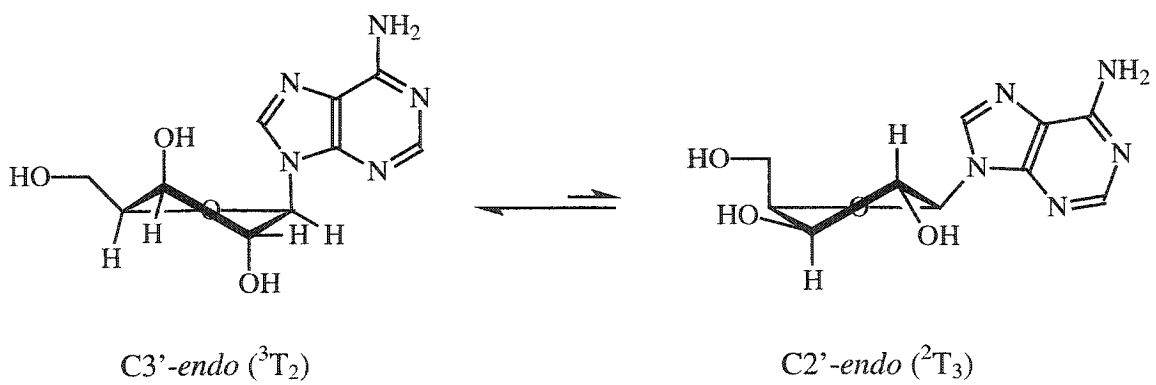

C3'-*endo* ($^3T_2$) C2'-*endo* ($^2T_3$)

Figure 2.4: Conformation of xylonucleosides observed in short single stranded oligonucleotides (trimers) and nucleosides.[179-182] The $^3T_2$ conformation is stabilized by two gauche effects (O4'-C4'-C3'-O3' and O4'-C1'-C2'-O2') and anomeric effect (axial disposition of adenine base).

3',5'-Linked-2'-deoxy-oligoxylonucleotides were first synthesized by Shabarnova *et al.*[183] and were studied independently by Seela *et al.*[184-188] Both studies showed that insertion of 3',5'-linked-2'-deoxy-xylonucleotides into DNA and sequences consisting

entirely of 3',5'-linked-2'-deoxy-xylonucleotides bind weakly to single stranded DNA and RNA. Seela *et al.* also showed that 3',5'-linked oligonucleotides comprised of 2'-deoxy-xylofuranose form left handed (Z-type) helices and that the sugar conformation is dramatically flattened, leaning towards a C3'-*exo* (Southern) conformation.[184-188] This unusual sugar pucker was ascribed to a steric interaction between the C3'-O-phosphate and the cis heterocyclic base making it impossible for the sugar to adopt a C3'-*endo* (Northern) conformation. Interestingly, 3',5'-linked 2'-deoxy-oligoxylonucleotides showed enhanced stability towards degradation by both calf-spleen and snake venom phosphodiesterases.[184-188]

The following sections describe the synthesis of xylonucleosides and their incorporation into 2',5'-linked oligonucleotides (2',5'-XNA). To the best of our knowledge, these studies are the first to describe the solid-phase synthesis of 2',5'-XNA as well as its physicochemical and biological (RNase H) properties.

2.2 SYNTHESIS OF PROTECTED β-D-OLIGOXYLONUCLEOTIDES-2'-O-PHOSPHORAMIDITES

As stated earlier, the synthesis of xylonucleosides is well established.[136,138,141,145-150,156-161,163-166,168-170] Our initial task was to synthesize xylonucleosides with appropriate protecting groups amenable to solid phase synthesis via phosphoramidite chemistry. The syntheses of the required pyrimidine nucleosides are outlined in **Figures 2.5** and **2.11**.

The route adopted for the synthesis of xyloU$^{5\text{-Me}}$ and xyloC involved the coupling of an appropriate sugar to the base. Imbach *et al.*[160] have shown, that 1,2,3,5-tetra-O-benzoyl-D-xylofuranose may be used effectively to couple different bases, which is in

agreement with our initial studies. In contrast, the tetra-O-acetylated sugar gave lower yields and more side products. This corroborates the finding of Gosselin *et al.*,[160] who found that the acetylated sugar is contaminated with both the pyranose form and the hexaacetylated sugar, and is difficult to purify.

Therefore, 1,2,3,5-tetra-O-benzoyl-D-xylofuranose was synthesized by the procedure of Kaz'mina *et al.*[190] Starting from D-xylose, the 1-O-methylated sugar was prepared by treatment with methanol/HCl, followed by benzoylation of the hydroxyl groups (**Figure 2.5**). The resulting sugar (**2.1**) was treated with HBr in AcOH to form the 1-brominated product, which was hydrolyzed using silver (I) carbonate, acetone and water. The viscous product was then benzoylated and recrystallized from ethyl acetate/ethanol to obtain the 1,2,3,5-tetra-O-benzoyl-α-D-xylofuranose as a white powder (53% overall yield from D-xylose).

5-Methyl-xylouridine (xyloU$^{5\text{-Me}}$, **2.3**) was synthesized in excellent yield by coupling the sugar (**2.1**) to silylated thymine via the Vorbrüggen reaction followed by treatment with methanolic ammonia. In order to use xyloU$^{5\text{-Me}}$ during solid phase synthesis using the phosphoramidite strategy, appropriate protecting groups were required.[190] To this end, the first step was protection of the 5'-OH with a monomethoxy trityl (MMT) group to obtain 5'-MMT-5-methyl-xylouridine (**2.4**) (assignment of the sugar protons and hydroxyls was achieved using ^{1}H NMR COSY experiments).

The preference for MMT over the more common dimethoxytrityl (DMT) group, is largely due to its stability.[203] The DMT group is more acid labile (about 10 times) and purification or storage of 5'-DMT nucleosides over a long period of time can be problematic, due to the loss of the DMT group. We had also envisioned the use of

xylonucleosides as precursors for the synthesis of other modified nucleosides and thus wished to use a protecting group (MMT) with greater stability.

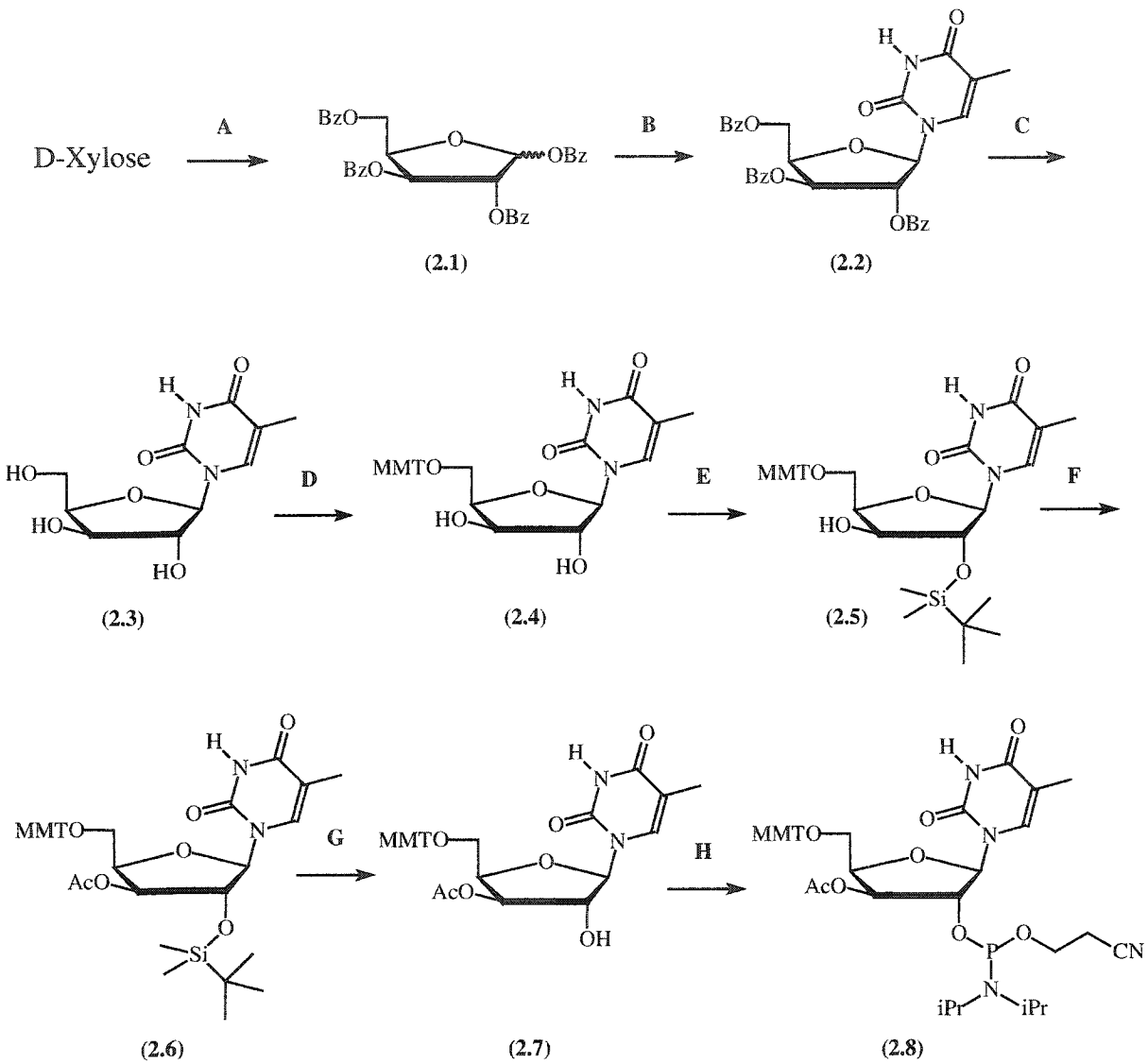

Figure 2.5: Scheme for the synthesis of xyloU$^{5\text{-Me}}$ amidite **(2.8)**. **A.** (i) 1% HCl, MeOH; (ii) Bz-Cl, pyr; (iii) 30% HBr in AcOH; (iv) Ag_2CO_3, acetone, H_2O; (v) Bz-Cl, pyr (53% over five steps); **B.** Thymine, $SnCl_4$, TMS-Cl, $(CH_3)_6Si_2NH$, reflux (86%); **C.** NH_4OH/MeOH, r.t., overnight (90%); **D.** MMT-Cl (1.2 eq.), DMAP (cat.), pyridine, r.t., overnight (99%); **E.** TBDMS-Cl, imidazole, DMF, r.t., overnight (88%); **F.** Ac_2O, DIPEA, DMAP, THF, r.t. (98%); **G.** TBAF, THF, r.t. (Quant.); **H.** Cl-P(OCE)(N-iPr_2) (1.2 eq), DIPEA (2.4 eq) (83%).

The next step was the silylation of the 2'-OH group (**Figure 2.5**). In the case of ribonucleosides, in which the C2' and C3'-OH are both pointing away from the 5'-MMT group, a mixture of 2' and 3'-silylated products are always obtained (**Figure 2.6**), requiring a difficult chromatographic separation. In addition, it is known that the 2'-hydroxyl has a lower pKa value and is more nucleophilic than the 3' (and even the 5'-) hydroxyls groups.[16] Therefore a slightly greater quantity of 2'-silylated product is generally obtained; however care must be taken to avoid a basic medium, which can cause 2'/3'-silyl isomerization, due to the ribo (or cis) configuration of the 2' and 3'-hydroxyls.

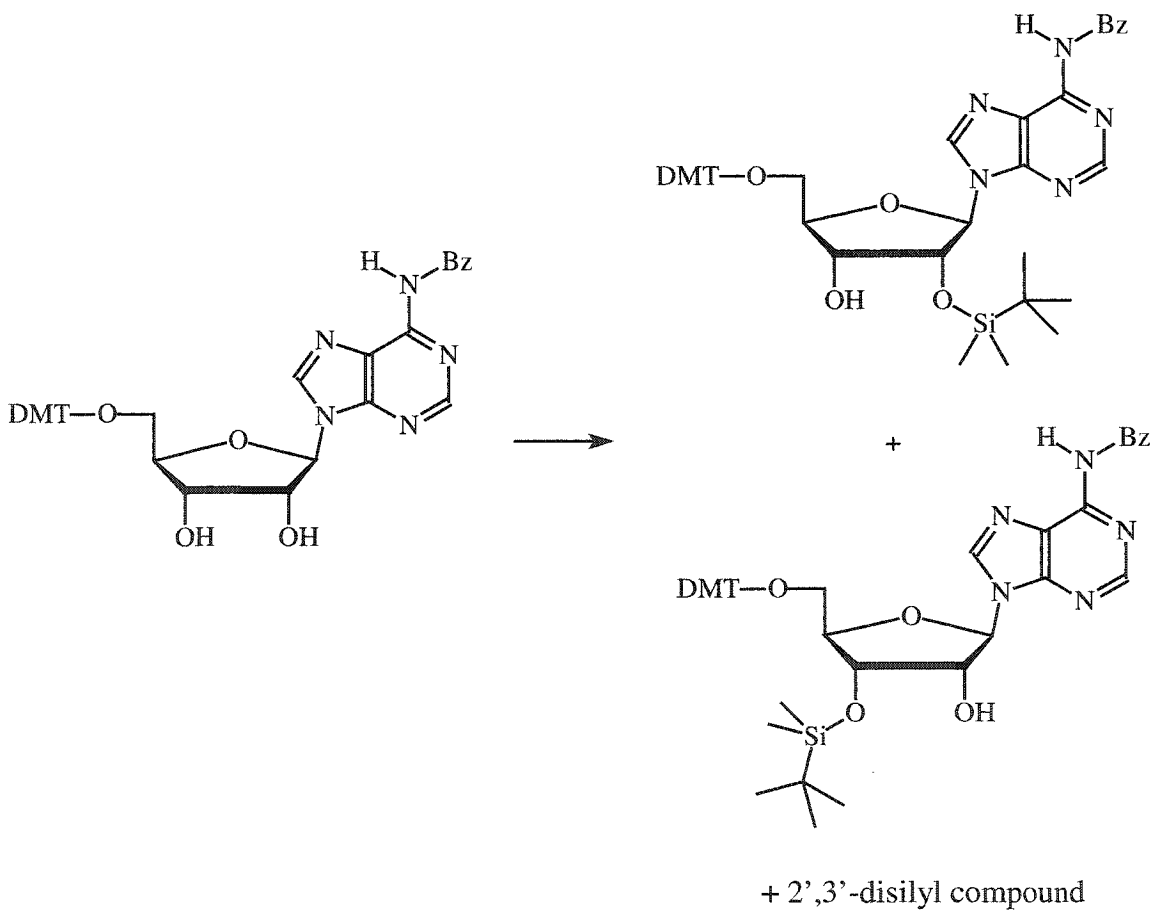

Figure 2.6: Products from the silylation reaction of ribonucleosides.

We perceived that in the case of xylonucleosides this reaction would proceed with a high degree of regioselectivity due to steric hindrance of the C3'-OH group by the bulky (cis) MMT group. Also the trans configuration of the 2' and 3'-hydroxyls in the xylonucleosides implied a slower rate of silyl migration in a basic medium compared ribonucleosides. Consistent with this notion, no 2'/3'-silyl migration was observed when 3',5'-di-O-benzoyl-2'-*tert*-butyldimethylsilylxyloadenosine was debenzoylated in a solution of sodium methoxide (**Figure 2.7**).[157]

Indeed as predicted, the silylation of 5'-MMT protected xyloU$^{5\text{-Me}}$ was regioselective, resulting in the exclusive formation of the 2'-silylated isomer (**Figure 2.5**). Following purification, 5'-MMT-2'-TBDMS-5-methyl-xylouridine (**2.5**) was obtained as a white foam (88% yield). The identity of the desired 2'-silyl isomer was confirmed by ^{1}H-NMR correlated spectroscopy (COSY) (**Figure 2.8**). Specifically, the ^{1}H NMR COSY spectrum showed a cross peak between H3' and the 3'-hydroxyl proton which disappeared upon addition of D_2O. Our synthetic strategy now called for acetylation of the remaining 3'-OH (98%) followed by removal of the 2'-TBDMS group (F^-/THF; 100% yield). The product, nucleoside (**2.7**), was now ready for the final 2'-phosphitylation reaction.

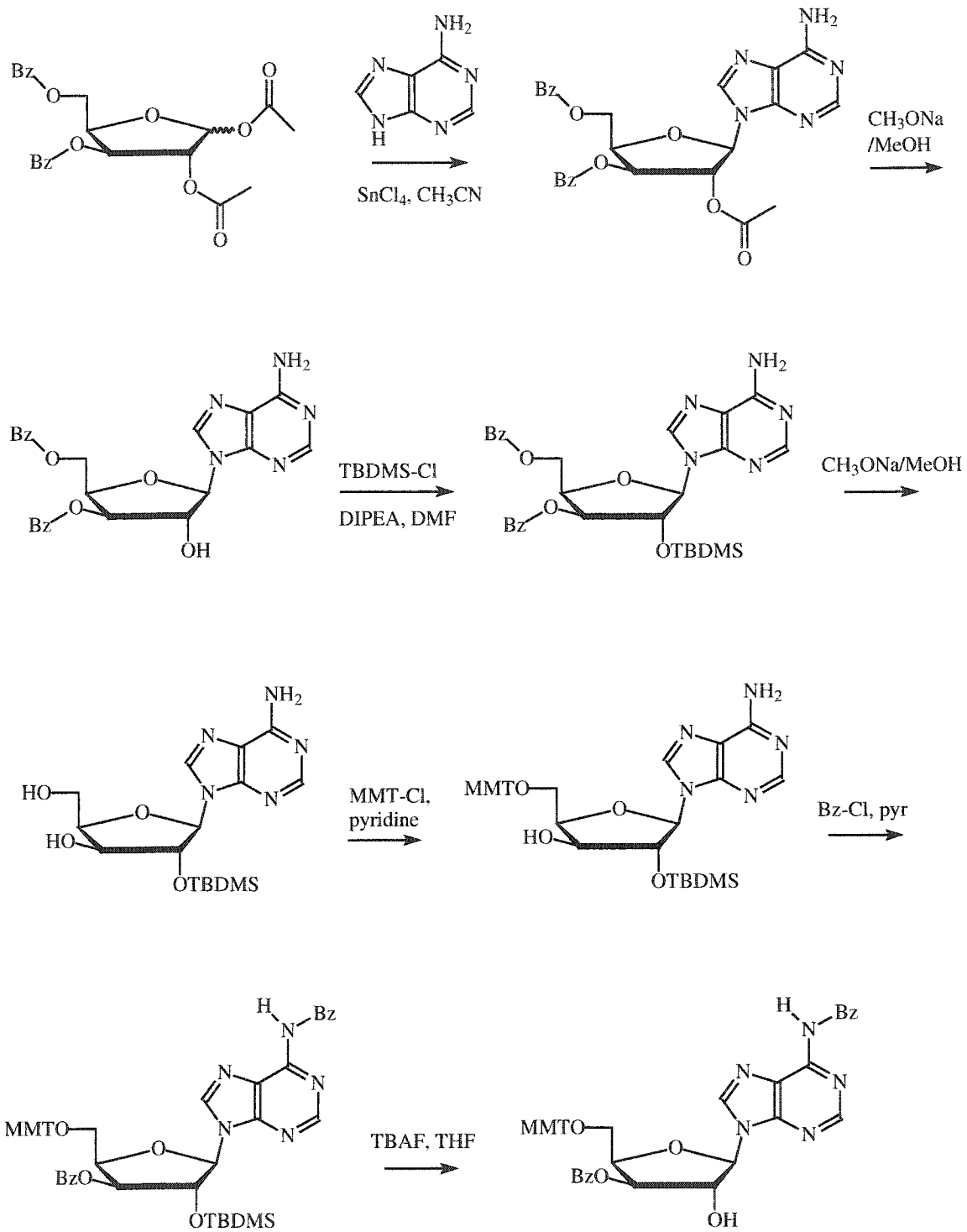

Figure 2.7: Synthesis of xyloA as reported by Imbach and coworkers.[157]

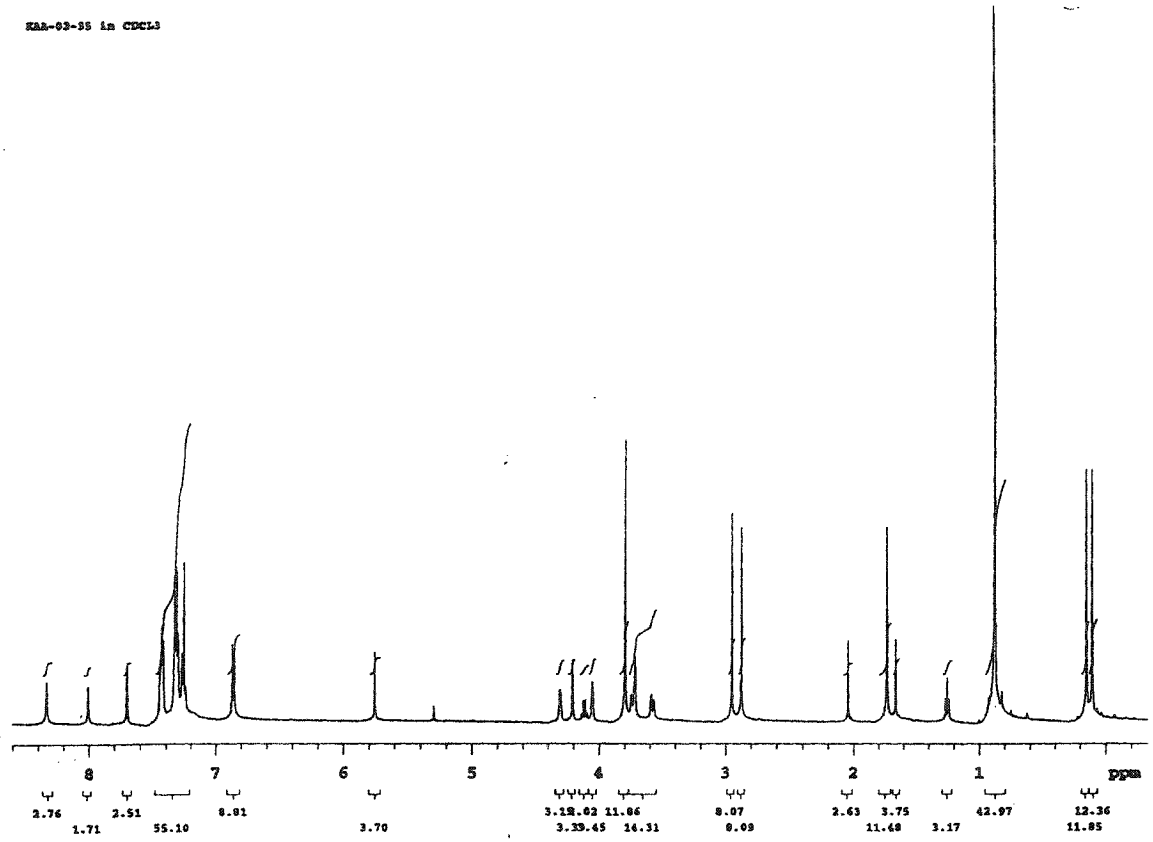

exp2 relayh

SAMPLE		DEC. & VT	
date	Mar 31 99	dn	H1
solvent	CDCl3	dof	0
file	/export/h-	dm	nnn
ome/unity500/damha-		dmm	c
/kazim/KAA_02_35_c-		dmf	200
	osy	dpwr	18
ACQUISITION		PROCESSING	
sfrq	499.843	sb	0.120
tn	H1	sbs	not used
at	0.239	wtfile	
np	2048	proc	ft
sw	4282.7	fn	2048
fb	2400	math	f
bs	32		
ss	2	werr	
tpwr	58	wexp	
pw	9.0	wbs	
p1	9.0	wnt	
d1	1.000	2D PROCESSING	
phase	0	sb1	0.060
tof	-393.7	sbs1	not used
nt	4	wtfile1	
ct	4	proc1	ft
alock	n	fn1	2048
gain	32	DISPLAY	
FLAGS		sp	1726.3
il	n	wp	1235.0
in	n	vs	500
dp	y	sc	10
hs	nn	wc	115
2D ACQUISITION		hzcm	10.74
sw1	4282.7	is	5239.71
ni	512	rf1	3659.2
2D DISPLAY		rfp	3618.9
sp1	1730.5	th	7
wp1	1214.0	ins	1.000
sc2	0	ai cdc nv	
wc2	115		
rf11	3659.2		
rfp1	3618.9		

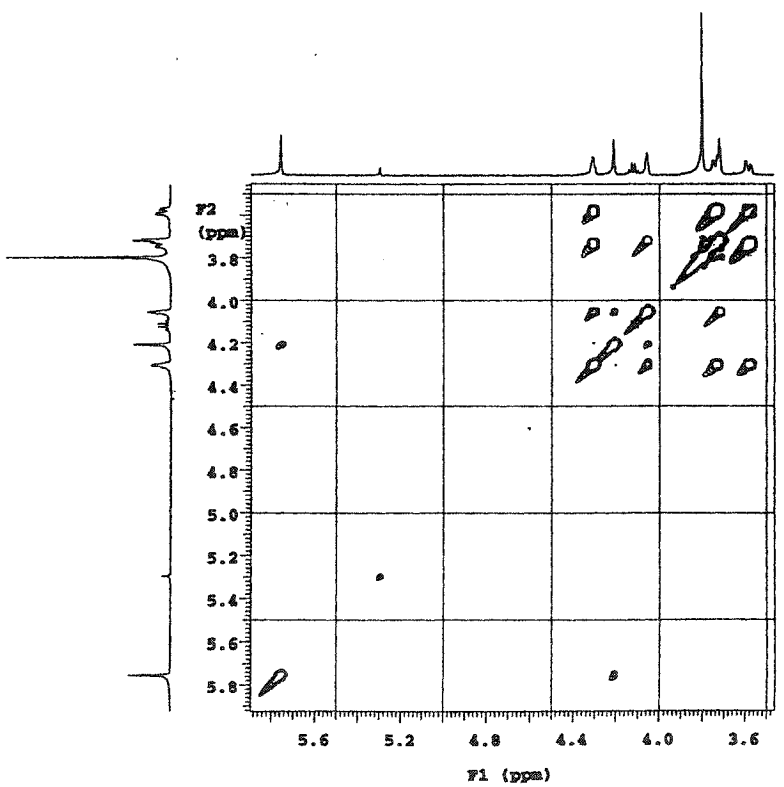

Figure 2.8: (A) The ^{1}H and (B) ^{1}H –COSY-NMR spectra of 5'-O-MMT-2'-O-TBDMS-5-methyl-xylouridine **(2.5)**.

A potential concern was the migration of the 3'-acetyl to the 2'-position, a characteristic reaction observed in 2'/3'-O-mono acetylated ribonucleosides. For example, it has been reported by Johnston[192] that in ribonucleosides, acetyl migration favors the movement of the acetyl group from the 2' to the 5'-hydroxyl position (i.e., in a direction opposite to the glycosidic linkage), whereas in xylonucleosides the rate of migration is significantly reduced. Taking into account the preference for the acetyl to move away from the glycosidic linkage and a slower rate of acetyl migration (3' → 2'), we felt comfortable that the isolated xylonucleoside **2.7** would not isomerize. This was indeed the case as confirmed by ^{1}H-NMR, i.e., only a single species was present consistent with the structure of **2.7**, with its H2' proton coupled to H1' and H3' (**Figure 2.9**).

5'-MMT-3'-O-acetyl-5-methyl-xylouridine (**2.7**) underwent 2'-phosphitylation cleanly, yielding the monomer (**2.8**) required for oligonucleotide synthesis (83% yield). The ^{1}H-NMR and COSY spectra of **2.8** are shown in **Figure 2.10**. In order to assist in the analysis of the sugar protons, separation of the P-diastereomers was carried out by column chromatography. The ^{1}H-COSY-NMR spectra (**Figure 2.10 C**) shows a large splitting for the H-2' caused by the ^3J coupling between H-2' and phosphorus. The small coupling constants observed for $^3J_{H1'\text{-}H2'}$ and $^3J_{H2'\text{-}H3'}$ suggested a C3'-*endo* conformation for the sugar moiety. The ^{31}P NMR shows two signals consistent with the diastereoisomeric nature of the (R_p and S_p at phosphorus) phosphoramidites (**Figure 2.10D**).

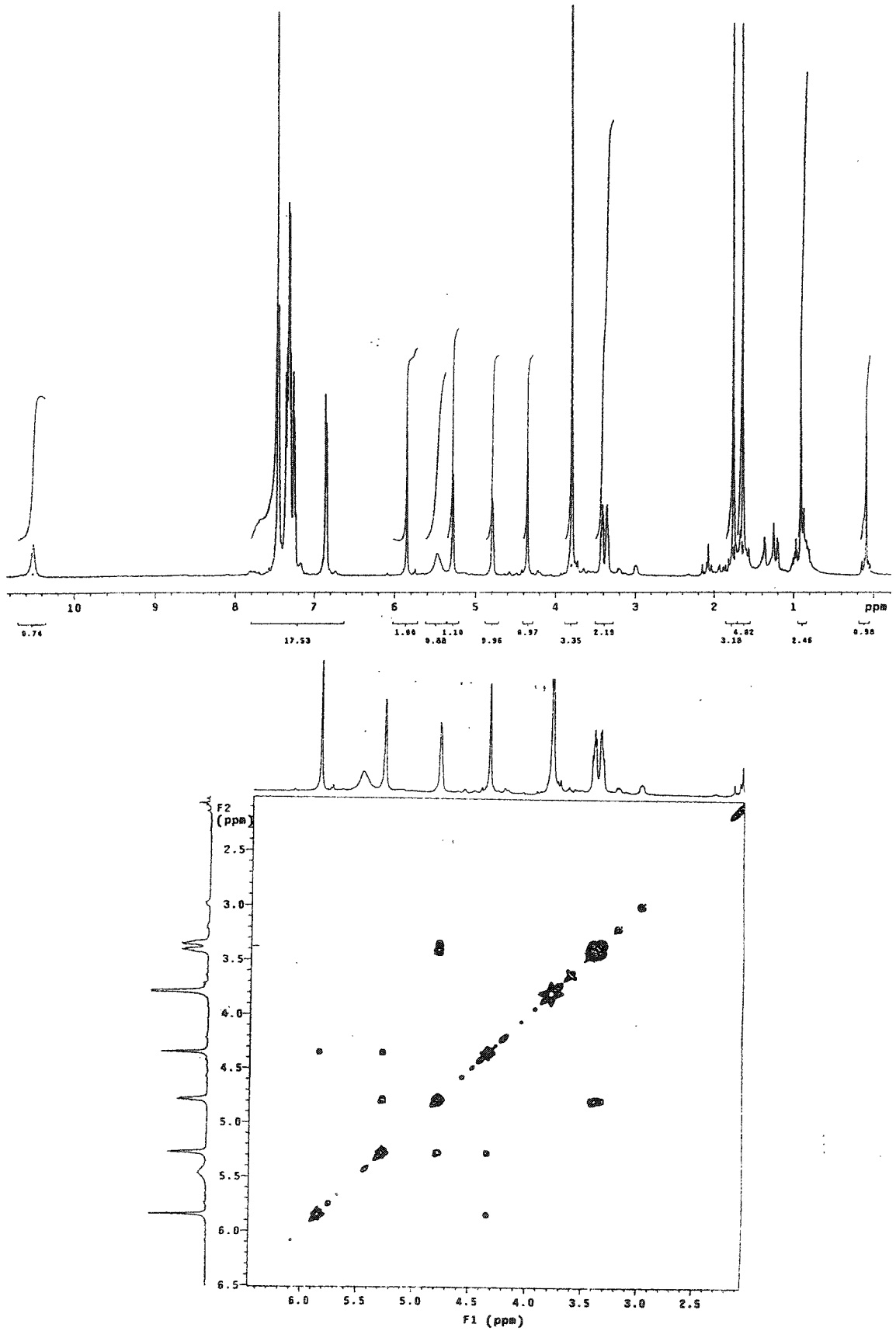

Figure 2.9: (A) The ^{1}H and (B) ^{1}H –COSY-NMR spectra of 5'-O-MMT-3'-O-Ac-5-methyl-xylouridine (2.6).

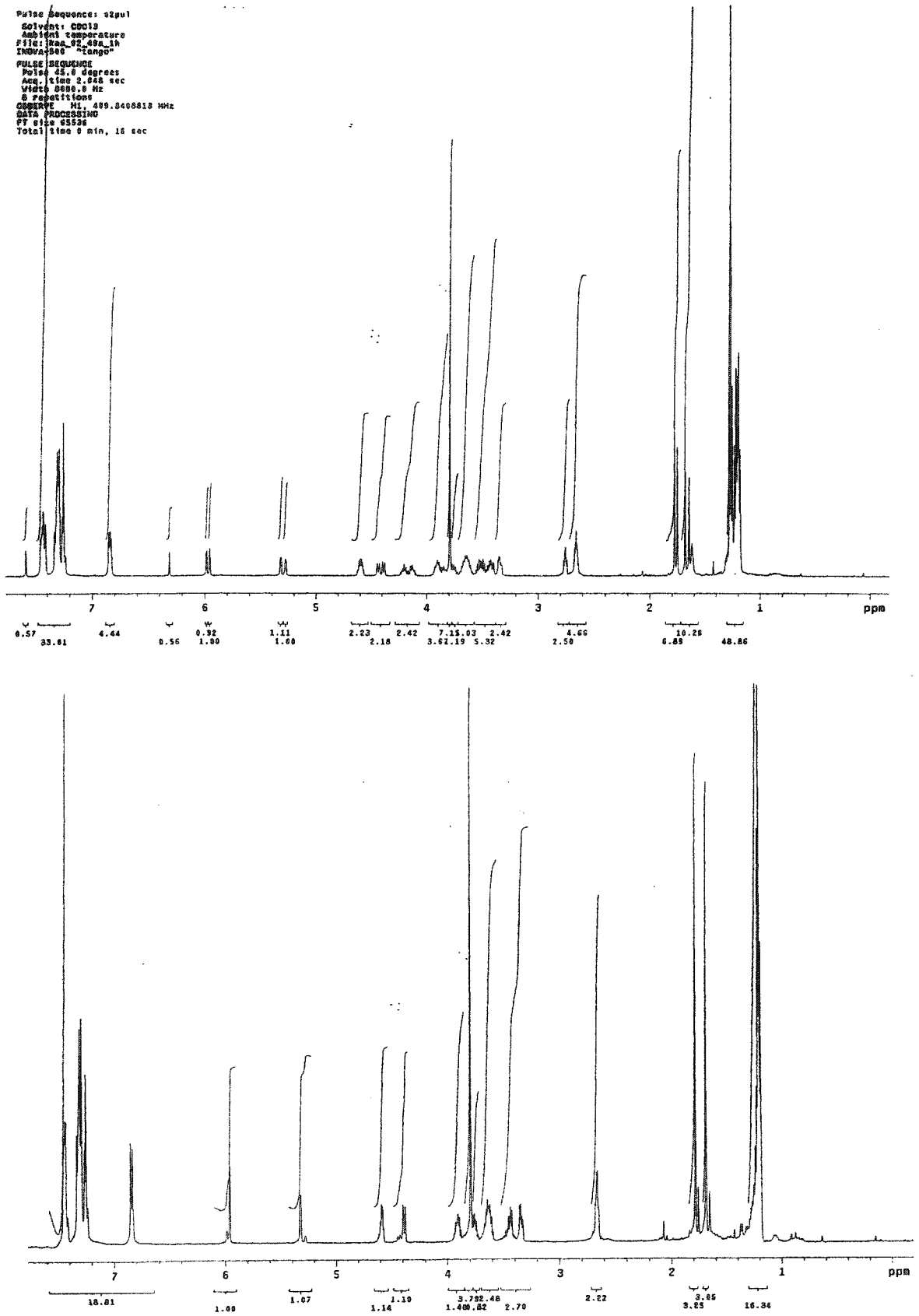

Figure 2.10: (A) The ^{1}H NMR spectra of both diastereosmers and **(B)** mostly single isomer of 5'-MMT-3'-O-Ac-5-methyl xylouridine-2'-O-phosphoramidite **(2.8)**.

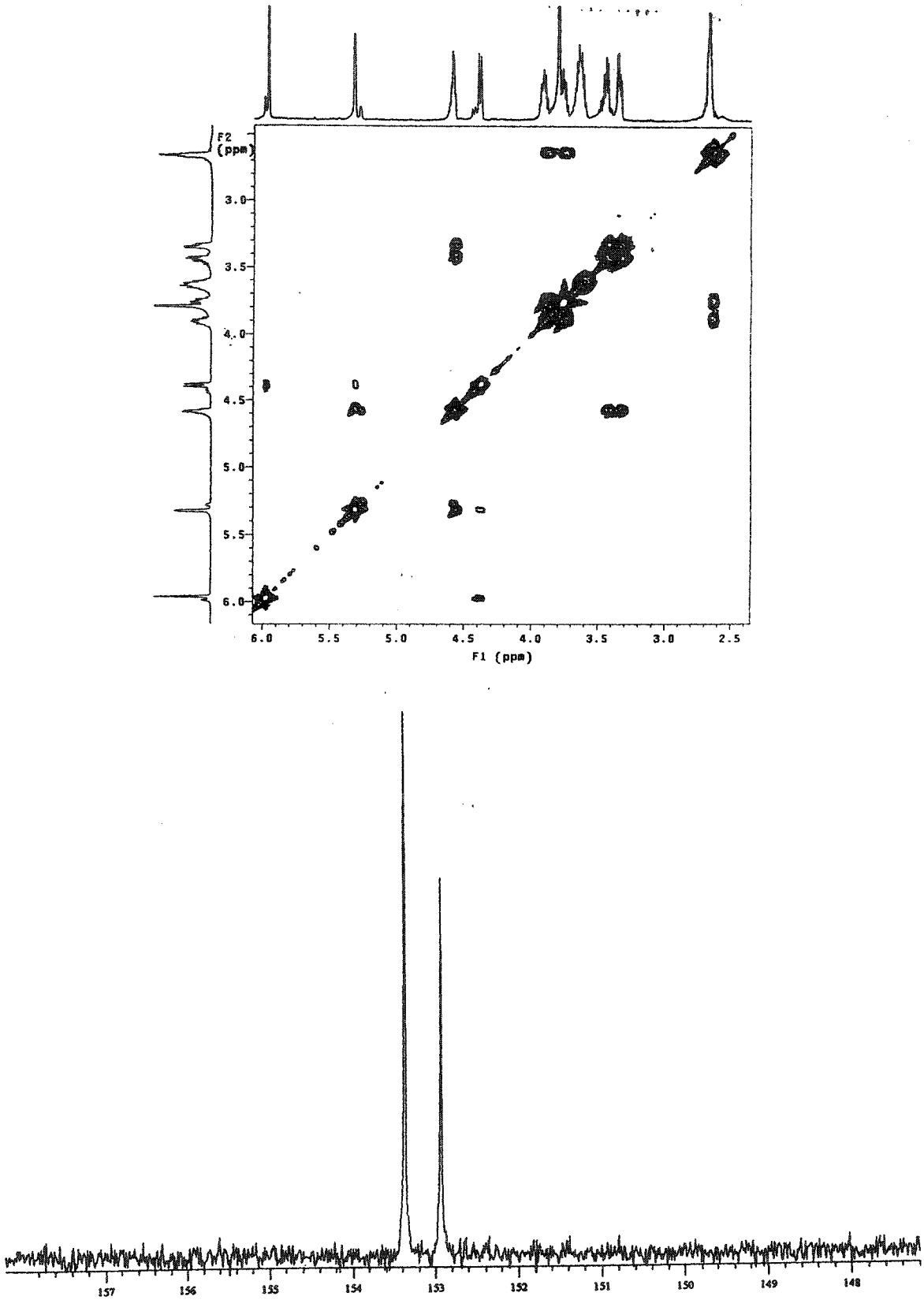

Figure 2.10: (C) The ^{1}H-COSY-NMR spectra and **(D)** ^{31}P NMR spectra of 5'-MMT-3'-O-Ac-5-methyl xylouridine-2'-O-phosphoramidite **(2.8)**.

An important and inherent advantage of the xylonucleoside-phosphoramidites over standard ribonucleoside-phosphoramidites is the absence of a silyl protecting group. This eliminates a further step (F^- treatment) after oligonucleotide synthesis and potential problems with chemical and/or enzymatic degradation that are characteristic of RNA synthesis.

A general observation with protected and unprotected xylonucleosides was a small ^3J coupling constant between H1' and H2', and H2' and H3', and a medium coupling constant between H3' and H4'. This is indicative of a C3'-*endo* type sugar conformation,[178] as it would make the dihedral angle between the H1' and H2', and H2' and H3' protons close to 90°, leading to a small $^3J_{1',2'}$ coupling constant (**Figure 2.4**).

Xylocytidine (**Figure 2.11**) and xyloadenosine (**Figure 2.12**) were prepared by direct coupling of sugar (**2.1**) to the unprotected cytosine or adenine, as described by Saneyoshi *et al.*[168, 169] and Imbach *et al.*[160] The reaction proceeded with exclusive formation of the N1-cytosine and N9-adenosine nucleosides due to the higher basicities and nucleophilicities of the heterocyclic nitrogens of these bases (N1 for cytidine and N9 for adenine). As observed previously during xylo$U^{5\text{-Me}}$ synthesis, the 1,2,3,5-tetra-O-benzoyl-D-xylofuranose sugar coupled with higher yields and lower abundance of side products as compared to the 1,2,3,5-tetra-O-acetylated-D-xylofuranose.

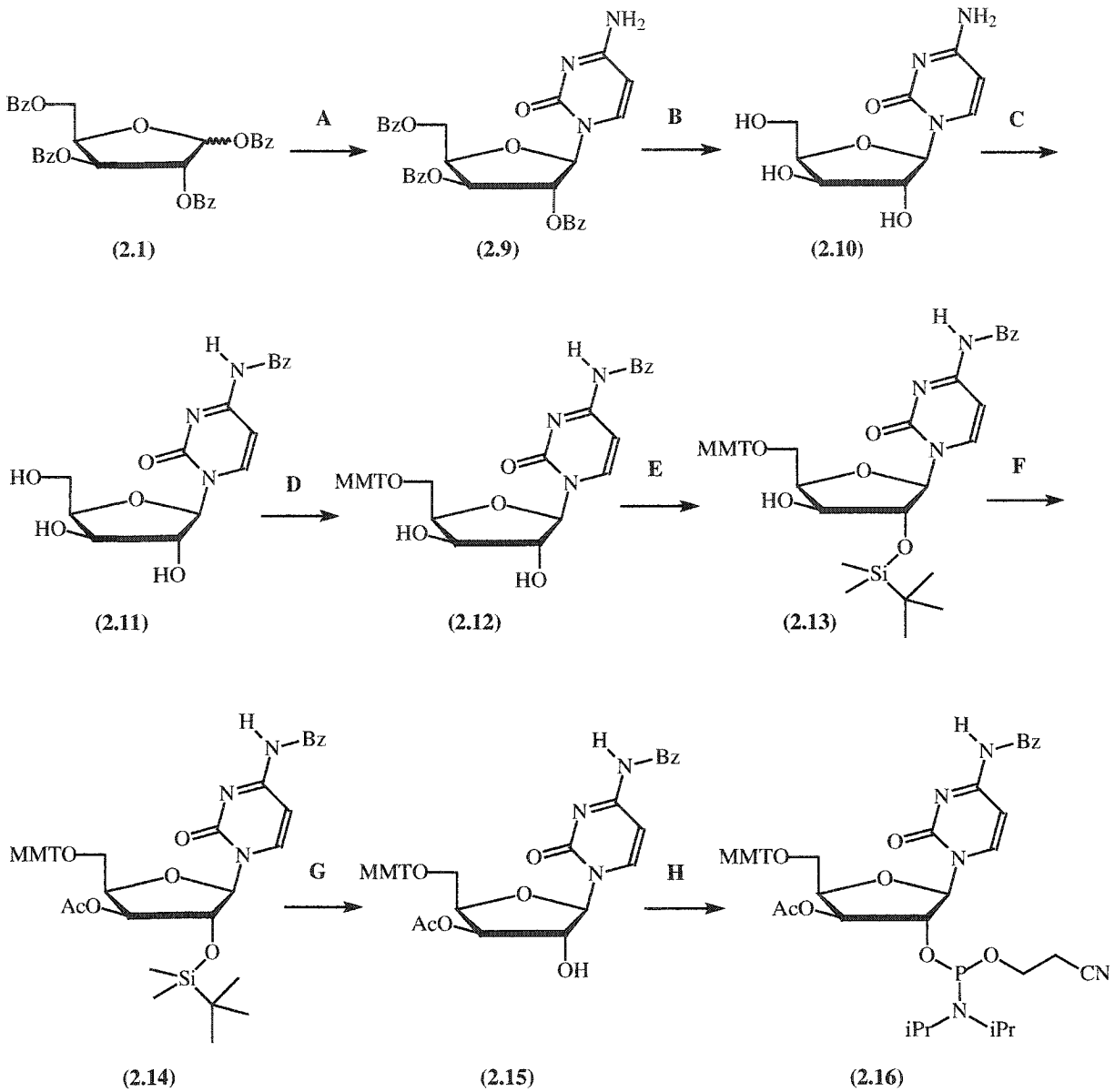

Figure 2.11: Scheme for the synthesis of xyloC amidite (**2.16**). **A.** Cytosine, $SnCl_4$, CH_3CN (79%); **B.** NH_4OH/MeOH, r.t., overnight (96%); **C.** (i) TMS-Cl, Bz-Cl, pyridine; (ii) NH_4OH (75%); **D.** MMT-Cl (1.2 equiv.), DMAP, pyridine, r.t., overnight (95%); **E.** TBDMS-Cl, imidazole, DMF, r.t., overnight (85%); **F.** Ac_2O, DMAP, DIPEA, THF, r.t. (98%); **G.** TBAF, THF, r.t. (Quant.); **H.** Cl-P(OCE)(N-iPr_2) (1.2 eq), DIPEA (2.4 eq) (79%).

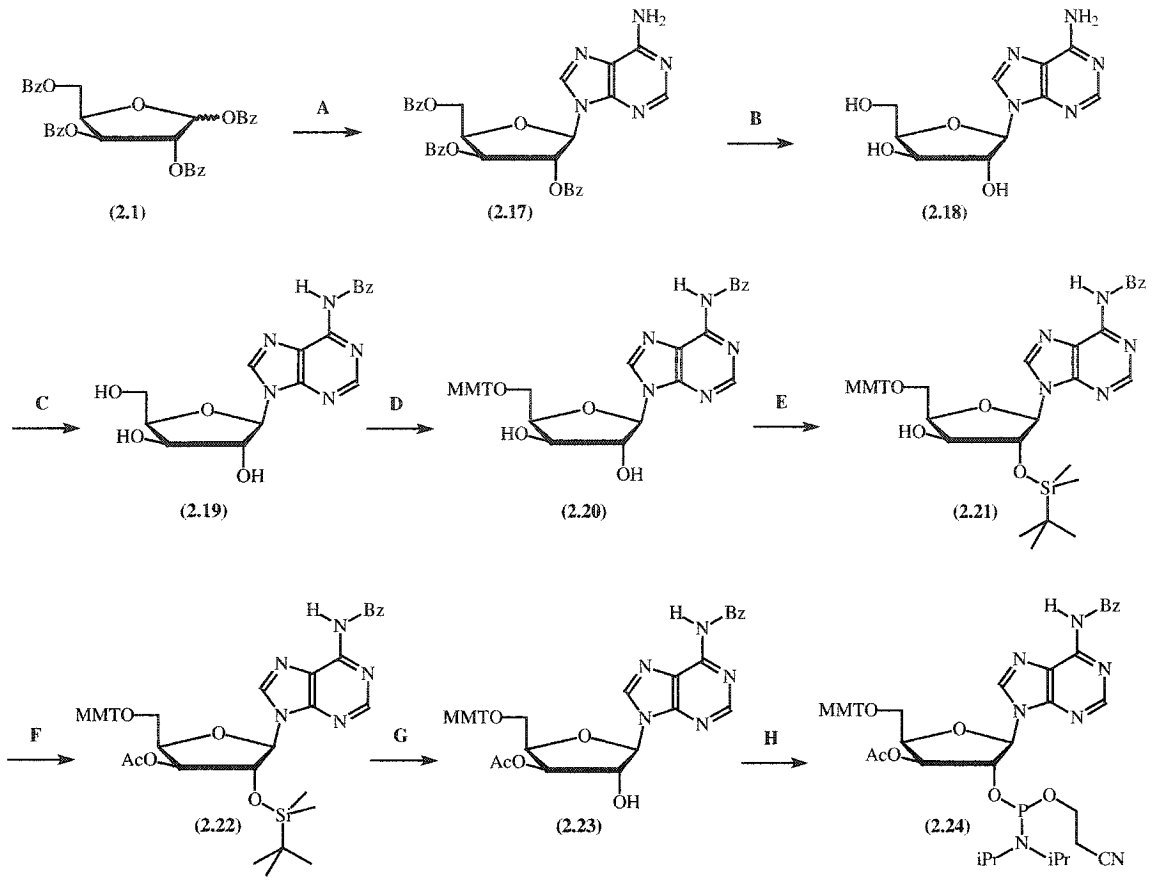

Figure 2.12: Scheme for the synthesis of XyloA phosphoramidite. **A.** Adenine, $SnCl_4$, CH_3CN (79%); **B.** NH_3/MeOH, r.t., overnight (96%); **C.** (i) TMS-Cl, Bz-Cl, pyridine; (ii) NH_4OH (75%); **D.** MMT-Cl (1.2 equiv.), DMAP, pyridine, r.t., overnight (95%); **E.** TBDMS-Cl, imidazole, DMF, r.t., overnight (85%); **F.** Ac_2O, DMAP, DIPEA, THF, r.t. (98%); **G.** TBAF, THF, r.t. (Quant.); **H.** Cl-P(OCE)(N-iPr_2) (1.2 eq), DIPEA (2.4 eq) (79%).

The xylocytidine-2'-O-phosphoramidite derivative (**2.16**) was synthesized from the nucleoside (**2.10**) by initial benzoylation of the exocyclic amine as described by Jones *et al.* (**Figure 2.11**).[201] The 5'-OH group was protected using monomethoxytrityl chloride to give the 5'-MMT-N-Bz-xylocytidine (**2.12**) as a white foam. The silylation proceeded selectively with only the 2'-silylated product (**2.13**) being observed, similar to the case of the 5-methyl-xylouridine. The structure of (**2.13**) was corroborated by ^1H NMR COSY experiments. As previously observed for (**2.7**), acetylation followed by

desilylation lead to the nucleoside (**2.15**), without any observed acetyl migration; this was supported by ^{1}H NMR COSY experiments. Phosphitylation of (**2.15**) afforded the phosphoramidite (**2.16**) in 79% yield (2 diastereomers by ^{31}P NMR).

The xyloadenosine phosphoramidite derivative was synthesized in a similar manner (**Figure 2.12**). The only difference was in the acetylation of N-Bz-5'-O-MMT-2'-O-TBDMS-xyloadenosine, which required only a small excess (1.05 equivalence) of the anhydrous acetic anhydride. When larger excesses of acetic anhydride were used (~1.3 to 1.5 equivalence), uncharacterized side products formed. These were probably N-Ac-N-Bz-protected-xyloadenosine by products, but no detailed analyses were carried out to prove this. The silylation of the purine nucleoside also went to completion, with selective formation of 5'-O-MMT-N-Bz-2'-O-TBDMS-xyloadenosine (^{1}H NMR COSY).

Xyloadenosine **2.23**, like its pyrimidine counterparts, did not undergo C3'-to-C2' acetyl migration under the conditions used to remove the 2'-silyl group (1M tetra-butylammonium fluoride in THF, r.t.) (^{1}H NMR COSY experiments). Reaction of 5'-MMT-N-Bz-3'-O-Ac-xyloadenosine with the chlorophosphoramidite proceeded cleanly to afford **2.24** as a mixture of two diastereomers (^{31}P NMR).

2.3 SYNTHESIS OF 2',5'-LINKED XYLOFURANOSE-NUCLEIC ACIDS (2',5'-XNA)

2.3.1 Background

As previously stated, studies on 2',5'-linked xylofuranose nucleic acids (2',5'-XNA) have been scarce. Most studies have focused on 2',5'-linked tri and tetranucleotide derivatives synthesized by solution-phase phosphotriester methods. The synthesis of 2',5'-XNA of mixed base composition has not been reported. In addition, there are no known studies of modified DNA or RNA strands incorporating a few 2',5'-linked xylonucleotide units, so the effect of such modifications on duplex stability is unknown. In this section we describe the solid-phase phosphoramidite synthesis of 2',5'-XNA and assess, for the first time, their ability to hybridize to complementary RNA, DNA and 2',5'-linked RNA.

2.3.2 Solid Phase Synthesis and Purification of 2',5'-Linked Xylofuranose-Nucleic Acids (2',5'-XNA)

Long chain alkyl amine-controlled pore glass (LCAA-CPG) was derivatized with protected 5-methyl-xyloU (xyloU$^{5\text{-Me}}$) **(2.4)**, xyloC^{Bz} **(2.12)** and xyloA^{Bz} **(2.20)** nucleosides according to the procedures of both Damha[193] and / or Pon.[194] The more recent procedure for derivatization, as described by Pon, leads to a higher nucleoside loading.[194] Typical loadings varied from 15-80μmol/g, with the general trend of pyrimidine loadings being slightly higher (71-80μmol/g) than those of the purine nucleosides (62-73μmol/g).

A variety of oligoxylonucleotides were synthesized. The standard solid phase RNA synthesis cycle was used for the synthesis of oligoxylonucleotides with minor modifications. An extended coupling time of 900 seconds for amidite coupling was used, along with a longer acid treatment in order to remove the more stable 5'-monomethoxytrityl protecting group (5'-dimethoxytrityl is more commonly used for RNA synthesis). The specific oligoxylonucleotide sequences prepared are listed in **Table 2.1**.

Table 2.1: List of 2',5'-XNA oligonucleotide sequences synthesized

Sequence	Designation	ODs Crude	ODs Pure[a]
5'- TTT TTT TTT TTT TTT TTT -3'	**2.25**	62	3.2
5'- AAA AAA AAA AAA AAA AAA -3'	**2.26**	70	5.6
5'- TTA TAT TTT TTC TTT CCC –3'	**2.27**	126	24.5

[a] Method of purification: polyacrylamide gel electrophoresis followed by desalting by gel filtration (Sephadex G-25, see Experimental Section 7.3.3).

During the initial course of the study, we encountered a much lower coupling efficiency for the xyloU$^{5\text{-Me}}$ amidite as compared to standard ribo-3' and 2'-amidites. In fact, this was a general trend observed for all xylo-amidite derivatives. When using tetrazole as the coupling agent (pK_a 4.9), the average coupling efficiency was typically 90% and ranged from 88 to 104%. Thus, the coupling efficiency was significantly lower than required to achieve a reasonable yield of oligomers, even if extended coupling times were used; in fact, in most cases, the desired oligonucleotide could not be isolated. By switching to a more acidic coupling agent, namely 5-ethylthio-tetrazole (pK_a 3.9), in

conjunction with a longer coupling time of 900 seconds, the problem was essentially eliminated and an adequate amount of oligonucleotide could be obtained for further studies.

The use of 5-ethylthio-tetrazole as coupling reagent can lead to the formation of oligonucleotides having higher than expected molecular weights ("n+1", "n+2" oligomers or "longmers").[202] This has been ascribed to the higher acidity of the thiotetrazole reagent, causing removal of the 5'-DMT protecting group during assembly of the oligonucleotide chain. Since the xylo-amidites contained the less labile 5'-monomethoxytrityl (MMT) protecting group, no observable presence of longmers was detected and the use of 5-ethylthio-tetrazole as an activating agent was deemed acceptable.

The lower coupling efficiency of the xylo-2'-O-phosphoramidite derivatives was somewhat unexpected. Given the trans configuration of the 3'-OAc group, we expected an improvement over the couplings of the bulkier ribo-3'-TBDMS-2'-amidite derivatives. Since this was not the case, we ascribe the lower coupling efficiency of xylo-phosphoramidites to the inductive withdrawal of electron density by O4' and the base away from the 2'-phosphoramidite moiety; this would require a more acidic activating agent to induce protonation of the N,N-diisopropylamine moiety at the 2'-phosphorus. Thus analogous to the 2'-O-ribophosphoramidites, the 2'-O-xylophosphoramidites require a more acidic activating agent.[96]

Initially, octadecanucleotides of 5-methyl-xylouridine ($xU^{5\text{-}Me}_{18}$) and xyloadenosine (xA_{18}) were synthesized and their physical properties evaluated. In addition, sequence **2.27** (referred to as the "CAT" sequence) was synthesized to evaluate

the properties of oligoxylonucleotides of mixed base composition. Deprotection of these oligoxylonucleotides involved treatment of the solid-support with conc. aqueous ammonia/ethanol according to a standard procedure.[190] Though not requiring the fluoride (1M TBAF in THF) step performed during RNA and 2',5'-RNA synthesis, recovery of these oligoxylonucleotides was moderate at best.

The purification and characterization of oligonucleotides were carried out using polyacrylamide gel electrophoresis (PAGE) or HPLC, and Matrix-Assisted Laser Desorption/Ionization-Time Of Flight Mass Spectrometry (MALDI-TOF MS). MALDI-TOF MS is a mild ionization technique commonly used for molecular weight determinations of large bio-molecules (polypeptides and nucleic acids).[96] **Figure 2.13 A** shows the electrophoretic mobilities of 2',5'-$xCAT_{18}$ and the corresponding RNA, DNA and 2',5'-RNA oligonucleotide sequences ($rCAT_{18}$, $dCAT_{18}$ and 2',5'-$xFCAT_{18}$, respectively). The gel shows that 2',5'-$xCAT_{18}$ migrates as a single species very closely to the corresponding native oligonucleotides. The observed molecular weights for oligomers **2.25-2.27** were in complete agreement with calculated values (**Table 2.2**), and a representative MALDI-TOF MS spectrum of **2.27** is shown in **Figure 2.13 B**.

Table 2.2: Observed and calculated MALDI-TOF mass spectra of 2',5'-XNA.

Sequence	Designation	MW (calc.)	MW (exp.)
5'- TTT TTT TTT TTT TTT TTT -3'	**2.25**	5701	5704
5'- AAA AAA AAA AAA AAA AAA -3'	**2.26**	5863	5863
5'- TTA TAT TTT TTC TTT CCC –3'	**2.27**	5659	5659

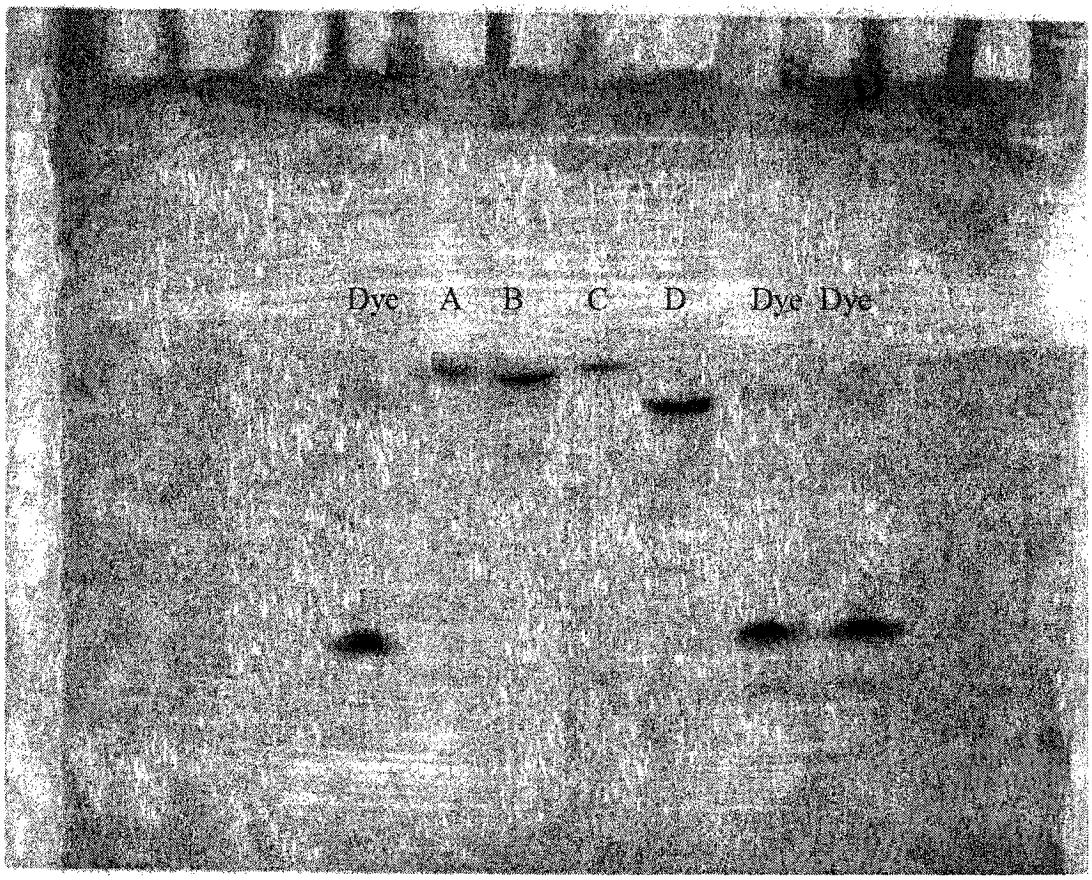

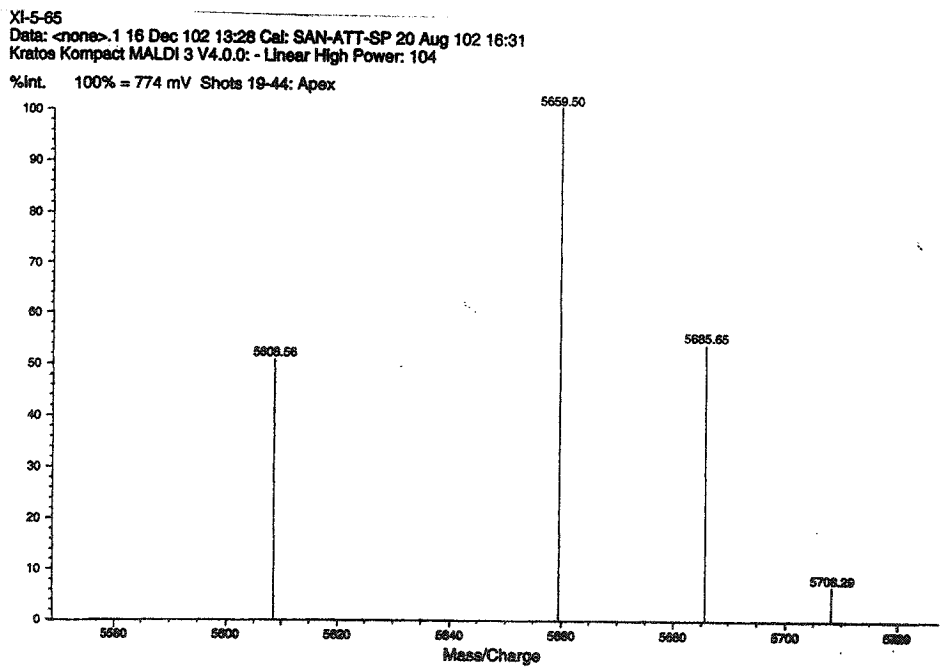

Figure 2.13: **(A)** Polyacrylamide Gel Electrophoresis (PAGE) of 18-unit long oligonucleotide using 24% polyacrylamide, 7M Urea in TBE buffer. Sequencec: 5'-TTA TAT TTT TTC TTT CCC-2' or 3'. In RNA T is replaced by U. **(B)** MALDI-TOF mass spectra 2',5'-XNA (5'-TTA TAT TTT TTC TTT CCC-2').
Lanes A: 2',5'-FXNA; B: RNA; C: 2',5'-XNA; D: DNA.

2.4 STUDIES ON DUPLEX FORMATION BY 2',5'-LINKED XYLOFURANOSE-NUCLEIC ACIDS (2',5'-XNA)

2.4.1 Background

As indicated above, NMR studies have shown that the sugars of 2',5'-linked tri and tetraxylonucleotides exist predominantly in a C3'-*endo* conformation, with the bases adopting the anti-conformation about the glycosidic bond. The sugar conformation of free xylonucleosides also favours the C3'-*endo* conformation, and this is likely the result of two gauche effects along the O3'-C3'-C4'-O4' and O2'-C2'-C1'-O4' frameworks.

In general, oligonucleotide analogs possessing a C3'-*endo* conformation ("RNA-like analogs) have a higher binding affinity towards complementary RNA relative to oligonucleotides that favour the C2'-*endo* conformation ("DNA-like analogs"). From this perspective, 2',5'-XNA oligos (C3'-*endo*) are expected to show enhanced RNA binding properties relative to oligodeoxynucleotides (ssDNA). However, according to a recent molecular modeling study by Yathindra and co-workers, the C3'-*endo* conformation of 2',5'-linked oligonucleotides (2',5'-RNA) is equivalent to the C2'-*endo* conformation of 3',5'-linked oligonucleotides and thus 2',5'-XNA would represent a "DNA-like" analog (**Chapter 1.4**). Therefore, understanding the binding and structural characteristics of oligoxylonucleotides would give further insight into the structure of 2',5'-linked oligonucleotides and possibly help develop novel and more potent antisense oligonucleotide analogs.

2.4.2 Duplex formation by homopolymeric 2',5'-XNA

To understand the behavior of 2',5'-XNA homopolymers, sequences based on thymine (5-methyl uracil) and adenine were first synthesized. Their binding affinity towards complementary RNA, DNA and 2',5'-RNA was evaluated by recording their thermal denaturation profiles. The hybridization properties of 2',5'-XNA were also compared to those of RNA, DNA and 2',5'-RNA of similar sequences, which were used as control sequences.

The associative properties (i.e. binding) and structure of oligodeoxy and oligoribonucleotides are well understood through the use of X-ray crystallography, CD and NMR spectroscopy.[16] The structure of 2',5'-RNA, the regioisomer of RNA is less well understood. Of particular interest is the ability of 2',5'-RNA to bind selectively to complementary RNA but not ssDNA. The same is true for 2',5'-DNA,[90,92,95,100] so this 'binding selectivity' appears to be a general property of 2',5'-linked oligonucleotides. We wondered whether this rather remarkable selective pairing behavior could be affected via stereochemical inversion at the sugar C3' chiral center (ribose → xylose).

To address this issue, the T_m (binding affinity) of various oligopyrimidines towards complementary adenosine oligonucleotides were recorded and these are summarized in **Table 2.3**.

Melting profiles of these single stranded oligonucleotides on their own showed no change in hyperchromicity or significant transition in absorbance, indicating lack of self association or complex formation. However, all oligonucleotides exhibited "sharp" monophasic transitions when mixed with a stoichiometric amount of complement, indicating the formation of single cooperative complexes. The stability of

homopolymeric A:T (U) duplexes differ from those of mixed base sequence. In homopolymeric duplexes based on the A:T (U) base composition, the order of stability is dA:dT > rA:dT > rA:rU > dA: rU.[195-198] The same trend in T_m values is observed in this study at high salt concentration, as shown in **Table 2.3**. These results may seem surprising given that the DNA duplex is more stable than the RNA duplex. The duplex structure formed by the dA:dT duplex, known as B'-DNA,[1] is the reason for this 'unexpected' result. The B'-DNA structure is also known as "propeller DNA" and, as the more common B-DNA helix, has the typical 10 base pairs per helical turn. The difference lies in the base pairing and interior stacking of the duplex, where there exists a bifurcating (three center) two hydrogen bond towards the major groove that involves the N6-amino group of adenine and two O4 atoms of the adjacent thymidines. This also leads to an increase in base stacking (higher percent hyperchromicity as observed in **Table 2.3**) and results in the formation of a more stable duplex.

Table 2.3: Melting temperature of various oligothymidylates towards complementary adenosine-oligonucleotides[a]

Sequence	RNA (rA_{18})		DNA (dA_{18})	
	T_m (°C)	%H	T_m (°C)	%H
rU_{18}	50.0	13.3	44.2	22.6
dT_{18}	52.1	27.2	59.0	27.0
2',5'-rU_{18}	36.4	17.5	--[b]	
2',5'-$xU^{5\text{-Me}}{}_{18}$	--[b]		--[b]	

[a] The melting temperatures (T_m) were taken to be the point of half-dissociation of an oligonucleotide duplex and were obtained by taking the maxima of the first derivative plot of the melting profile (dA_{260} vs. dTemperature). Buffer: 1M NaCl, 100mM Na_2HPO_4, pH = 7.2. [b] No T_m observed above 5°C. %H = percent hyperchromicity.

Duplex stability is also affected by base sequence. In 3',5'-linked oligonucleotides, the presence of thymine (or 5-methyl uracil) has a more stabilizing effect on the duplex relative to uracil. Also known as the "methyl effect", the C5-methyl group improves base stacking due to greater polarizability and hydrophobicity created between adjacent base pairs.[199] However in duplexes comprising only of 2',5'-linked oligonucleotide strands, no such "methyl effect" has been observed. On the contrary, uracil seems to impart greater stability in pure 2',5'-linked duplexes relative to pure 3',5'-duplexes rich in thymine.[90] This effect may not be as significant to the present studies, since the 2',5'-linked strand is hybridized to a native (3',5') complementary strand.

As mentioned above, 2',5'-linked oligonucleotides (homo and mixed base sequence) are known to bind selectively to RNA over DNA.[96, 98-103] This property is also characteristic of 2',5'-XNA under the salt concentration used (**Table 2.3**). The structure of RNA:2',5'-RNA hybrid duplexes have been shown to be similar to the native RNA:DNA hybrid structure and their stabilities follow the order RNA:DNA> RNA:2',5'-RNA. This was confirmed by our studies which show that rA_{18}:dT_{18} and rA_{18}:rU_{18} are significantly more stable than rA_{18}:2',5'-rU_{18}. Contrary to what is found for 2',5'-rU_{18}, no association was observed between 2',5'-$xU^{5\text{-}Me}{}_{18}$ and complementary dA_{18} and rA_{18} (**Table 2.3**). From this result we conclude that inversion of configuration at C3'of ribose is detrimental to duplex formation. This could be explained in terms of steric factors involving the 3'-hydroxyl or, more likely, by an inappropriate structure of 2',5'-$xU^{5\text{-}Me}{}_{18}$ to form duplexes. Previous studies indicate that the sugars of 2',5'-xA_3 adopt a C3'-*endo* conformation,[179] likely the result of two gauche effects along the O3'-C3'-C4'-O4' and

O2'-C2'-C1'-O4' frameworks. Similarly, a C3'-*endo* conformation in 2',5'-$xU^{5\text{-}Me}_{18}$ would force the sugar-phosphate backbone to adopt an '*extended*' conformation of almost equivalent length to that found in the native DNA (*i.e.* C2'-*endo*) conformation.[77,94,104] Oligonucleotides that are pre-organized in an '*extended*' (or DNA-like) conformation bind weakly, if at all, to a '*compact*' RNA target. Such conformational incompatibility or spatial "mismatching" of two strands likely explains why 2',5'-XNA ('*extended*') binds poorly to an RNA strand ('*compact*'). By contrast, both 2',5'-RNA (C2'-*endo*) and RNA (C3'-*endo*) adopt '*compact*' sugar-phosphate backbones that are compatible for binding to '*compact*' RNA targets (*i.e.*, in this case, a compact/compact "match" can be realized).

To determine whether the properties of 2',5'-$xU^{5\text{-}Me}_{18}$ are representative of all 2',5'-xylose nucleic acids, the binding properties of an oligoadenylate homopolymer was next evaluated (**Table 2.4**).

Table 2.4: Melting temperature of various oligoadenylates towards complementary thymidine-oligonucleotides[a]

Sequence	RNA (rU_{18})		DNA (dT_{18})	
	T_m (°C)	%H	T_m (°C)	%H
rA_{18}	50.0	13.3	52.1	27.2
dA_{18}	44.2	22.6	59.0	27.0
2',5'-rA_{18}	47.8	17.1	9.5	9.1
2',5'-xA_{18}	58.0	10.2	27.5	7.2

[a] The melting temperatures (T_m) were taken to be the point of half-dissociation of an oligonucleotide duplex and were obtained by taking the maxima of the first derivative plot of the melting profile (dA_{260} vs. dTemperature). Buffer: 1M NaCl, 100mM Na_2HPO_4, pH = 7.2. %H = percent hyperchromicity.

The data shows that 2',5'-rA_{18}, unlike rA_{18}, show selective hybridization toward RNA over DNA, characteristic of all 2',5'-linked oligonucleotides. Under the conditions used, the duplex formed between 2',5'-rA_{18} and rU_{18} is slightly more stable than the corresponding dA_{18}:rU_{18} duplex, also in agreement with previous studies.[99, 100]

Remarkably, the 2',5'-xA_{18}:rU_{18} duplex, is more stable (T_m 58°C) than the 2',5'-rA_{18}:rU_{18} duplex (T_m 47.8°C) or even the rA_{18}:rU_{18} duplex (T_m 50.0°C) (**Table 2.4**). In fact, this is the first 2',5'-linked oligoadenylate sequence showing better binding affinity towards RNA compared to the native oligoriboadenylate. Of note, the selectivity in binding towards RNA over DNA is still maintained upon inversion of stereochemistry at the C3'-position. Relative to 2',5'-rA_{18}, there is slight decrease in selectivity for RNA over DNA (2.15 °C/bp for 2',5'-rA_{18} vs. 1.70 °C/bp for 2',5'-xA_{18}). These results underscore the importance of preparing oligomers of varied base compositions before reaching conclusions about the binding behavior of a particular nucleic acid modification.

The associative properties of 2',5'-linked oligonucleotides towards 2',5'-linked complementary sequences have been studied from an etiological perspective,[90,91,92,95] i.e., to help answer the question "why did nature choose a 3',5'-phosphodiester over a 2',5'-phosphodiester as the internucleotide linkage?" The greater stability of complexes formed by 3',5'-nucleic acids is an important factor generally attributed as to why nature chose the 3',5'-phosphodiester linkage. Xylooligonucleotides are interesting to study from this perspective as well, as their association with complementary 2',5'-linked oligonucleotides would give further insight into why nature chose 3',5' over 2',5'-linkage.

The associative properties of 2',5'-xyloA$_{18}$ and 2',5'-xyloU$_{18}$ towards complementary 2',5'-linked oligonucleotides are summarized in **Table 2.5**.

Table 2.5: Association of 2',5'-linked oligopyrimidines with complementary 2',5'-linked oligonucleotides.

Sequence	2',5'-RNA (2',5'-rA$_{18}$)		2',5'-XNA (2',5'-xA$_{18}$)	
	T_m (°C)	%H	T_m (°C)	%H
2',5'-rU$_{18}$	36.5	13.8	14.0	4.2
2',5'-x U$^{5\text{-Me}}{}_{18}$	--[b]		--[b]	

[a] The melting temperatures (T_m) were taken to be the point of half-dissociation of an oligonucleotide duplex and were obtained by taking the maxima of the first derivative plot of the melting profile (A_{260} vs. Temperature). Buffer: 1M NaCl, 100mM Na_2HPO_4, pH = 7.2. %H = percent hyperchromicity. [b] No T_m observed above 5°C. %H = percent hyperchromicity.

Based on the T_m data, the duplex 2',5'-xA$_{18}$:2',5'-rU$_{18}$ (14°C) is significantly less stable than the isomeric 2',5'-rA$_{18}$:2',5'-rU$_{18}$ (36.5°C) and rA$_{18}$:rU$_{18}$ (50°C) duplexes. No association between 2',5'-xA$_{18}$ and 2',5'-xU$^{5\text{-Me}}{}_{18}$ was observed. Based on recent studies this is perhaps not unexpected, as a change in linkage modification in both strands (3',5'→2',5') would result in a mandatory slide and displacement of the Watson-Crick base pairs.[77] This would cause weaker intra-strand base stacking between adjacent base pairs and result in a lower melting temperature. Another factor resulting from the 2',5'-linkage modification is a shift in the phosphate backbone, such that the major groove expands with concomitant compression of the minor groove.[104] In B-DNA the minor groove width is about 5.7 Å and modeling studies have shown that in a 2',5'-B-DNA the groove width decreases by as much as 4 Å. [104] Thus with 2',5'-XNA, which also likely possess an extended B-like structure, serious phosphate charge repulsions would occur.

This, coupled with slide and displacement of the base pairs may explain why the 2',5'-xA_{18}:2',5'-$xU^{5\text{-}Me}{}_{18}$ duplex was not observed.

The shift in the phosphate linkage from 3',5' to 2',5' is also the most probable cause for the inability of 2',5'-nucleic acids (2',5'-DNA, 2',5'-RNA, 2',5'-XNA) to bind favourably with target ssDNA. The movement of the phosphate linkage closer to the DNA strand would lead to greater phosphate-phosphate electrostatic repulsion. This, combined with the reluctance of DNA to adjust to the conformation of the 2',5'-sequence under these conditions, results in selective binding to RNA.

2.5 CIRCULAR DICHROISM (CD) SPECTRA OF 2',5'-LINKED XYLOFURANOSE-NUCLEIC ACIDS (2',5'-XNA)

To understand the effect of sugar structure on the conformation of 2',5'-XNA, circular dichroism spectroscopy was performed on the single and duplexed strands. As mentioned earlier, CD spectroscopy is a qualitative method commonly used in the study of nucleic acid structure and generates insight into the overall topological structure of a duplex. An advantage of CD spectroscopy over other techniques for structural determination, such as NMR and X-ray crystallography, is that only small amounts of sample are required (μmol vs. mmol).

The CD spectra of single stranded oligopyrimidines and oligopurines are shown in **Figure 2.14** and **Figure 2.15**, respectively. The CD spectra of rU_{18} and dT_{18} are similar to the respective reference spectra of the polynucleotides (poly U and poly T).[200]

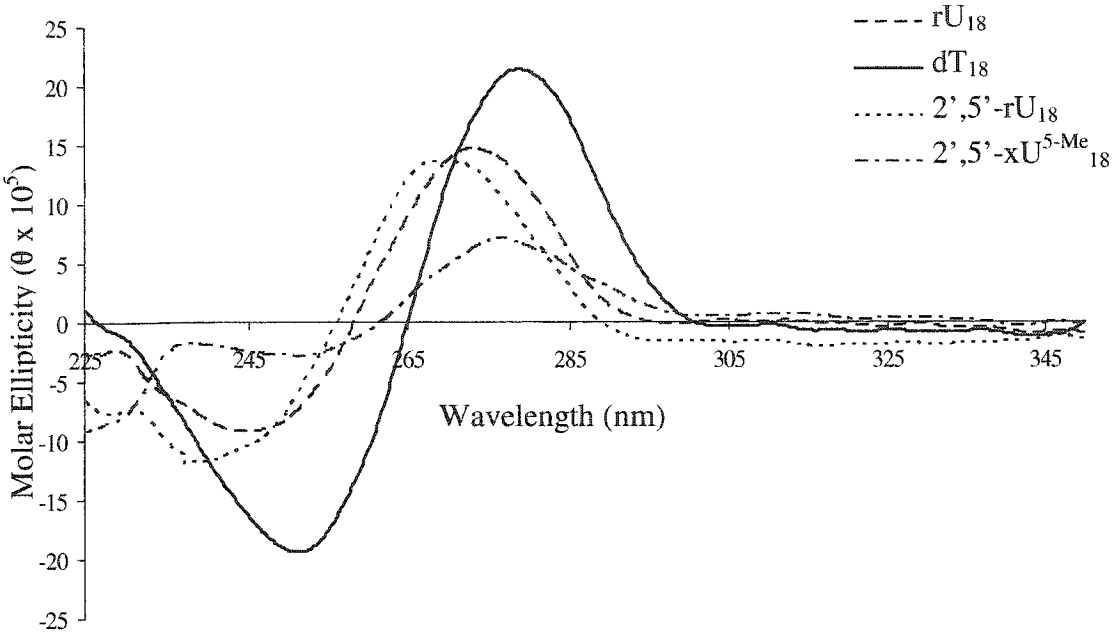

Figure 2.14: CD spectra of various single stranded pyrimidine oligonucleotides at 5°C (1M NaCl, 100mM Na_2HPO_4, pH = 7.2).

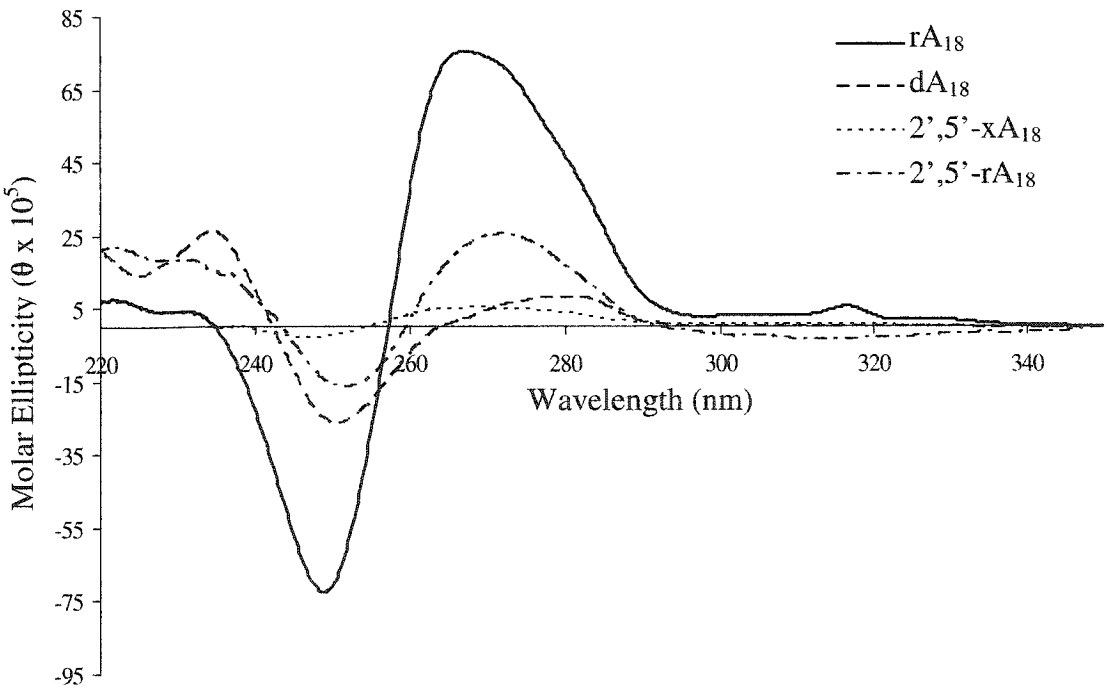

Figure 2.15: CD spectra of various single stranded purine oligonucleotides at 5°C (1M NaCl, 100mM Na_2HPO_4, pH = 7.2).

The overall CD profile of the oligo-pyrimidines is very similar, showing an initial positive Cotton effect followed by a crossover leading to a negative Cotton effect. For example, the CD spectrum of dT_{18} shows a positive λ_{max} around 278 nm, a crossover at 265 nm with a negative λ_{max} at 251 nm. Relative to it, the ribouridylates (both 3',5' and 2',5') show a hypsochromic shift for both the B_{2u} and B_{1u} transition and have a very similar CD profile. Upon inversion of stereochemistry at the C3' position as in 2',5'-XNA, the CD spectra becomes very similar to the CD signatures of DNA. The positive λ_{max} (at 276nm), crossover (261nm) and negative λ_{max} (252 nm) all shift from an RNA-like (shown by 2',5'-RNA) to a DNA-like CD spectra (2',5'-XNA). The intensity of molar ellipticities displayed by 2',5'-XNA is much lower than those of DNA, RNA and 2',5'-RNA, which may be indicative of weaker intra-strand base stacking.

Another structural difference between the pyrimidine sequences lies in the substitution at C5 of bases. Both the DNA and 2',5'-XNA sequences are composed of thymine (5-methyluracil) while both the 3',5' and 2',5' RNA oligomers are composed of uracil. A change in base structure (composition) may also have a slight effect on the overall CD spectra of these oligonucleotides.

Figure 2.15 shows the CD spectra of single-stranded oligoadenylates. The CD spectra of rA_{18} and dA_{18} are distinctly different. The large intensity of the CD bands seen for rA_{18} is due to the sugar-influenced orientation adopted by the bases.[200] The sugars in RNA are restricted in conformation due to the 2'-hydroxyl, resulting in greater intrastrand base stacking and formation of a more 'ordered' stacked structure, causing an increase in the CD signal at around 264nm. The spectrum of 2',5'-rA_{18} is similar to that

of rA_{18} but of lower intensity, while that of 2',5'-xA_{18} more closely resembles that of dA_{18}. Both 2',5'-xA_{18} and dA_{18} have rather weak positive and negative CD bands.

The CD spectra of the homopolymer duplexes are shown in **Figure 2.16** The rA_{18}:rU_{18} duplex adopts an A-form conformation with positive and negative maxima at 270 and 247 nm, respectively, and a crossover at 256 nm. The conformation of the rA_{18}:dT_{18} hybrid is intermediate between the A and B-forms, but resembling more the A-form. Thus in this case, the duplex structure is "dictated" by the more rigid RNA strand (rA_{18}) and is able to force the rather flexible DNA (dT_{18}) into the A-like form. The crossover and negative maxima of these duplexes are very similar, with the intensity difference in the negative maxima probably due to better base stacking with dT_{18}. The difference lies in the positive Cotton effect, with the rA_{18}:dT_{18} duplex showing a broad intense positive band between 260-290 nm.

Based on the CD profiles, the rA_{18}:2',5'-rU_{18} duplex is closer to rA_{18}:rU_{18} than to the rA_{18}:dT_{18} duplex, although the positive maxima and crossover in rA_{18}:rU_{18} are slightly blue shifted. The CD spectrum of a 1:1 mixture of rA_{18} and $xU^{5\text{-}Me}{}_{18}$ (5°C) showed characteristics very similar to the rA_{18}:dT_{18} duplex. This was unexpected, as the thermal denaturation studies suggested that the rA_{18}:$xU^{5\text{-}Me}{}_{18}$ duplex did not form in the 5-85°C temperature range. The CD spectrum of the rA_{18}:$xU^{5\text{-}Me}{}_{18}$ "duplex" shows a similar broad positive maximum (between 255-290 nm) as the rA_{18}:dT_{18} duplex, with weaker intensity attributable to decreased stacking of the bases.

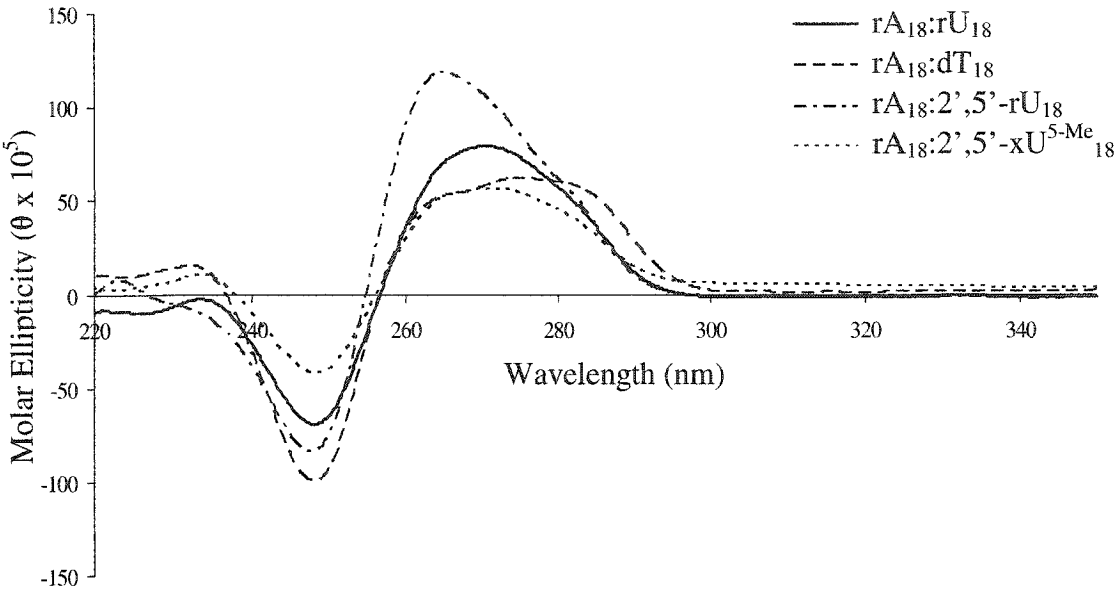

Figure 2.16 A: CD spectra of ribooligoadenylates hybridized to pyrimidine-oligonucleotides at 5°C (1M NaCl, 100mM Na_2HPO_4, pH = 7.2).

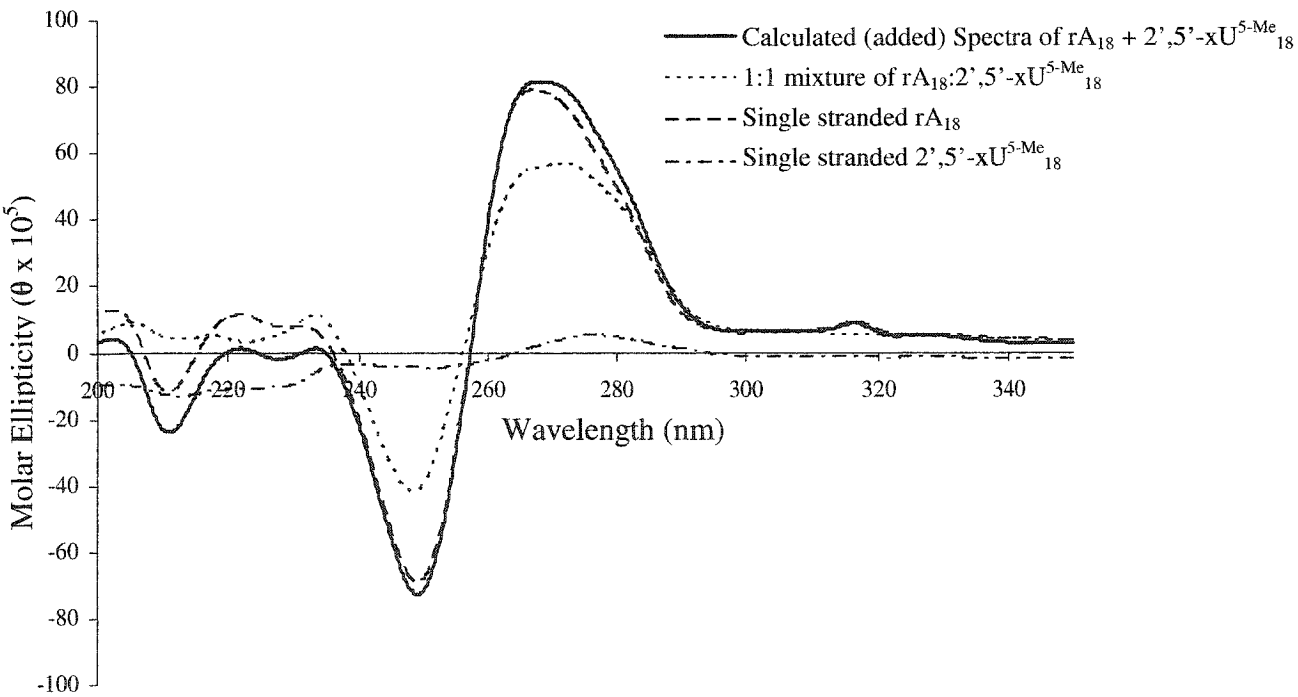

Figure 2.16 B: Comparison of the summed CD spectra of rA_{18} + $xU^{5\text{-}Me}_{18}$, duplex and single strand oligonucleotides at 5°C (1M NaCl, 100mM Na_2HPO_4, pH = 7.2).

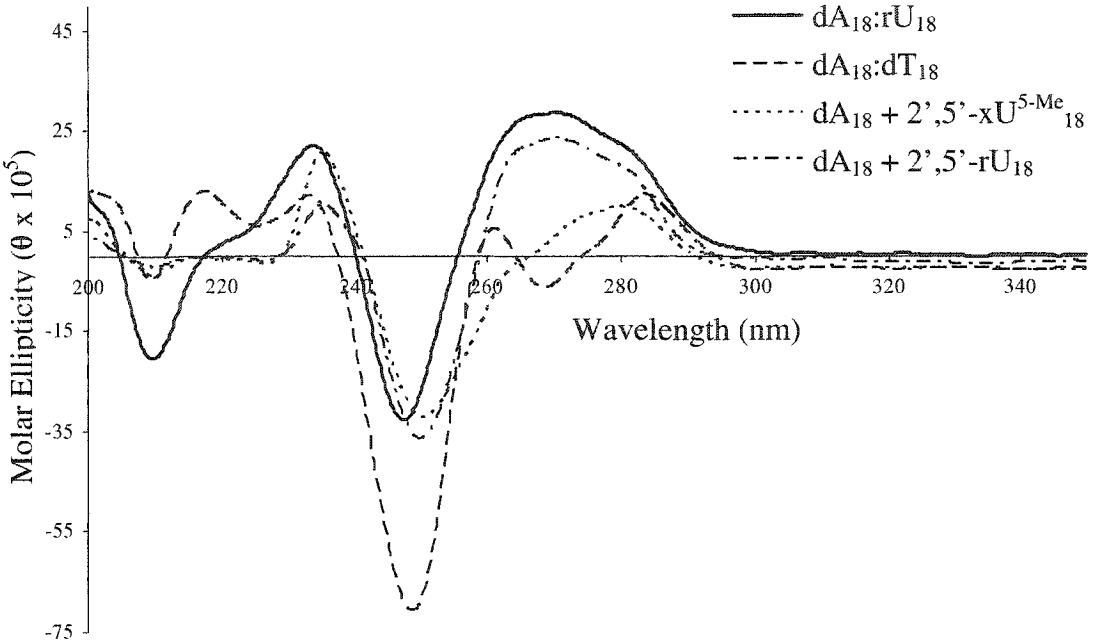

Figure 2.16 C: CD spectra of oligodeoxyadenylates hybridized to oligopyrimidine at 5°C (1M NaCl, 100mM Na_2HPO_4, pH = 7.2).

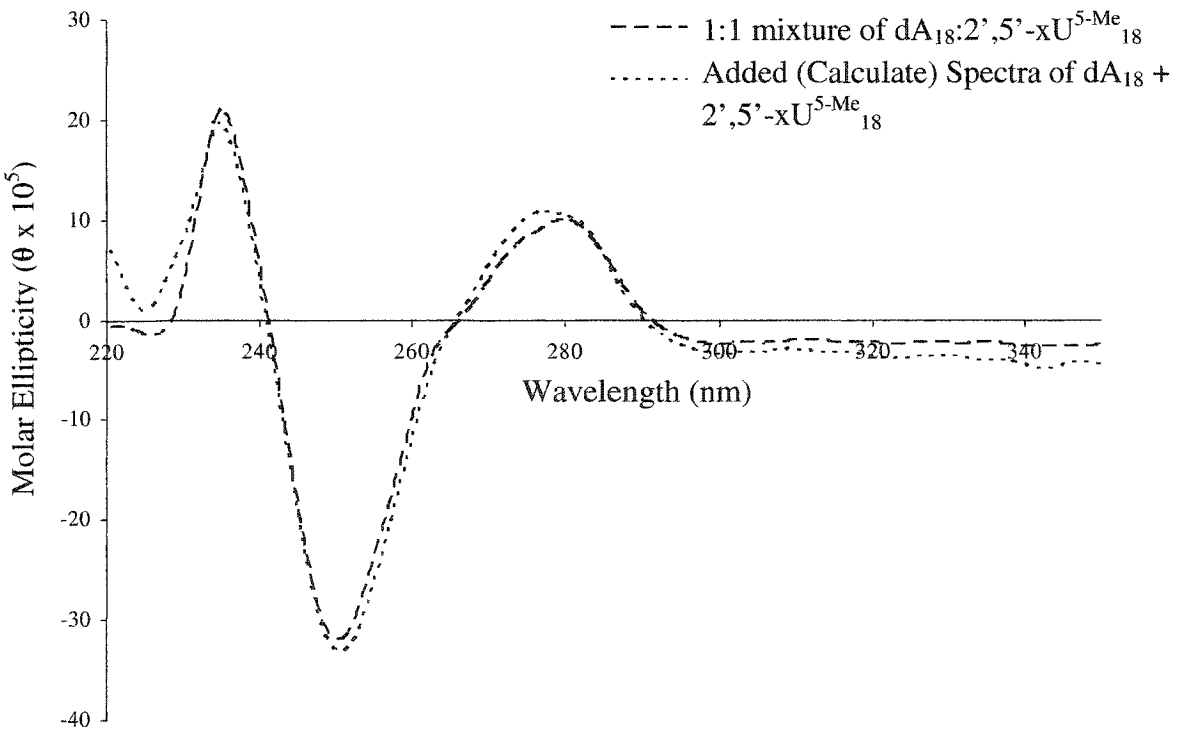

Figure 2.16 D: Comparison of the summed CD spectra of dA_{18} and $xU^{5\text{-}Me}{}_{18}$ with hybridized CD spectra of dA_{18}:$xU^{5\text{-}Me}{}_{18}$ at 5°C (1M NaCl, 100mM Na_2HPO_4, pH = 7.2).

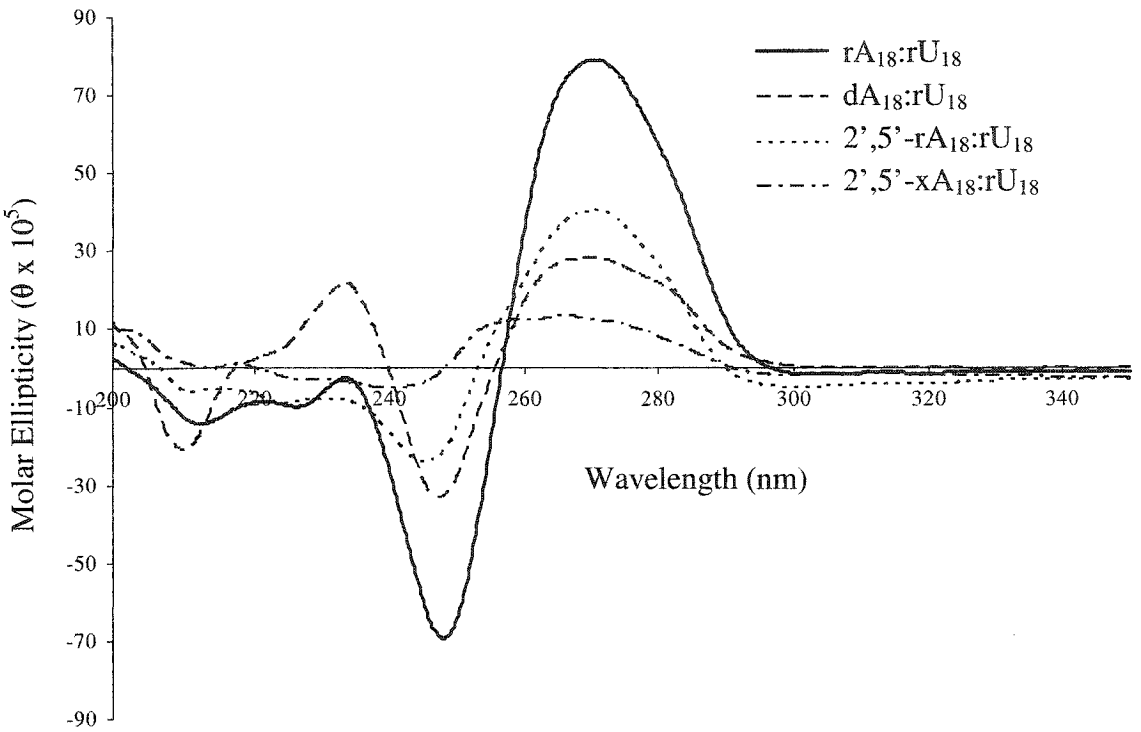

Figure 2.16 E: CD spectra of pyrimidine-oligonucleotides hybridized to purine-oligonucleotides at 5°C (1M NaCl, 100mM Na_2HPO_4, pH = 7.2).

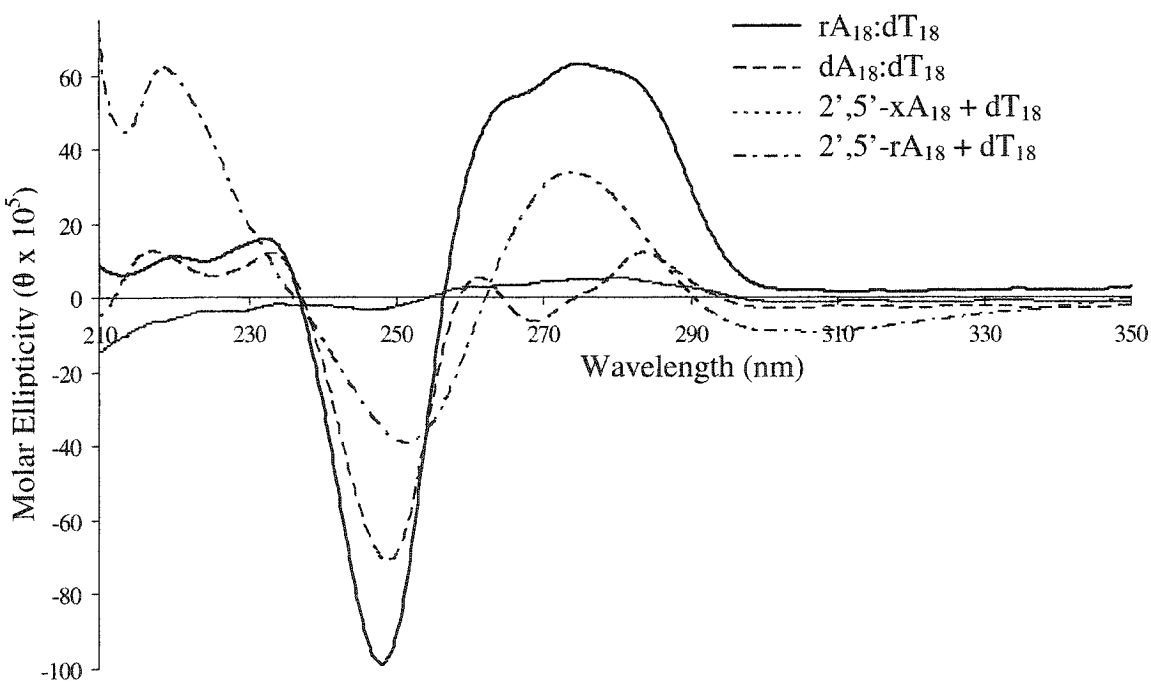

Figure 2.16 F: CD spectra of deoxyoligothymidylates hybridized to purine-oligonucleotides at 5°C (1M NaCl, 100mM Na_2HPO_4, pH = 7.2).

Based on these observations, it is possible that a weak duplex between rA_{18} and $xU^{5\text{-}Me}{}_{18}$ is formed (T_m ~ 5°C) and this, coupled with decreased stacking, could be responsible for the lack of a distinct sigmoidal curve in the T_m study. To test this hypothesis, the spectrum of the putative "duplex" (1:1, rA_{18} + $xU^{5\text{-}Me}{}_{18}$ mixture) was compared to the individual spectrum of rA_{18} and $xU^{5\text{-}Me}{}_{18}$ single strands, and to the calculated additive spectra. As shown in **Figure 2.16 B**, the summed spectrum is very similar to that of single stranded rA_{18}. This is not surprising given that oligoadenylates display much more intense bands relative to oligopyrimidines (attributed to the greater efficiency of purines to base-base stack). However, when the calculated spectrum is compared to that of the 1:1 rA_{18} + $xU^{5\text{-}Me}{}_{18}$ mixture, some differences are revealed **(Figure 2.16B)**, i.e., the latter exhibited a weaker and broader positive peak, and both the crossover point and the negative peak were blue-shifted relative those in the summed spectra. This is consistent with a weak association between the rA_{18} and 2',5'-$xU^{5\text{-}Me}{}_{18}$ strands.

The CD spectra of duplexes formed by dA_{18} oligonucleotide are shown in **Figure 2.16 C**. The dA_{18}:dT_{18} duplex belongs to the B'-family with characteristic peaks of low intensity around 260 and 285 nm and a strong negative band around 248 nm. The dA_{18}:rU_{18} duplex spectrum is intermediate between the A and B forms with a broad positive band between 255 and 290 nm and a negative peak around 245 nm. The spectrum also shows a positive and negative peak in the lower wavelength region, around 230 and 210 nm, respectively. The spectrum of dA_{18}:2',5'-rU_{18} has signatures similar to the dA_{18}:rU_{18} spectrum, being more A-like but with lower intensity. The crossover point and negative Cotton effect is slightly red shifted. No complex was observed by UV

melting between 2',5'-$xU^{5\text{-}Me}_{18}$ and dA_{18}. In order to test whether a weak association was taking place, as in the case of 2',5'-$xU^{5\text{-}Me}_{18}$ and rA_{18}, the CD spectrum of a mixture of dA_{18} and 2',5'-$xU^{5\text{-}Me}_{18}$ was measured. This exhibited a similarity to the dA_{18}:dT_{18} spectrum. However, comparison with the additive spectral effects of the single strands, dA_{18} and $xU^{5\text{-}Me}_{18}$ (**Figure 2.16 D**), shows that the CD spectrum of the $xU^{5\text{-}Me}_{18}$+rA_{18} mixture is the summed spectra of the single strands, and therefore we conclude that no duplex is formed under these conditions (5°C).

Next, the structural properties of duplexes formed by 2',5'-xA_{18} were studied. The CD spectra of duplexes formed by rU_{18} with various oligoadenylates are shown in **Figure 2.16 E**. As mentioned earlier, the rA_{18}:rU_{18} duplex adopts a helical conformation typical of the A-form, whereas that of dA_{18}:rU_{18} is intermediate between the A and B-form, but being more A-like. The 2',5'-rA_{18}: rU_{18} spectrum is also intermediate between the A and B-form and exhibits CD bands of larger magnitude than those observed for the dA_{18}:rU_{18} duplex. Its conformation is closer to the A-form than the B-form (or "A-like"). In comparison, the 2',5'-xA_{18}:rU_{18} spectrum shows very small positive and negative bands. There is a weak, broad positive Cotton effect from 245 to 290 nm, which is similar to that observed for the dA_{18}:rU_{18} duplex, which is in turn weaker and broader than those of the rA_{18}:rU_{18} duplex. However the structure of the 2',5'-xA_{18}:rU_{18} duplex is likely very different from the dA_{18}:rU_{18} structure, as indicated by their different CD spectra.

Figure 2.16 F shows the CD spectra of duplexes formed by dT_{18}. As stated previously, dA_{18}:dT_{18} and rA_{18}:dT_{18} adopt, respectively, the B' and A-like conformations. The CD spectra of 2',5'-rA_{18}:dT_{18} and rA_{18}:dT_{18} are alike, exhibiting similar positive and

negative Cotton effects. In contrast, the CD spectrum of 2',5'-xA_{18}:dT_{18} shows very small positive or negative Cotton effects. These features were also observed with the duplex formed with rU_{18} (2',5'-xA_{18}:rU_{18}), indicating that the conformation of these duplexes is dictated by the 2',5'-xA_{18} strand. This is supported by the strong similarity observed between the CD spectra of the duplexes (2',5'-xA_{18}:rU_{18} and 2',5'-xA_{18}:dT_{18}) and the single strand (2',5'-xA_{18}).

2.6 BINDING STUDIES ON DUPLEXES OF 2',5'-XNA OF MIXED BASE COMPOSITION WITH RNA AND DNA

In order to gain a better understanding of the binding properties of 2',5'-XNA towards RNA and DNA, a mixed base sequence of 2',5'-XNA, complementary to the HIV-1 genomic sequence, was synthesized.[203] **Table 2.6** shows the T_m values of the duplexes formed between 2',5'-XNA and its complementary RNA, DNA or 2',5'-RNA strand.

As expected for native oligonucleotides of mixed-base composition, the RNA:RNA duplex is more stable than the DNA:DNA duplex. The binding of 2',5'-RNA to complementary RNA and DNA oligonucleotides also follows the same trend, i.e. 2',5'-RNA:RNA > 2',5'-RNA:DNA.[77,94,104] Generally, the stability of RNA:DNA hybrids depends upon the purine content of the RNA strand, with purine-rich strands giving rise to the most stable hybrids. When the 2',5'-RNA strand is purine rich, a weak association with DNA is observed, and no duplex formation occurs between a DNA strand and a pyrimidine-rich 2',5'-RNA strand (**Table 2.6**). For 2',5'-XNA (**2.27**) a weaker duplex with DNA than with RNA is observed, thus exhibiting the 'RNA selectivity'

characteristic of 2',5'-linked oligonucleotides. A low hyperchromicity is indicative of weak base stacking interactions, in agreement with properties reported for 2',5'-linked oligoribonucleotides. Also no complexation was observed between 2',5'-RNA and 2',5'-XNA (**2.27**), consistent with our previous studies on homopolymers, where no duplex formation was detected between 2',5'-xyloT$_{18}$ (**2.25**) and 2',5'-rA$_{18}$.

Table 2.6: Thermal melting (T_m) data obtained upon binding of 2',5'-XNA (**2.27**) of mixed base composition with complementary RNA, DNA and 2',5'-RNA.[a]

Sequence[b]	RNA target {%H}[c]	DNA target {%H}[c]	2',5'-RNA target {%H}[c]
RNA	56.0 {20.8}	30.0 {18.1}	34.1 {15.5}
DNA	53.0 {18.2}	51.0 {22.1}	8.0 {11.6}
2',5'-RNA	36.0 {17.8}	<5.0	24.1 {14.6}
2',5'-XNA	24.1 {13.6}	<5.0	<5.0

[a] All duplexes were 2.3 x 10^{-6} M in concentration. All transitions were monophasic. Buffer: 140 mM KCl, 1 mM $MgCl_2$, 5mM Na_2HPO_4, pH = 7.2
[b] Sequence: 5'-TTA TAT TTT TTC TTT CCC-3' or 2'[d]
[c] Target: 5'-GGG AAA GAA AAA ATA TAA-3' or 2'
[d] For RNA and 2',5'-RNA, T is replaced by U

The low T_m value of 2',5'-XNA:RNA (**Table 2.6**) duplex is probably due to the "DNA-like" (extended) conformational behavior of 2',5'-XNA (as previously stated, DNA analogs bind to native RNA less avidly compared to RNA analogs). To test this hypothesis and to further understand the structure adopted by 2',5'-XNA, circular dichroism spectroscopy was carried out on 2',5'-XNA:DNA and 2',5'-XNA:RNA duplexes.

2.7 CD STUDIES ON 2',5'-XNA:RNA and 2',5'-XNA:RNA OF MIXED BASE COMPOSITION

The CD spectra of single strands are shown in **Figure 2.17** and that of duplexes formed with RNA are shown in **Figure 2.18**.

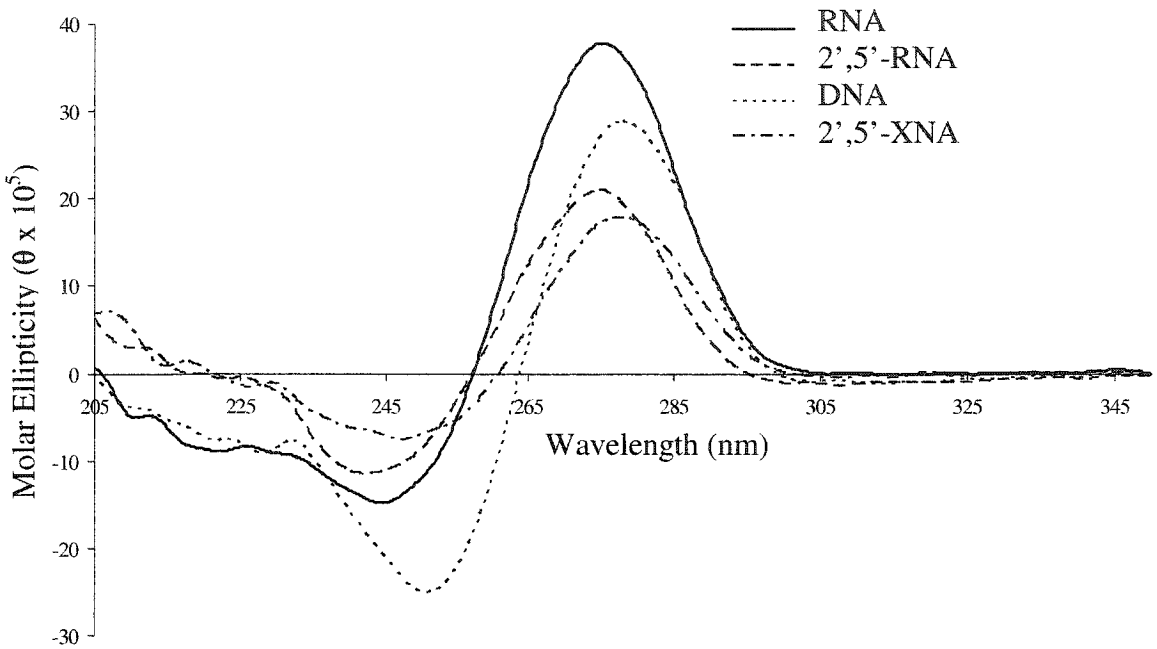

Figure 2.17: CD spectra of single strands of oligonucleotides complementary to HIV-1 genomic sequence at 5°C. The sequences are shown in **Table 2.1**. Buffer: 140 mM KCl, 1 mM $MgCl_2$, 5 mM Na_2HPO_4, pH = 7.2). Concentration of single strands was 2.3 μM.

The overall spectral features of the single strands are similar with a few key differences. The CD spectrum of RNA is slightly blue shifted relative to DNA with Cotton effects of larger magnitudes. The RNA spectrum has a positive maxima around 274 nm, crossover at 256 nm and a negative maxima at 243 nm while the positive maxima of DNA is about 277 nm, with a distinctly different crossover and negative maxima at 263 and 250 nm, respectively. The CD spectra of 2',5'-RNA and RNA are very similar, with nearly identical wavelengths for the crossover, and positive and

negative peaks. Upon inversion of stereochemistry at C3' (2',5'-RNA → 2',5'-XNA), the CD spectrum changes from 'RNA like' to more 'DNA like'. That is, the observed positive Cotton effect with a λ_{max} at 276 nm, cross over at 260 nm and negative peak at 247 nm all are closer to those of the DNA spectrum. This is consistent with the notion that 2',5'-linked oligoxylonucleotides, despite their C3'-*endo* conformation, adopt a 'extended' backbone geometry characteristic of DNA. The weaker intensity of the Cotton effects observed in the 2',5'-XNA duplexes could be the result of decreased base stacking.

The CD spectra shown in **Figure 2.18** distinctly shows the structural similarities between 2',5'-XNA:RNA and DNA:RNA duplexes. The RNA:RNA spectrum is representative of the A-form structure, while the DNA:RNA spectrum is characteristic of an 'A-like' hybrid. Most notable are the positive maxima at longer wavelength, with a similar shift in the cross-over wavelength and a strong negative Cotton effect. The 2',5'-RNA:RNA duplex shows spectral features very similar to the A-form with two positive maxima. The crossover points along with amplitudes and wavelengths of negative Cotton effect are nearly identical, showing the A-like characteristics of 2',5'-RNA. The 2',5'-XNA:RNA spectrum is similar to the DNA:RNA spectrum. The broad positive peak could be an effect of the 2',5'-linkage in this sequence.

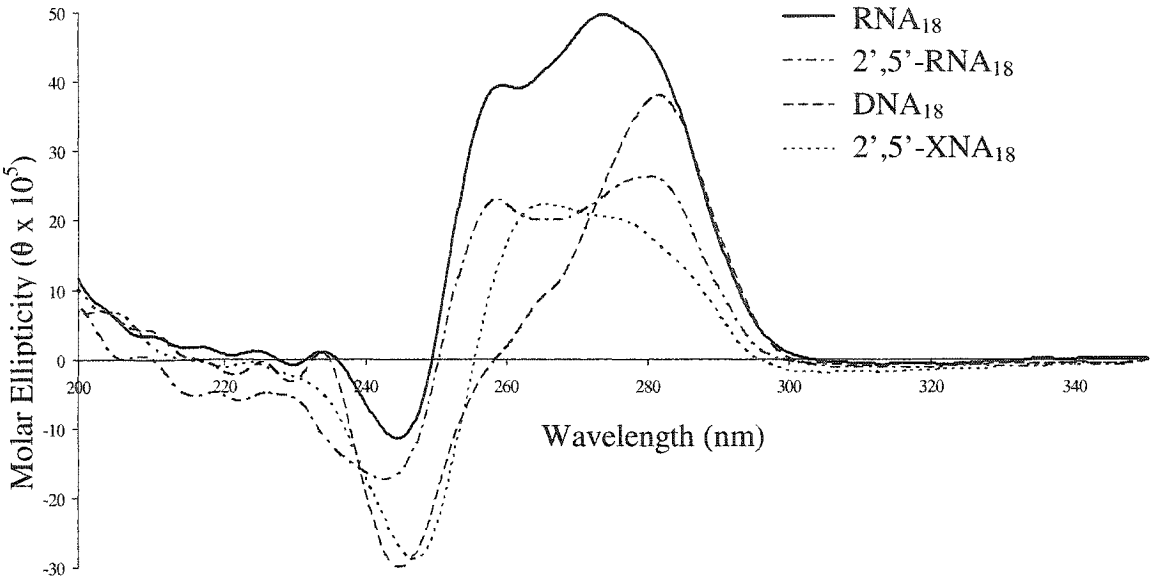

Figure 2.18: CD spectra of duplexes formed with a common RNA target at 5°C. The legend shows the antisense strand used and the sense strand sequence (**2.27**) is reported in **Table 2.1**. Buffer: 140 mM KCl, 1 mM $MgCl_2$, 5 mM Na_2HPO_4, pH = 7.2). Duplex concentration was 2.3 μM.

The T_m and CD studies strongly suggests that the structure of 2',5'-XNA resembles the "extended" DNA conformation as described recently by Yathindra and coworkers. In other words, the 'extended' conformation of 2',5'-XNA, (a result of its C3'-*endo* sugar conformation) causes it to behave as a structural mimic of DNA.

2.8 ENZYME ACTIVATION BY 2',5'-XYLOFURANOSE OLIGONUCLEOTIDES (2',5'-XNA) FOR ANTISENSE APPLICATION

As emphasized in the introduction, oligonucleotide analogs have potential use in therapeutic applications (antisense strategy). A primary mechanism of action of antisense drugs is the the activation of RNase H, an enzyme that degrades the RNA strand of the antisense/RNA hybrids. Cleavage requires the presence of divalent cations (Mg^{+2} and

Mn^{+2}) and affords 5'-O-phosphate and 3'-hydroxyl oligoribonucleotides fragments.[204] RNase H is known to possess both endonucleolytic and 3',5'-exonuclease activity and is involved in replication and repair of DNA.

E. coli RNase H was used in our studies to test the ability of 2',5'-XNA to induce degradation of a target RNA. The bacterial enzyme is composed of a single polypeptide chain of 155 amino acids and is similar in sequence to the RNase H domain of retroviral reverse transcriptase (RT), such as HIV-1-RT. [204] The active site consists of three acidic amino acids (Asp-10, Glu-48 and Asp-70) and divalent cation (Mg^{+2} or Mn^{+2}), along with the hybrid duplex closely bound to it. The enzyme binds within the minor groove of the RNA:antisense hybrid and its activity is influenced by the sugar conformation adopted by the oligonucleotide bound to the RNA. It is also well known that RNase H binds to RNA:RNA duplexes without cleaving it.

As previously described, 2',5'-RNA and its analogues have been used in mRNA degradation by interferon-induced activation of a latent enzyme RNase L. Also 2',5'-RNA and 2',5'-DNA have been tested for their ability to activate RNase H but without success.[90,96] These 2',5'-linked oligonucleotides when bound to the RNA target showed structural similarity to the native RNA:RNA duplex and therefore were unlikely to act as susbstrates. On the other hand, our studies have shown that the 2',5'-XNA(**2.27**):RNA duplex shows structural similarity to the native DNA:RNA heteroduplex and that 2',5'-XNA poses as a "DNA analogue" with 2',5'-phosphodiester linkages. Therefore it was hoped that the 2',5'-XNA:RNA hybrid would be a substrate of RNase H.

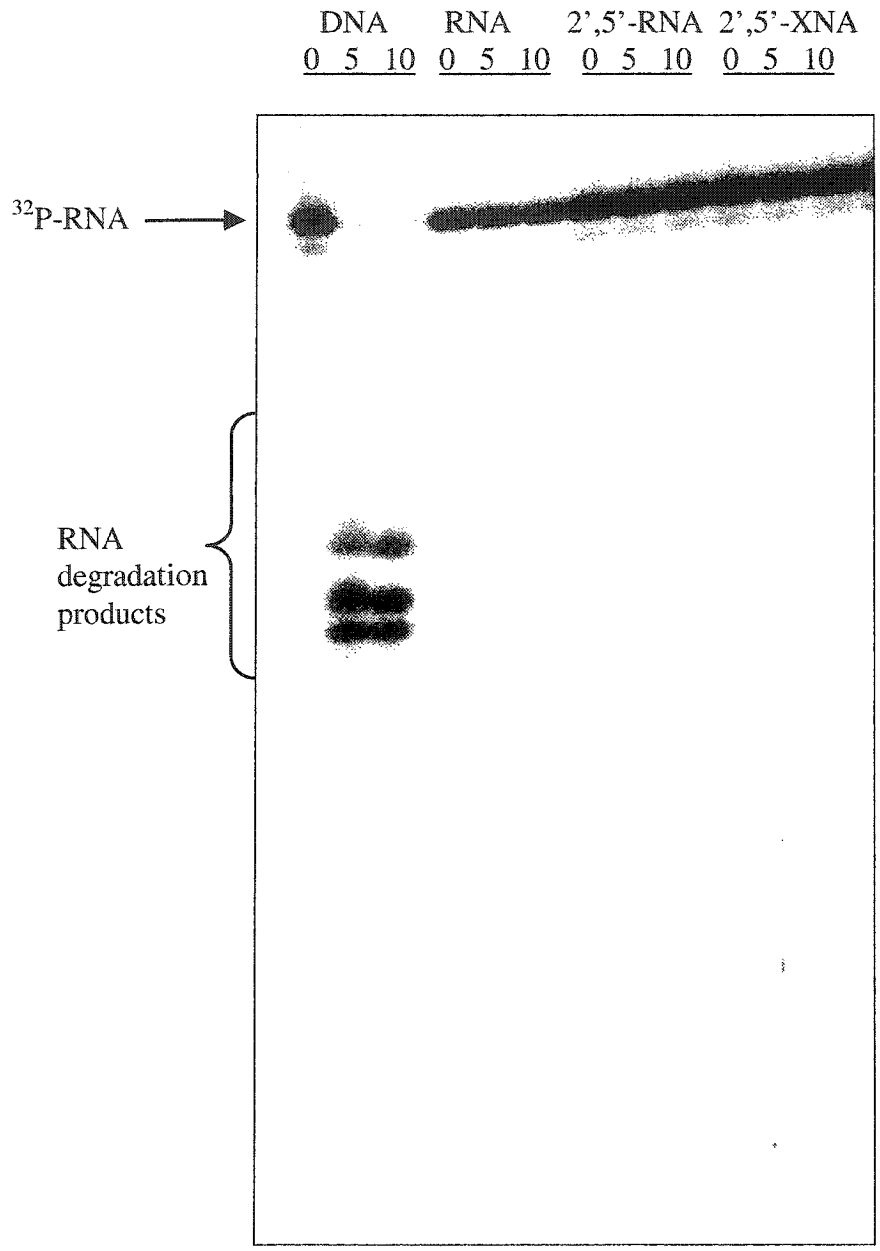

Figure 2.19: PAGE analysis of RNA degradation by RNase H using antisense oligonucleotides (Sequence: 5'-TTA TAT TTT TTC TTT CCC-3' or 2' with T replaced U in RNA and 2',5'-RNA). 1 pmol of target 5'-[^{32}P]-RNA and 10 pmol of antisense oligonucleotide were incubated in 60mM TRIS-HCl (pH 7.8), 2mM DTT, 60mM KCl and 2.5mM $MgCl_2$. Reaction was initiated by the addition of *E. coli* RNase H at 15 °C and quenched at 0, 5 and 10 minute intervals. The gel was visualized by autoradiography.

Briefly the enzymatic assay was carried out as follows: the 5'-hydroxyl end of the target RNA strand was 5'-^{32}P radiolabelled using γ-^{32}P ATP and T4 RNA ligase. The antisense oligonucleotides (2',5'-XNA, 2',5'-RNA, DNA or RNA) were incubated along with the target ^{32}-P-labeled RNA strand in an appropriate buffer at 17°C. The reaction was then initiated by the addition of *E. coli* RNase H and quenched after 5 and/or 10min. The products were resolved by gel electrophoresis and visualized by autoradiography. If the ^{32}P-RNA substrate results in RNA degradation, a "degradation ladder" of the cleavage product is generally observed.

As clearly seen in Figure **2.19**, the 2',5'-XNA:RNA hybrid was not a substrate of RNase H. According to these results and our CD studies, we can make the following conclusions. We can consider 2',5'-XNA nucleotides as DNA mimics at the global helical level in the context of DNA:RNA hybrids. However, at the local level, the movement of the linkage from 3' to 2' introduces rather significant perturbations in the antisense strand of the hybrid. It is generally assumed that a key element of RNase H recognition of a DNA:RNA hybrids is the width of its minor groove. Thus it is very likely that 2',5'-XNA:RNA hybrids are not optimally recognized by the RNase H enzyme, given the 'slide' or displacement of the phosphate groups, irrespective of whether the backbone adopts an extended (2',5'-XNA, 2',5'-DNA) or compact (2',5'-RNA) geometry.

CHAPTER III

SYNTHESIS, PHYSICOCHEMICAL AND BIOCHEMICAL PROPERTIES OF 3'-DEOXY-3'-FLUORO-XYLONUCLEOSIDES AND OLIGONUCLEOTIDES

3.1 BACKGROUND

The inversion of stereochemistry at the C3'-hydroxyl of 2',5'-RNA, to give 2',5'-XNA, results in weaker associations with complementary oligonucleotides (**Chapter II**). This effect has previously been observed for 3',5'-linked arabinofuranose nucleic acids (ANA) in which an analogous inversion at C2'-OH of the ribofuranose sugar moiety was made (**Figure 3.1**).[206] The significant drop in T_m values was attributed to the steric hindrance created within the major groove by the arabinose's C2'-hydroxyl.[206] One way to prevent or reduce such steric effects, while maintaining the conformation of the nucleotide is to substitute the hydroxyl group with a fluorine atom. Recent findings by our group and others have shown that replacement with fluorine has caused very little electronic perturbation, while resulting in reduced steric repulsions and improved binding (i.e. higher T_m) in duplex formation, e.g. RNA→2'-fluoro-RNA (2'F-RNA) and ANA→2'-fluoroANA (2'F-ANA).[203] The reason for the higher T_ms has been attributed to the fluorine-induced pre-organization of the oligonucleotide prior to complexation to the complementary strand.[203] Alternatively, it may also be attributed to the decrease in the entropic gain upon denaturation of two strands as the pre-organized or conformationally biased strand (2'F-ANA or 2'F-RNA) is made less advantageous than a more flexible single strand (DNA or RNA).

A recent review[212] on fluorinated nucleosides indicated that over 77% of the nucleosides synthesized to date bear a fluorine atom at the C2'-position and less than

12% have focused on 3'-fluorinated nucleosides. Therefore relatively little structural information is available on C3'-fluorinated nucleosides and the corresponding oligonucleotides.

The application of fluorine as a 'hydroxyl mimic' in organic molecules is well established.[207] From an electronic perspective, fluorine and oxygen are very similar, where fluorine is the most electronegative of all the elements, having a value of 4.0 (vs. 3.5 for oxygen) on the Pauling electronegativity scale. [208] In terms of steric interactions, fluorine is smaller than oxygen, having a van der Waals radius (1.35Å) that is intermediate between that of oxygen (1.57Å) and hydrogen (1.2Å).[209] This results in similar C-F and C-OH bond lengths and dipole moments. The hydrogen-bonding ability of fluorine is limited in comparison to a hydroxyl moiety, as it can only act as a H-bond acceptor and not a donor. While a hydrogen bond formed between F····H (2.48kcal/mol) is only half as strong as an O····H hydrogen bond (~5 kcal/mol), fluorine still retains the ability to act as an effective hydrogen bond acceptor (the F····H bond distance is estimated at 1.9Å).[210] The reason for the weak hydrogen bond forming ability of fluorine is thought to be due to its high nuclear charge, which pulls electrons closer to the nucleus. Thus in order for a hydrogen-fluorine bond to form, the proton has to come closer to the fluorine nucleus relative to one involving oxygen and this leads to nuclear repulsion. The effect of fluorine substitution in nucleosides has also been extensively studied.[211-215] Fluorine essentially 'locks' the furanose in a conformation that is dependent on both the location and stereochemistry of the C2'/C3' carbon bearing the fluorine atom.

As mentioned previously, small oligonucleotides (up to trimers) of 2',5'-xylo-fluoro-adenosines have been synthesized for the application of interferon induced

degradation of RNA and their structures studied via one and two-dimensional NMR spectroscopy.[181,216] These studies nicely showed that the nucleotide conformation is governed by the fluorine configuration. In the case of xylo-fluoro-adenosine, the nucleotide conformation exists mainly in the C3'-*endo* form while the non-fluorinated nucleotides (2',5'-xyloadenosine trinucleotides) are slightly more flexible.

Based on the above, the substitution of 2',5'-XNA's 3'-hydroxyl groups with fluorine should have minimal electronic effects while reducing potential steric effects. It would also result in the 'locking' of the nucleotide units in a North (C3'-*endo*) conformation. A similar sugar conformation exists in xyloadenosine and 2',5'-XNA (3'-OH; **Chapter II**). The pre-organization induced by fluorine allows us to address the following questions: (a) are there any steric interactions between C3'-OH of 2',5'-XNA within a duplex?; (b) does substitution of a hydroxyl with fluorine in the sugar moiety generally result in improvement of overall T_ms due to pre-organization?; and most importantly for the creation of an oligonucleotide analog with 2',5'-phosphodiester linkage, (c) do the effects of sugar conformation switch upon 3',5'- to 2',5'-backbone modification?[77,94,104]

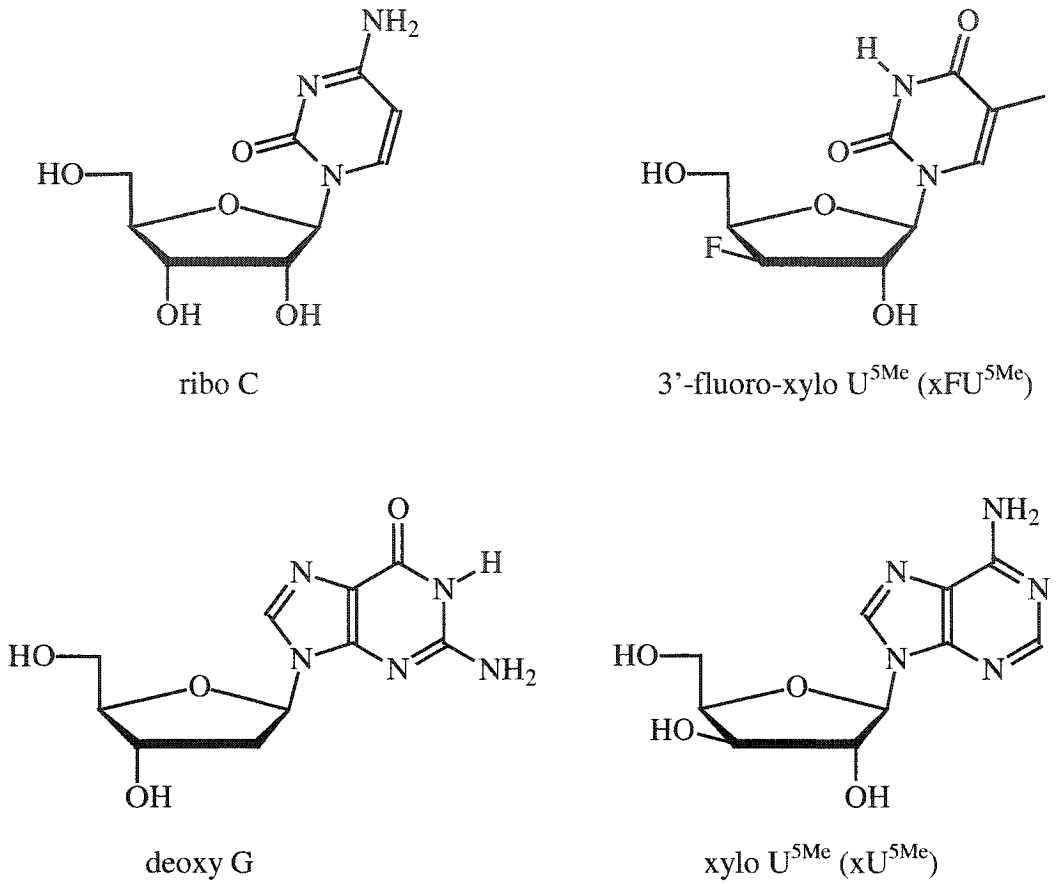

Figure 3.1: Structural comparison of 3'-deoxy-3'-fluoro-xylonucleoside to other nucleosides.

In an attempt to answer these questions, we undertook the synthesis of 3'-fluoroxylonucleosides and a series of 2',5'-linked 3'-fluoro-oligoxylonucleotides (2',5'-XFNA). We compared the structural implications of this modification in hybrids with DNA and RNA via T_m and CD measurements, and also examined the 2',5'-XFNA:RNA duplex in the context of RNase H recognition.

3.2 SYNTHESIS OF PROTECTED 3'-DEOXY-3'-FLUORO-β-D-XYLOFURANOSYL-NUCLEOSIDES

3'-Deoxy-3'-fluoro-xylonucleosides have been investigated as potential antitumor and antiviral agents.[217-8] Trinucleotide derivatives of these nucleosides have been found to elicit RNase L,[219] and increase the lytic activity of human lymphocytes.[220]

3'-Deoxy-3'-fluoro-xyloadenosine was the first to be synthesized[221] by condensing the appropriate sugar with the mercuric adenine salt. Analogous synthesis of 3'-fluoro-xylocytosine proved to be difficult and condensation of a 1-brominated sugar with silylated cytidine appeared to be more advantageous.[222] Later Robins *et al.* showed an elegant transformation of a ribonucleoside 2',3'-epoxide into 3'-fluoro-xylonucleosides[150] but these transformations in the pyrimidine series have not been reported. Opening of a purine 2',3'- cyclic sulfate nucleoside has led to a mixture of the xylo and arabino products.[223] Watanabe *et al.*[230] have looked at the effect of sugar conformation on the efficiency of fluorination mediated by diethylaminosulfur trifluoride (DAST) **(Figure 3.2).** If the "triflate-like" (O2'-SF_2-NEt_2) intermediate that forms is anti-periplanar to the vicinal proton (H3'), the elimination product predominates. If the proton occupies an equatorial position, substitution at C2' occurs to afford the fluorinated nucleoside. Interestingly, these requirements are more stringent at the C2'-position than to the C3' position, but other factors such as temperature and basicity of the reaction medium also impact the E2/S_N2 product distribution.

Recently, Marquez *et al.* have described the synthesis of 3'-fluoro-5-methyl-xylouridine via Vorbrüggen coupling of 1,2-di-O-acetyl-3-fluoro-5-O-benzoyl-xylofuranose with silylated thymine.[224] As in the case of xylo and ribonucleoside

synthesis, anchimeric assistance of the C2'-acetate controls the stereselectivity of the glycosylation reaction and the β-product is exclusively formed.

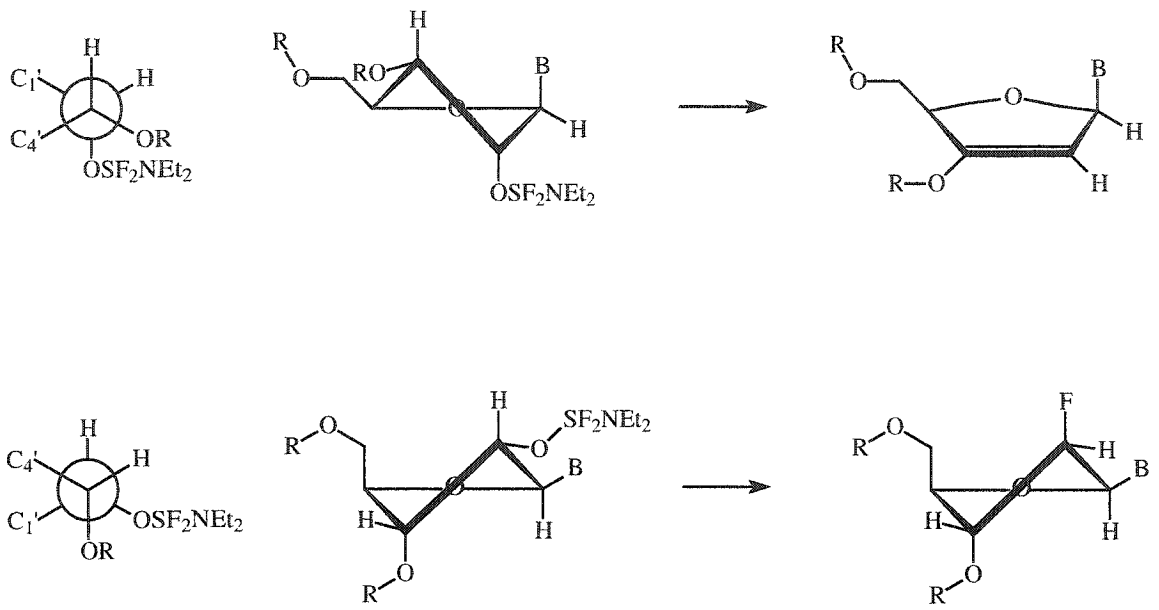

Figure 3.2: Effect of sugar conformation on fluorination reaction using DAST. The anti-periplanar conformation of a proton relative to the triflate-like intermediate leads to elimination (top row); while absence of an anti-periplanar proton leads to the desired fluorination.[230]

An efficient synthesis of the sugar precursor is key to the large scale preparation of the xylo-fluoro-nucleosides. Webber *et al.*[225] have shown that a C3-O-tosyloxy group of 1,2:5,6-di-O-isopropylidene-α-D-allofuranose can be displaced by fluoride derived from tetrabutylammonium fluoride. Analogously, Fox *et al.*[226] have carried out the displacement using potassium fluoride in acetamide at ~210 °C. This was improved upon by Tewson *et al.*[227] who demonstrated that reaction of the same non-tosylated sugar with DAST followed by vacuum distillation avoided an extra step (tosylation of C3-hydroxyl). An alternative route to synthesis of xylo-fluoro-nucleoside was described by Gosselin *et al.*,[228] but it is more laborious; furthermore they used rather harsh conditions resulting in

poor overall yields. Marquez adopted a similar route[224] as that of Tewson and performed chromatographic purification of the fluorinated product.

We decided to follow the synthetic route described by Marquez[224] in the preparation of 1,2-di-O-acetyl-5-O-benzoyl-3-deoxy-3-fluoro-D-xylofuranose (**Figure 3.3**). However, due to the cost of the starting material required, we started out with the readily available 1,2:5,6-di-O-isopropylidene-α-D-glucofuranose sugar. This was oxidized-reduced at the C3-hydroxyl[229] to give the protected allofuranose **(3.1)** in 85% yield, ready for fluorination.

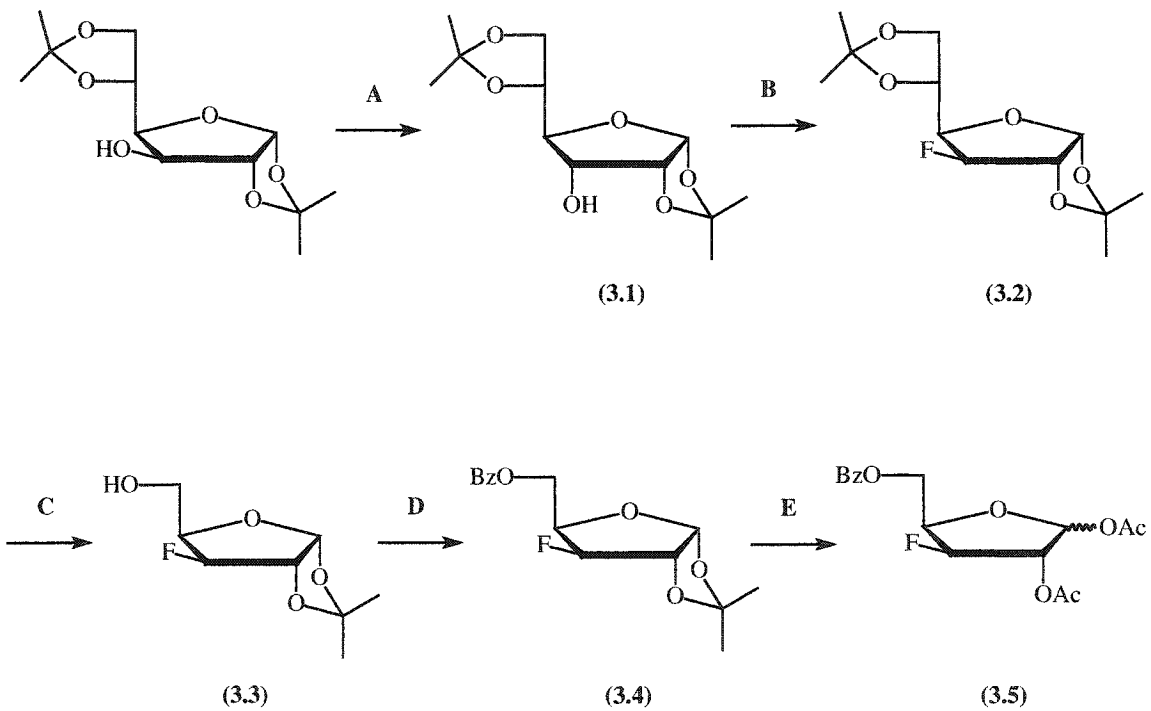

Figure 3.3: Scheme for the synthesis of sugar precursor 5-O-benzoyl-3-deoxy-3'-fluoro-1,2-di-O-Acetyl xylofuranose **(3.5)** for coupling to heterocyclic bases. **A.** (i) PCC, Ac_2O, DCM, reflux, 2hrs (ii) $NaBH_4$, EtOH (85%); **B.** DAST, pyr, DCM, 0°C→r.t., overnight (59%); **C.** (i) 80% AcOH, r.t., 2days; $NaHCO_3$; $NaIO_4$, 0°C; $NaBH_4$/EtOH (93%); **D.** Bz-Cl, pyr (92%); **E.** glacial AcOH, Ac_2O, H_2SO_4, 0°C (99%).

The expected inversion of stereochemistry took place upon fluorination (DAST) to afford derivative **3.2** (59%). Selective hydrolysis of the 5,6-O-isopropylidene moiety, followed by sequential periodate oxidation and hydride reduction afforded the xylofuranose derivative **3.3** in 93% yield (three steps from **3.2**). In the ensuing three steps, compound **3.3** was benzoylated at the C5-hydroxyl (92%), the 1,2-O-isopropylidene moiety was cleaved, and the resulting hemiacetal esterified (in situ) using acetic acid, acetic anhydride and sulfuric acid (99%). The desired sugar (**3.5**) was isolated in 48% overall yield (from the diisopropylidende glucofuranose). Gosselin *et al.* have reported[228] that the final esterification reaction produces an equal amount of the open chain acetylated product, however, our results agreed with those of Marquez[224] and the reaction proceeded cleanly to give **3.5** in excellent yield.

The synthetic steps leading to the 3'-deoxy-3'-fluoro-5-methyl-xylouridine-2'-phosphoramidite derivative are shown in **Figure 3.4**. First, bis-O-silylated thymine (prepared by refluxing thymine with hexamethyldisilazane in chlorotrimethylsilane) was coupled to sugar (**3.5**) in the presence of trimethylsilyl trifluoromethanesulfonate (TMSOTf), to afford exclusively the β-product (**3.6**).[162] The spectral properties (NMR and MS) agreed with those reported in the literature.[224] Deprotection with conc. aqueous ammonia/methanol (overnight) led to cleavage of the esters to yield the desired nucleoside (xFU^{5Me}) (**3.7**).

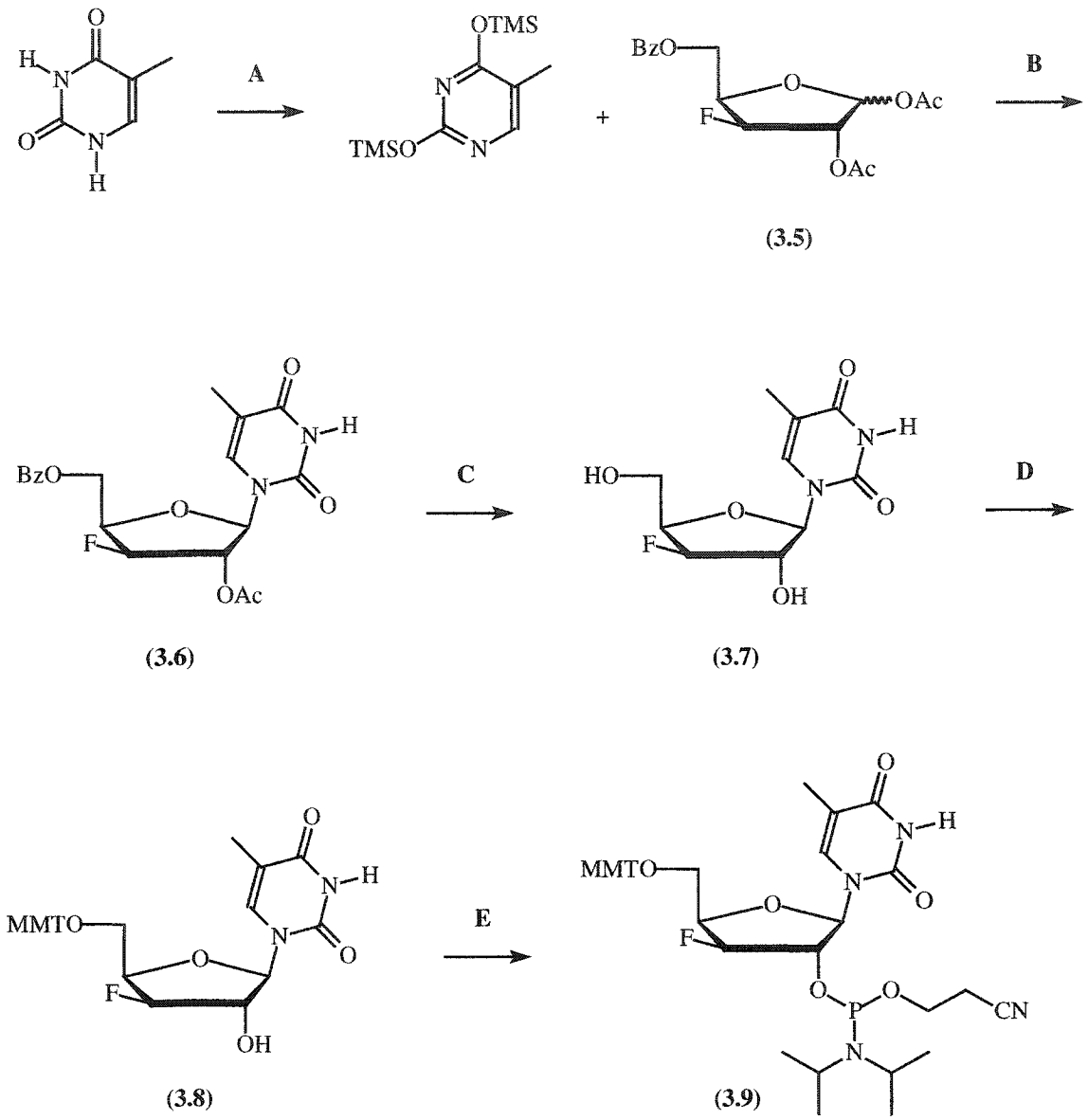

Figure 3.4: Scheme for the synthesis of xyloFU$^{5\text{-Me}}$-2'-phosphoramidite **A.** thymine, HMDS, TMS-Cl, reflux. **B.** TMSOTf, CH_3CN (70%). **C.** NH_4OH/MeOH, overnight (90%). **D.** MMT-Cl (1.2 equiv.), DMAP (cat.), pyridine, r.t., overnight (90%). **E.** Cl-P(OCE)($NiPr_2$) (1.2 equiv.), DIPEA (2.4 equiv.), THF, r.t., 2h (69%).

In order to prepare the nucleoside for solid phase oligonucleotide synthesis appropriate protecting groups were attached.[191] The first step was protection of the 5'-hydroxyl using monomethoxytrityl chloride to give the 5'-tritylated nucleoside (**3.8**).

The tritylated nucleoside is more easily manipulated than the nucleoside. The ^{1}H, COSY and ^{19}F NMR of 5'-O-MMT-3'-deoxy-3'-fluoro-5-methyl-xylouridine (**3.8**) is shown in **Figure 3.5**. The small $^{3}J_{1',2'}$ splitting (vicinal coupling constant) is indicative of a C3'-*endo* sugar conformation, similar to what was observed for the xylonucleoside series (3'-OH; **Chapter II**). The assignment of the sugar protons was done by a ^{1}H-COSY experiment (**Figure 3.5 B**). Clearly, the largest splitting observed is for H3' due to geminal coupling to the 3'-fluorine (nuclear spin ^{19}F = ½). The ^{19}F-NMR resonance appears as a doublet-of-doublet-of-doublet (ddd) due to coupling to the geminal (H3') and vicinal protons (H1'/H4').

Fortunately for the fluorinated nucleoside synthesized, no silyl or ester protection was required. The nucleoside was readily phosphitylated forming the 2'-amidite (**3.9**). The sugar H2' proton of this derivative displays splitting to both ^{19}F and ^{31}P nuclei. The ^{31}P-NMR spectra show two peaks (d) due to the diastereomeric nature of compound **3.9**. In the ^{31}P-NMR spectrum of the corresponding 2'-deoxy-2'-fluoro-*arabinose*-3'-phosphoramidite, one observes a longe range ^{19}F (2') - ^{31}P (3') coupling consistent with a C2'-*endo* sugar pucker and a "W"-type pathway between these nuclei,.[203] Interestingly, no such splitting was observed for xylonucleoside 2'-amidite (**3.9**), indicating that in spite of a possible C3'-*endo* pucker, no such "W" arrangement (F3'-C3'-C2'-O2'-P2') exists in this case.

Xylo-fluoro-cytosine (xFC) was synthesized via Saneyoshi coupling[168-9] of the base to the di-acetyl-fluorinated sugar affording the β anomer exclusively and in good yields. This derivative was converted to the desired xFC-2'-O-phosphoramidite as shown in **Figure 3.6**.

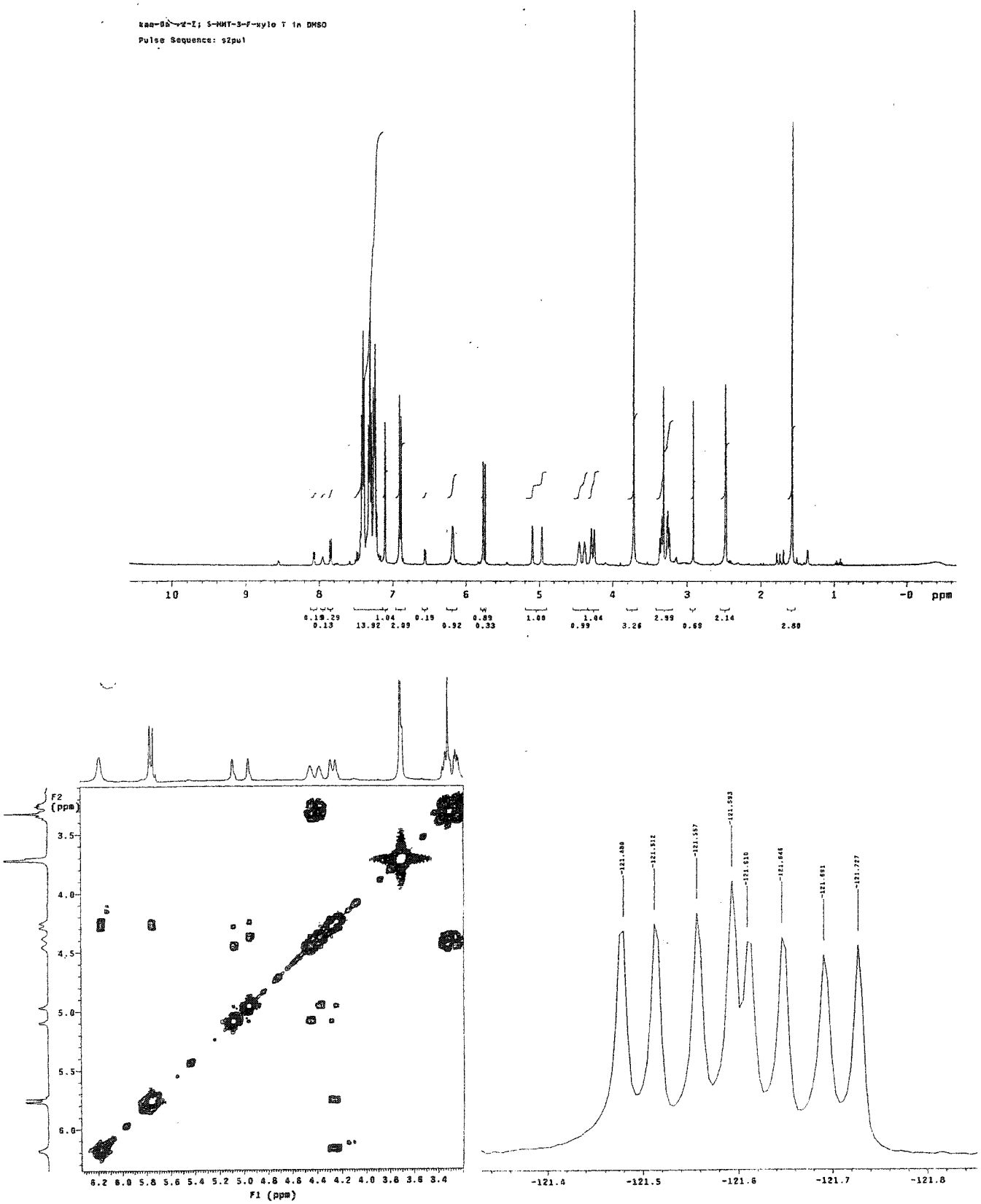

Figure 3.5: The ^{1}H, COSY and ^{19}F NMR spectra of 5'-MMT-3'-deoxy-3'-fluoro-5-methyl-xylouridine **(3.8)**.

It is known that the presence of fluorine substitution on a sugar (particularly at C2') makes the formation of the oxonium ion intermediate difficult, making it possible to control the stereoselectivity of the coupling reaction under S_N2 conditions. Although the effect of fluorine under Saneyoshi coupling conditions is relatively unexplored, our studies indicate that a remote 3'-fluorine atom has a minimal effect on coupling and in fact, higher yields are obtained relative to Vorbrüggen-type coupling conditions (discussed later in this section). A side product was also formed resulting from hydrolysis of the 2'-OAc group. This compound, ($^{5'\text{-Bz}}$xFC$_{2'\text{OH}}$), and $^{5'\text{-Bz}}$xFC$_{2'\text{OAc}}$ (**3.10**) converged to the same product (**3.11**) upon treatment with *aq.* NH_3/methanol (NMR, MS and UV spectroscopic results). These xylo-fluoro-nucleosides ($^{5'\text{-Bz}}$xFC$_{2'\text{OH}}$ and $^{5'\text{-Bz}}$xFC$_{2'\text{OAc}}$) were combined to determine the yield of the coupling reaction (70%).

The standard "transient protecting group strategy"[201] was applied to install the exocyclic amine benzoyl protecting group (**Figure 3.6**; step C), affording N-benzoyl-xFC (**3.12**) in 73% yield. The nucleoside was then tritylated (95%) and phosphitylated (79%) to afford the desired 2'-phosphoramidite derivative (**3.14**). The ^{1}H, ^{19}F and ^{31}P NMR spectra of compound (**3.14**) were similar to those of the xFU^{5Me}-phosphoramidite. The sugar protons showed splitting due to both fluorine and phosphorus and no long range coupling was observed between the 3'-fluorine and the 2'-phosphorus.

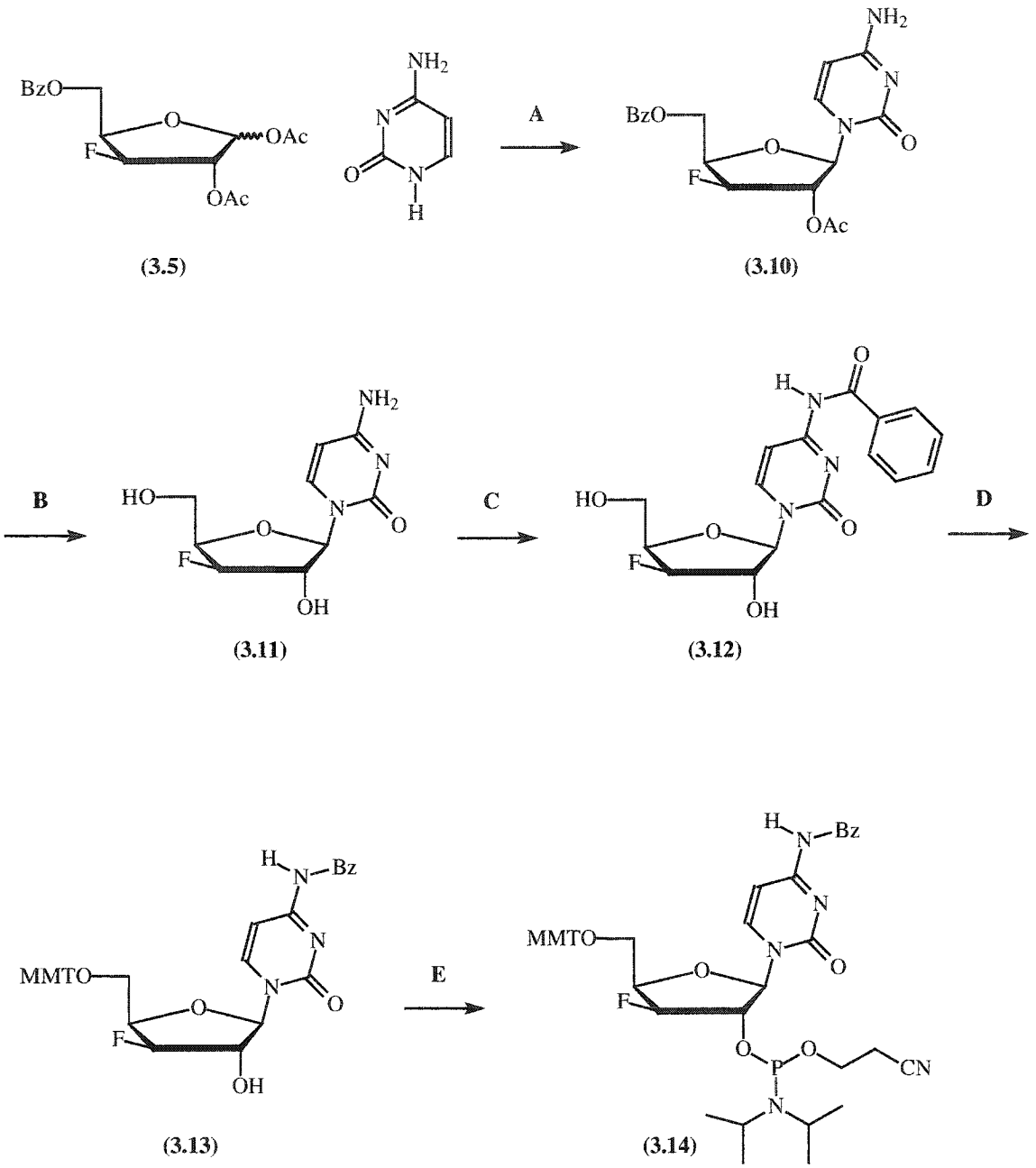

Figure 3.6: Scheme for the synthesis of 3'-deoxy-3'-fluoro-xylocytidine-2'-phosphoramidite (**3.14**). **A.** Cytosine, $SnCl_4$, CH_3CN (47%); **B.** NH_4OH/MeOH, r.t., overnight (70%); **C.** (i) TMS-Cl, Bz-Cl, pyridine; (ii) NH_4OH (73%); **D.** MMT-Cl (1.2 equiv.), DMAP, pyridine, r.t., overnight (95%); **E.** Cl-P(OCE)(N-iPr_2) (1.2 eq), DIPEA (2.4 eq) (79%).

The synthesis of xylo-fluoro-adenosine (xFA) and its protected-2'-O-phosphoramidite derivative followed a route similar to that described for the cytosine analogue (**Figure 3.7**). The unprotected base was coupled to the protected sugar (**3.5**) under Saneyoshi conditions to yield exclusively the β-product. The yields obtained were also higher than those obtained using the Vorbrüggen reaction, in which a mixture of N-7 and N-9 anomers were also obtained. As in the case of xFC, the exocyclic amine of xFA was protected with the benzoyl group after transient silylation of the sugar hydroxyl groups to yield N-Bz-xFA (**3.17**). The primary 5'-hydroxyl was reacted with monomethoxytrityl chloride to give the nucleoside (**3.18**) ready for phosphitylation.

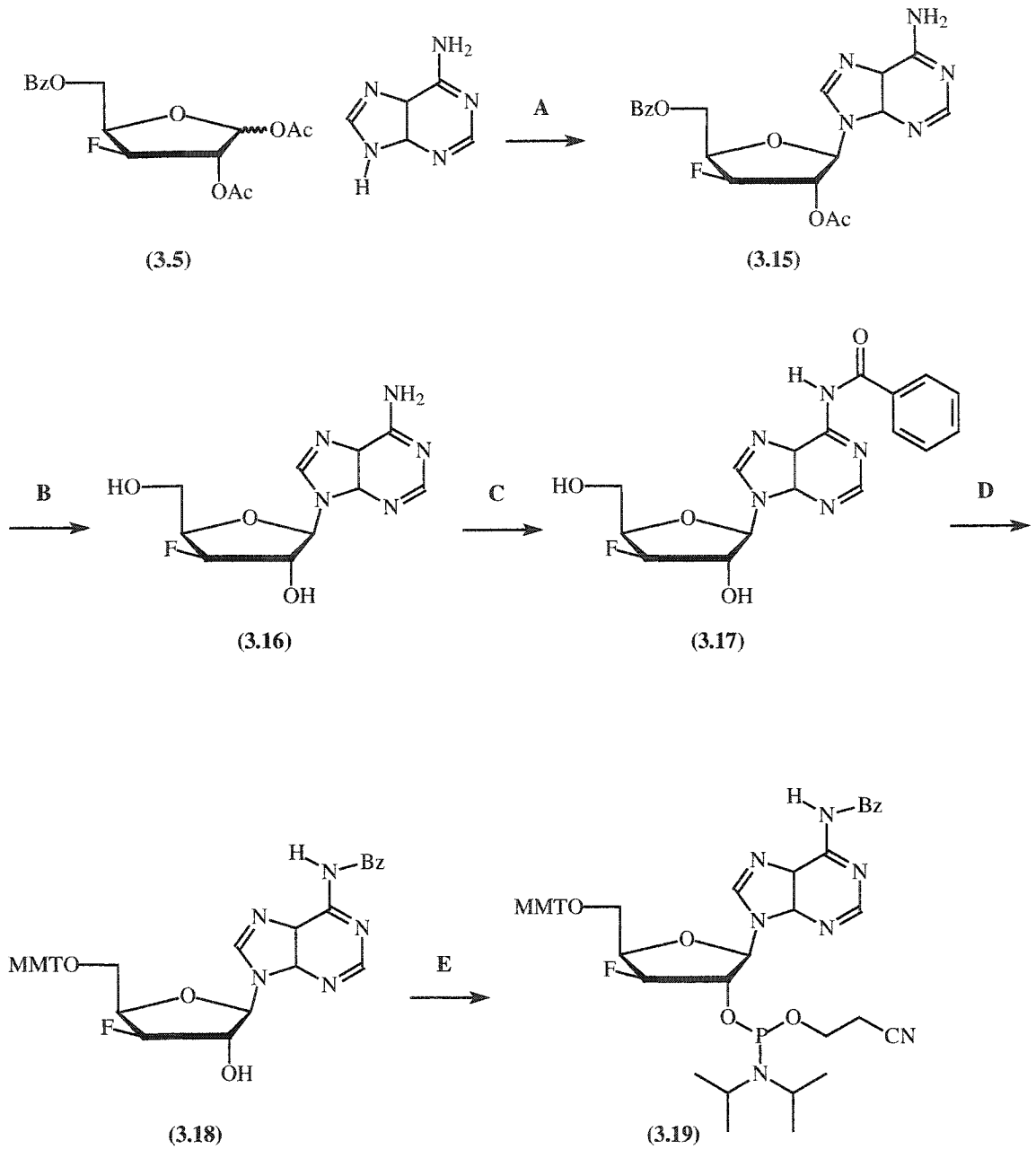

Figure 3.7: Scheme for the synthesis of 3'-deoxy-3'-fluoro-xyloadenosine-2'-phosphoramidite (**3.19**). **A.** Adenine, $SnCl_4$, CH_3CN (58%); **B.** NH_4OH/MeOH, r.t., overnight (82%); **C.** (i) TMS-Cl, Bz-Cl, pyridine; (ii) NH_4OH (63%); **D.** MMT-Cl (1.2 equiv.), DMAP, pyridine, r.t., overnight (72%); **E.** Cl-P(OCE)(N-iPr_2) (1.2 eq), DIPEA (2.4 eq) (88%).

3.3 SOLID-PHASE SYNTHESIS OF 2',5'-LINKED-3'-FLUORO-XYLOFURANOSE NUCLEIC ACIDS (2',5'-FXNA)

LCAA-CPG was derivatized with protected xFU^{5Me}, xFC and xFA nucleosides according to the procedure of Pon.[194] Typical loadings varied from 60-80 μmol/g, with pyrimidine giving higher loadings than purines. A similar trend was observed with the $xyloU^{5\text{-}Me}$, xyloC and xyloA building blocks (**Chapter II**).

A number of 2',5'-FXNA oligonucleotides were synthesized and their sequences are listed in **Table 3.1**. The RNA synthetic cycle was used with minor modifications, e.g., an extended coupling time (900 s) for monomer coupling, and a longer detritylation time to allow complete removal of the 5'-monomethoxytrityl group, which is more stable towards acid hydrolysis than the 5'-dimethoxytrityl group present in RNA monomers.

Table 3.1: List of 2',5'-FXNA oligonucleotide sequences synthesized

Sequence	Designation	ODs Crude	ODs Pure[a]
5'- TTT TTT TTT TTT TTT TTT -3'	**3.15**	59.0	34.7
5'- AAA AAA AAA AAA AAA AAA -3'	**3.16**	62.3	27.5
5'- TTA TAT TTT TTC TTT CCC –3'	**3.17**	74.4	36.9

[a] Method of purification: polyacrylamide gel electrophoresis followed by desalting by gel filtration (Sephadex G-25, see Experimental Section 7.3.3).

Taking into consideration the problems of low coupling efficiencies that we encountered with 2',5'-XNA (**Chapter II**), we chose to use a different coupling reagent, namely 4,5-dicyanoimidazole (DCI). Dicyanoimidazole is known to be a better activating agent than tetrazole[194b] and does not cause any 5'-detritylation during coupling.

In fact, monomer coupling efficiencies ranged from 89 to 103%, which are similar to those obtained for 2',5'-XNA using 5-ethylthiotetrazole as an activating reagent. Deprotection of these oligonucleotides was carried out according to the standard procedure used for DNA synthesis.[191] Recovery of oligonucleotides after purification (PAGE and size-exclusion chromatography) was moderate (28-37% yield). Sequence **3.17** (CAT) was also synthesized to study the properties of 2',5'-XFNA of mixed base composition. A representative gel of a purified 2',5'-FXNA sequence is shown in **Figure 3.8**. The oligomers were characterized by MALDI-TOF mass spectrometry (see **Chapter VI, section 6.4.2**). Experimentally determined molecular weights were in excellent agreement with calculated values **(Table 3.2)**.

Table 3.2: Observed and calculated molecular weights of 2',5'-FXNA determined by MALDI-TOF mass spectrometry.

Sequence	Designation	MW (calc.)[a]	MW (exp.)[a]
5'- TTT TTT TTT TTT TTT TTT -3'	**3.15**	5737	5737
5'- AAA AAA AAA AAA AAA AAA -3'	**3.16**	5899	5899
5'- TTA TAT TTT TTC TTT CCC –3'	**3.17**	5695	5695

[a] g/mol. Matrix: 20mM ammonium citrate(50% acetonitrile: 50% water) buffer containing 10 mg/mL of 6-aza-2-thiothymidine.

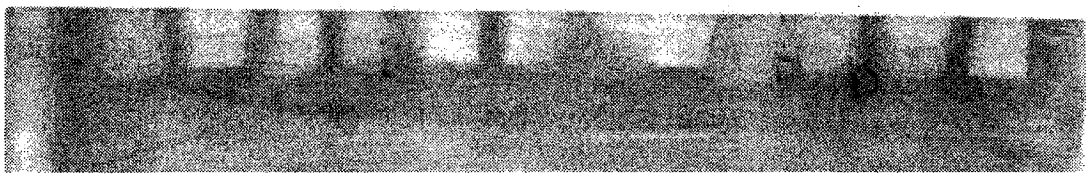

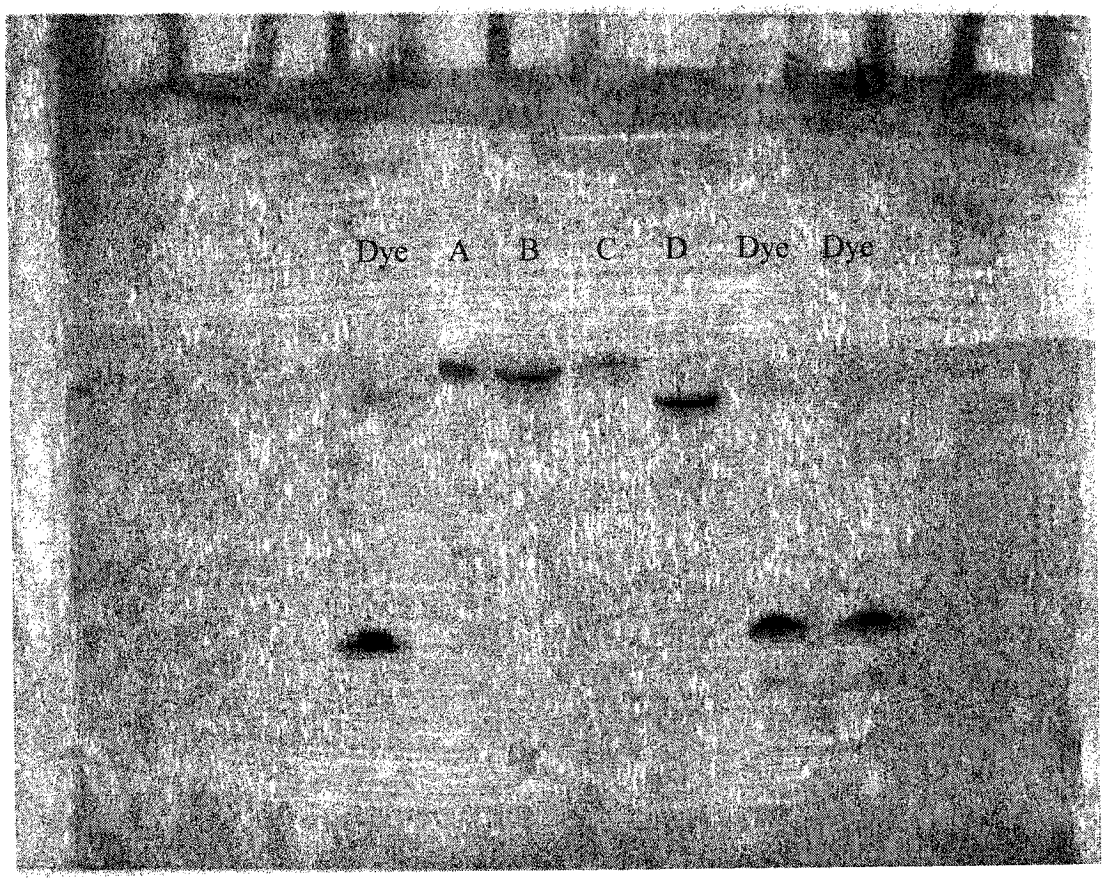

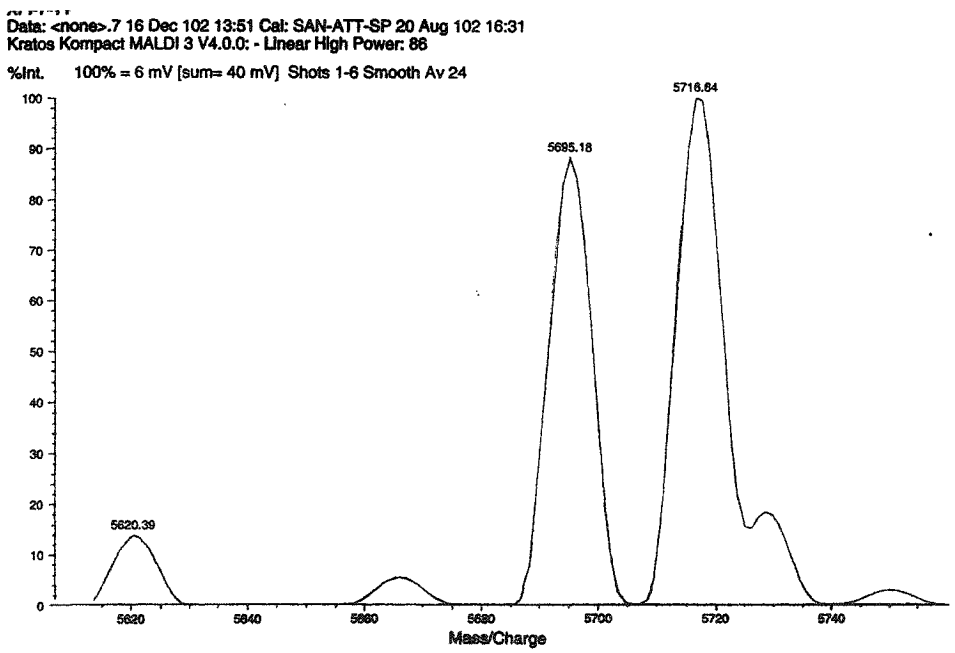

Figure 3.8: **(A)** Polyacrylamide Gel Electrophoresis (PAGE) of 18-unit long oligonucleotides (24% polyacrylamide, 7 M Urea in TBE buffer). **(B)** MALDI-TOF mass spectra of 2',5'-linked xylo-fluoro-oligonucleotides. The base composition of the sequence was 5'- TTA TAT TTT TTC TTT CCC-3' and in RNA 'T' is replaced by 'U'. Lanes A: 2',5'-FXNA; B: RNA; C: 2',5'-XNA; D: DNA.

3.4 DUPLEX FORMATION BY 2',5'-LINKED-3'-DEOXY-3'-FLUORO-XYLOFURANOSE-NUCLEIC ACIDS (2',5'-FXNA)

There are no known studies on the binding properties of 2',5'-FXNA. The presence of fluorine on the sugar moiety has two possible effects; as mentioned previously, one being an improvement in the binding affinity to complementary oligonucleotides, as seen for other fluorinated oligonucleotides,[203] alternatively, reduction in associative property as a result of pre-organization of the oligonucleotide in an undesirable conformation (the desired conformation would lead to an enhancement of T_m values).

Analogous to the study performed on 2',5'-XNA (**Chapter II**), homopolymers of 2',5'-xylo-fluoro-5-methyl-uridine and adenosine were synthesized and their ability to form duplexes with complementary strands of DNA and RNA was studied. The T_m values (binding affinity) of various oligopyrimidines towards complementary dA_{18} and rA_{18} are summarized in **Table 3.3**.

Table 3.3: Melting temperature of various oligopyrimidylates towards complementary adenosine-oligonucleotides

Sequence	rA_{18} (RNA)		dA_{18} (DNA)	
	T_m (°C)	%H	T_m (°C)	%H
rU_{18}	50.0	13.3	44.2	22.6
dT_{18}	52.1	27.2	59.0	27.0
2',5'-rU_{18}	36.4	17.5	--[b]	
2',5'-$xFU^{5\text{-}Me}{}_{18}$	10.7	6.2	--[b]	

Buffer: 1M NaCl, 100mM Na_2HPO_4, pH = 7.2. [b] No T_m observed above 5°C. %H = percent hyperchromicity.

All duplexes exhibited "sharp" monophasic transitions, indicating the formation of single cooperative complexes (the binding properties of the native oligonucleotides are discussed in **Chapter II**). As seen in **Table 3.3**, $xFU^{5Me}{}_{18}$ associates weakly with RNA (11.0°C) and no duplex was observed with target ssDNA. The same was observed with the 5-methyl-xylouridine oligonucleotides ($xU^{5\text{-}Me}{}_{18}$:rA_{18}, T_m ~5°C; **Chapter II**). Therefore we conclude that steric bulk at the C3'-position (xylo-configuration) is not responsible for the observed reduced binding by xylooligonucleotides. Rather, it is likely due to the C3'-*endo* or 'extended' conformation of the 2',5'-linked sugar phosphate backbone, which in turn renders 2',5'-XNA and 2',5'-FXNA more selective in binding to complementary RNA (over DNA).

Homopolymers of adenosine were also synthesized and studied for their associative properties. Their T_m values are given in **Table 3.4**.

Table 3.4: Melting temperature of various oligoadenylates towards complementary oligopyrimidylates[a]

Sequence	rU_{18} (RNA)		dT_{18} (DNA)	
	T_m (°C)	%H	T_m (°C)	%H
rA_{18}	50.0	13.3	52.1	27.2
`dA_{18}	44.2	22.6	59.0	27.0
2',5'-rA_{18}	47.8	17.1	9.5	9.1
2',5'-xFA_{18}	65.0	21.6	38.1	27.9

Buffer: 1M NaCl, 100mM Na_2HPO_4, pH = 7.2. %H = percent hypochromicity.

The duplex 2',5'- xFA_{18}:rU_{18} exhibited a greater percent hyperchromicity than the 2',5'-xA_{18}:rU_{18} duplex, indicating an improvement in base stacking geometry within the helical structure. Furthermore, 2',5'- xFA_{18}:rU_{18} showed enhanced binding to RNA, in fact, it was more stable than the corresponding rA_{18}:rU_{18} duplex; a property also observed

for the 2',5'- xA_{18}:rU_{18} duplex (**Chapter II**). This is surprising given the results observed for xFU_{18} (**Table 3.3**), and likely does not represent the general properties of 2',5'-FXNA. In this regard, it is appropriate to point out that several modified adenylates ($araA_{18}^{2'\text{-}OH}$, L-dA_{18}, 2',5'-rA_{18}, 2',5'-xA_{18}, etc) exhibit superior binding properties than their native counterparts (rA_{18}), yet, the same does not hold true when mixed-base strands bear the same modifications. In fact, as shown below, 2',5'-FXNA of mixed base composition ("CAT") exhibits poor association to both ssDNA and RNA targets.

As shown in **Table 3.3** a stronger duplex is formed between 2',5'-xFA_{18} and dT_{18} than between 2',5'-rA_{18} and dT_{18}. This parallels the observation that dA_{18}:dT_{18} is more stable than rA_{18}:dT_{18}, and suggests that 2',5'-xFA_{18} is a closer mimic of dA_{18}. In other words if the xylo-fluoro-adenosine oligonucleotides are "DNA analogs" then their binding affinity towards dT_{18} would be higher relative to the analogous riboadenosine analog (2',5'-rA_{18}).

To further understand the associative and structural properties of 2',5'-linked oligonucleotides, the binding properties of 2',5'-FXNA towards complementary 2',5'-RNA and 2',5'-FXNA was investigated. The T_m values are given in **Table 3.5**. Melting profiles of single stranded oligonucleotides showed no change in hyperchromicity, indicating lack of self association or complex formation. Melting of all the oligonucleotide duplexes exhibited "sharp" monophasic transitions, indicating the formation of single cooperative complexes.

Table 3.5: Melting temperature of 2',5'-linked oligothymdylates towards complementary 2',5'-linked oligonucleotides.

Sequence	2',5'-rA_{18} (2',5'-RNA)		2',5'-xFA_{18} (2',5'-FXNA)	
	T_m (°C)	%H	T_m (°C)	%H
2',5'-rU_{18}	36.5	13.8	14.0	4.2
2',5'-$xFU^{5\text{-}Me}{}_{18}$	--[b]		45.2	11.9

Buffer: 1M NaCl, 100mM Na_2HPO_4, pH = 7.2. %H = percent hypochromicity. [b] No T_m observed above 5°C. %H = percent hypochromicity.

The 2',5'-$xFU^{5Me}{}_{18}$ oligonucleotide does not bind to 2',5'-rA_{18}, in line with the properties of 2',5'-$xU^{5Me}{}_{18}$ (**Chapter II**). Interestingly, the pure 2',5'-FXNA duplex (i.e., 2',5'-xFA_{18}:2',5'-$xFU^{5\text{-}Me}{}_{18}$; T_m 45.2°C) is more stable than the 2',5'-rA_{18}:2',5'-rU_{18} duplex. This is very similar to the property observed in 3',5'-linked homopolymer oligonucleotides, where dA_{18}:dT_{18} (T_m 59.0°C) duplex (B'-form) is more stable than the rA_{18}:rU_{18} (T_m 50.0°C) duplex. This points to the resemblance of 2',5'-FXNA to DNA in terms of its extended backbone conformation, a notion that is fully supported by the CD studies described below. In sharp constrast, the pure 2',5'-XNA duplex (2',5'-xA_{18}:2',5'-$xU^{5\text{-}Me}{}_{18}$) was not observed, pointing to destabilizing steric interactions (3'-OH versus 3'-F) in this case.

3.5 CIRCULAR DICHROISM (CD) SPECTRA OF 2',5'-LINKED-3'-DEOXY-3'-FLUORO-XYLOFURANOSE-NUCLEIC ACIDS (2',5'-FXNA)

The CD spectra of single strand oligopyrimidines and oligopurines are shown in **Figures 3.9** and **Figure 3.10**, respectively. The CD spectra of the single stranded RNA and DNA controls are similar to the respective spectra of polynucleotides.[200]

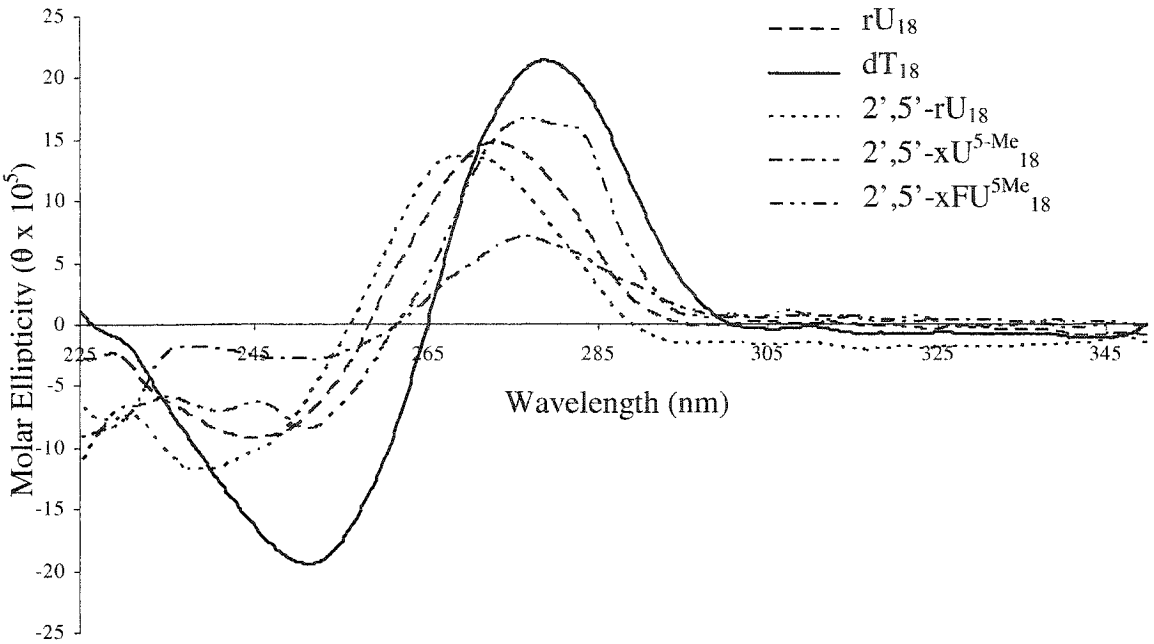

Figure 3.9: CD spectra of various single stranded pyrimidine oligonucleotides at 5°C (1M NaCl, 100mM Na_2HPO_4, pH = 7.2).

The overall CD profiles of the oligopyrimidylates are quite similar. The spectrum of dT_{18} shows a positive λ_{max} around 278 nm, a cross-over at 265 nm with a negative λ_{max} at 251 nm. The corresponding bands of the ribouridylates, namely 3',5'-rU_{18} and 2',5'-rU_{18}, are slightly blue shifted; however, both 3',5'-rU_{18} and 2',5'-rU_{18} display very similar CD profiles. Interestingly, the CD profile of $xFU^{5Me}{}_{18}$ is distinctly different from that of 2',5'-rU_{18}. the former being more "DNA-like" in character. For example, it has a slightly broadened positive Cotton effect around 278 nm (similar to dT_{18}), a blue-shifted cross-over at 261 nm. This crossover is similar to that seen for DNA (dT_{18}). A weak negative Cotton effect is also observed at 251 nm, which is similar to the corresponding DNA (dT_{18}) band but of reduced intensity.

The oligopyrimidines 2',5'-$xU^{5Me}{}_{18}$ and 2',5'-$xFU^{5Me}{}_{18}$ exhibited very similar CD profiles (**Figure 3.9**), although the intensity of the bands were significantly greater for the

latter oligonucleotide. This probably indicates a strong pre-organization of the oligonucleotide and/or higher intramolecular base stacking interactions within the 2',5'-xFU^{5Me}_{18} strand.

Figure 3.10 shows the CD profiles of oligoadenylate single strands. As discussed in **Chapter II**, the CD profile of rA_{18} is quite different from that of dA_{18}, the former displaying more dominant Cotton effects as a consequence of the greater pre-organized nature of the RNA strand. In this regard, 2',5'-rA_{18} resembles rA_{18}, although the bands of the 2',5'-isomer are slightly shifted (negative Cotton effect and cross-over position) and of lower intensity. As pointed out previously, this does not necessarily reflect reduced stacking in 2',5'-rA_{18} strands relative to normal RNA strands since the spectra of these isomeric compounds have slightly different band positions.[96] A more plausible explanation of the CD results is that the angle between the transition moments of the bases differs between rA_{18} and 2',5'-rA_{18}, resulting in a smaller rotational strength for the 2',5'-rA_{18}–strand stacks relative to the 3',5'-strand stacks. In fact, NMR and hypochromicity data indicate that the overlapping of the bases in single-stranded 2',5'-RNA is more extensive than in single-stranded RNA. However, the same may not apply to the 2',5'-xFA_{18} oligomer, which exhibits a very different (weak) CD profile that somewhat resembles that of DNA (dA_{18}).

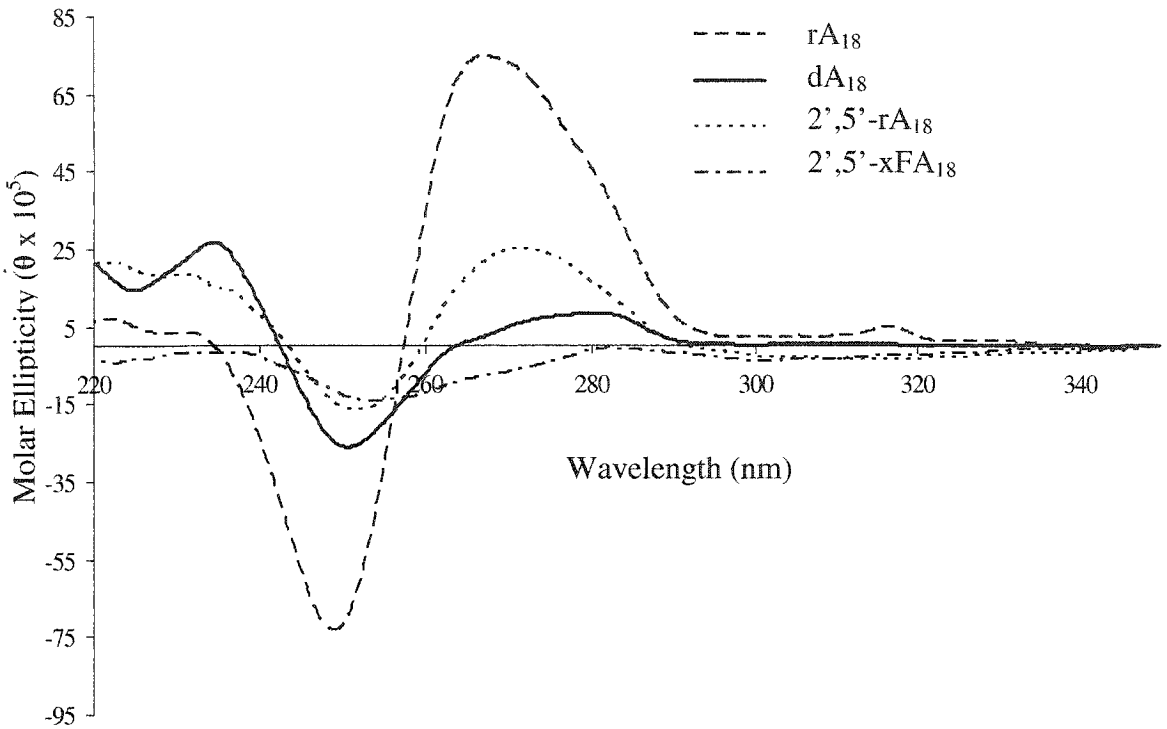

Figure 3.10: CD spectra of various single stranded purine oligonucleotides at 5°C (1M NaCl, 100mM Na_2HPO_4, pH = 7.2).

The CD spectra of various duplexes in which the target RNA strand is rA_{18}, are shown in **Figure 3.11**. The rA_{18}:2',5'-rU_{18} duplex is closer in structure to the rA_{18}:rU_{18} duplex than to the rA_{18}:dT_{18} duplex. The CD spectra of rA_{18}:2',5'-xFU^{5Me}_{18} shows characteristics similar to the spectra of both rA_{18}:dT_{18} and rA_{18}:2',5'-rU_{18}, namely, a broad positive cotton effect and cross-over wavelength as seen for rA_{18}:dT_{18} and a negative band similar to that seen for the rA_{18}:2',5'-rU_{18} duplex. This is probably due to the more rigid ribopurine which dictates the overall structure of the hybrid duplex.

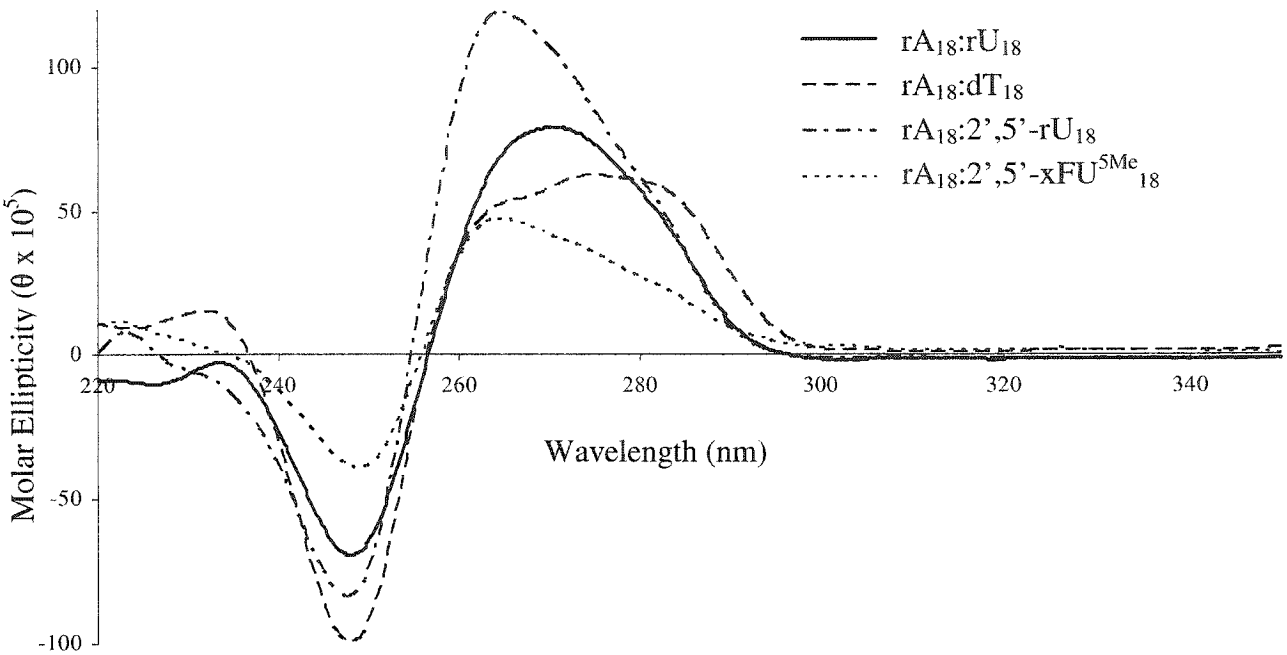

Figure 3.11: CD spectra of ribooligoadenylates hybridized to pyrimidine-oligonucleotides at 5°C (1M NaCl, 100mM Na_2HPO_4, pH = 7.2).

The duplex rA_{18}:2',5'-$xFU^{5\text{-}Me}{}_{18}$ is quite weak (T_m 10.7°C), as is the case for the analogous rA_{18}:2',5'-$xU^{5\text{-}Me}{}_{18}$ hybrid (T_m < 5°C; **Chapter II**). To confirm the formation of rA_{18}:2',5'-$xFU^{5\text{-}Me}{}_{18}$, its spectrum was compared to the summed spectra of the individual strands (rA_{18} + 2',5'-$xFU^{5\text{-}Me}{}_{18}$; **Figure 3.12**). The CD bands of rA_{18} are more intense than those of 2',5'-$xFU^{5\text{-}Me}{}_{18}$, and this is likely due to the more effective base stacking of the larger purines. As a result, the calculated rA_{18} + 2',5-$xFU^{5Me}{}_{18}$ spectrum is very similar to that of rA_{18} By contrast, the hybrid spectrum (rA_{18}:2',5'-$xFU^{5\text{-}Me}{}_{18}$) displays significantly weaker molar ellipticities (positive and negative), confirming the interaction (albeit weak) between 2',5'-$xFU^{5\text{-}Me}{}_{18}$ and rA_{18}.

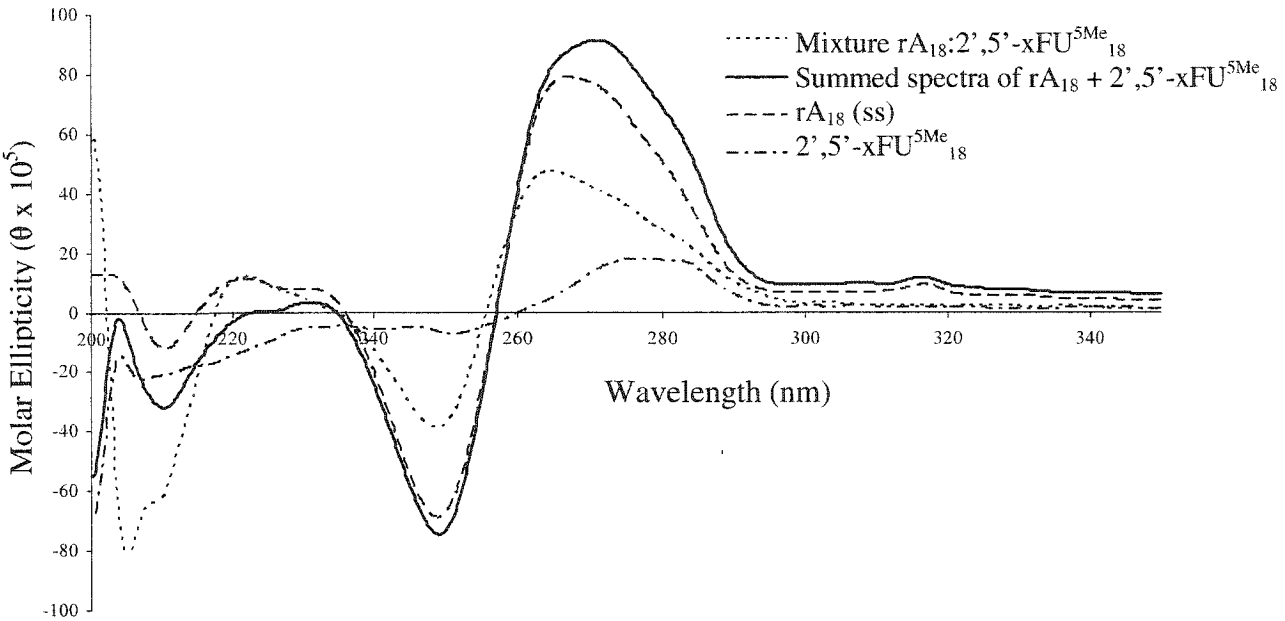

Figure 3.12: Comparison of the summed CD spectra of rA_{18}:$xFU^{5\text{-}Me}{}_{18}$, duplex and single strand oligonucleotides at 5°C (1M NaCl, 100mM Na_2HPO_4, pH = 7.2).

The spectra of duplexes formed with dA_{18} are shown in **Figure 3.13**. No duplex association was observed for the dA_{18}+2',5'-$xFU^{5Me}{}_{18}$ mixture (UV studies). The CD spectral profile of the summed spectra of dA_{18} and 2',5'-$xFU^{5Me}{}_{18}$ is very similar to the experimentally obtained spectrum of the mixture, indicating a lack of association between these strands. This would be in agreement with the observed properties of 2',5'-linked oligonucleotides, which show selective binding to RNA over DNA.

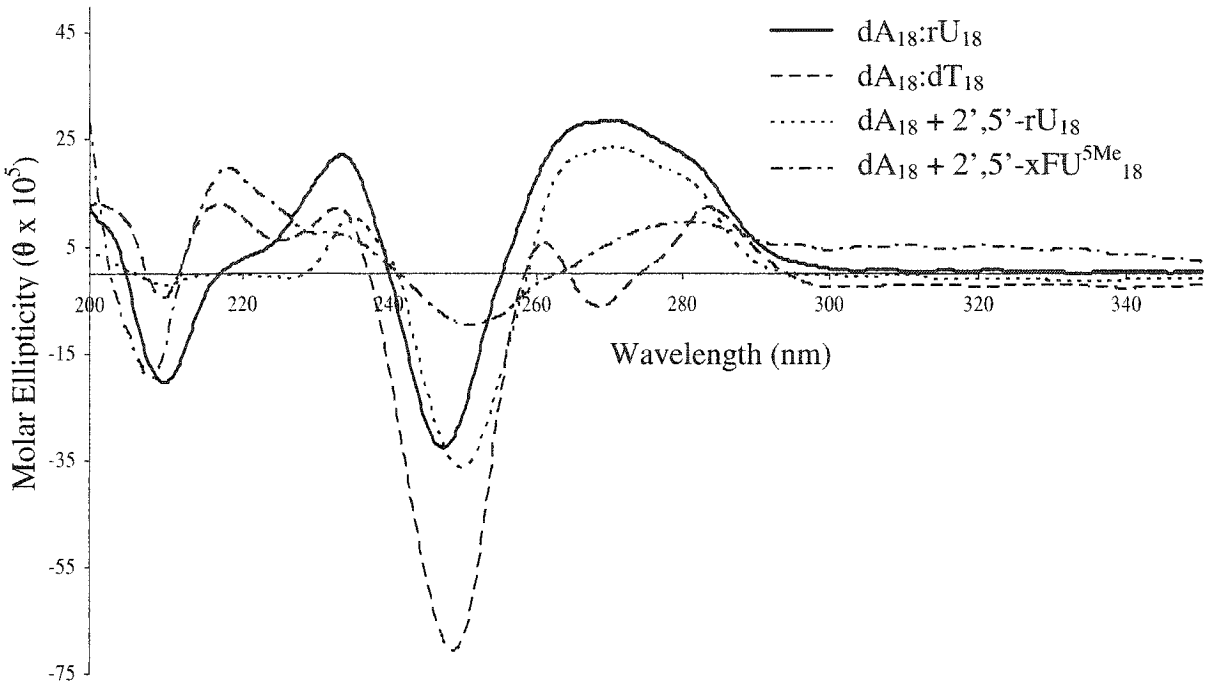

Figure 3.13: CD spectra of deoxy-oligoadenylates hybridized to pyrimidine-oligonucleotides at 5°C (1M NaCl, 100mM Na_2HPO_4, pH = 7.2).

Next, the structural properties of duplexes formed with 2',5'-xFA_{18} were assessed, and compared with those of other nucleic acid duplexes. The spectrum of 2',5'-xFA_{18}:rU_{18} **(Figure 3.14)** shows strong similarity to the dA_{18}:rU_{18} spectrum, although the former exhibits weaker bands. The positive cotton effects (260-290nm), the crossover wavelength (255nm) and the negative band (246nm) are nearly identical for these two hybrids. The weaker molar ellipticities observed for 2',5'-xFA_{18}:rU_{18} are not due to weak stacking interactions since a strong hyperchromic shift was observed upon melting of this duplex. Therefore, it is probable that the particular (pre-organized) structure adopted by the 2',5'-xFA_{18}:rU_{18} duplex results in reduced absorption of the circularly polarized light.

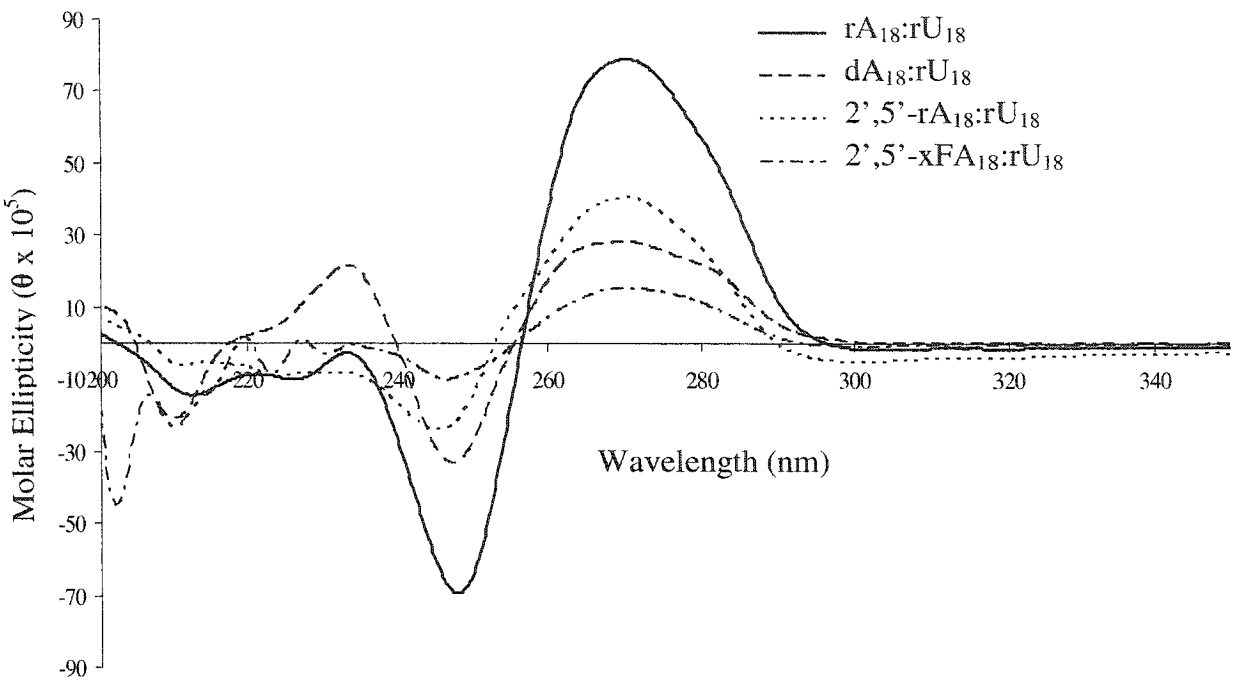

Figure 3.14: CD spectra of ribo-oligouridylates hybridized to purine-oligonucleotides at 5°C (1M NaCl, 100mM Na_2HPO_4, pH = 7.2).

Figure 3.15 shows the spectra of duplexes formed with dT_{18}. As previously stated, the dA_{18}:dT_{18} duplex forms the typical B'-structure whereas the rA_{18}:dT_{18} duplex is "A-like". The spectrum of the 2',5'-xFA_{18}:dT_{18} duplex is different from all other duplex spectra. Since the structure of a duplex is dominated by the purine rich strand, the CD spectral signatures are likely indicative of the structure formed by 2',5'-xFA_{18}. Evidently this is quite different from the stability and structure of duplexes formed by dA_{18} and rA_{18} and their complementary (dT_{18}) strands.

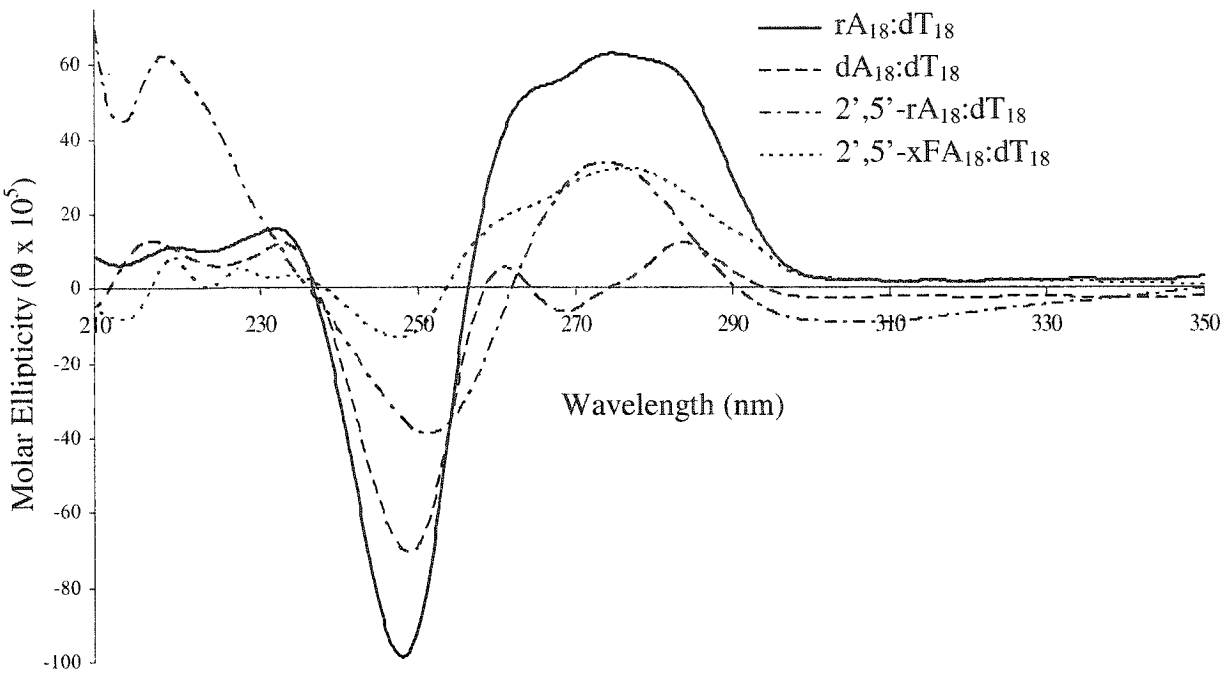

Figure 3.15: CD spectra of deoxy-oligothymidylates hybridized to purine-oligonucleotides at 5°C (1M NaCl, 100mM Na_2HPO_4, pH = 7.2).

To further improve our understanding of the binding and structural properties of 2',5'-FXNA, studies on an oligonucleotide of mixed base composition were carried out.

3.6 STUDIES ON 2',5'-FXNA/RNA and 2',5'-FXNA/DNA DUPLEXES OF MIXED BASE COMPOSITION

A 2',5'-FXNA sequence of mixed base composition ("CAT") was designed and prepared to be complementary to the genomic HIV-1 RNA sequence. Melting curves of 2',5'-XFNA annealed to complementary RNA and single-stranded DNA were obtained in a buffer containing 140 mM K^+, 1 mM Mg^+, and 5 mM Na^+ (pH 7.2), which is representative of intracellular conditions. Thermal dissociation (T_m) data for the complexes formed are summarized in **Table 3.6**.

The 2',5'-FXNA:RNA shows a single cooperative transition at 24.1 °C, while an equimolar mixture of 2',5'-FXNA and DNA showed no transition. This is consistent with earlier findings that 2',5'-linked oligonucleotides can form duplexes with RNA, but they associate only weakly, or not at all, with single-stranded DNA.[97,98] The weak percent hyperchromicity observed for 2',5'-FXNA:RNA (13.6%) relative to RNA:RNA (20.8%) is also characteristic of duplexes formed by 2',5'-linked oligonucleotides.

Furthermore, no duplex formation is observed upon mixing of 2',5'-FXNA with 2',5'-RNA, in agreement with our homopolymer studies (above), in which no complexation was detected between 2',5'-$xFU^{5\text{-}Me}_{18}$ and 2',5'-rA_{18} (**Table 3.5**).

Table 3.6: Thermal melting (T_m) data obtained upon binding of 2',5'-FXNA (**3.17**) of mixed base composition with complementary RNA, DNA and 2',5'-RNA.[a]

Sequence[b]	RNA target {%H}[c]	DNA target {%H}[c]	2',5'-RNA target {%H}[c]
RNA	56.0 {20.8}	30.0 {18.1}	34.1 {15.5}
DNA	53.0 {18.2}	51.0 {22.1}	8.0 {11.6}
2',5'-RNA	36.0 {17.8}	<5.0	24.1 {14.6}
2',5'-FXNA	24.1 {13.6}	<5.0	<5.0

[a] All duplexes were 2.3 x 10^{-6} M in concentration. All transitions were monophasic. Buffer: 140mM KCl, 1mM $MgCl_2$, 5mM Na_2HPO_4, pH = 7.2
[b] Sequence: 5'-TTA TAT TTT TTC TTT CCC-3' or 2'
[c] Target: 5'-GGG AAA GAA AAA ATA TAA-3' or 2
[d] For RNA and 2',5'-RNA, T is replaced by U

Interestingly the binding properties of 2',5'-FXNA are nearly identical to those observed for the 2',5'-XNA sequence, i.e., a weak binding to RNA with a low percent hyperchromicity and no duplex formation with DNA or 2',5'-RNA. This suggests that the weak association properties of 2',5'-XNA and 2',5'-FXNA are a result of the

conformation of the constituent nucleotides rather than steric interactions caused by the 3'-substituent. Another possible explanation is that 2',5'-FXNA and 2',5'-XNA act as a 'DNA mimics', as predicted by the structural models of Yathindra *et al.*[77,104] To further test these ideas, circular dichroism spectroscopy on the duplexes was carried out.

3.7 CD STUDIES ON MIXED BASE 2',5'-FXNA/RNA AND 2',5'-FXNA/DNA DUPLEXES

The spectra of single strands and duplexes are shown in **Figures 3.16 A&B** and **Figure 3.17**, respectively. The spectra of single stranded RNA, DNA and 2',5'-RNA were already discussed in **section 2.7**. The overall spectra are very similar with small but important differences. The CD signatures of the RNA strand are slightly blue shifted relative to those observed for the DNA strand and show a stronger positive Cotton effect. The CD profile of 2',5'-FXNA very closely resembles that of DNA, with only slight differences in the intensity of the bands. This shows that the single stranded 2',5'-FXNA sequence adopts a structure that is similar to the structure of DNA. In other words, the 'extended' conformation adopted by the 2',5'-FXNA strand (C3'-*endo*) is equivalent to the 'extended' conformation adopted by 3',5'-DNA (C2'-*endo*), as predicted by the Yathindra model.[77]

A comparison of the CD spectra of 2',5'-FXNA and 2',5'-XNA are shown in **Figure 3.16 B**. The CD signatures are nearly identical for the two oligonucleotides with the xylo-fluoro-oligomer showing stronger molar ellipticities; this is probably a reflection of the more rigid (locked) backbone of the 3'-fluorinated oligonucleotide.

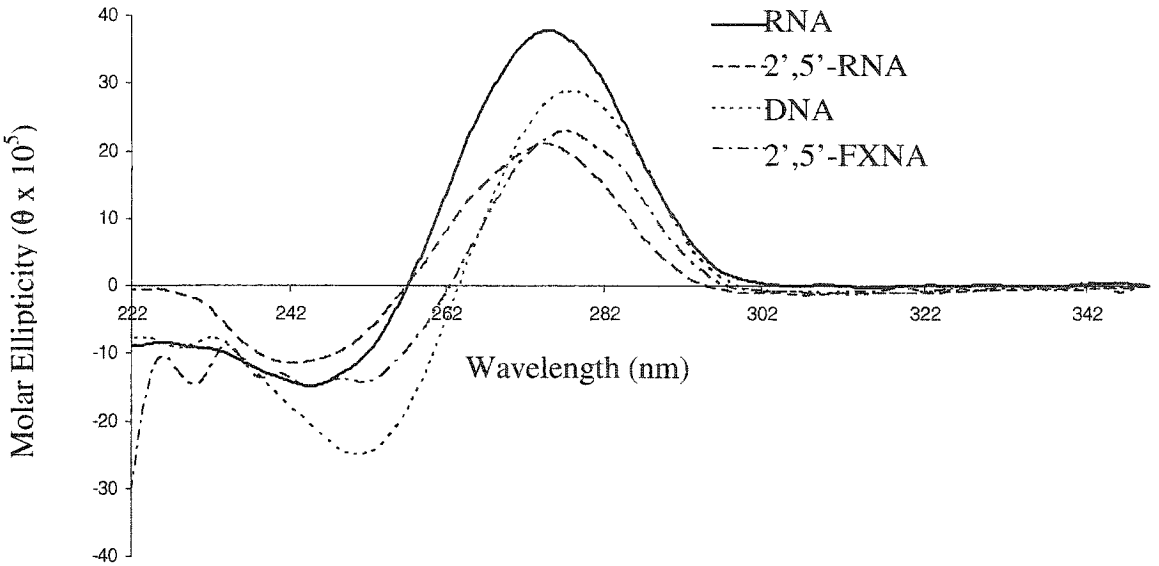

Figure 3.16 A: CD spectra of single strands of oligonucleotides complementary to HIV-1 genomic sequence at 5°C. The sequence (**3.17**) is shown in **Table 3.1**. Buffer: 140mM KCl, 1mM $MgCl_2$, 5mM Na_2HPO_4, pH = 7.2). Concentration of single strands was 2.3 μM.

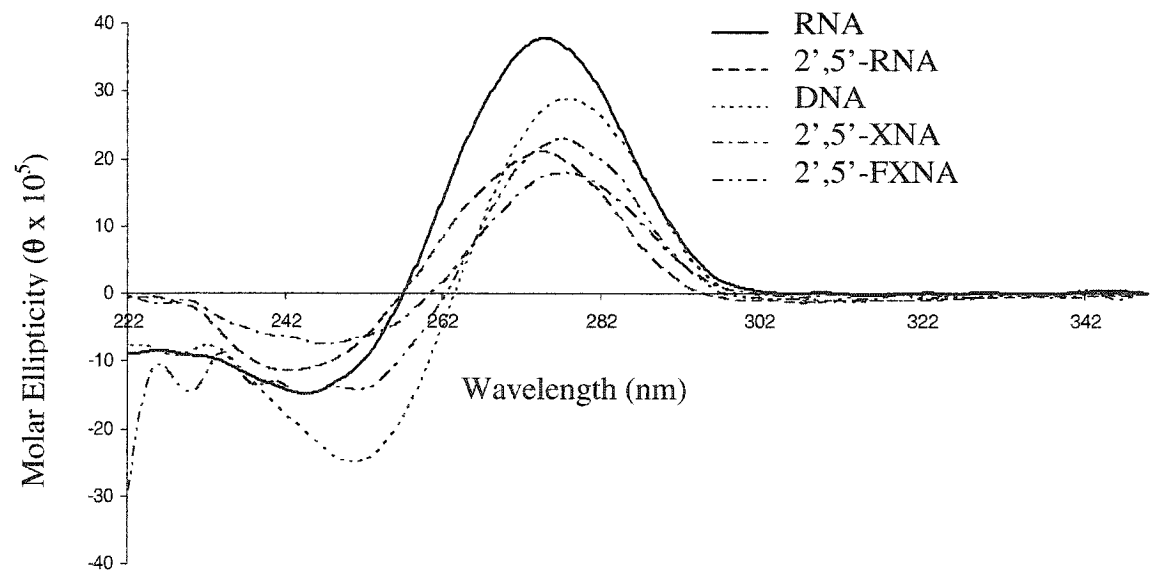

Figure 3.16 B: CD spectra of single strands of oligonucleotides complementary to HIV-1 genomic sequence at 5°C. The sequence (**3.17**) is shown in **Table 3.1**. Buffer: 140mM KCl, 1mM $MgCl_2$, 5mM Na_2HPO_4, pH = 7.2). Concentration of single strands was 2.3 μM.

The CD spectra of duplexes formed with target RNA are shown in **Figure 3.17**. The RNA:2',5'-FXNA duplex has CD signatures that resemble those seen for the RNA:DNA and RNA:2',5'-RNA duplexes. The positive cotton effect is composed of two bands, one around 280nm (as seen in RNA:DNA) and another around 262 nm (observed in RNA:2',5'-RNA). Thus the band at 262nm could be a result of the topological structure imposed by the 2',5'-phosphodiester linkage. The other significant spectral feature are the cross-over wavelength (254nm for RNA:2',5'-FXNA and 257nm for RNA:DNA) and strong negative cotton effect (247nm for RNA:2',5'-FXNA vs. 245nm for RNA:DNA). This, along with the overall shape of the CD spectra, indicates that 2',5'-FXNA behaves as a 'DNA mimic'.

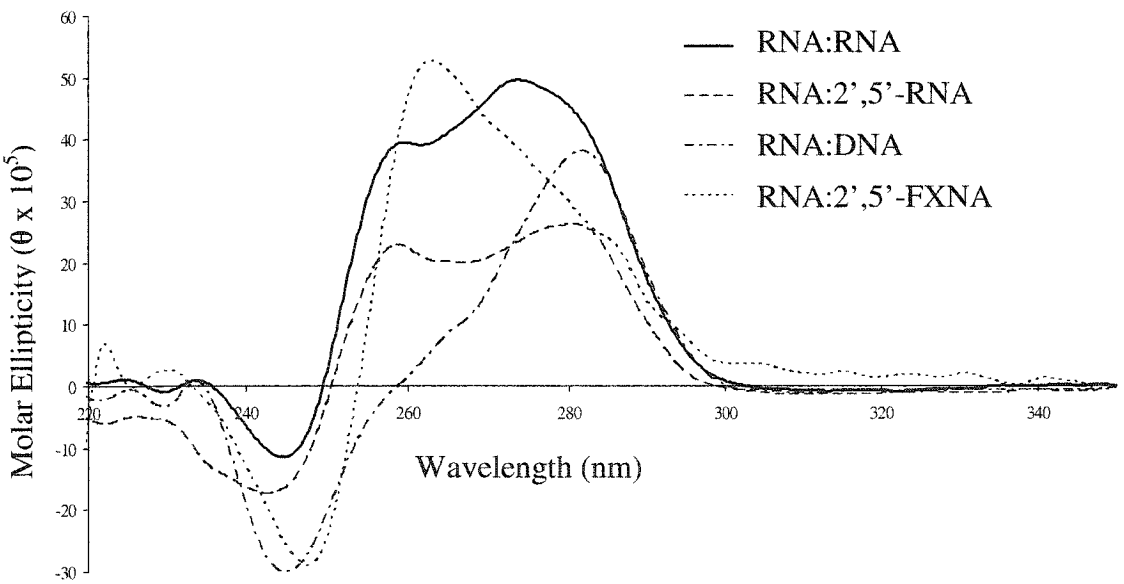

Figure 3.17: CD spectra of duplexes formed with a common RNA target at 5°C. The legend shows the antisense strand used and the sequence (**3.17**) is reported in **Table 3.1**. Buffer: 140mM KCl, 1mM $MgCl_2$, 5mM Na_2HPO_4, pH = 7.2). Duplex concentration was 2.3 μM.

3.8 INVESTIGATING RNase H ACTIVATION BY 2',5'-XYLO-3'-FLUORO-OLIGONUCLEOTIDES (2',5'-FXNA)

The reader is referred to **section 1.3** for a background on antisense technology as a means for gene silencing. The ability of xylo-fluoro-oligonucleotides to elicit RNase H activity has not preveiously been assessed.

Figure 3.18 shows PAGE analysis of the enzyme assays carried out. As control, we also examined the ability of the native RNA:DNA hybrid of the same sequence to serve as substrates for RNase H. The reaction was stopped after five and ten minutes, and the sample was denatured and loaded onto a denaturing acrylamide gel. As seen in Figure 3.18 RNase H was only able to degrade RNA in the RNA:DNA hybrid; the RNA:2',5'-FXNA heteroduplex did not serve as a substrate for RNase H, despite the fact that CD studies indicate that this duplex mimics the global helical structure of DNA:RNA substrate. This indicates that the 2',5'-backbone upon duplex formation yields a structure that is still slightly different with respect to its minor groove dimensions, the site of RNase H binding.

Based on studies of 2',5'-FXNA, the same conclusions are attained as 2',5'-XNA. Overall, at the global level the 2',5'-FXNA behaves as an 'extended' oligonucleotide and a DNA analogue with 2',5'-linkage.

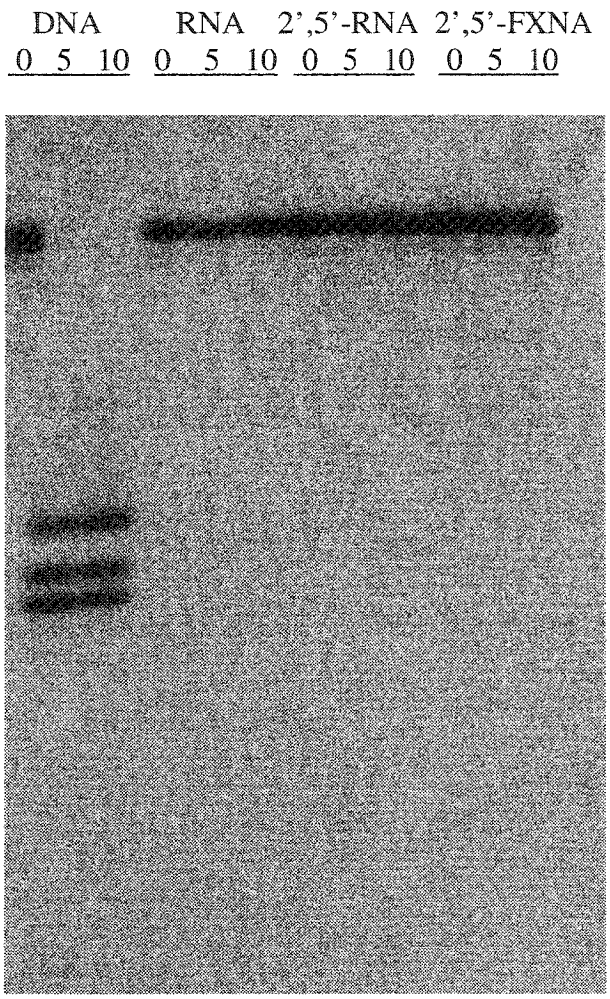

Figure 3.18: PAGE analysis of RNA degradation by RNase H using antisense oligonucleotides (Sequence: 5'-TTA TAT TTT TTC TTT CCC-3' or 2' with T replaced by U in RNA and 2',5'-RNA). 1pmol of target 5'-[^{32}P]-RNA and 10pmol of antisense oligonucleotide were incubated in 60mM TRIS-HCl (pH 7.8), 2mM DTT, 60mM KCl and 2.5mM $MgCl_2$. Reaction was initiated by the addition of *E. coli* RNase H at 15 °C and quenched at 0, 5 and 10 minute intervals. The gel was visualized by autoradiography.

CHAPTER IV

SYNTHESIS, PHYSICOCHEMICAL AND BIOCHEMICAL PROPERTIES OF 3'-DEOXY-3'-FLUORO-OLIGORIBONUCLEOTIDES

4.1 BACKGROUND

Our studies on 2',5'-linked xylose and 3'-fluoroxylose containing oligonucleotides strongly suggest that these compounds have an 'extended' C3'-*endo* sugar-phosphate backbone conformation that is characteristic of native 3',5'-linked DNA (C2'-*endo* sugar conformation) (**Chapter 3**). Conversely, 2',5'-linked nucleic acids that adopt a C2'-*endo* sugar conformation are expected to have a 'compact' backbone structure that is characteristic of the native RNA (C3'-*endo* sugar conformation). Consistent with this notion, 2',5'-RNA (C2'-*endo*) is structurally similar to RNA and, in fact, exhibits higher binding affinities to complementary oligonucleotides compared to 2',5'-XNA and 2',5'-FXNA. In order to obtain further experimental evidence of the relationship of sugar pucker and backbone geometry, we synthesized a 2',5'-linked octadecamer of 3'-deoxy-3'-fluoro-5-methyl-ribouridine ($rFU^{5\text{-}Me}_{18}$) and studied its physicochemical and biochemical properties (**Figure 4.1**). $rFU^{5\text{-}Me}_{18}$ is the 3'-epimer of the previously studied $xFU^{5\text{-}Me}_{18}$ oligonucleotide (**Chapter 3**) and, as described below, is expected to adopt a C2'-*endo*/compact geometry and hence to bind favourably with complementary RNA. Such binding would give robust support to the theory of sugar conformational switch (Yathindra's structural basis of 2',5'-nucleic acids)[77,94,104] that occurs in 3',5'-RNA ('compact' C3'-*endo*) and 2',5'-linked RNA oligonucleotides ('compact' C2'-*endo*).

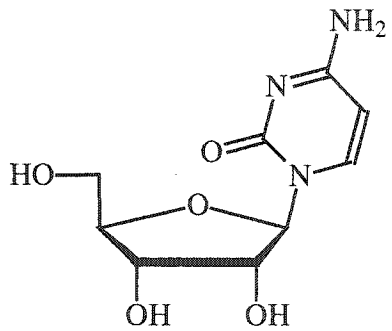

ribo C

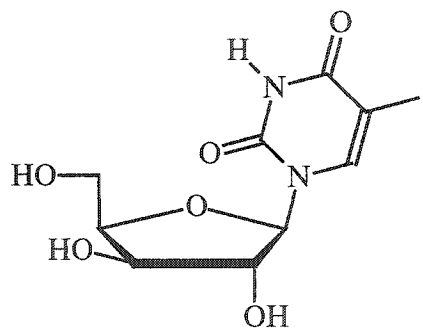

xyloU$^{5\text{-Me}}$

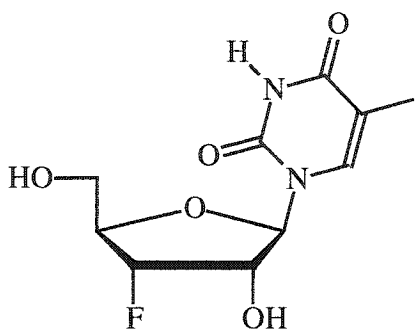

3'-deoxy-3'-fluoro-riboU$^{5\text{-Me}}$

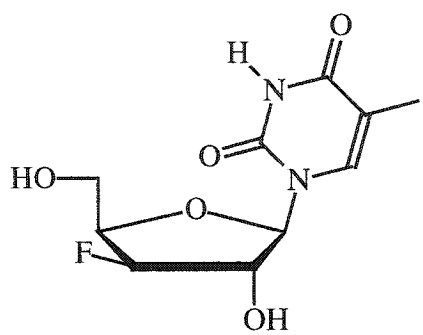

3'-deoxy-3'-fluoro-xyloU$^{5\text{-Me}}$

Figure 4.1: Structural comparison of 3'-deoxy-3'-fluoro-5-methyl-ribouridine nucleoside to natural and 3'-modified nucleosides.

The effect of fluorine substitution for a hydroxyl has been discussed previously (**Section 3.1**). Interest in the synthesis of 3'-fluoro-2',3'-dideoxyribonucleosides arose due to their cytostatic and antiviral properties.[231-8] The pyrimidine 2',3'-dideoxy-3'-fluoronucleosides were prepared by reaction of O^2,3'-anhydrothymidine with a nucleophilic fluoride source, while the purines were obtained via trans-glycosylation of the fluorinated pyrimidines.[239]

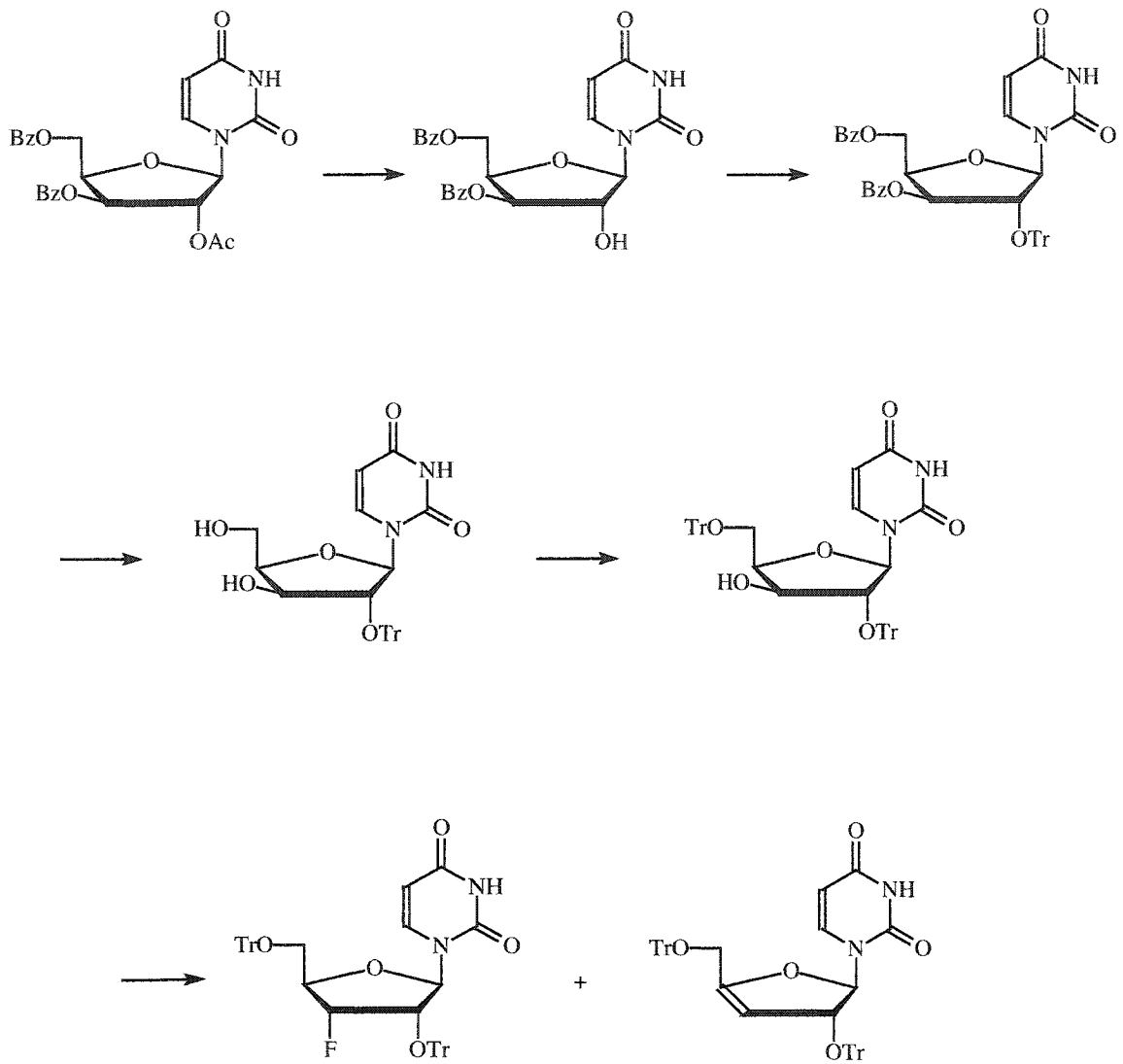

Figure 4.2: Synthesis of 3'-deoxy-3'-fluoro-ribofuranosyl-nucleoside from xylo-nucleoside.[240]

Alternatively, 3'-deoxy-3'-fluoro-ribonucleosides can be obtained by either direct modification of nucleosides or by coupling of the appropriate sugar to various heterocyclic bases. It was initially shown that 3'-fluoro-ribonucleosides could be synthesized directly from xylonucleosides[240] (**Figure 4.2**). Preparation has also been described starting from adenosine (**Figure 4.3**), which involves laborious purification of

mixtures of 2' and 3'-protected isomers.[241-3] The appropriate sugar precursor, for base coupling, was prepared as shown in **Figure 4.4**.[245-6]

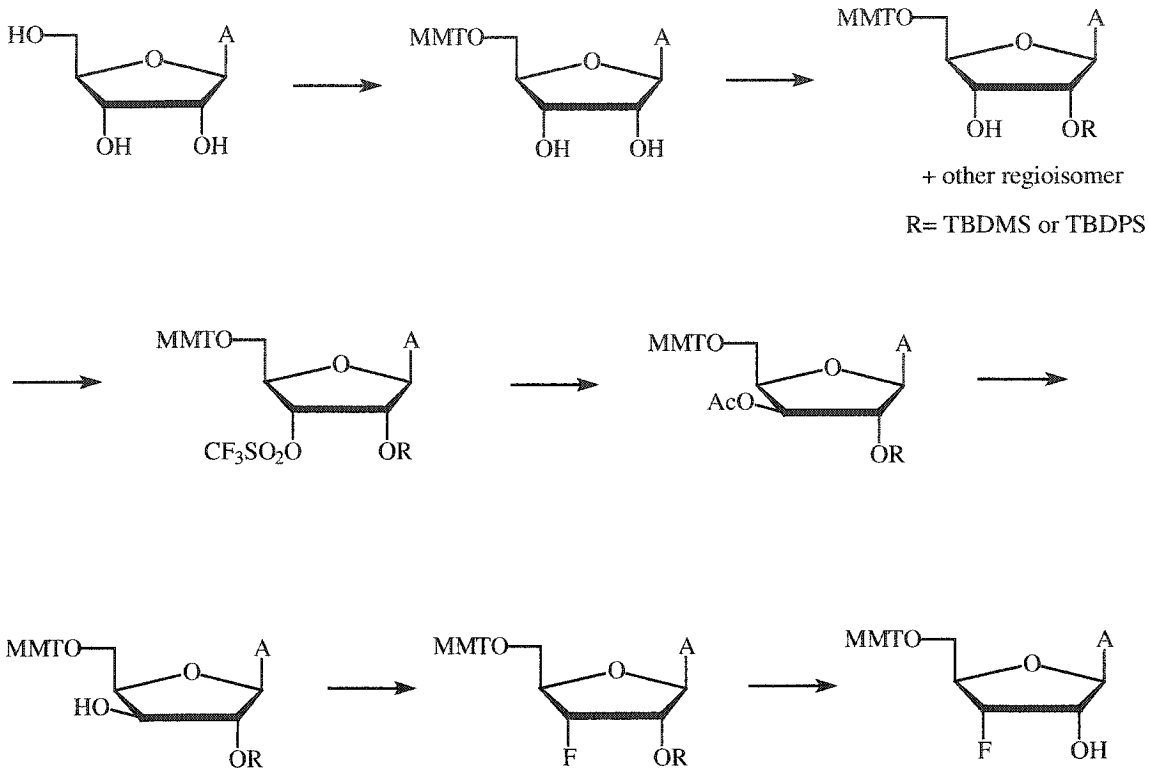

Figure 4.3: Synthesis of 3'-deoxy-3'-fluoro-ribofuranosyl nucleoside starting from ribo-nucleoside.[241-243]

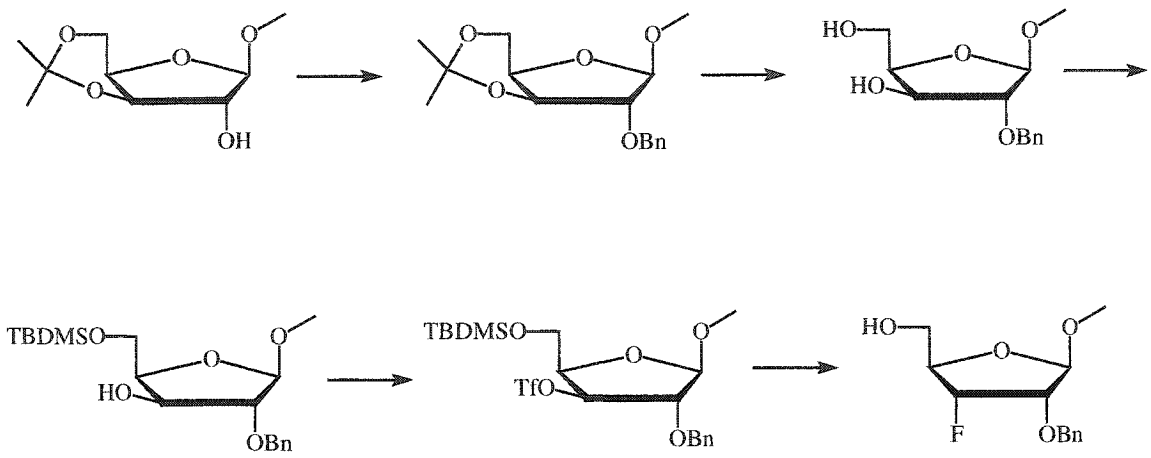

Figure 4.4: Synthesis of 3-fluoro-ribofuranosyl sugar precursor for coupling to heterocyclic bases.[244,245]

2',5'-Linked trinucleotides containing 3'-fluoroadenosine have been synthesized,[247] and studied from a structural perspective.[216,219] These compounds have also found application for studying RNA degradation by induction of RNase L.[209,248] As for 2',5'-linked rApApA, conformational NMR analysis of these compounds indicated that the sugar units existed exclusively in the C2'-*endo* (Southern) form (**Figure 4.5**). This data agreed with the enzyme binding assay performed which indicated that the 2',5'-linked-3'-deoxy-3'-fluoro-ribonucleic acids (2',5'-FRNA) behave in similar manner as 2',5'-linked RNA with respect to induction of RNaseL.

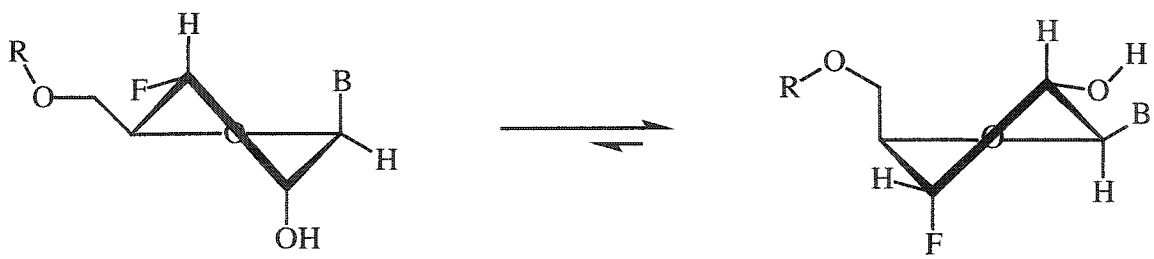

Figure 4.5: Sugar conformation of 3'-deoxy-3'-fluoro-ribonucleosides. The C2'-*endo* conformation is favored in short oligonucleotides.

The following sections describe the synthesis and properties of rFU^{5Me} and $rFU^{5Me}{}_{18}$. The ability of the latter compound to activate RNase H was also assessed.

4.2 SYNTHESIS OF PROTECTED 3'-DEOXY-3'-FLUORO-β-D-RIBONUCLEOSIDE-2'-PHOSPHORAMIDITES

During the course of this study, we pursued two routes to the synthesis of 3'-deoxy-3'-fluoro-5'-methylribouridine, i.e. via modification of a nucleoside, as well as coupling of an appropriate sugar precursor to thymine. The desired nucleoside, $rFU^{5\text{-}Me}$, was successfully prepared from 5-methyl-xylouridine. Described in this section are also attempts to couple a 3-fluoro-ribofuranose sugar precursor to thymine via the Vorbrüggen procedure.

Synthesis of 3'-deoxy-3'-fluoro-5-methyl-ribouridine was achieved by taking advantage of the selective silylation of xylonucleosides, discovered by us during the course of this study (**Chapter 2**), along with literature precedence on synthesis of 3'-fluoro-riboadenosine (**Figure 4.3**).[241,242] The drawback of the literature procedure[241,242] is that mixtures of 2' and 3'-silylated ribonucleoside are obtained which necessitates difficult separation. This is completely avoided with our protocol (**Figure 4.6**).

The sugar conformation of xylonucleosides is predominantly C3'-*endo* (N-conformation).[178] During the course of reaction with DAST, an intermediate would be formed with a pseudo-axial C4'-proton and O3'-triflate like group which would lead to the elimination product (Watanabe et al.) (**CHAPTER II**).[230] However Watanabe *et al.* do point out that in the case of xylonucleosides, fluorination at the C3'-position does take place (S_N2) and that other factors like basicity of the reaction medium is also responsible

for the extent of competing elimination product (E2). We utilized both TBDMS and TBDPS silyl protecting groups for the 2'-hydroxyl and found that a better yield of the desired 3'-fluorinated product was obtained when TBDPS was used. This could be due to the larger protecting group occupying a pseudo axial position which may shift the sugar pucker away from the C3'-*endo* conformation.

A second concern was the potential desilylation of the nucleoside by fluoride ions during the DAST reaction, however Battistini and coworkers noted that this reaction is minimized by using the TBDPS instead of the TBDMS group.[241] Our results with the pyrimidine nucleoside are in complete agreement with their observations. Interestingly we found out that use of pyridine in the DAST reaction resulted in 2'-desilylation along with fluorination at C3', a convenient way to carry out two steps under the same conditions. However side products were also obtained under these conditions making purification more difficult.

The synthetic route for 3'-fluoro-ribopyrimidines as described by Battistini could pose another problem. During the inversion of stereochemistry at C3' (from ribo to xylonucleoside) participation of the exocyclic base oxygen (O^2) could yield an O^2,C3'-anhydronucleoside, which upon hydrolysis, affords a mixture of xylo and ribo-nucleosides. The use of xylo-nucleoside starting materials would avert this problem. The xylo-configuration of the nucleoside would also prevent any exocyclic nucleophilic participation during DAST reaction.

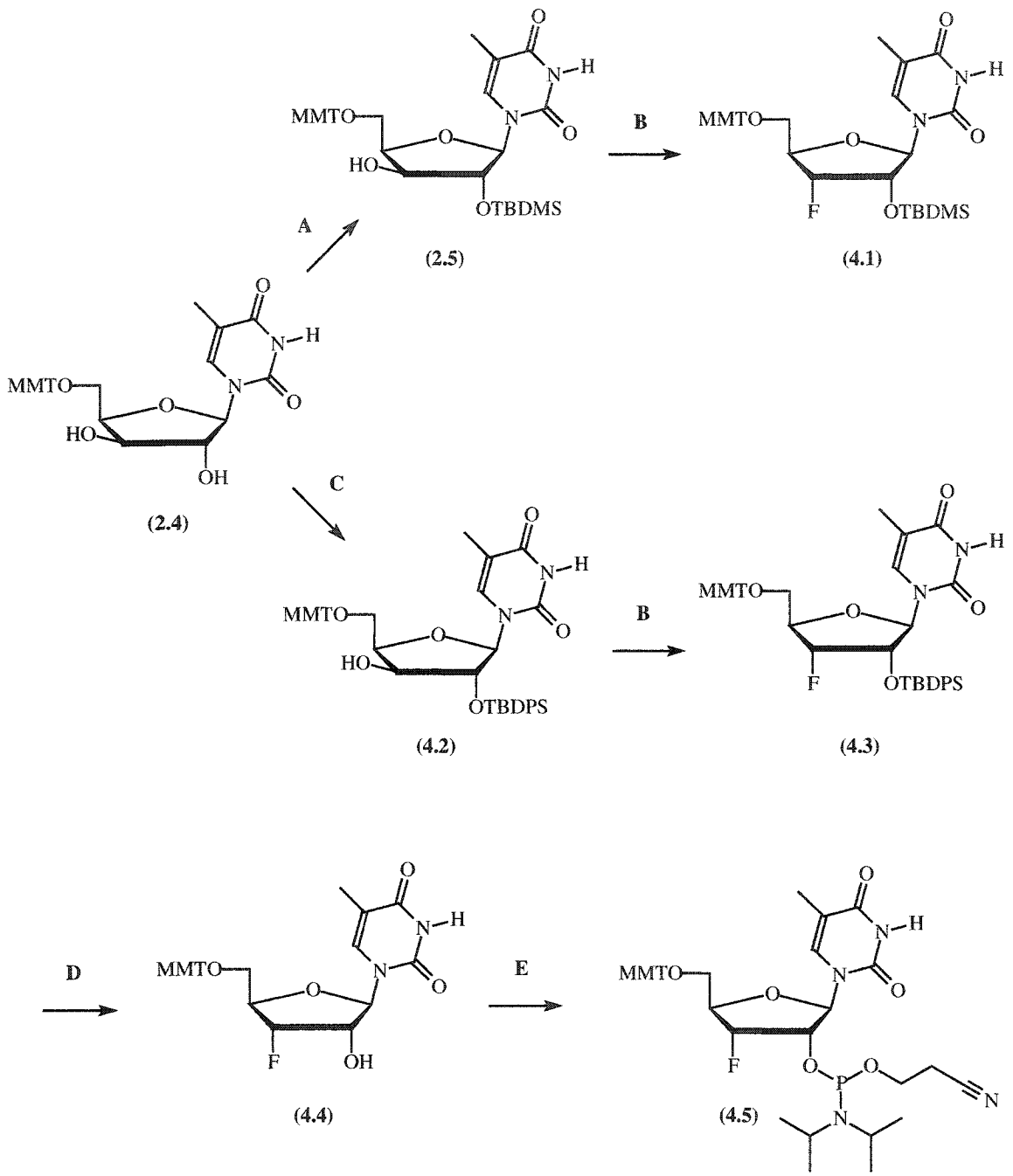

Figure 4.6: Scheme for the synthesis of 5'-O-MMT-3'-deoxy-3'-fluoro-5-methyl-ribouridine-2'-O-cyanoethyl phosphoramidite (**4.5**). **A.** TBDMS-Cl, imidazole, DMF, r.t., overnight (88%); **B.** DAST, CH_2Cl_2, r.t. (58%); **C.** TBDPS-Cl, imidazole, DMF, r.t., overnight (quant.); **D.** TBAF, THF, r.t. (quant.); **E.** Cl-P(OCE)(N-iPr_2) (1.2 eq), DIPEA (2.4 eq) (85%).

The synthesis of 5'-MMT-2'-phosphoramidite derivative of 3'-deoxy-3'-fluoro-5-methyl-ribouridine is shown in **Figure 4.6**. Starting from 5'-MMT-2'-TBDMS-5-methyl-xylouridine (**2.5**), fluorination using DAST gave the desired 3'-fluorinated-ribonucleoside. However the yields obtained were low and purification was complicated by the presence of impurities. Therefore 5'-MMT-5-methyl-xylouridine was silylated using TBDPS-Cl to obtain (**4.2**); the silylation also proceeded selectively with only the 2'-silylated being formed. The DAST reaction of (**4.2**) resulted in formation of 5'-MMT-2'-TBDPS-3'-fluoro-5-methyl-ribouridine (**4.3**) with acceptable yield (58%).

Compound (**4.3**) was characterized by NMR. The ^{19}F NMR spectra consisted of a ddd (seven peaks due to overlap of 2 peaks) as expected due to coupling of 3'-F with H-3', H-2' and H-4'. ^{1}H and COSY-NMR spectroscopy led to the assignment of the sugar protons and are shown in **Figure 4.7**. The large ^{1}H-^{1}H coupling observed between H1' and H2', was expected, and is indicative of a C2'-*endo* like sugar conformation. The 3'-proton shows the largest splitting due to geminal coupling with the 3'-fluorine atom, this being proof that fluorine is at the 3'-carbon. To confirm that the desired 3'-fluoro-ribonucleoside had formed a NOESY experiment was carried out and is shown in **Figure 4.8**. The spectra shows nuclear Overhauser effects between H-3' and H-5' further corroborates the xylo to ribo configurational change during the fluorination reaction.

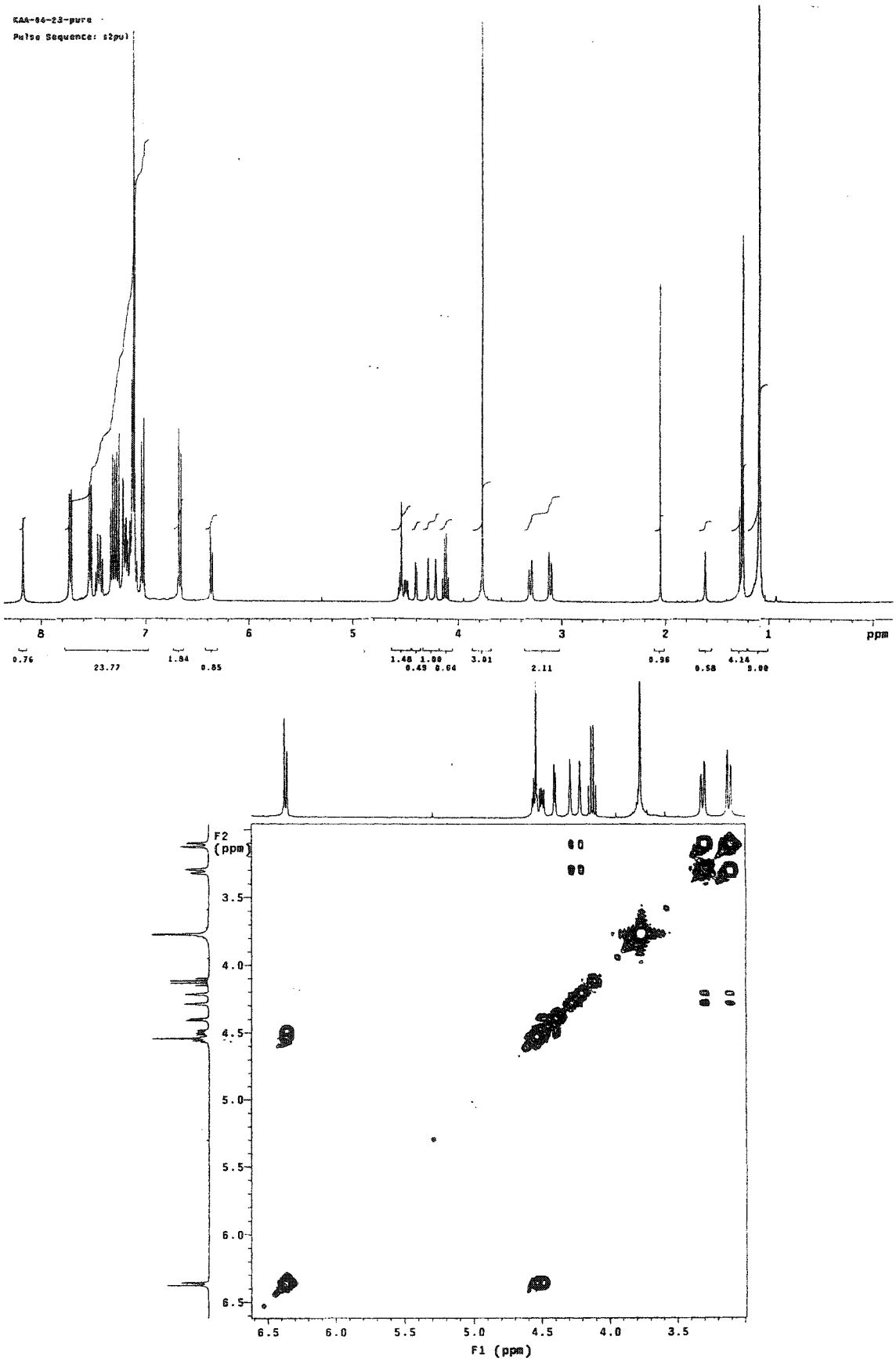

Figure 4.7: The ^{1}H and ^{1}H-COSY NMR spectra of 5'-O-MMT-3'-deoxy-3'-fluoro-2'-O-TBDPS-5-methyl-ribouridine (**4.3**).

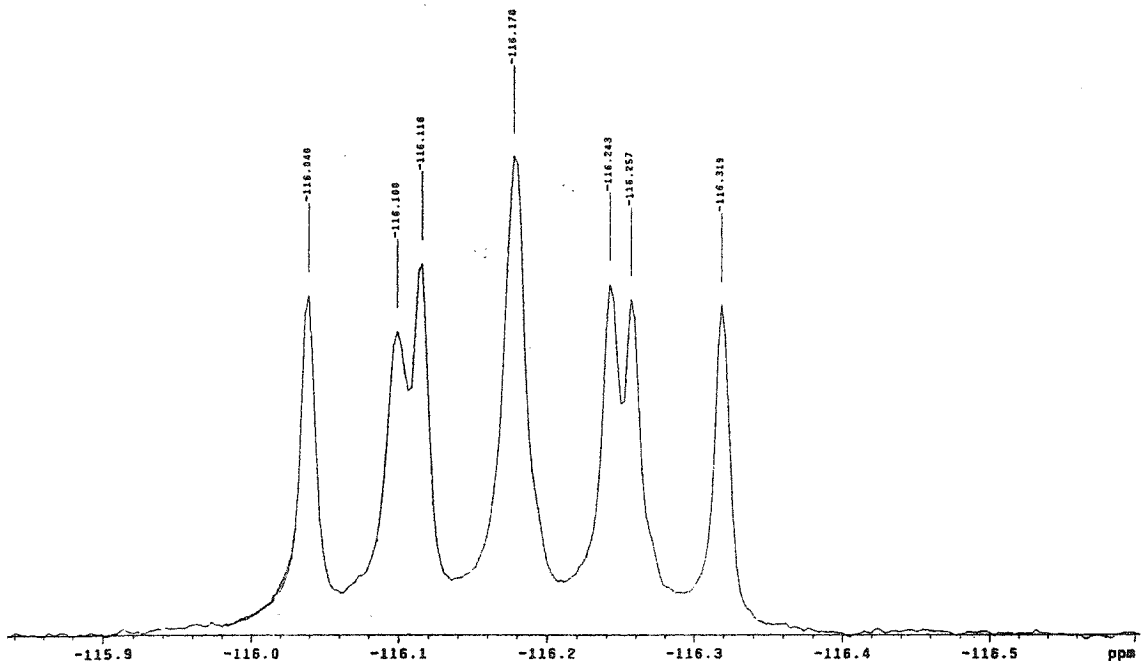

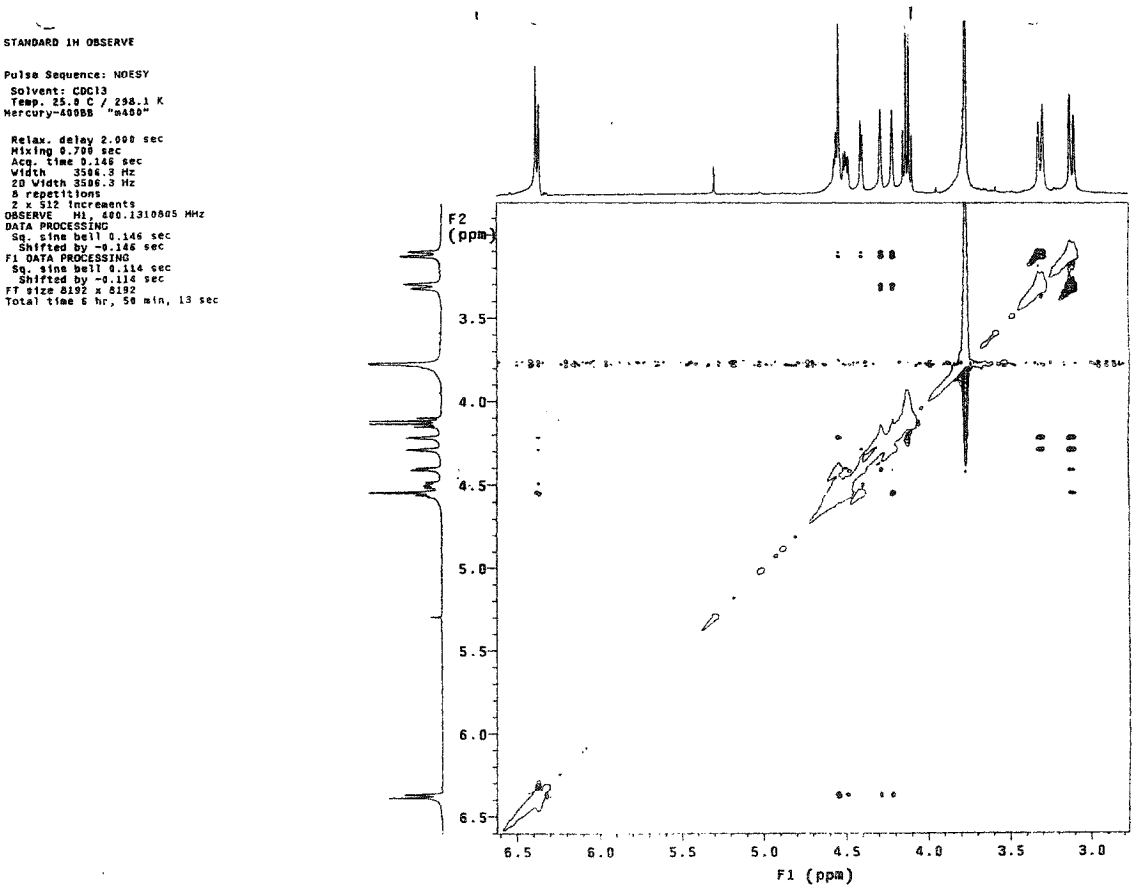

Figure 4.8: The ^{19}F and NOESY spectra of 5'-O-MMT-3'-deoxy-3'-fluoro-2'-O-TBDPS-5-methyl-ribouridine (**4.3**).

The silyl-protection was removed using TBAF to obtain (**4.4**) in excellent yield; the ^{1}H-NMR and COSY spectra are shown in **Figure 4.9**. The different sugar protons are nicely resolved which simplified their assignment (COSY). The normal ^{1}H-NMR pattern of ribo-nucleosides follows the order: H-1', H-2'/ H-3', H-4', H-5' and H-5", with H-1' being the most deshielded proton (5.5 – 6.5 ppm). A similar pattern is observed with 3'-fluoro-ribonucleosides with H-3' being more deshielded than H-2' due to the electronegative fluorine atom. Also observed is the expected large splitting of H-3' due to geminal coupling with fluorine. The nucleoside was then phosphitylated to obtain 5'-MMT-3'-deoxy-3'-fluoro-5-methyl-ribouridine-2'-cyanoethyl phosphoramidite (**4.5**), which is the immediate precursor to oligonucleotide synthesis.

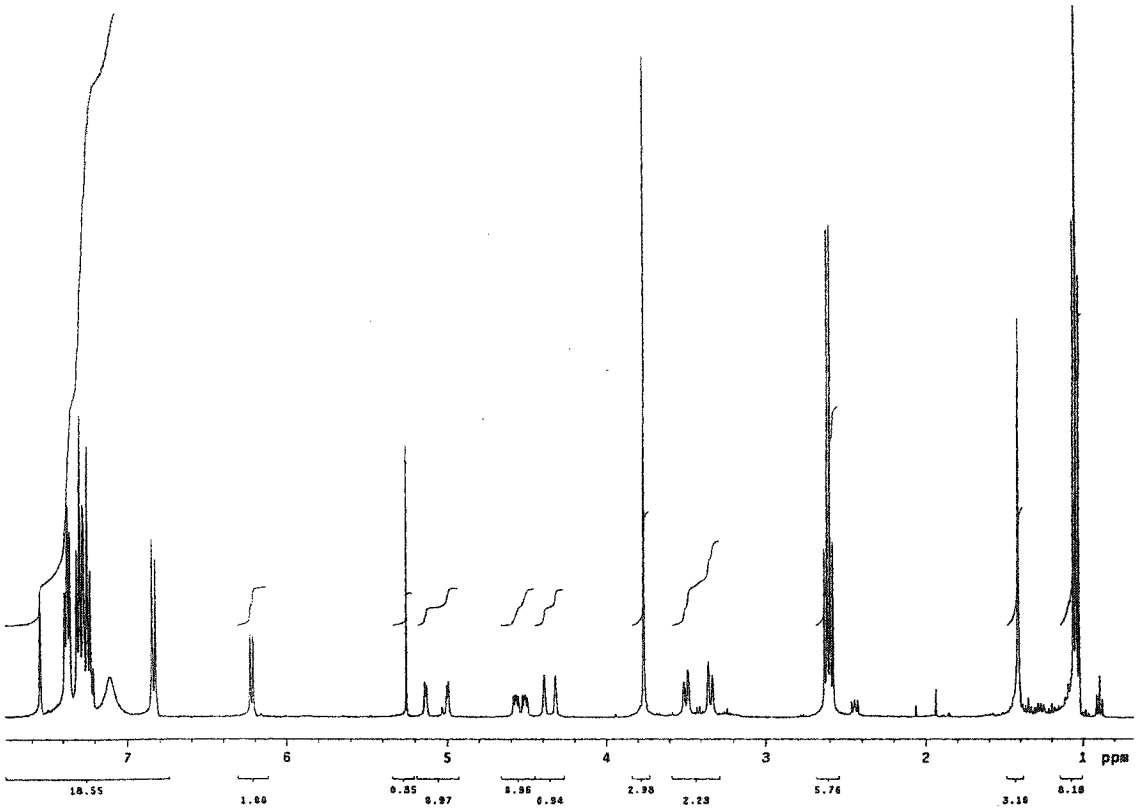

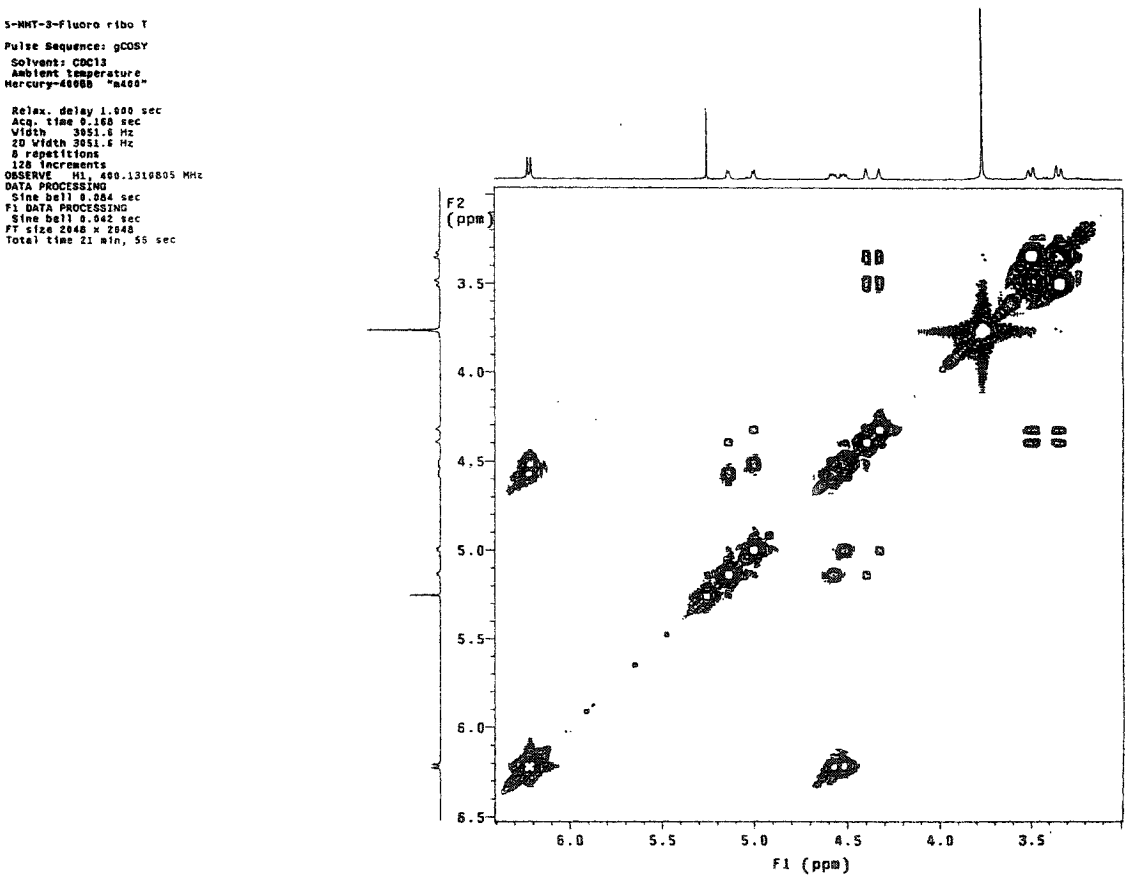

Figure 4.9: The ^{1}H-NMR and COSY spectra of 5'-O-MMT-3'-deoxy-3'-fluoro-5-methyl-ribouridine (**4.4**).

The synthesis of 3-deoxy-3-fluoro-ribofuranose sugar, for nucleoside synthesis via a Vorbrüggen type reaction was also attempted (**Figure 4.10**). Starting from commercially available 1,2-O-isopropylidene-D-xylofuranose, the 5-hydroxyl was selectively protected using p-toluoyl chloride. This was followed by reaction with triflic anhydride to yield the 3-triflate derivative. However experimental conditions are yet to be determined for conversion of the 3-O-triflate derivative to the desired 3-fluoro-ribofuranose.

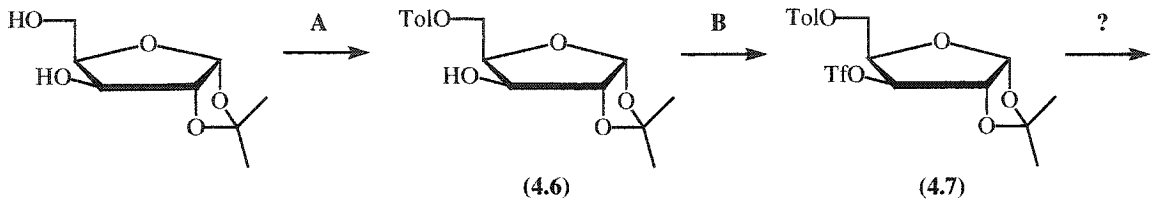

Figure 4.10: Attempted synthesis of a sugar precursor amenable to heterocyclic base coupling for synthesis of 3'-fluoro-ribonucleosides.

4.3 SYNTHESIS OF 2',5'-LINKED-3'-DEOXY-3'-FLUORO-RIBOFURANOSE NUCLEIC ACIDS (2',5'-FRNA)

LCAA-CPG was activated and succinylated as described by Damha *et al.*[192] and the nucleoside was coupled according to Pon's procedure.[194] Loading of 5'-MMT-3'-deoxy-3'-fluoro-5-methyl-ribouridine on the solid support was ~85μmol/g. Only one oligonucleotide, namely 2',5'-$rFU^{5\text{-}Me}{}_{18}$ (**Seq. 4.8**) was synthesized. An RNA synthesis cycle was utilized for synthesis of this oligonucleotide with minor modifications. An extended coupling time (900 s) for amidite coupling was used along with a longer detritylation time to remove the more stable 5'-monomethoxytrityl group. The activator used for oligonucleotide synthesis was 4,5-dicyanoimidazole and the coupling efficiency

ranged from 98-101%. This was higher than previously observed for 2',5'-FXNA synthesis (96-101%), indicating that the 2',3'-trans configuration of functional groups requires a superior activator. Deprotection and purification of 2',5'-rFU$^{5\text{-Me}}_{18}$ was performed under standard conditions used for DNA synthesis, with a moderate recovery of the product. Characterization of the oligonucleotide was carried out by gel electrophoresis and MALDI-TOF spectrometry (**Figure 4.11**). The mobility of the oligonucleotide was very similar to that of DNA and RNA strands of same chain length and base composition. MALDI-TOF MS confirmed the identity of the oligonucleotide sequence (theoretical: 5736 g/mol; calculated: 5736 g/mol).

Binding studies were carried out with complementary DNA and RNA; and the structures of these oligonucleotides and duplexes were studied via CD spectroscopy. The ability of xFU$^{5\text{-Me}}_{18}$ to elicit RNase H activity was also assessed.

A

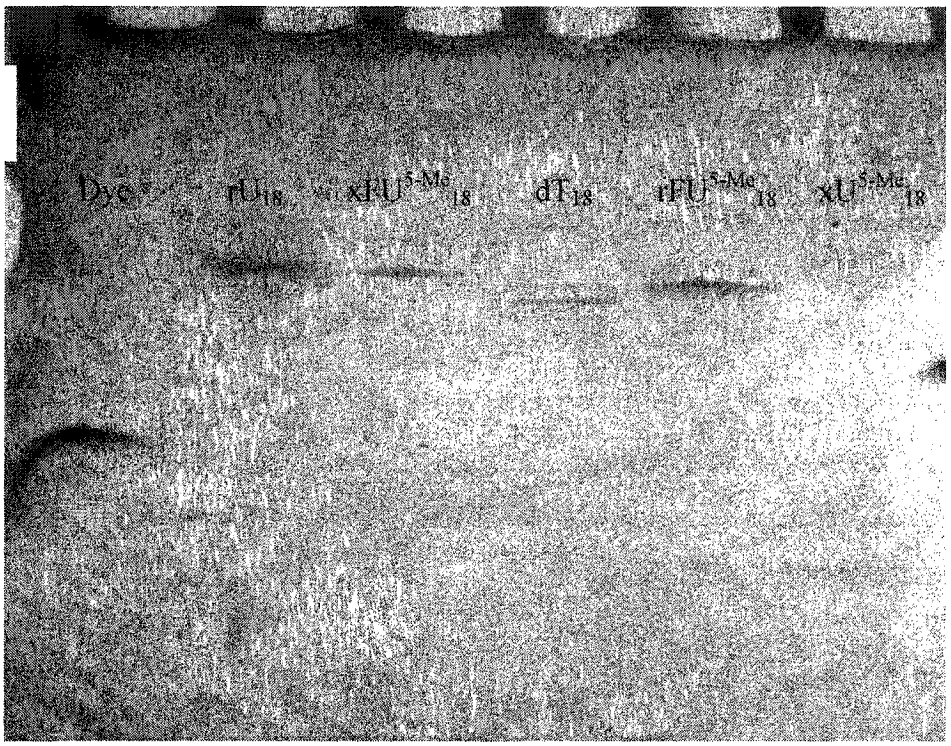

B

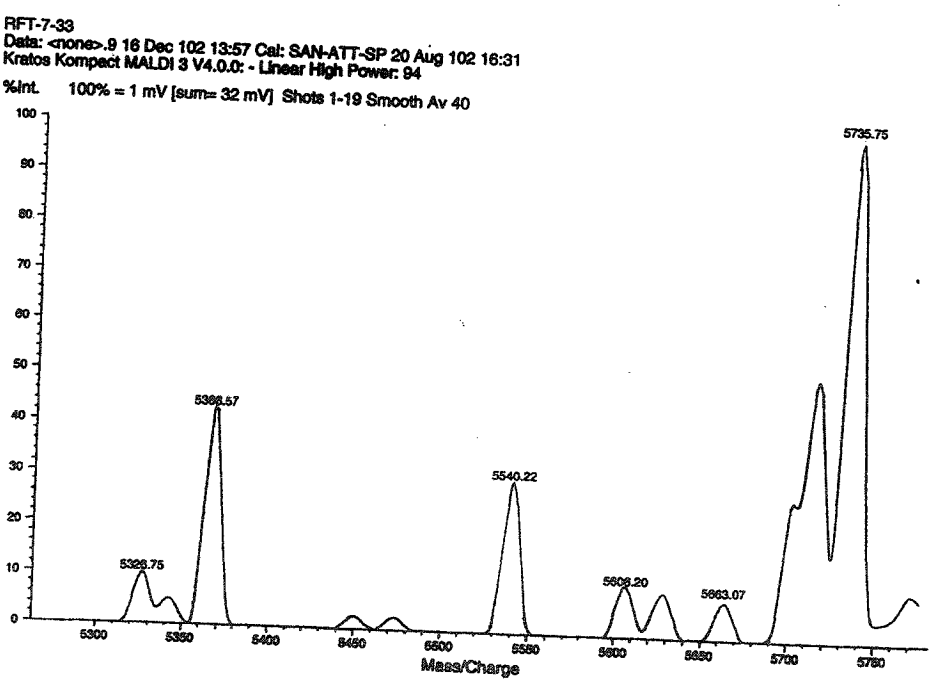

Figure 4.11: (A) Polyacrylamide Gel Electrophoresis (PAGE) of 18-unit long oligonucleotides (24% polyacrylamide, 7 M Urea in TBE buffer). (B) MALDI-TOF mass spectra of 2',5'-linked rFU$^{5\text{-Me}}_{18}$.

4.4 DUPLEX FORMATION BY 2',5'-LINKED-3'-DEOXY-3'-FLUORO-5-METHYL-RIBOURIDYLIC ACID (2',5'-rFU$^{5\text{-Me}}_{18}$)

To the best of our knowledge, there are no previous studies on the binding properties of 2',5'-FRNA oligonucleotides. The binding properties of 2',5'-rFU$^{5\text{-Me}}_{18}$, along with those of its corresponding DNA, RNA and 2',5'-RNA sequences, are summarized in **Table 4.1**.

Table 4.1: Melting temperature of various oligo-pyrimidines towards complementary adenosine-oligonucleotides[a]

Sequence	RNA (rA_{18})		DNA (dA_{18})	
	T_m (°C)	%H	T_m (°C)	%H
rU_{18}	50.0	13.3	44.2	22.6
dT_{18}	52.1	27.2	59.0	27.0
2',5'-rU_{18}	36.4	17.5	--[b]	
2',5'- rFU$^{5\text{-Me}}_{18}$	40.0	21.2	--[b]	

[a] Buffer: 1M NaCl, 100mM Na_2HPO_4, pH = 7.2. [b] No T_m observed above 5°C. %H = percent hyperchromicity.

Melting curves of oligomers annealed to complementary RNA and single-stranded DNA were obtained in a buffer containing 1M NaCl, 100mM Na_2HPO_4, pH = 7.2. The duplex of rFU$^{5\text{-Me}}_{18}$ with rA_{18} showed a single cooperative transition centered at 40°C (Table 1), whereas no complex was detected between rFU$^{5\text{-Me}}_{18}$ and its complementary DNA strand.

This is consistent with earlier findings that 2',5'-linked oligonucleotides associate with RNA, but they associate only weakly, if at all, with single-stranded DNA. [98] Of note, the 2',5'-rFU$^{5\text{-Me}}_{18}$:rA_{18} hybrid is of higher thermal stability than the 2',5'-rU_{18}:rA_{18} hybrid (ΔTm = 3.6 °C), although less stable than the native RNA duplex

(rU_{18}:rA_{18}; ΔT_m = 10 °C). The fact that 2',5'-$rFU^{5\text{-}Me}{}_{18}$:rA_{18} is significantly more stable than 2',5'-$xFU^{5\text{-}Me}{}_{18}$:rA_{18} and 2',5'-$xU^{5\text{-}Me}{}_{18}$:rA_{18} (duplexes not detected; Chapters 2 & 3). This is highly supportive of the notion that 2',5'-$rFU^{5\text{-}Me}{}_{18}$ adopts a 'compact' RNA-like conformation. In addition, these observations nicely substantiate Yathindra's model[77,104] about the effect of sugar pucker on the backbone geometry of 2',5'-linked oligonucleotides.

4.5 CIRCULAR DICHROISM (CD) SPECTRA OF 2',5'-LINKED-3'-DEOXY-3'-FLUORO-5-METHYL-RIBOURIIDINE (2',5'-$rFU^{5\text{-}Me}{}_{18}$)

Analogous to our previous studies, in order to get insight into the structure of 2',5'-FRNA and the duplexes it forms, circular dichroism spectroscopy was carried out.

The CD spectra of single strand oligothymidylates and oligouridylates are shown in **Figure 4.12**. **Figure 4.12a** compares the spectra of 2',5'-$rFU^{5\text{-}Me}{}_{18}$ to rU_{18} and dT_{18}. The overall CD profile is quite similar to that of rU_{18}. **Figure 4.12b** compares the CD spectra of all pyrimidine oligonucleotides synthesized. The general trend observed is that 2',5'-linked oligoribonucleotides display spectra similar to RNA, whereas 2',5'-linked oligoxylonucleotides have spectral signatures that resemble those of DNA.

Figure 4.13a compares the CD spectra of 2',5'-$rFU^{5\text{-}Me}{}_{18}$, rU_{18} and dT_{18} bound to rA_{18}. **Figure 4.13b** compares CD profiles of all pyrimidine strands/rA_{18} combinations. The crossover wavelength and negative cotton effects of duplexes of 2',5'-$rFU^{5\text{-}Me}{}_{18}$, rU_{18} and dT_{18} bound to rA_{18} are very similar under these conditions. The major difference lies in the positive peak, where rA_{18}:dT_{18} shows a broad band while rA_{18}:rU_{18} shows a sharper and more distinct positive λ_{max}. The CD profile of rA_{18}:2',5'-$rFU^{5\text{-}Me}{}_{18}$ closely

resembles that of the pure RNA duplex (rA_{18}:rU_{18}), displaying a sharp positive cotton effect with a prominent λ_{max}. All in all, the CD spectra further corroborate Yathindra's basis of sugar conformational effects on the structure of 2',5'-linked oligonucleotides. 2',5'-Oligoribonucleotides and their analogues adopt the C2'-*endo* sugar conformation and a 'compact oligonucleotide' structure that resembles the native RNA structure, whereas 2',5'-oligoxylonucleotides (with a C3'-*endo* sugar conformation) exhibit an extended backbone resembling that of DNA.

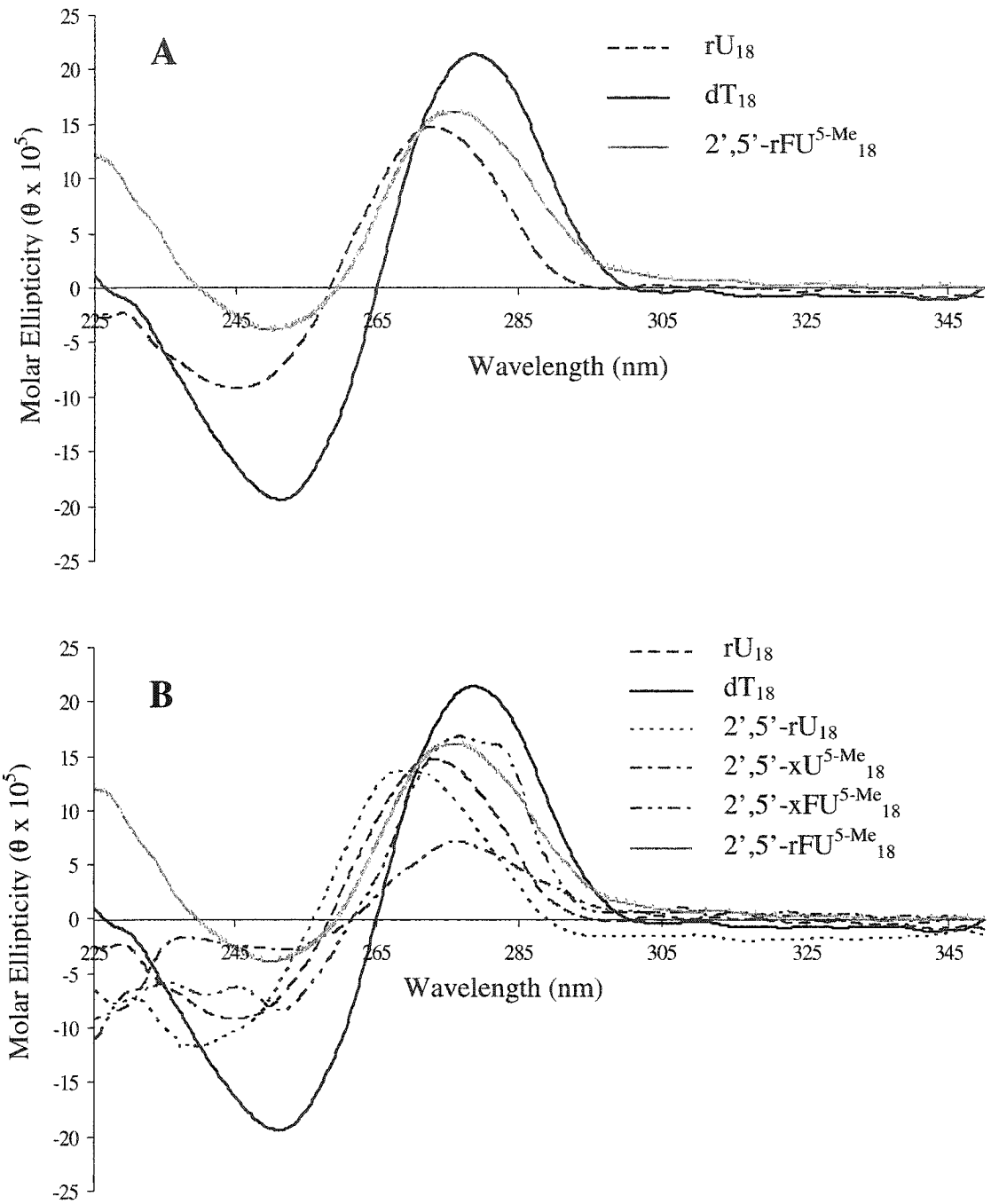

Figure 4.12: CD spectra of various single stranded pyrimidine oligonucleotides at 5°C (1M NaCl, 100mM Na_2HPO_4, pH = 7.2).

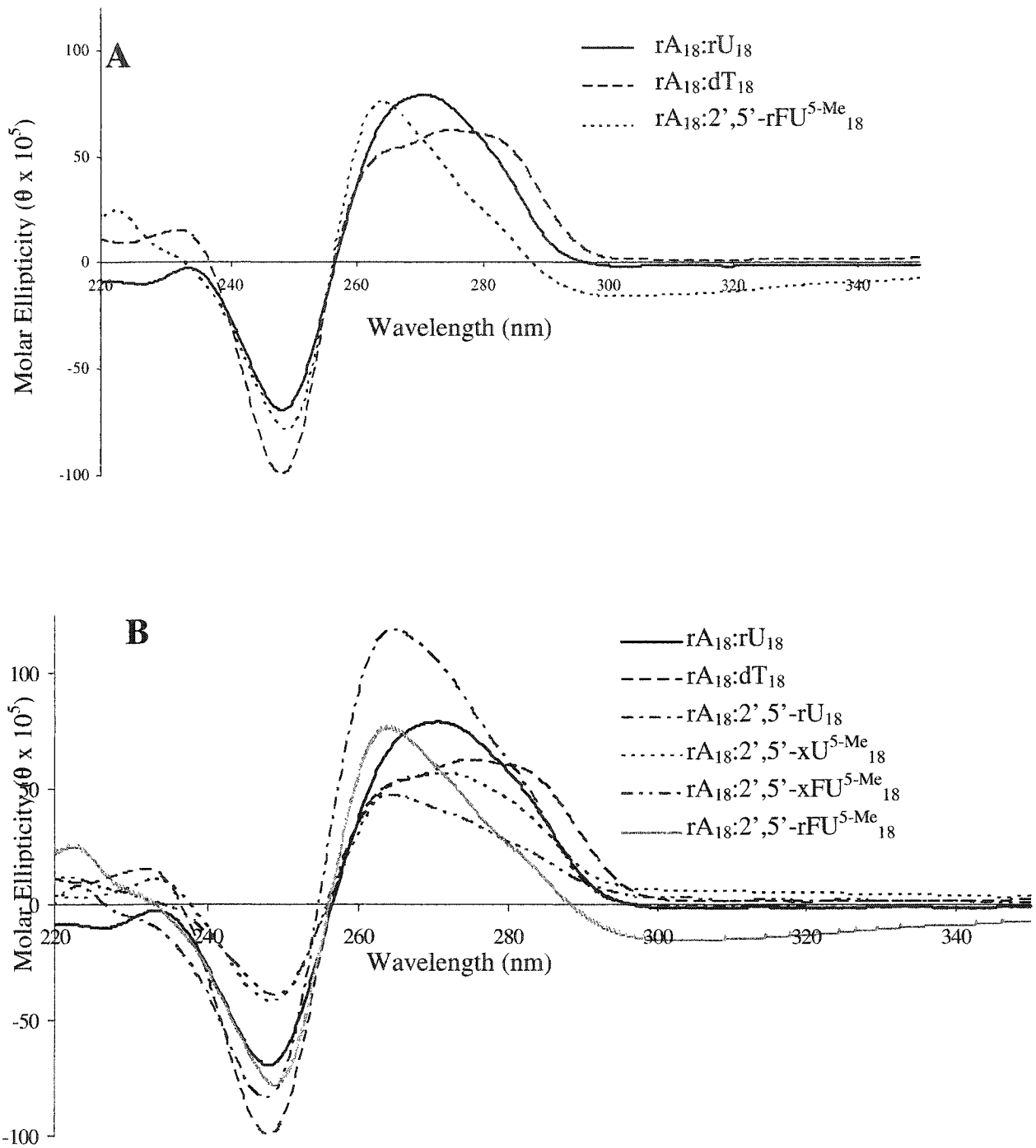

Figure 4.13: CD spectra of ribo-oligoadenylates hybridized to pyrimidine-oligonucleotides at 5°C (1M NaCl, 100mM Na_2HPO_4, pH = 7.2).

4.6 INVESTIGATING RNase H ACTIVATION BY 2',5'-LINKED 3'-FLUORO-RIBOFURANOSYL OLIGONUCLEOTIDES (2',5'-FRNA)

Our preliminary findings with 2',5'-rFU$^{5\text{-Me}}{}_{18}$ suggests that oligonucleotides constructed from 3'-fluoro-ribofuranose nucleotide units linked by 2',5'-phosphodiester bonds associate more strongly with complementary RNA than any other 2',5'-linked oligonucleotide studied to date. Given that the structure of 2',5'-rFU$^{5\text{-Me}}{}_{18}$:rA$_{18}$ resembles that of an RNA:RNA duplex, it was not expected that this hybrid would be a substrate of RNase H. Nevertheless, this hybrid adopts an A type conformation that appears to be essential for RNase H to effectively recognize and bind to hybrid substrates. Therefore a follow up study was carried out to determine whether such oligonucleotide could be used for RNA degradation by activation of RNase H. For a background on antisense strategy and RNase H the reader is referred to the introductory chapter and **section 2.8** respectively.

Figure 4.14 shows PAGE analysis of the enzyme assays carried out. As control, we also examined the ability of the native RNA:DNA hybrid of the same sequence to serve as substrates for RNase H. The reaction was stopped after fifteen minutes, and the sample was denatured and loaded onto a denaturing acrylamide gel. As seen in Figure 4.14 RNase H was only able to degrade RNA in the RNA:DNA hybrid; the RNA:2',5'-rFRNA heteroduplex did not serve as a substrate for RNase H. The lack of activity of RNase H with the RNA:2',5'-rFRNA duplex could be rationalized through a comparison of the structural dissimilarities possessed by these hybrids (close to the pure A-form RNA-RNA helical structure) in relation to the natural DNA:RNA substrates ("A-like").

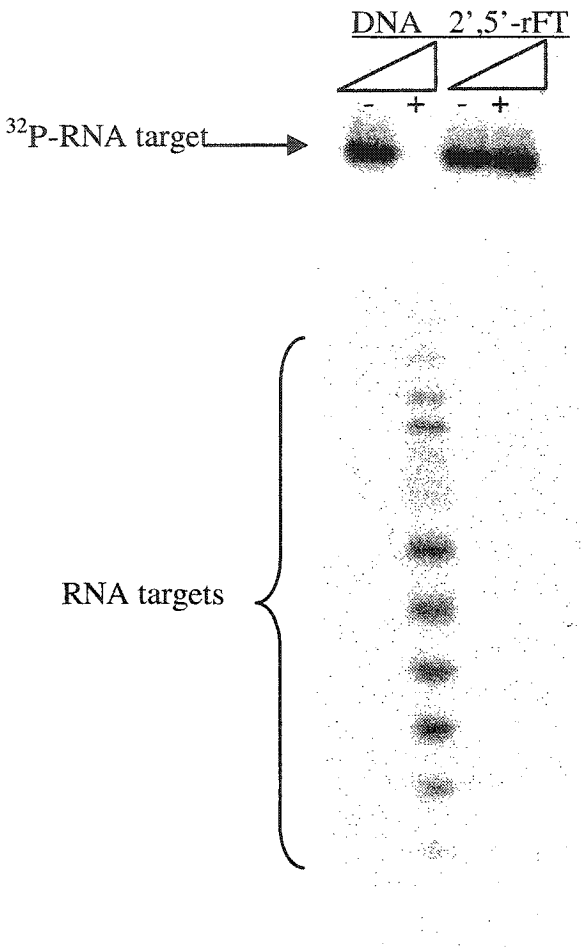

Figure 4.14: PAGE analysis of RNase H mediated RNA degradation using antisense oligonucleotides (Sequence: 5'-TTT TTT TTT TTT TTT TTT-3' or 2' with T replaced U in RNA and 2',5'-RNA). 1 pmol of target 5'-[^{32}P]-RNA and 10 pmol of antisense oligonucleotide were incubated in 60mM TRIS-HCl (pH 7.8), 2mM DTT, 60mM KCl and 2.5mM $MgCl_2$. Reaction was initiated by the addition of *E. coli* RNase H at 15 °C and quenched at 0 and 15 minute intervals. The gel was visualized by autoradiography.

CHAPTER V

CONTRIBUTION TO KNOWLEDGE

SYNTHESIS OF C3'-MODIFIED NUCLEOSIDES

Nucleosides with various modifications at the C3'-position, amenable to solid phase synthesis, were synthesized and characterized by NMR and mass spectra. Of the 3 chemical modifications explored in this work, both the xylofuranose and 3'-deoxy-3'-fluoro-xylofuranose nucleosides synthesized contained the following bases: adenine, cytidine and thymidine, while that of the 3'-deoxy-3'-fluoro-ribofuranose involved preparation of only the thymidine derivative. However, the synthetic routes examined may suitably be implemented toward the synthesis of any nucleobase-containing analogue.

An interesting property discovered during the course of this study was the selective silylation of the 2'-hydroxyl group in xylonucleosides. Thus, unlike the natural ribonucleosides, purification of a xylonucleoside is significantly simplified and the 2'-silylated precursor can further be utilized for selective manipulation at the C3'-position, as performed for the synthesis of 3'-fluoro-ribonucleosides. Another advantage of the protecting groups utilized to prepare the xylo-oligonucleotides is that, unlike RNA and 2',5'-RNA synthesis, no desilylation was required in the final deprotection step.

SOLID PHASE SYNTHESIS OF OLIGONUCLEOTIDES

Optimization of the 2',5'-linked-3'-modified oligonucleotide solid phase synthesis was crucial for improving the efficiency with which the 3'-modified derivatives

undergo solid phase internucleotide coupling and chain extension. This was accomplished by modification of the activator used (dicyanoimidazole or 5-ethylthio tetrazole in place of tetrazole), as well as an increase in the coupling time of the incoming phosphoramidite and a longer detritylation time of the growing chain. All compounds were characterized by gel electrophoresis and MALDI-TOF mass spectrometry to confirm the success of each synthesis and purity of the isolated oligonucleotides.

It is worth noting that monomers for synthesis of 2',5'-linked xylo and 3'-fluoro-xylooligonucleotides coupled more weakly than those for 2',5'-ribo and 3'-fluoro-ribooligonucleotides, despite the fact that the former are less sterically hindered.

BINDING PROPERTIES OF 2',5'-LINKED OLIGONUCLEOTIDES

The pyrimidine (5-methyl uridine) xylo and 3'-fluoro-xylooligonucleotides bound very weakly to complementary riboadenylate strands, while 3'-fluoro-ribooligonucleotides bound quite strongly to their RNA complements. No binding of these oligonucleotides was observed with complementary DNA, demonstrating that selective binding of 2',5'-linked oligonucleotides towards RNA over DNA is retained upon C3'-modification.

In the case of xyloadenosine and 3'-fluoro-xyloadenosine homopolymers, very strong binding was observed with complementary RNA. In fact, this is the first example of a 2',5'-linked oligoadenylate analogue that shows better binding affinity towards RNA than the native oligoriboadenylate. The selective binding towards RNA over DNA is still retained by these strong binding oligonucleotides.

In the case of duplexes composed of mixed base sequence, when hybridized with complementary RNA, the order of stability is as follows: 2',5'-FXNA:RNA ≈ 2',5'-XNA:RNA < 2',5'-RNA:RNA < DNA:RNA < RNA:RNA. No association of 2',5'-linked xylo and 3'-fluoro-xylooligonucleotides was observed with complementary DNA.

Overall, these binding properties of 2',5'-linked xylo, 3'-fluoro-xylo and 3'-fluoro-ribooligonucleotides support Yathindra's theory that the global helical conformation of a 2',5'-linked C3'-*endo* ('extended') oligonucleotide is equivalent to a C2'-*endo* ('compact') 3',5'-linked oligonucleotide, and vice versa.

STRUCTURAL PROPERTIES (CD) OF 2',5'-LINKED OLIGONUCLEOTIDES

The CD spectra of single stranded xylo and 3'-fluoroxylooligonucleotides suggest similar conformational characteristics to those acquired by DNA, while 3'-fluoro-ribooligonucleotides adopt helicities that are reminiscent of the conformational properties of RNA single strands. These findings are also maintained upon examining the overall conformational disposition of mixed sequence hybrid duplexes with target RNA, and thereby support the same conclusion regarding conformational mimicry of these analogues with the natural DNA and RNA strands, respectively. Furthermore, CD spectroscopic studies on xylo, xylo-fluoro and ribo-fluoro oligonucleotides corroborate the conclusions of the binding studies (T_m), that a sugar conformational switch must take place when going from 3',5'-to 2',5'-linkage in order to retain the global helical conformation of an oligonucleotide.

RNASE H INDUCTION BY 2',5'-LINKED OLIGONUCLEOTIDES

None of the 2',5'-linked oligonucleotide (xylo, xylo-fluoro and ribo-fluoro) hybrid duplexes formed with target single stranded RNA were able to induce RNA degradation by activation of RNase H. This is probably due to the change in linkage, such that going from a 3',5'-linked to 2',5'-oligonucleotide likely modifies the local conformation of the hybrid duplex where the enzyme binds and ultimately abolishes any ensuing enzyme activity.

PUBLICATIONS

As a direct result of the studies herein, the following publications have appeared:

Agha, K.A. and Damha, M. J. "Synthesis and binding properties of a homopyrimidine 2',5'-linked xylose nucleic acids (2',5'-XNA)", Nucleosides, Nucleotides and Nucleic Acids, **2003**, *22*, 1175.

Carriero, S.; Mangos, M.M.; Agha, K.A.; Noronha, A.M. and Damha, M.J. "Branch point sugar stereochemistry determines the hydrolytic susceptibility of branched RNA fragments by yDBR", Nucleosides, Nucleotides and Nucleic Acids, **2003**, *22*, 1599.

CONFERENCE PRESENTATIONS

Agha, K.A. and Damha, M.J. "Hybridization and Biochemical Properties of 2',5'-linked Oligonucleotides", XV International Roundtable on Nucleosides, Nucleotides and Nucleic Acids, Leuven, Belgium, September 10-14, 2002.

Agha, K.A. and Damha, M.J. "Effect of sugar conformation on 2',5'-linked oligonucleotides", McGill Organic Seminar Series, McGill University, Montreal, Quebec, February 27, 2002.

Agha, K.A. and Damha, M.J. "2',5'-FXNA: Physicochemical and Biochemical Properties", 8th Annual Ottawa Life Sciences International Conference & Exhibition, Ottawa, Ontario, November 5-7, 2001.

Agha, K.A. and Damha, M.J. "Physicochemical and Biochemical Properties of 2',5'-Xylo-oligonucleotides", 84th Canadian Society for Chemistry Conference and Exhibition, Montreal, Quebec, May 23-27, 2001. (**Best Poster Presentation**).

Damha, M.J.; Viazovkina, K; Agha, K.A.; Mangos, M.M. and Yazbeck, D. "Effect of sugar substitution on Arabino & Xylo Nucleic Acids", 84th Canadian Society for Chemistry Conference and Exhibition, Montreal, Quebec, May 23-27, 2001.

Agha, K.A. and Damha, M.J. "Synthesis and binding properties of homopyrimidine 2',5'-linked xylooligonucleotides", 3rd Annual Concordia Graduate Student Chemistry and Biochemistry Conference, Montreal, Quebec, March 17, 2000.

Agha, K.A. and Damha, M.J. "Synthesis of 2'-Xylo-Amidites and advances towards the binding and structural studies of 2',5'-linked Xylo-Oligonucleotides", Quebec/Ontario Minisymposium in Synthetic and Bioorganic Chemistry, Saint-Sauver-des-Monts, Quebec, November 5-7, 1999.

CHAPTER VI

EXPERIMENTAL

6.1 GENERAL METHODS

6.1.1 Reagents and Solvents

Pyridine (Caledon Laboratories Ltd., Georgetown, ON) was dried over Barium Oxide (BaO) and distillated following reflux under a nitrogen atmosphere; it was stored over activated 4 Å molecular sieves. Dichloromethane (DCM), N, N, N-triethylamine (TEA) (Aldrich Chemical Company, Milwaukee, WI) and collidine (Aldrich) were dried by reflux and distilling over calcium hydride (CaH_2) and stored over activated 4 Å molecular sieves. Tetrahydrofuran (THF) (BDH) was constantly refluxed over sodium (Na) and benzophenone (Aldrich) in a nitrogen atmosphere, and collected before use. Acetonitrile (MeCN) (Caledon) was dried by refluxing over phosphorus pentoxide (P_2O_5) followed by distillation. It was kept dry by constant reflux over CaH_2 in an inert atmosphere and collected before use. Anhydrous N, N-diisopropylamine (DIPEA) (Aldrich), N-methylimidazole (NMI) (Aldrich) and N, N-dimethylformamide (DMF) (Aldrich) were either used as received or dried by distillation over CaH_2. Chloroform, ethyl acetate, acetone, ethanol, methanol (BDH), hydrochloric acid (HCl) and diethyl ether (Caledon) were used as obtained.

The following chemicals were used as received (Aldrich): triethylamine tris(hydrofluoride) (TREAT HF), 1-(3-dimethylaminopropyl)-3-ethylcarbodiimide hydrochloride, diethylaminosulfur trifluoride (DAST), chlorotrimethylsilane (TMS-Cl), *p*-anisylchlorodiphenylmethane (MMT-Cl), tetra-*n*-butylammonium fluoride (1.0 M TBAF in THF), 4-dimethylaminopyridine (DMAP), tin (IV) tetrachloride ($SnCl_4$), thymine, adenine, cytosine, benzoyl chloride (Bz-Cl), D-xylose, isobutyryl chloride (iBu-

Cl) (Aldrich). The sugars 1,2,3,5-tetra-O-benzoyl-D-xylofuranose and 1,2:5,6-di-isopropylidene allofuranose were either purchased from Pfanstiehl or synthesized in house. Analytical reagent grade glacial acetic acid, anhydrous sodium sulfate, anhydrous magnesium sulfate, ammonium acetate, sodium chloride, magnesium chloride, 95% ethanol, acetone, analytical grade ethylenediammine tetra acetate (EDTA), triethylamine were all obtained from BDH, disodium hydrogen phosphate (Fischer Scientific Fairlawn, NJ), manganese chloride ($MnCl_2$), sodium acetate (Aldrich) TRIS (Bio-Rad).

6.1.2 Chromatography

Column chromatography was performed with silica gel [40-63 micron silica gel 60 (Silicycle Montreal, QC)].

Thin-layer chromatography (TLC) was performed using Merck Kiesselgel 60 F-254 aluminum-back analytical gel sheets (0.2 m thickness, EM Science, Gibbstown, NJ). Compounds were visualized on TLC plate by illumination with a UV light source (Mineralite, emission wavelength *ca.* 254 nm), and further stained by trifluoroacetic acid vapours for trityl containing compounds. Sugars and other compounds could also be visualized by staining in 10% H_2SO_4 in methanol. This was done by first dipping the TLC in the solution, followed by heating to obtain the charred spots.

6.1.3 Instruments

UV Spectroscopy

UV-VIS spectra were recorded using a CARY I spectrophotometer (Varian:Mulgrave, Victoria, Australia). Oligonucleotide thermal denaturation profiles

were obtained in the ultraviolet spectrum using a CARY I spectrophotometer equipped with a 6X6 cell holder thermally stabilized with an external temperature controller. Monitoring the temperature and data collection was done using manufacturers supplied software (Cary Win UV version: 2.00) and processed on a PC.

NMR Spectroscopy

Spectra were recorded at ambient temperature, on a Varian XL-500, XL-400, XL-300 or XL-200. Chemical shifts reported are in ppm downfield from tetramethylsilane (TMS) for ^{1}H and ^{13}C spectra; while for ^{31}P NMR spectra, 85% phosphoric acid (H_3PO_4) was used as an external reference. For characterization of new compounds, all ^{1}H and ^{13}C spectral assignments were done by 2-D NMR experiments: homonuclear correlated spectroscopy (COSY), nuclear Overhauser and exchange spectroscopy (NOESY) and ^{1}H-detected heteronuclear multiple quantum coherence spectroscopy (HMQC). Deuterated solvents used were: acetone-D_6 (CDN Isotopes, Quebec, Canada), dimethylsulfoxide- D_6 (Cambridge Isotopes Laboratories Andover, MA), chloroform-$CDCl_3$ (Isotec Inc. Miamisburg, OH).

Circular Dichroism (CD) Spectroscopy

CD spectra were collected on a Jasco J-710 spectropolarimeter equipped with a thermoelectrically controlled external constant temperature NESLAB RTE-111 circulating bath. Data were processed using a Windows based software supplied by the manufacturer (JASCO, Inc.).

FAB Mass Spectroscopy

Fast Atom Bombardment (FAB) mass spectra were collected by the McGill University Analytical Services using a Kratos MS25RFA high resolution mass spectrometer. Nitrobenzyl alcohol (NBA) matrix was used unless otherwise specified.

MALDI TOF Mass Spectroscopy

Matrix-Assisted laser desorption/ionization time of flight (MALDI TOF) mass spectra were recorded on a Kratos Kompact-III TOF instrument with a minimum laser output of 6mW at a wavelength of 337 nm light, 3 ns pulse width, 100 mm diameter spot. The MALDI instrument was operated in a positive (reflection and linear) mode.

6.2 OLIGONUCLEOTIDE SYNTHESIS

6.2.1 Reagents for nucleoside derivatization

All nucleosides (deoxy and ribo) and N, N-diisopropyl-2-cyanoethylphosphonamidic chloride were purchased from either ChemGenes (Ashland, MA) or Dalton Chemical Laboratories (DCL, Toronto, ON). Chlorotrimethylsilane (TMS-Cl), *p*-anisylchlorodiphenylmethane (MMT-Cl), benzoyl chloride (Bz-Cl), *tert*-butyldimethylsilyl chloride (TMDMS-Cl), 4-dimethylaminopyridine (DMAP) and 1M tetrabutylammonium fluoride (TBAF) in THF were obtained from Aldrich.

Reagent grade acetic anhydride (Ac_2O) (BDH), trichloroacetic acid (TCA) (Aldrich), aqueous ammonium hydroxide (BDH), 1,2-dichloroethane (Caledon), N-methylimmidazole (NMI) (Aldrich), iodine (Aldrich), DNA synthesis grade tetrazole

(DCL), 5-(ethylthio)-1*H*-tetrazole (ChemGenes) and 4,5-dicyanoimmidazole (AIC) were used as received.

Double distilled water (Millipore, Mississuaga, ON) was treated with diethyl pyrocarbonate (Aldrich) to form a 0.1% solution and autoclaved (1hour, 121°C, 1.3 atm).

6.2.2 Solid Support Derivatization

Long-chain alkyl amine controlled pore glass (LCAA-CPG), 500 Å pore size, density *ca* 0.4 g/ml (DCL) was derivatized according to literature.[192,194] A prolonged acid activation time was needed to achieve desired nucleoside loading; the LCAA-CPG was shaken over 5% TCA in DCE for 24-72 h. For coupling of the nucleoside to the succinylated LCAA-CPG the procedure of Pon *et al.* was more efficient (higher loading in shorter coupling time).[194] The loading determined was based upon spectrophotometric quantitation of mono and dimethoxytrityl cation. The support was dried by placing *in vacuo* over P_2O_5 for 24h before use; then placed into an empty column with replacable filters (Applied Biosystems Inc. (ABI) Foster City, CA), crimped closed with aluminum seals (Pierce) and installed on the instrument.

6.2.3 Monomers for Gene Machine Synthesis

All protected amidite monomers for DNA, RNA and 2',5'-RNA were purchased from ChemGenes (Ashland, MA) . They were stored at -20°C and placed overnight under vacuum over P_2O_5 before use.

6.2.4 Automated Oligonucleotide Synthesis

a. Chain Assembly

DNA and RNA oligonucleotides were synthesized on either Applied Biosystems DNA/RNA 381A or Applied Biosystems Expedite™ 8909 Nucleic Acid Synthesizer. All modified oligonucleotides were synthesized on the Applied Biosystems 381A synthesizer. Oligomers were synthesized on a 1 μmol scale using succinylated LCAA-CPG (500 Å) derivatized from the 3'-nucleoside end as described.

All reagents for oligonucleotide automated synthesizer were purchased from ABI, DCL or prepared as follows.

Solvents were dried as follows: Tetrahydrofuran (THF) (BDH) was constantly refluxed over sodium/benzophenone (Aldrich) in an inert atmosphere and collected before use. Anhydrous acetonitrile (MeCN) (Caledon) was dried by refluxing over phosphorous pentoxide (P_2O_5) followed by distillation. It was kept dry by constant reflux over CaH_2 in an inert atmosphere and collected before use. Pyridine (Caledon Laboratories Ltd., Georgetown, ON) was dried over Barium Oxide (BaO) by distillation following reflux, in a nitrogen atmosphere and stored over activated 4 Å molecular sieves. N-methylimidazole (NMI) (Aldrich) was either used as received or dried by distillation over CaH_2. Collidine (Aldrich) was dried by reflux and distilling over calcium hydride (CaH_2) and stored over activated 4 Å molecular sieves.

Prior to oligonucleotide synthesis, the solid support was capped, to prevent oligomer synthesis from other reactive sites, using capping reagents described above. Monomers for oligonucleotide assembly were dissolved in freshly distilled acetonitrile, collected from a constant reflux apparatus under inert atmosphere. The concentrations of

the amidite solutions were as follows: 0.1 M for DNA and 0.15 M for RNA and modified oligonucleotides. All modified amidites solutions were filtered through a 0.45 μm pore Teflon® filter by use of a 'swinny' filter apparatus (Millipore, Mississuaga, ON) before placement on the automated synthesizer.

Assembly of sequences on the 381 A synthesizer was carried out using the following reagents and synthesis steps: (1) detritylation: for DNA and RNA, 3% trichloroacetic acid in dichloroethane delivered in 100 s (+ 40s 'burst') steps. For modified oligonucleotides an extended time of 120s (+ 60s 'burst') step was used. Monomer coupling yields were based on UV spectroscopic trityl cation (DMT^+: λ=504 nm, ε = 76000 $L.mol^{-1}.cm^{-1}$, deoxy and ribo; MMT^+: λ=478 nm, ε = 56000 $L.mol^{-1}.cm^{-1}$, xylo, xylo-fluoro and ribo-fluoro) assay of the eluate collected; (2) phosphoramidite coupling time of 90s (dA, dT and dC), 180s (dG), 600s (rA, rU and rC) and 900s (rG) and 30 min (xylo, xylo-fluoro and ribo-fluoro) and branch point nucleotides; (3) Capping: acetic anhydride/2,4,6-collidine/THF 1:1:8 (volume ratio, Cap A) and 1-methyl-1*H*-imidazole/THF 16:84 (volume ration, Cap B) delivered in 15s + 600s "wait" steps; (4) Oxidation: 0.1M iodine in THF/pyridine/water 25:20:2, delivered in 20s + 20s "wait" steps. The coupling efficiencies for xylo oligonucleotides (XNA) ranged from 88-104%, xylo-fluoro (FXNA) from 89-103% and ribo-fluoro (FRNA) from 96-101%.

b. Oligonucleotide Deprotection

After oligonucleotide synthesis, the solid support CPG linked oligomer was separated into two equal halves (0.5 μmol). Each half was treated with aqueous ammonia/ethanol (3:1 v/v, 1.2 mL) for 24-48 hours at r.t. to cleave the oligomer off the

support and remove exocyclic amino protecting groups. The time for deprotection depended upon the base sequence; those containing only A, C and U (T) were treated for 24 h, while oligomers containing G were allowed to react for 48 h. Following cleavage, the solid support was centrifuged and the supernatant collected. The solid support was washed three times with absolute EtOH. All supernatants were pooled and then evaporated to obtain a pellet. RNA oligonucleotides were desilylated by treatment with triethylamine trihydrofluoride (TREAT.HF) (100 μL per μmol scale of synthesis). Oligonucleotides were quantified by UV absorbance at λ=260 nm and amounts reported in optical density (OD) units. An OD unit represents the amount of sample that when dissolved in 1mL of water, in a 1cm path cuvette, gives an absorbance of one (A_{260}).

6.3 Oligonucleotide Purification

Following deprotection, the crude oligonucleotides were purified from shorter sequences either via polyacrylamide gel electrophoresis (PAGE) or high pressure liquid chromatography (HPLC).

6.3.1 Polyacrylamide Gel Electrophoresis (PAGE)

Crude oligonucleotides were purified by vertical plate polyacrylamide gel electrophoresis (PAGE) using a BioRad Proteam II or Hoefer Scientific units (San Francisco, CA). The reagents (electrophoresis grade acrylamide, N, N'-methylene-bis(acrylamide) (BIS), ammonium persulfate (APS), N,N,N',N'-tetramethylenediamine (TEMED), bromophenol blue (BPB) and xylene cyanol (XC)) were purchased from BioRad (Mississauga, ON). Other reagents required were: boric acid, formamide and

disodium ethylenediaminetetraacetate dehydrate (EDTA) (BDH), Trishydroxy-methylaminomethane (Tris), sucrose (Aldrich) and urea (Caledon), and were used as described.[191]

The thickness of the gels were 0.75 mm and 1.5 mm for the analytical and preparative gels, respectively. Most commonly gels were composed of 14-24% (w/v) acrylamide and 5% (with respect to mass of acrylamide) BIS, *i.e.*, 19:1 acrylamide: BIS. A Tris/boric acid (TBE) buffer (89 mM Tris/boric acid, 2.5 mM EDTA, pH=8.3)[6] was used for running the gels. Formamide was stirred over an ion-exchange resin (Bio Rad AG 501-X8) for deionization. The denaturing loading buffer was 8:2 deionized formamide / 10x TBE. Approximately 1 O.D. (in each well) and 30 O.D. units were loaded in analytical and preparative gels respectively. The desired bands were excised, crushed and shaken overnight in 8-10 mL of water. Following water extraction, the aqueous layer was evaporated and desalted as described.

6.3.2 Oligonucleotide Visualization

After completion of the PAGE, the apparatus was disassembled and the gel wrapped in Saran Wrap®, placed over a fluorescent TLC plate and illuminated using a hand held UV lamp. The gel was photographed using a Polariod PolaPan® camera with a 4x5" Instant Sheet Film, #52, medium contrast, ISO 400/21°C; f 4.5, 16 second and a Kodak Wratten gelatin filter (#58).

Analytical gels could be visualized with higher sensitivity via staining, using All-stain (Bio-Rad)® , which is a solution containing 1-ethyl-2-(3-[1-ethylnapthol(1,2-d)-thiazolin-2-ylidene]-2-methylpropenyl)napthol(1,2-d)-thiazolium bromide. The gels

were placed in this solution overnight for staining and photographed without the filter, using the same film (f 11, 0.30s).

6.3.3 Desalting of Oligonucleotides

The oligonucleotide was further purified from salts and other low molecular weight impurities by size exclusion chromatography (SEC) using Sephadex G-25 (Pharmacia, Baie d'Urfe, QC). The sephadex was stored in distilled deionized water and autoclaved (1h, 120°C, 1.3atm.) using an All American Electric Steam Sterilizer-Model No. 25X (Wisconsin Aluminum Co., Inc. Manitowoc, WI). The chromatography was performed in appropriately sized, sterile, disposable 10 mL syringe (Becton Dickinson & Co., Franklin Lakes, NJ), plugged with autoclaved glass wool (Chromatographic Specialties Inc., Brockville, ON). After packing the column, the sephadex was washed with ~10mL of distilled deionized autoclaved water. The oligonucleotide was dissolved in 1mL of double distilled autoclaved water, loaded onto the Sephadex, eluted (with autoclaved H_2O) and collected in 0.7-1.0mL fractions. The UV absorbance (260 nm) of these fractions were measured, those predominantly containing oligonucleotide were evaporated and pooled to a final volume of 1mL. This stock solution was stored at -20°C and thawed before use.

6.3.4 High Pressure Liquid Chromatography (HPLC)

Oligonucleotides were also purified using high pressure liquid chromatography (HPLC). A Waters HPLC instrument equipped with a W600E multisolvent delivery system, two pump heads (225 µL), w U6K injector, a temperature controller and a M486

tunable absorbance detector was used. The anion exchange column (semi-preparative) used was Protein Pak DEAE-5PW (7.5 mm X 7.5 mm) from Waters. Lithium perchlorate was purchased from BDH. All solutions were made using dd H_2O, filtered through a 0.45 μm filter and degassed with helium before use.

The oligonucleotides were purified using a linear gradient of 0-20% of 1M $LiClO_4$, at a flow rate of 1 mL per minute, during a 60 minute run at a constant temperature of 50°C (for disassociation of any secondary structure), which resulted in reasonable separation from the shorter oligonucleotides. Analytical injections were done on 0.5-1.0 OD units dissolved in 10 μL of water and the detector wavelength set at 260 nm. For preparative injections, ~20 OD's of the sample was injected at a concentration of 0.5 OD per μL of water and a detector wavelength of 270 nm. Fractions containing the pure oligonucleotide was collected, pooled and evaporated.

Desalting of the oligonucleotide was done by either size-exclusion chromatography (SEC) (as described above) or by n-butanol precipitation.

6.4 OLIGONUCLEOTIDE CHARACTERIZATION

6.4.1 Physicochemical Studies

a. UV-Thermal Melt (T_m) Studies

Hybridization properties of oligonucleotides were studied by observing the change in UV absorbance with temperature, generating a UV denaturation profile ("melting curve"). The studies were conducted using a Varian Cary I UV-VIS spectrophotometer equipped with a Pelletier temperature controller. During spectrum collection, samples were placed in Hellman QS-1.000-104 cells, the absorbance

measured at 1°C interval and temperature ramped at a rate of 0.5 °C/min. The spectrophotometer was set at 260 nm on dual optical mode to reduce optical drift. The instrument parameters were controlled using manufacturers supplied software (Cary Win UV, version 2.00).

The data was initially stored in a 'batch' (.bsw) format and then converted into an 'Spreadsheet Ascii' (.CSV) format for manipulations in Excel. In order to compare absorbance change, normalized ΔA plots were developed[7] according to the formula: $(A_t-A_i)/A_f$, where A_t is the absorbance at temperature (T), A_i is the initial absorbance and A_f is the final absorbance. This allows for a uniform comparison for samples at identical concentrations in the same buffer[8]. Hyperchromicity (H%) values were used to approximate base stacking in a complex[9,10], using the formula: $(A_S-A_D)/A_S$; where A_S and A_D is the absorbance of single and double strands respectively. The T_m is defined as the inflection point in the melting curve (the maximum of the first derivative of the T_m) and was determined using the "recalculate function" of manufacturer supplied software. The curve was smoothed and derivative calculated using a filter size of 5 and data intervals at 1°C.

Molar extinction coefficients for all oligonucleotides were estimated using a web based software (www.paris.chem.yale.edu/extinct.html). The coefficients for 2',5'-XNA, 2',5'-FXNA and 2',5'-FRNA were assumed to be the same as normal DNA.

For thermal denaturation profiles, equimolar mixture of the samples were lyophilized to dryness and then re-dissolved in the appropriate buffer. Prior to the T_m run, samples were heated to 80-90 °C for 15 min, allowed to cool slowly to r.t., degassed by ultrasound sonication and then incubated at 4 °C over night.

b. Circular Dichroism Spectroscopy

CD spectra were collected on a Jasco J-710 spectropolarimeter equipped with a thermoelectrically controlled external constant temperature NESLAB RTE-111 circulating bath. Spectra were recorded using either fused Quartz cells (Hellma 165-QS) or Hellman QS-1.000-104 cells with 1 cm optical path length. The samples were prepared in a similar manner as described above for the T_m study; and equilibrated for 5-10min at the acquisition temperature before scanning. An initial scan was done to ensure that the voltage did not exceed 800 at the low wavelength (for acceptable signal to noise ratio). The data recorded was an average of 5 scans, collected at a rate of 100nm/min, band width of 1nm intervals and sampling wavelength of 0.2nm. The CD spectra were recorded from 350 to 200nm at 5°C and normalized by subtraction of buffer spectra. The molar ellipticity was calculated from the equation $[\theta] = \theta / cl$, where θ is the relative intensity, c is the molar concentration of oligonucleotides and l is the path length. Data processing was done using manufacturers supplied software (JASCO, Inc. J-700 for Windows Standard Analysis, version 1.10.00).

6.4.2 Matrix Assisted Laser Desorption/Ionization Time of Flight Mass Spectra (MALDI-TOF)

The purified oligonucleotide were analyzed by MALDI-TOF mass spectroscopy using a 20 mM ammonium citrate (Fluka) (50% acetonitrile: 50% water) buffer containing 10 mg/mL of 6-aza-2-thiothymidine (Aldrich) as the matrix[12]. The positive ion MALDI-TOF mass spectra were obtained in the reflectron and linear mode to give the correct molecular weight with excellent signal to noise ratio.

Sample preparation was done by dissolving the oligonucleotide in water with a concentration of 0.2-1mmol. An aliquot of 5 μL of this sample was mixed with 5 μL of the matrix; and 1-3 5 μL of the final solution was applied to a stainless steel sample slide and air dried prior to analysis.

6.5 BIOLOGICAL STUDIES

E. coli RNase H were obtained from Pharmacia and [γ-^{32}P]-ATP was purchased from Amersham. The 18mer RNA template corresponding to the CAT sequence was ^{32}-P, 5'-end labeled using T4 polynucleotide kinase and then purified by 16% polyacrylamide gel electrophoresis (PAGE).

The ability of oligonucleotides to induce RNaseH based degradation of the target RNA was determined in assays consisting of 1pmol of the 5'-[^{32}P]-target RNA and 8pmol of the test oligonucleotide in 60mM Tris-HCl (pH 7.8, 25°C) containing 2mM dithiothreitol, 60mM KCl and 2.5mM $MgCl_2$. Reaction was initiated by addition of *E. coli* RNase H, with incubation at 17°C for xylo and 3'-fluoro-xylooligonucleotides, and r.t. for 3'-fluoro-ribooligonucleotide. The reactions were quenched by the addition of the loading buffer, composed of 98% deionized formamide containing 10mM EDTA and 1mg/mL of bromophenol blue and xylene cyanol each. This was followed by heating to 100°C for 5min, followed by resolution of the reaction products by electrophoresis on sequencing gel. The gel was prepared from 16% acrylamide and 7M Urea, and the products were visualized by autoradiography.

6.6 MONOMER PREPARATION

1,2,3,5-Tetra-O-benzoyl-α-D-xylofuranose [2.1]

D-xylose (20g, 0.13 mol) was stirred in anhydrous MeOH (500mL) containing 1% HCl at r.t. for 5 h. Pyridine (20mL) was added and the solution evaporated to dryness. The residue was dissolved in pyridine (200mL) and benzoyl chloride (80mL, 0.69mol) was added. The reaction was stirred overnight, poured over ice and extracted with benzene. The extracts were washed with 3N H_2SO_4 and $NaHCO_3$, dried (Na_2SO_4), filtered through activated charcoal, and evaporated to obtain a syrup. The syrup was stirred in 30% HBr in AcOH (150mL) for 2 hours at r.t., diluted in benzene (200mL) and washed with cold water, $NaHCO_3$ and water. The organic phase was stirred with acetone (360mL), water (10mL) and Ag_2CO_3 (20g) for 30 minutes, filtered and evaporated. The oil obtained was reacted with benzoyl chloride (56mL, 0.48 mol) in pyridine (200mL) for overnight at r.t. The reaction was taken up in dichloromethane (200mL), washed with cold water (100mL), 3N H_2SO_4 (100mL) and $NaHCO_3$ (100mL), dried with $MgSO_4$, filtered through activated charcoal and evaporated. The residue was dissolved in boiling ethyl acetate (80mL) and ethanol (200mL) was added to it. The solution was kept overnight at 0°C to obtain the desired product as white precipitate (43.05 g, 57.1%).

^{1}H NMR (400 MHz, ppm, $CDCl_3$): 4.60 (m, 2 H, H-5 & H-5'), 5.07 (m, 1 H, H-4); 5.94 (q, 1 H, H-2), 6.20 (t, 1 H, H-3), 6.93 (d, 1 H, H-1), 7.3-8.2 (m, 20 H, 4 x Ph).

ESI-MS (MeOH): 589.21 g/mol (calc. 566.56 g/mol + sodium).

1-(2',3',5'-Tri-O-benzoyl-β-D-xylofuranosyl)-5-methyluridine [2.2]

A mixture of 1,2,3,5-tetra-O-benzoyl-α-D-xylofuranose (10g, 17.6 mmol) and thymine (2.44 g, 19.3mmol) was stirred in anhydrous acetonitrile (200mL). To this tin (IV) tetrachloride (2.48mL, 21.2mmol), chlorotrimethylsilane (1.96mL, 15.4mmol) and 1,1,1,3,3,3-Hexamethyldisilazane (3.28mL, 15.5mmol) was added. The solution was refluxed for one hour, followed by dilution in dichloromethane (400mL). The organic phase was washed with 5% sodium bicarbonate (400mL), sodium chloride (400mL). Any remaining tin salts could be removed by passing through celite. The organic phase was dried (Na_2SO_4), evaporated and purified by column chromatography using dichloromethane: methanol (with a gradient of 0 to 5% methanol) as an eluent. The fractions containing the desired product were evaporated to obtain a white foam (8.56g, 85.6%).

R_f (SiO_2): 0.56 {dichloromethane: methanol (95:5)}

^{1}H NMR (400 MHz, ppm, $CDCl_3$): 1.70 (s, 3 H, C5-CH_3), 4.69-4.8 (m, 2 H, H-5' & H-5''), 4.94 (m, 1 H, H-4'), 5.72 (t, 1 H, H-2'), 5.92 (q, 1 H, H-3'), 6.20 (d, 1 H, H-1'), 7.45-8.10 (m, 16 H, 3 x Ph & H-6), 11.43 (bs, 1 H, N-H).

ESI-MS (MeOH): 571.0 g/mol (calc. 570.68 g/mol).

1-(β-D-Xylofuranosyl)-5-methyluridine [2.3]

Nucleoside **[2.2]** (1g) was dissolved in MeOH (40mL) and concentrated ammonium hydroxide (20mL) was added. The solution was stirred overnight and then evaporated to dryness. The nucleoside was either taken to the next step, or purified by

absorbing onto silica and performing flash chromatography using chloroform: ethanol (3:1) as eluant (0.40 g, 90%).

R_f (SiO_2): 0.16 {dichloromethane: methanol (9:1)}

UV: λ_{max}= 267 nm (MeOH); dT: λ_{max}= 266 nm (MeOH)

^{1}H NMR (400 MHz, ppm, DMSO-d_6): 1.74 (s, 3 H, C5-CH_3), 3.62-3.72 (m, 2 H, H-5' & H-5''), 3.90 (bs, 1 H, C2'-OH), 3.93 (bs, 1 H, C3'-OH), 4.03 (q, 1 H, H-2'), 4.73 (t, 1 H, H-3'), 5.39 (d, 1 H, C5'-OH), 5.64 (d, 1 H, H-1'), 7.6 (s, 1 H, H-6).

CI-MS (MeOH): 259.0 g/mol (calc. 258.23 g/mol).

1-[5'-O-(4-Monomethoxytrityl-β-D-xylofuranosyl)]-5-methyluridine [2.4]

Nucleoside **[2.3]** (4.35 g, 16.85mmol) was co-evaporated with pyridine (45mL).. Pyridine (90mL), followed by addition of 4-monomethoxytrityl chloride (6.25 g, 20.21mmol) and DMAP (catalytic), were added and the solution stirred overnight at r.t. under a N_2 atmosphere. The reaction was quenched by the addition of 5% $NaHCO_3$ (50mL) and evaporated. Extraction was performed using CH_2Cl_2, brine and water. The organic phase was dried (Na_2SO_4), evaporated and purified by flash chromatography using dichloromethane: methanol (with a gradient of 0 → 5%): triethylamine (0.2%). The desired fractions were evaporated to obtain the product as a white foam (8.90 g, 99.6%).

R_f (SiO_2): 0.43 {dichloromethane: methanol (9:1)}

^{1}H NMR (500 MHz, ppm, $CDCl_3$): 1.57 (s, 3 H, C5-CH_3), 3.57 (m, 2 H, H-5' and H-5''), 3.67 (s, 1 H, OH-3'), 3.78 (s, 3 H, O-CH_3), 4.21 (s, 1 H, H-3'), 4.43 (s, 1 H, H-2'), 4.54

(m, 1 H, H-4'), 5.33 (bs, 1 H, OH-2'), 5.74 (s, 1 H, H-1'), 6.8-7.6 (m, 15 H, 3 x Ph and H-6), 10.72 (bs, 1 H, N-H).

EI-MS (MeOH): 553.2 g/mol (calc. 530.59 g/mol + Na).

1-[5'-O-(4-Monomethoxytrityl)-2'-*tert*-butyldimethylsilyl-(β-D-xylofuranosyl)]-5-methyluridine [2.5]

Nucleoside **[2.4]** (1 g, 1.88 mmol), imidazole (0.32 g, 4.71 mmol) and *tert*-butyldimethylsilyl chloride (0.34 g, 2.26 mmol) was dissolved in anhydrous DMF (15 mL) and stirred overnight at r.t. The reaction was quenched by the addition of 5% $NaHCO_3$ (10mL). The solution was evaporated, the residue dissolved in CH_2Cl_2 (20mL) and extracted with brine (10mL) and water (10mL). The organic phase was dried (Na_2SO_4), evaporated and purified by column chromatography using a gradient of dichloromethane: ethyl acetate (from 7:1 to 3:1) to obtain the product as a white foam (1.05 g, 88.0%).

R_f (SiO_2): 0.56 {dichloromethane: ethyl acetate (2:1)}

^1H NMR (500 MHz, ppm, $CDCl_3$): 0.11 (s, 3 H, Si-CH_3), 0.16 (s, 3 H, Si-CH_3), 0.89 (s, 9 H, -$C(CH_3)_3$), 1.74 (s, 3 H, C5-CH_3), 3.66 (ddd, 2 H, H-5' and H-5''), 3.73 (s, 1 H, OH-3'), 4.06 (s, 1 H, H-3'), 4.21 (s, 1 H, H-2'), 4.30 (m, 1 H, H-4'), 5.77 (s, 1 H, H-1'), 6.8-8.4 (m, 15 H, 3 x Ph and H-6).

FAB-MS (NBA): 645.22 g/mol (calc. 644.84 g/mol).

1-[5'-O-(4-Monomethoxytrityl)-2'-O-*tert*-butyldimethylsilyl-3'-O-acetyl-(β-D-xylofuranosyl)]-5-methyluridine [2.6]

Nucleoside **[2.5]** (1.5 g, 2.33mmol) and DMAP (150 mg) were dissolved in anhydrous THF (15mL), followed by addition of DIPEA (2.8mL). The solution was kept under N_2 at r.t. and Ac_2O (0.90mL) was added dropwise. The reaction was diluted with CH_2Cl_2 (30mL) and extracted with 5% $NaHCO_3$ (2 x 15mL) and brine (2 x 15mL). The aqueous layer was back extracted with CH_2Cl_2 and the organic phase dried (Na_2SO_4) and evaporated to obtain a white foam. The compound was purified by column chromatography using dichloromethane: ethyl acetate (from 7:1 to 3:1) (1.57 g, 98.1%).

R_f (SiO_2): 0.64 {ether}

^{1}H NMR (500 MHz, ppm, $CDCl_3$): 0.18 (s, 6 H, Si-$(CH_3)_2$), 0.93 (s, 9 H, C$(CH_3)_3$), 1.61 (s, 3 H, C5-CH_3), 1.79 (s, 3 H, CH_3-CO), 3.41 (m, 2 H, H5' and H5''),3.82 (s, 3 H, O-CH_3), 4.29 (s, 1 H, H-2'), 4.64 (m, 1 H, H-4'), 5.05 (d, 1 H, H-3'), 5.84 (s, 1 H, H-1'), 6.8-7.6 (m, 15 H, 3 x Ph and H-6), 8.52 (bs, 1 H, N-H).

FAB-MS (NBA): 687.21 g/mol (calc. 686.87 g/mol).

1-[5'-O-(4-Monomethoxytrityl)-3'-O-acetyl-(β-D-xylofuranosyl)]-5-methyluridine [2.7]

Nucleoside **[2.6]** (0.99 g, 1.4 mmol) was dissolved in anhydrous THF (10mL) and TBAF (1M in THF, 0.22mL) was added. The reaction was stirred in a nitrogen atmosphere at r.t. for 1 hour. The solution was then evaporated, dissolved in CH_2Cl_2 (20mL) and extracted with brine (2 x 10mL) and water (2 x 10mL). The organic phase was dried (Na_2SO_4), evaporated and purified by flash chromatography using

dichloromethane: methanol (0 → 5% as gradient) to obtain the product as a white foam (0.82 g, quantitative).

R_f (SiO_2): 0.28 {dichloromethane: methanol (95:5)}

^{1}H NMR (500 MHz, ppm, $CDCl_3$): 1.64 (s, 3 H, C5-CH_3), 1.77 (s, 3 H, CH_3-CO), 3.39 (m, 2 H, H-5' and H-5''), 3.81 (s, 3 H, O-CH_3), 4.35 (s, 1 H, H-2'), 4.79 (d, 1 H, H-4'), 5.29 (s, 1 H, H-3'), 5.50 (bs, 1 H, OH-2'), 5.86 (s, 1 H, H-1'), 6.8-7.6 (m, 15 H, 3 x Ph and H-6), 10.50 (bs, 1 H, N-H).

FAB-MS (NBA): 573.93 g/mol (calc. 572.61 g/mol).

1-[5'-O-(4-monomethoxytrityl)-3'-O-acetyl-2'-O-(β–cyanoethyl-N,N-diisopropylphosphoramidite)-β-D-xylofuranosyl]-5-methyluridine [2.8]

Nucleoside **[2.7]** (0.20 g) was dissolved in anhydrous THF (2mL) and DIPEA (1.3 equiv.) was added to it. The solution was cooled in an ice bath, kept under a N_2 atmosphere and N,N-diisopropyl-β-cyanoethylphosphoramidic chloride (1.2 equiv.) was added dropwise. The solution was allowed to come to r.t. and stirred for 2 hours. The solution became cloudy indicating salt formation. The reaction was quenched by adding EtOAc (prewashed with 5% $NaHCO_3$) (3mL), further diluting it in EtOAc (20mL) and extracting with brine (2 x 10mL). The organic phase was dried (Na_2SO_4), evaporated and purified by flash chromatography using dichloromethane: hexane: triethylamine (50:45:5) to obtain a white foam.

R_f (SiO_2): 0.3 & 0.2 {dichloromethane: hexanes: triethylamine (50:45:5)}

FAB-MS (NBA): 773.0 g/mol (calc. 772.84 g/mol).

^{31}P NMR (202.3MHz, ppm, acetone-d_6): 152.94, 153.36

1-(2',3',5'-Tri-O-Benzoyl-β-D-xylofuranosyl) cytosine [2.9]

A mixture of 1,2,3,5-tetra-O-benzoyl-α-D-xylofuranose (14.75 g, 26.0 mmol) and cytosine (2.89 g, 26.0mmol) was stirred in anhydrous acetonitrile (300mL) under a nitrogen atmosphere. To this, tin (IV) tetrachloride (7.62mL, 65.1mmol) was added and stirred at r.t. for 48 h. The reaction was poured in an equal volume of 5% $NaHCO_3$ and CH_2Cl_2 (300mL) and stirred till bubbling subsided. The organic phase was washed with $NaHCO_3$, brine and evaporated. The crude product was purified by column chromatography using dichloromethane: methanol (with a gradient of 0 → 5%) as an eluent (14.52 g, 79.4%).

R_f (SiO_2): 0.55 {dichloromethane: methanol (9:1)}

^1H NMR (400 MHz, ppm, $CDCl_3$): 4.63-4.79 (m, 2 H, H-5' and H-5''), 4.90 (m, 1 H, H-4'), 5.71 (s, 1 H, H-2'), 5.77 (d, 1 H, H-3'), 5.83 (d, 1 H, H-5), 6.24 (s, 1 H, H-1'), 7.2-8.1 (m, 16 H, 3 x Ph and H-6), 8.50 (bs, 1 H, N-H).

FAB-MS (NBA): 556.0 g/mol (calc. 556.57 g/mol).

1-(β-D-xylofuranosyl) cytosine [2.10]

Nucleoside **[2.9]** (11.59g, 20.8mmol) was dissolved in MeOH (470mL) and concentrated ammonium hydroxide (230mL) was added. The solution was stirred overnight and then evaporated to dryness. The nucleoside was either taken to the next step, or purified by absorbing onto silica and performing flash chromatography using chloroform: ethanol (3:1) as eluant (4.93 g, 95.7%).

R_f (SiO_2): 0.08 {dichloromethane: methanol (9:1)}

UV: λ_{max}= 264 nm (MeOH); rC: λ_{max}= 265 nm (MeOH)

^{1}H NMR (400 MHz, ppm, DMSO-d_6): 3.55-3.74 (m, 2 H, H-5' and H-5''), 3.86 (m, 1 H, H-3'), 3.89 (m, 1 H, H-2'), 4.06 (m, 1 H, H-4'), 4.86 (t, 1 H, OH-5'), 5.46 (d, 1 H, OH-3'), 5.58 (s, 1 H, H-1'), 5.75 (d, 1 H, OH-2'), 5.81 (d, 1 H, H-5), 7.75 (d, 1 H, H-6).

FAB-MS (NBA): 244.1 g/mol (calc. 243.21 g/mol).

1-[N-Benzoyl-(β-D-xylofuranosyl)] cytosine [2.11]

Nucleoside **[2.10]** (2.5 g, 10.2 mmol) was co-evaporated with pyridine (3 x 25mL) and then suspended in pyridine (70mL). To this trimethylsilyl chloride (9.15mL, 72.0mmol) was added. After stirring the mixture for 10 minutes benzoyl chloride (8.35mL, 72.0mmol) was added at r.t. and stirring was continued for 3 hours. The reaction was cooled in an ice bath, water (15mL) added, followed by concentrated ammonium hydroxide (25mL). The reaction was stirred at r.t. for 30 min and evaporated to near dryness. The nucleoside was taken up in water (150mL) and extracted with ethyl acetate (2 x 75mL). The aqueous layer was separated, allowed to stand and the precipitate formed was collected (2.33g, 65.2%).

R_f (SiO_2): 0.16 {dichloromethane: methanol (9:1)}

^{1}H NMR (400 MHz, ppm, DMSO-d_6): 3.34 (s, 1 H, OH), 3.79 (ddd, 2 H, H-5' and H-5''), 3.90 (s, 1 H, H-2'), 4.01 (d, 1 H, $^3J_{3',4'}$ 4.0 Hz, H-3'), 4.23 (m, 1 H, H-4'), 4.80 (t, 1 H, OH-5'), 5.25 (d, 1 H, OH-2'), 5.63 (s, 1 H, H-1'), 5.86 (d, 1 H, OH-3'), 7.2-8.2 (m, 7 H, Ph, H-5 and H-6), 11.15 (bs, 1 H, N-H).

FAB-MS (NBA/NaCl): 348.1 g/mol (calc. 347.32 g/mol).

1-[N-Bz-5'-O-(4-monomethoxytrityl)-(β-D-xylofuranosyl)] cytosine [2.12]

Nucleoside **[2.11]** (1.80g, 5.18mmol) was co-evaporated with pyridine (20mL), followed by addition of 4-monomethoxytrityl chloride (1.92g, 6.22mmol) and DMAP (catalytic). Pyridine (90mL) was added and the solution stirred overnight at r.t. under a N_2 atmosphere. The reaction was quenched by the addition of 5% $NaHCO_3$ (50mL) and evaporated. Extraction was performed using CH_2Cl_2, brine and water. The organic phase was dried (Na_2SO_4), evaporated and purified by flash chromatography using dichloromethane: methanol (with a gradient of 0 → 5%): triethylamine (0.2%). The desired fractions were evaporated to obtain the product as a white foam (3.05g, 95.1%).

R_f (SiO_2): 0.42 {dichloromethane: methanol (95:5)}

^1H NMR (400 MHz, ppm, $CDCl_3$): 3.5-3.74 (m, 3 H, H-4', H-5' and H-5''), 3.80 (s, 3 H, O-CH_3), 4.32 (d, 1 H, H-2'), 4.69 (t, 1 H, H-3'), 5.69 (s, 1 H, H-1'), 6.8-7.9 (m, 21 H, 4 x Ph, H-5 and H-6), 8.80 (bs, 1 H, N-H).

FAB-MS (NBA): 620.1 g/mol (calc.619.67 g/mol).

1-[N-Bz-5'-O-(4-monomethoxytrityl)-2'-*tert*-butyldimethylsilyl-(β-D-xylofuranosyl)] cytosine [2.13]

Nucleoside **[2.12]** (2.44g, 3.94mmol), imidazole (0.67g, 9.84mmol) and *tert*-butyldimethylsilyl chloride (0.77g, 5.11mmol) was dissolved in anhydrous DMF (25mL) and stirred overnight at r.t. The reaction was quenched by the addition of 5% $NaHCO_3$ (25mL). The solution was evaporated, the residue dissolved in CH_2Cl_2 (60mL) and extracted with brine (30mL) and water (30mL). The organic phase was dried (Na_2SO_4),

evaporated and purified by column chromatography using a gradient of CH_2Cl_2:EtOAc (from 7:1 to 3:1).

R_f (SiO_2): 0.56 {dichloromethane: ethyl acetate (2:1)}

^1H NMR (400 MHz, ppm, DMSO-d_6): 0.09 (s, 3 H, Si-CH_3), 0.16 (s, 3 H, Si-CH_3), 0.86 (s, 9 H, Si-$C(CH_3)_3$), 3.2-3.6 (m, 2 H, H-5' and H-5''), 3.77 (s, 3 H, O-CH_3), 3.81 (t, 1 H, H-3'), 4.12 (s, 1 H, H-2'), 4.37 (m, 1 H, H-4'), 5.33 (bs, 1 H, OH-3'), 5.62 (s, 1 H, H-1'), 6.8-8.1 (m, 21 H, 4 x Ph, H-5 and H-6), 11.22 (bs, 1 H, N-H).

FAB-MS (NBA): 734.1 g/mol (calc.733.93 g/mol).

1-[N-Benzoyl-5'-O-(4-monomethoxytrityl)-2'-O-*tert*-butyldimethylsilyl-3'-O-acetyl-(β-D-xylofuranosyl)] cytosine [2.14]

Nucleoside **[2.13]** (0.40g, 0.65mmol) and DMAP (catalytic) were dissolved in anhydrous THF (5mL), followed by addition of DIPEA (0.8mL). The solution was kept under N_2 at r.t. and Ac_2O (0.07mL, 0.71mmol) was added dropwise. The reaction was diluted in CH_2Cl_2 (10mL) and extracted with 5% $NaHCO_3$ (2 x 5mL) and brine (2 x 5mL). The aqueous layer was back extracted with CH_2Cl_2 and the organic phase dried (Na_2SO_4) and evaporated to obtain a white foam. The compound was purified by column chromatography using hexanes:ether (3:1 → 0:1) (0.41g, 97.6%).

R_f (SiO_2): 0.78 {dichloromethane: ethyl acetate (4:1)}

^1H NMR (400 MHz, ppm, $CDCl_3$): 0.19 (s, 3 H, Si-CH_3), 0.26 (s, 3 H, Si-CH_3), 0.93 (s, 9 H, Si-$C(CH_3)_3$), 1.72 (s, 3 H, CH_3-CO), 3.45-3.55 (ddd, 2 H, H-5' and H-5''), 3.83 (s, 3 H, O-CH_3), 4.27 (s, 1 H, H-2'), 4.76 (m, 1 H, H-3'), 4.99 (m, 1 H, H-4'), 5.78 (s, 1 H, H-1'), 6.8-8.0 (m, 21 H, 4 x Ph, H-5 and H-6), 7.96 (bs, 1 H, N-H).

EI-MS (MeOH): 798.3 g/mol (calc.775.97 g/mol + Na).

1-[N-Benzoyl-5'-O-(4-monomethoxytrityl)-3'-O-acetyl-(β-D-xylofuranosyl)] cytosine [2.15]

Nucleoside **[2.14]** (0.93g, 1.23mmol) was dissolved in anhydrous THF (10mL) and TBAF (1M in THF, 2.46mL) was added. The reaction was stirred in a nitrogen atmosphere at r.t. for 1 hour. The solution was then evaporated, dissolved in CH_2Cl_2 (20mL) and extracted with brine (2 x 10mL) and water (2 x 10mL). The organic phase was dried (Na_2SO_4), evaporated and purified by flash chromatography using dichloromethane: methanol (0 → 5% as gradient) (0.75g, 92.6%).

R_f (SiO_2): 0.27 {dichloromethane: methanol (95:5)}

^{1}H NMR (400 MHz, ppm, $CDCl_3$): 1.79 (s, 3 H, CH_3-C(O)), 3.36-3.47 (ddd, 2 H, H-5' and H-5''), 3.8 (s, 3 H, O-CH_3), 4.39 (s, 1 H, H-2'), 4.83 (q, 1 H, H-4'), 5.33 (q, 1 H, H-3'), 5.81 (s, 1 H, H-1'), 6.86 (d, 1 H, H-5), 7.2-8.0 (m, 20 H, 4 x Ph and H-6), 8.86 (bs, 1 H, N-H).

EI-MS (MeOH): 684.3 g/mol (calc. 661.71 g/mol + Na^+)

1-[-Benzoyl-5'-O-(4-monomethoxytrityl)-3'-O-acetyl-2'-O-(β–cyanoethyl-N,N-diisopropylphosphoramidite)-β-D-xylofuranosyl]cytosine [2.16]

Nucleoside **[2.15]** (0.90g, 1.36mmol) was dissolved in anhydrous THF (16mL) and DIPEA (1.0mL, 5.71mmol) was added to it. The solution was cooled in an ice bath, kept under a N_2 atmosphere and N,N-diisopropyl-β-cyanoethylphosphoramidic chloride (0.40mL, 1.77mmol) was added dropwise. The solution was allowed to come to r.t. and

stirred for 2 hours. The solution became cloudy indicating salt formation. The reaction was quenched by adding EtOAc (prewashed with 5% $NaHCO_3$) (5mL), further diluting it in ethyl acetate (20mL) and extracting with brine (2 x 10mL). The organic phase was dried (Na_2SO_4), evaporated and purified by flash chromatography using dichloromethane: hexane: triethylamine (50:45:5) to obtain a white foam (0.92g, 78.7%).

R_f (SiO_2): 0.44 & 0.56 {ethyl acetate: hexanes: triethylamine (70:25:5)}

^{31}P NMR (500 MHz, ppm, d_6-acetone): 150.34, 150.90

FAB-MS (NBA): 862.0 g/mol (calc. 861.94 g/mol).

9-(2',3',5'-Tri-O-benzoyl-β-D-xylofuranosyl) adenine [2.17]

A mixture of 1,2,3,5-tetra-O-benzoyl-α-D-xylofuranose (5.66g, 10mmol) and adenine (1.35 g, 10mmol) was stirred in anhydrous acetonitrile under a nitrogen atmosphere. To this tin (IV) tetrachloride (1.76mL, 15mmol) was added and stirred at r.t. for 48 hrs. The reaction was poured in an equal volume of 5% $NaHCO_3$ and CH_2Cl_2 (100mL) and stirred till bubbling subsided. The organic phase was washed with $NaHCO_3$, brine and evaporated. The crude product was purified by column chromatography using dichloromethane: methanol (with a gradient of 0 → 5%) as an eluent (4.86g, 83.9%).

R_f (SiO_2): 0.5 {dichloromethane: methanol (9:1)}

^1H NMR (400 MHz, ppm, $CDCl_3$): 4.77 (m, 2 H, H-5' & H-5''), 5.00 (m, 1 H, H-4'), 5.98 (d, 1 H, H-3'), 6.28 (s, 1 H, H-2'), 6.43 (s, 1 H, H-1'), 7.26-8.26 (m, 17 H, 3 x Ph, H-2 & H-8).

EI-MS (MeOH): 602.3 g/mol (calc. 579.69 g/mol + Na^+).

9-(β-D-xylofuranosyl) adenine [2.18]

Nucleoside **[2.17]** (1g, 1.72mmol) was dissolved in MeOH (40mL) and concentrated ammonium hydroxide (20mL) was added. The solution was stirred overnight and then evaporated to dryness. The nucleoside was either taken to the next step, or purified by absorbing onto silica and performing flash chromatography using chloroform: ethanol (3:1) as eluant (0.40 g, 88.0%).

R_f (SiO_2): 0.08 {dichloromethane: methanol (9:1)}

UV: λ_{max}= 260 nm (MeOH); rA: λ_{max}= 260 nm (MeOH)

^{1}H NMR (400 MHz, ppm, DMSO-d_6): 3.69 (ddd, 2 H, H-5' and H-5''), 4.05 (d, 1 H, H-3'), 4.18 (q, 1 H, H-4'), 4.31 (s, 1 H, H-2'), 6.01 (s, 1 H, H-1'), 8.50 and 8.62 (2 x s, 2 H, H-2 and H-8).

FAB-MS (NBA): 267.0 g/mol (calc. 267.24 g/mol).

9-[N-Benzoyl-(β-D-xylofuranosyl)] adenine [2.19]

Nucleoside **[2.18]** (4.5 g, 16.8mmol) was co-evaporated with pyridine (3 x 40mL) and then suspended in pyridine (100mL). To this trimethylsilyl chloride (15mL, 0.12mmol) was added, the mixture was stirred for 10 minutes followed by addition of benzoyl chloride (10mL, 84.2mmol) at r.t. and stirring continued for 3 hours. The reaction was cooled in an ice bath and water (20mL) added, followed by concentrated ammonium hydroxide (40 ml). The reaction was stirred at r.t. for 30 min and evaporated to near dryness. The nucleoside was taken up in water (300mL) and extracted with ethyl acetate (2 x 100mL). The aqueous layer was separated, allowed to stand and the precipitate formed was collected (4.53 g, 72.4%).

R_f (SiO_2): 0.18 {dichloromethane: methanol (9:1)}

^1H NMR (400 MHz, ppm, DMSO-d_6): 1.48 (bs, 1 H, N-H), 3.73 (ddd, 2 H, H-5' and H-5''), 4.14 (d, 1 H, H-3'), 4.24 (q, 1 H, H-4'), 4.40 (s, 1 H, H-2'), 6.06 (s, 1 H, H-1'), 7.0-8.1 (m, 5 H, Ph), 8.60 and 8.74 (2 x s, 2 H, H-2 and H-8).

ESI-MS (MeOH): 394.1 g/mol (calc. 371.35 g/mol + Na^+).

9-[N-Benzoyl-5'-O-(4-monomethoxytrityl)-(β-D-xylofuranosyl)] adenine [2.20]

Nucleoside **[2.19]** (5.75 g, 15.5mmol) was co-evaporated with pyridine (45mL), followed by addition of 4-monomethoxytrityl chloride (5.74 g, 18.6mmol) and DMAP (catalytic). Pyridine (90mL) was added and the solution stirred overnight at r.t. under a N_2 atmosphere. The reaction was quenched by the addition of 5% $NaHCO_3$ (50mL) and evaporated. Extraction was performed using CH_2Cl_2, brine and water. The organic phase was dried (Na_2SO_4), evaporated and purified by flash chromatography using dichloromethane: methanol (with a gradient of 0 → 5%): triethylamine (0.2%). The desired fractions were evaporated to obtain the product as a white foam (7.95 g, 79.8%).

R_f (SiO_2): 0.36 {dichloromethane: methanol (9:1)}

^1H NMR (400 MHz, ppm, $CDCl_3$): 3.55 (d, 2 H, H-5' and H-5''), 3.76 (s 3 H, O-CH_3), 4.23 (bs, 1 H, H-3'), 4.46 (m, 1 H, H-4'), 4.64 (s, 1 H, H-2'), 5.23 (bs, 1 H, OH-3'), 5.96 (s, 1 H, H-1'), 6.7-8.1 (m, 19 H, 4 x Ph), 8.21 (s, 1 H, H-2), 8.66 (s, 1 H, H-8).

EI-MS (MeOH): 666.3 g/mol (calc. 643.69 g/mol + Na^+).

9-[N-Benzoyl-5'-O-(4-monomethoxytrityl)-2'-*tert*-butyldimethylsilyl-(β-D-xylofuranosyl)] adenine [2.21]

Nucleoside **[2.20]** (4.02 g, 6.25mmol), imidazole (1.06 g, 15.6mmol) and *tert*-butyldimethylsilyl chloride (1.13 g, 7.5mmol) was dissolved in anhydrous DMF (65mL) and stirred overnight at r.t. The reaction was quenched by the addition of 5% $NaHCO_3$ (50mL). The solution was evaporated, the residue dissolved in CH_2Cl_2 (150mL) and extracted with brine (75mL) and water (75mL). The organic phase was dried (Na_2SO_4), evaporated and purified by column chromatography using a gradient of dichloromethane: ethyl acetate (from 7:1 to 3:1) to obtain the product as a white foam (3.85 g, 81.3%).

R_f (SiO_2): 0.60 {dichloromethane: ethyl acetate (2:1)}

^1H NMR (400 MHz, ppm, $CDCl_3$): 0.20 (s, 6 H, Si-$(CH_3)_2$), 0.82 (s, 9 H, Si-C$(CH_3)_3$), 3.54 (m, 2 H, H-5' and H-5''), 3.70 (s, 3 H, O-CH_3), 3.98 (dd, 1 H, H-3'), 4.30 (m, 1 H, H-4'), 4.42 (s, 1 H, H-2'), 5.46 (d, 1 H, OH-3'), 5.83 (s, 1 H, H-1'), 6.7-8.0 (m, 19 H, 4 x Ph), 8.16 (s, 1 H, H-2), 8.66 (s, 1 H, H-8), 8.96 (bs, 1 H, N-H).

EI-MS (MeOH): 780.4 g/mol (calc. 757.96 g/mol + Na^+).

9-[N-Benzoyl-5'-O-(4-monomethoxytrityl)-2'-*tert*-butyldimethylsilyl-3'-O-acetyl-(β-D-xylofuranosyl)] adenine [2.22]

Nucleoside **[2.21]** (0.48 g, 0.64mmol) and DMAP (40 mg) were dissolved in anhydrous THF (15mL), followed by addition of DIPEA (0.80mL, 4.5mmol). The solution was kept under N_2 at r.t. and Ac_2O (0.075mL, 0.77mmol) was added dropwise. The reaction was diluted in dichloromethane (30mL) and extracted with 5% $NaHCO_3$ (2 x 15mL) and brine (2 x 15mL). The aqueous layer was back extracted with

dichloromethane and the organic phase dried (Na_2SO_4) and evaporated to obtain a white foam. The compound was purified by column chromatography using dichloromethane: ethyl acetate (from 7:1 to 3:1) (0.44 g, 85.7%).

R_f (SiO_2): 0.60 {ether}

^1H NMR (400 MHz, ppm, $CDCl_3$): -0.08 (s, 3 H, Si-CH_3), 0.04 (s, 3 H, Si-CH_3), 0.83 (s, 9 H, Si-C(CH_3)$_3$), 1.79 (s, 3 H, CH_3-CO), 3.29 (ddd, 2 H, H-5' and H-5''), 3.71 (s, 3 H, O-CH_3), 4.57 (q, 1 H, H-4'), 4.98 (t, 1 H, H-2'), 5.21 (q, 1 H, H-3'), 6.10 (d, 1 H, H-1'), 6.8-8.1 (m, 19 H, 4 x Ph), 8.37 (s, 1 H, H-2), 8.70 (s, 1 H, H-8), 11.21 (bs, 1 H, N-H).

EI-MS (MeOH): 822.4 g/mol (calc. 799.99 g/mol + Na^+).

9-[N-Benzoyl-5'-O-(4-monomethoxytrityl)-3'-O-acetyl-(β-D-xylofuranosyl)]adenine [2.23]

Nucleoside **[2.22]** (50 mg, 0.06mmol) was dissolved in anhydrous THF (1mL) and TBAF (1M in THF, 0.12mL) was added. The reaction was stirred in a nitrogen atmosphere at r.t. for 1 hour. The solution was then evaporated, dissolved in CH_2Cl_2 (5mL) and extracted with brine (2 x 2mL) and water (2 x 2mL). The organic phase was dried (Na_2SO_4), evaporated and purified by flash chromatography using dichloromethane: methanol (0 → 5% as gradient) to obtain the product as a white foam (40 mg, 93.0%)

R_f (SiO_2): 0.5{dichloromethane: methanol (9:1}

^1H NMR (500 MHz, ppm, $CDCl_3$): 1.84 (s, 3 H, CH_3-CO), 3.36 (ddd, 2 H, H-5' and H-5''), 3.79 (s, 3 H, O-CH_3), 4.80 (q, 1 H, H-4'), 4.89 (t, 1 H, H-2'), 5.44 (t, 1 H, H-3'), 6.15 (d, 1 H, H-1'), 6.80-8.10 (m, 19 H, 4 x Ph), 8.27 (s, 1 H, H-2), 8.79 (s, 1 H, H-8), 9.10 (bs, 1 H, N-H).

EI-MS (MeOH): 708.3 g/mol (calc. 687.75 g/mol + Na^+).

9-[N-Benzoyl-5'-O-(4-monomethoxytrityl)-3'-O-acetyl-2'-O-(β–cyanoethyl-N,N-diisopropylphosphoramidite)-β-D-xylofuranosyl)] adenine [2.24]

Nucleoside **[2.23]** (0.37 g, 0.54mmol) was dissolved in anhydrous THF (5mL) and DIPEA (0.40mL) was added to it. The solution was cooled in an ice bath, kept under a N_2 atmosphere and N,N-Diisopropyl-β-cyanoethylphosphoramidic chloride (0.40mL, 2 mmol) was added dropwise. The solution was allowed to come to r.t. and stirred for 2 hours. The solution became cloudy indicating salt formation. The reaction was quenched by adding EtOAc (prewashed with 5% $NaHCO_3$) (3mL), further diluting it in EtOAc (20mL) and extracting with brine (2 x 10mL). The organic phase was dried (Na_2SO_4), evaporated and purified by flash chromatography using dichloromethane: hexane: triethylamine (50:45:5) to obtain a white foam (0.39g, 81.9%).

R_f (SiO_2): 0.34 & 0.3 {ethyl acetate: hexanes: triethylamine (50:45:5)}

^{31}P NMR (202.3 MHz, ppm, d_6-acetone): 150.08, 150.20

FAB-MS (NBA): 886.9 g/mol (calc. 885.95 g/mol).

1,2:5,6-Di-O-isopropylidene-α-D-allofuranose [3.1]

1,2:5,6-Di-isopropylidene glucofuranose (10g, 39.4mmol) was stirred in methylene chloride (25mL). To this pyridinium chlorochromate (10.2g, 29.2mmol) in dichloromethane (70mL) was added, followed by acetic anhydride (11mL). The solution was refluxed for 2h, cooled and then filtered through celite. The celite was washed with dichloromethane (2 x50mL) and then evaporated. The residue was taken up in ethanol (50mL) and cooled in an ice bath. Sodium borohydride (6.0g, 0.159mol) was added, till

bubling subsided. The solution was stirred for 2h, quenched by the addition of water and evaporated to near dryness. The residue was taken up in dichloromethane (100mL) and washed with water (2 x 50mL), dried with $MgSO_4$, evaporated and purified by flash column chromatography using hexanes:ether (1:1 to 1:5) to obtain the product as a white powder (8.5g, 85.0%)

^{1}H NMR (400 MHz, ppm, $CDCl_3$): 1.37-1.58 (4 x s, 12 H, 2 x $C(CH_3)_2$), 2.58 (s, 1 H, OH), 3.80-3.83 (q, 1 H, H-4), 3.96-4.12 (m, 3 H, H-5, H-6 and H-6'), 4.28-4.33 (q, 1 H, H-3), 4.61 (t, 1 H, H-2), 5.80 (d, 1 H, H-1).

CI-MS (MeOH): 261.0 g/mol (calc. 260.25 g/mol).

3-Deoxy-3-Fluoro-1,2:5,6-Di-O-isopropylidene-α-D-glucofuranose [3.2]

Anhydrous pyridine (32mL) was added to a solution of 1,2:5,6-Di-O-isopropylidene-α-D-allofuranose (32g, 0.12 mol) in anhydrous dichloromethane (250mL), followed by the dropwise addition of diethylaminosulfur trifluoride (25.9mL, 0.19 mol) at 0°C under a nitrogen atmosphere. The reaction was allowed to come to r.t. and stirred overnight, then quenched by pouring it slowly in a solution of saturated $NaHCO_3$ (200mL). The organic layer was separated, washed with brine (150mL), dried ($MgSO_4$) and evaporated. The residue was purified by silica column chromatography using petroleum ether: ethyl acetate (5:1) as eluent (15.38g, 50.9%).

R_f (SiO_2): 0.53 {Petroleum ether: ethyl acetate (5:1)}

^{1}H NMR (400 MHz, ppm, $CDCl_3$): 1.29, 1.33, 1.41, 1.46 (4 x s, 12 H, 2 x $C(CH_3)_2$), 3.9-4.1 (m, 1 H, H-4), 3.9-4.3 (m, 2 H, H-5 and H-5'), 4.66 (dd, 1 H, H-2, $^3J_{H2,\,F}$ 10.8 Hz), 4.97 (dd, 1 H, H-3, $^2J_{H3,\,F}$ 49.6 Hz), 5.91 (d, 1 H, H-1)

^{19}F NMR (400 MHz, ppm, $CDCl_3$): -128.56 (ddd, F-3)

CI-MS (MeOH): 263.1 g/mol (calc. 262.27 g/mol).

3-Deoxy-3-fluoro-1,2-O-isopropylidene-α-D-xylofuranose [3.3]

A solution of 3-deoxy-3-fluoro-1,2:5,6-Di-O-isopropylidene-α-D-glucofuranose **[3.2]** (9.66g, 36.8mmol) in 80% acetic acid (250mL) was stirred for 2 days at r.t. The solvent was evaporated and the residue dissolved in methanol (250mL). Solid $NaHCO_3$ (5.0g, 59.5mmol) was added, followed by the dropwise addition of aqueous $NaIO_4$ (12.5g in 150mL) at 0°C. After half an hour, $NaBH_4$(3g, 79.4mmol) was added and the mixture stirred for half an hour; then filtered, washed with methanol and neutralized with glacial acetic acid. The volume was reduced to half and the mixture partitioned between water and ethyl acetate. The organic phase was washed with $NaHCO_3$ and brine, dried (Na_2SO_4) and evaporated. The residue obtained was purified by silica gel chromatography using petroleum ether: ethyl acetate (3:1) to obtain the desired product (6.57g, 92.5%).

R_f (SiO_2): 0.16 {Petroleum ether: ethyl acetate (3:1)}

^1H NMR (400 MHz, ppm, $CDCl_3$): 1.25 (s, 3 H, CH_3), 1.41 (s, 3 H, CH_3), 3.82 (m, 2 H, H-$5_{a,b}$), 4.28 (m, 1 H, H-4), 4.62 (dd, 1 H, $^3J_{2,F}$ 11.1, $J_{2,1}$ 3.8 Hz, H-2), 4.92 (dd, 1 H, $^2J_{3,F}$ 50.4, $J_{3,4}$ 2.3 Hz, H-3), 5.91 (d, 1 H, J 3.8 Hz, H-1).

CI-MS (MeOH): 193.0 g/mol (calc. 192.19 g/mol).

^{19}F NMR (400 MHz, ppm, $CDCl_3$): -125.60 (ddd, F-3)

5-O-Benzoyl-3-deoxy-3-fluoro-1,2-O-isopropylidene-α-D-xylofuranose [3.4]

The sugar 3-Deoxy-3-fluoro-1,2-O-isopropylidene-α-D-xylofuranose **[3.3]** (1g, 5.3mmol) was dried by coevaporating with anhydrous pyridine (2 x 10mL), dissolved in anhydrous pyridine (20mL); followed by the addition of benzoyl chloride (1.4mL, 10.4mmol). The reaction was stirred under a nitrogen atmosphere at r.t. for 2 hours and quenched by the addition of ice. The solution was evaporated, dissolved in ethyl acetate (65mL) and washed with saturated $NaHCO_3$ and brine. The organic phase was dried ($MgSO_4$), evaporated and purified by silica gel chromatography using petroleum ether: ethyl acetate (5:1) as eluent (1.42g, 92.1%)

R_f (SiO_2): 0.50 {Petroleum ether: ethyl acetate (5:1)}

^{1}H NMR (400 MHz, ppm, $CDCl_3$): 1.29 (s, 3 H, CH_3), 1.48 (s, 3 H, CH_3), 4.52 (m, 3 H, H-4, H-$5_{a, b}$), 4.72 (dd, 1 H, $^3J_{2, F}$ 10.9, $J_{2, 1}$ 3.8 Hz, H-2), 5.04 (dd, 1 H, $^2J_{3, F}$ 50.3, $J_{3, 4}$ 1.7 Hz, H-3), 6.01 (d, 1 H, J 3.8 Hz, H-1), 7.35-8.10 (m, 5 H, Ph).

CI-MS (MeOH): 296.9 g/mol (calc. 296.29 g/mol).

^{19}F NMR (400 MHz, ppm, $CDCl_3$): -129.78 (ddd, F-3)

1,2-Di-O-Acetyl-5-O-benzoyl-3-deoxy-3-fluoro-D-xylofuranose [3.5]

The aglycon 5-O-Benzoyl-3-deoxy-3-fluoro-1,2-O-isopropylidene-α-D-xylofuranose **[3.4]** (7.5g, 25.3mmol) in glacial acetic acid (127.5mL) and acetic anhydride (15mL) was treated with concentrated H_2SO_4 (1.13mL) at 0°C. The reaction was allowed to slowly come to r.t. and stirred for 15 hours. The solution was carefully poured into 10% aqueous NaOAc (200mL), stirred for half an hour at 0°C, and extracted with chloroform (3 x 200mL). The organic phase was combined, washed with saturated

$NaHCO_3$ (200mL) and brine (200mL), dried ($MgSO_4$) and evaporated. The residue obtained was purified by column chromatography (hexanes: ethyl acetate {5:1} as eluent) to give a colorless syrup (8.5g, 98.6%).

R_f (SiO_2): 0.58 & 0.64 {Hexanes: ethyl acetate (1:1)}

^1H NMR (400 MHz, ppm, $CDCl_3$): 2.01, 2.03, 2.05 and 2.09 (singlets, 6 H, 2 x $OCOCH_3$), 4.40-4.80 (m, 3 H, H-4 and H-$5_{a, b}$), 5.00-5.50 (m, 2 H, H-2 and H-3), 6.19 (s, 0.4 H, H-1), 6.50 (d, 0.6 H, $J_{1,2}$ 4.6 Hz, H-1), 7.38-8.05 (m, 5 H, Ph).

CI-MS (MeOH): 358.0 g/mol (calc. 340.31 g/mol + ammonium).

^{19}F NMR (400 MHz, ppm, $CDCl_3$): -125.53 (m, F-3)

2,4-Bis-O-(trimethylsilyl) thymine

A mixture of thymine(1.12g, 8.9mmol), ammonium sulfate (catalytic) in 1,1,1,3,3,3-hexamethyldisilazane (30mL) was refluxed overnight. The mixture became clear indicating product formation. The excess 1,1,1,3,3,3-hexamethyldisilazane was evaporated and the silylated base used for coupling.

Alternatively, thymine (3g), chlorotrimethylsilane (4mL) and 1,1,1,3,3,3-hexamethyldisilazane (40mL) was refluxed till the mixture became clear. The excess reagent was evaporated, leaving behind the silylated base used for coupling.

1-(2'-O-Acetyl-5'-O-benzoyl-3'-deoxy-3'-fluoro-β-D-xylofuranosyl)-5-methyluridine [3.6]

A solution of the silylated thymine base, prepared above, (2.78g, 22.0mmol) in anhydrous acetonitrile (50mL) was added to 1,2-Di-O-acetyl-5-O-benzoyl-3-deoxy-3-

fluoro-D-xylofuranose **[3.5]** (2.5g, 7.35mmol) in anhydrous acetonitrile (20mL). Trimethylsilyl trifluoromethanesulfonate (2.66mL, 14.7mmol) was added dropwise and the reaction was refluxed for 2 hours. The reaction was allowed to come to r.t. and added to equal portions of chloroform (100mL) and saturated $NaHCO_3$. After stirring for 30 minutes, the organic layer was separated, washed with brine (50mL), dried ($MgSO_4$) and evaporated. The nucleoside was purified by silica gel column chromatography using chloroform:methanol (20:1) as eluent to give the desired product as a white foam (2.08g, 69.5%).

R_f (SiO_2): 0.30 {chloroform: methanol (20:1)}

^{1}H NMR (400 MHz, ppm, $CDCl_3$): 1.89 (s, 3 H, C5-CH_3), 2.14 (s, 3 H, CH_3-CO), 4.42-4.56 (dm, 1 H, $^3J_{4',F}$ 28.8 Hz, H-4'), 4.6-4.8 (dm, 2 H, H-5' and H-5''), 5.13 (dd, 1 H, $^2J_{3',F}$ 69.8 Hz, $^3J_{3',4'}$ 2.4 Hz, H-3'), 5.22 (distorted triplet, 1 H, H-2'), 6.15 (d, 1 H, $^3J_{1',2'}$ 2.5 Hz, H-1'), 7.18 (s, 1 H, H-6), 7.42-8.08 (m, 5 H, Ph), 8.48 (br s, 1 H, N-H).

FAB-MS (NBA): 406.9 g/mol (calc. 406.42 g/mol).

^{19}F NMR (400 MHz, ppm, $CDCl_3$): -122.80 (ddd, F-3)

1-[3'-Deoxy-3'-fluoro-(β-D-xylofuranosyl)]-5-methyluridine [3.7]

The nucleoside **[3.6]** (2.67g, 6.57mmol) was dissolved in MeOH (50mL) and concentrated ammonium hydroxide (25mL) was added. The solution was stirred overnight and then evaporated to dryness. The nucleoside was either taken to the next step, or purified by absorbing onto silica and performing flash chromatography using chloroform: ethanol (3:1) as eluant (90%).

R_f (SiO_2): 0.31 {dichloromethane: methanol (9:1)}

UV: λ_{max}= 265 nm (MeOH); dT: λ_{max}= 266 nm (MeOH)

^{1}H NMR (400 MHz, ppm, DMSO-d_6): 1.58 (s, 3 H, C5-CH_3), 3.23-3.38 (ddd, 2 H, H-5' and H-5''), 3.72 (s, 3 H, O-CH_3), 4.27 (d, 1 H, $^3J_{2',F}$ 16.4 Hz, H-2'), 4.37-4.47 (m, 1 H, $^3J_{4',F}$ 29.2 Hz, H-4'), 4.96-5.10 (m, 1 H, $^3J_{3',F}$ 53.2 Hz, H-3'), 5.77 (d, 1 H, $^4J_{1',F}$ 2 Hz, H-1'), 6.18 (bs, 1 H, OH-2'), 6.89-7.42 (m, 15 H, 3 x Ph and H-6).

CI-MS (MeOH): 261.0 g/mol (calc. 260.22 g/mol).

1-[5'-O-(4-Monomethoxytrityl)-3'-deoxy-3'-fluoro-(β-D-xylofuranosyl)]-5-methyluridine [3.8]

Nucleoside **[3.7]** (2g, 7.68mmol) was co-evaporated with pyridine (3 x 20mL), followed by addition of 4-monomethoxytrityl chloride (2.85, 9.2mmol) and DMAP (catalytic). Pyridine (40mL) was added and the solution stirred overnight at r.t. under a N_2 atmosphere. The reaction was quenched by the addition of 5% $NaHCO_3$ (20mL) and evaporated. Extraction was performed using CH_2Cl_2, brine and water. The organic phase was dried (Na_2SO_4), evaporated and purified by flash chromatography using CH_2Cl_2: MeOH (with a gradient of 0 → 5%): TEA (0.2%)

R_f (SiO_2): 0.55{dichloromethane: methanol (9:1)}

^{1}H NMR (400 MHz, ppm, DMSO-d_6): 1.58 (s, 3 H, C5-CH_3), 3.23-3.38 (ddd, 2 H, H-5' and H-5''), 3.72 (s, 3 H, O-CH_3), 4.27 (d, 1 H, $^3J_{2',F}$ 16.4 Hz, H-2'), 4.37-4.47 (m, 1 H, $^3J_{4',F}$ 29.2 Hz, H-4'), 4.96-5.10 (m, 1 H, $^3J_{3',F}$ 53.2 Hz, H-3'), 5.77 (d, 1 H, $^4J_{1',F}$ 2 Hz, H-1'), 6.18 (bs, 1 H, OH-2'), 6.89-7.42 (m, 15 H, 3 x Ph and H-6).

ESI-MS (MeOH): 555.19 g/mol (calc. 532.57 g/mol + Na^+).

^{19}F NMR (400 MHz, ppm, $CDCl_3$): -118.50 (ddd, F-3)

1-[5'-O-(4-Mmonomethoxytrityl)-3'-deoxy-3'-fluoro-2'-O-(β–cyanoethyl-N,N-diisopropylphosphoramidite)-β-D-xylofuranosyl]-5-methyluridine [3.9]

Nucleoside **[3.8]** (0.75g, 1.41mmol) was dissolved in anhydrous THF (15mL) and DIPEA (1.0mL) was added to it. The solution was cooled in an ice bath, kept under a N_2 atmosphere and N,N-Diisopropyl-β-cyanoethyl phosphoramidic chloride (0.375mL, 1.68mmol) was added dropwise. The solution was allowed to come to r.t. and stirred for 2 hours. The solution became cloudy indicating salt formation. The reaction was quenched by adding EtOAc (prewashed with 5% $NaHCO_3$) (5mL), further diluting it with EtOAc (20mL) and extracting with brine (2 x 10mL). The organic phase was dried (Na_2SO_4), evaporated and purified by flash chromatography using dichloromethane: hexane: triethylamine (50:45:5) to obtain a white foam (712mg, 68.9%).

R_f (SiO_2): 0.38 & 0.56{dichloromethane: ether(2:1)}

^{31}P NMR (202.3MHz, ppm, acetone-d_6): 150.60, 150.81

2,4-Bis-O-(trimethylsilyl)cytosine

Cytidine (3g), chlorotrimethylsilane (4mL) and 1,1,1,3,3,3-hexamethyldisilazane (40mL) was refluxed till the mixture became clear (normally overnight). The excess reagent was evaporated, leaving behind the silylated base used for coupling.

1-(2'-O-Acetyl-5'-O-benzoyl-3'-deoxy-3'-fluoro-β-D-xylofuranosyl) cytosine [3.10]

To a mixture of cytosine (0.5g, 4.41mmol) and 1,2-di-O-acetyl-5-O-benzoyl-3-deoxy-3-fluoro-D-xylofuranose (1g, 2.94mmol) in anhydrous acetonitrile (40mL), tin (IV) tetrachloride (0.86mL, 7.34mmol) was added. The reaction was stirred at r.t. in a

nitrogren atmosphere for 48 hours. The reaction was poured in an equal volume of 5% $NaHCO_3$ and CH_2Cl_2 (75mL) and stirred till bubbling subsided. The organic phase was washed with $NaHCO_3$, brine and evaporated. The crude product was purified by column chromatography using dichloromethane: methanol (with a gradient of 0 → 5%) as an eluent (541mg, 47.0%).

R_f (SiO_2): 0.40 {dichloromethane: methanol (9:1)}

^{1}H NMR (400 MHz, ppm, $CDCl_3$): 2.18 (s, 3 H, CH_3-CO), 4.6-4.7 (dm, 1 H, $^3J_{4',F}$ 30.0 Hz, H-4'), 4.74-4.86 (ddd, 2 H, H-5' and H-5''), 5.12 (dd, 1 H, $^2J_{3',F}$ 49.6 Hz, H-3'), 5.42 (d, 1 H, $^3J_{2',F}$ 12.8 Hz, 6.16 (s, 1 H, H-1'), 7.4-8.1 (m, 7 H, Ph, H-5 and H-6), 8.08 (br s, 1 H, N-H).

FAB-MS (NBA): 391.86 g/mol (calc. 391.36g/mol).

^{19}F NMR (400 MHz, ppm, $CDCl_3$): -118.19 (ddd, F-3)

1-[3'-deoxy-3'-fluoro-(β-D-xylofuranosyl)] cytosine [3.11]

The nucleoside (1.14g, 2.6mmol) was dissolved in methanol (40mL) and concentrated ammonium hydroxide (20mL) was added. The solution was stirred overnight and then evaporated to dryness. The nucleoside was either taken to the next step, or purified by absorbing onto silica and performing flash chromatography using chloroform: ethanol (3:1) as eluant (451mg, 70.0%).

R_f (SiO_2): 0.3 {chloroform: ethanol (3:1)}

^{1}H NMR (400 MHz, ppm, DMSO-d_6): 3.66-3.79 (m, 2 H, H-5' and H-5''), 4.13 (dd, 1 H, $^3J_{2',F}$ 14.0 Hz, H-2'), 4.21 (ddt, 1 H, $^3J_{4',F}$ 31.6 Hz, H-4'), 4.89 (dm, 1 H, $^3J_{3',F}$ 51.2 Hz, H-3'), 5.67 (s, 1 H, H-1'), 5.77 (d, 1 H, H-6), 7.44 (d, 1 H, H-5).

^{19}F NMR (400 MHz, ppm, DMSO-d_6): -117.19 (ddd, F-3').

APCI-MS (MeOH): 245.0 g/mol (calc. 245.21 g/mol).

1-[N-Benzoyl-3'-deoxy-3'-fluoro-(β-D-xylofuranosyl)] cytosine [3.12]

Nucleoside **[3.11]** (1.1g, 4.65mmol) was co-evaporated with pyridine (3 x 10mL) and then suspended in pyridine (25mL). To this trimethylsilyl chloride (6.4mL, 50mmol) was added, the mixture was stirred for 10 minutes followed by addition of benzoyl chloride (5.8mL, 50mmol) at r.t. and stirring continued for 3 hours. The reaction was cooled in an ice bath, water (5mL) added; followed by concentrated ammonium hydroxide (10mL). The reaction was stirred at r.t. for 30 min and evaporated to near dryness. The nucleoside was taken up in water (75mL) and extracted with ethyl acetate (2 x 25mL). The aqueous layer was separated, allowed to stand and the precipitate formed was collected (1.62g, 72.8%).

R_f (SiO_2): 0.36 {dichloromethane: methanol (91)}

^1H NMR (400 MHz, ppm, $CDCl_3$): 3.8-3.85 (m, 2 H, H-5' and H-5''), 4.25-4.29 (dd, 1 H, H-2', $^3J_{H2',F}$ 11.6 Hz), 4.28-4.45 (dm, 1 H, H-4'), 4.95 (dd, 1 H, H-3', $^2J_{H3',F}$ 52.8 Hz), 5.1 (t, 1 H, C5'-OH), 6.31 (d, 1 H, H-1'), 7.36-8.06 (m, 7 H, Ph, H-5 and H-6), 11.23 (bs, 1 H, N-H).

^{19}F NMR (400 MHz, ppm, $CDCl_3$): -116.49 (ddd, F-3)

FAB-MS (NBA): 349.50 g/mol (calc. 349.32 g/mol).

1-[N-Benzoyl-5'-O-(4-monomethoxytrityl)-3'-deoxy-3'-fluoro-(β-D-xylofuranosyl)] cytosine [3.13]

Nucleoside **[3.12]** (1.2g, 3.43mmol) was co-evaporated with pyridine (3 x 15mL), followed by addition of 4-monomethoxytrityl chloride (1.38g, 4.47mmol) and DMAP (catalytic). Pyridine (30mL) was added and the solution stirred overnight at r.t. under a N_2 atmosphere. The reaction was quenched by the addition of 5% $NaHCO_3$ (15mL) and evaporated. Extraction was performed using CH_2Cl_2, brine and water. The organic phase was dried (Na_2SO_4), evaporated and purified by flash chromatography using dichloromethane: methanol (with a gradient of 0 → 5%): triethylamine (0.2%)

R_f (SiO_2): 0.54 {dichloromethane: methanol (9:1)}

^{1}H NMR (400 MHz, ppm, $CDCl_3$): 3.5-3.78 (ddd, 2 H, H-5' and H-5''), 3.81 (s, 3 H, O-CH_3), 4.50 (d, 1 H, H-2', $^3J_{H2',\ F}$ 13.2 Hz), 4.7-4.81 (dt, 1 H, H-4', $^3J_{H4',\ F}$ 32.8 Hz), 5.0 (dd, 1 H, H-3', $^2J_{H2',\ F}$ 50.4 Hz), 6.86 (d, 1 H, H-5), 7.2-8.2 (m, 18 H, 4 x Ph and H-6).

^{19}F NMR (400 MHz, ppm, $CDCl_3$): -121.33 (ddd, F-3)

ESI-MS: 644.3 g/mol (calc. 621.66 g/mol + Na^+).

1-[5'-O-(4-Monomethoxytrityl)-3'-deoxy-3'-fluoro-2'-O-(β–cyanoethyl-N,N-diisopropylphosphoramidite)-β-D-xylofuranosyl] cytosine [3.14]

Nucleoside **[3.13]** (0.50g, 0.80mmol) was dissolved in anhydrous THF (5mL) and DIPEA (0.5mL) was added to it. The solution was cooled in an ice bath, kept under a N_2 atmosphere and N,N-Diisopropyl-β-cyanoethyl phosphoramidic chloride (188μL, 0.84mmol) was added dropwise. The solution was allowed to come to r.t. and stirred for 2 hours. The solution became cloudy indicating salt formation. The reaction was

quenched by adding EtOAc (prewashed with 5% $NaHCO_3$) (3mL), further diluting it in EtOAc (20mL) and extracting with brine (2 x 10mL). The organic phase was dried (Na_2SO_4), evaporated and purified by flash chromatography using dichloromethane: hexane: triethylamine (50:45:5) to obtain a white foam.

R_f (SiO_2): 0.18 & 0.30 {dichloromethane: ether (2:1)}

^{31}P NMR (202.3MHz, ppm, acetone-d_6): 151.56, 154.09

FAB-MS (NBA): 822.24 g/mol (calc. 821.89g/mol).

9-(2'-O-Acetyl-5'-O-benzoyl-3'-deoxy-3'-fluoro-β-D-xylofuranosyl) adenine [3.15]

To a mixture of adenine (2.38g, 17.6mmol) and 1,2-di-O-acetyl-3-deoxy-3-fluoro-D-xylofuranose (3g, 8.82mmol) in anhydrous acetonitrile (60mL), tin (IV) tetrachloride (2.1mL, 17.6mmol) was added. The reaction was stirred under a nitrogen atmosphere at r.t. for 48 hours. The reaction was poured in an equal volume of 5% $NaHCO_3$ and CH_2Cl_2 (75mL) and stirred till bubbling subsided. The organic phase was washed with $NaHCO_3$, brine and evaporated. The crude product was purified by column chromatography using dichloromethane: methanol (with a gradient of 0 → 5%) as an eluent (2.13g, 58.2%).

R_f (SiO_2): 0.54 {dichloromethane: methanol (9:1)}

^1H NMR (400 MHz, ppm, DMSO-d_6): 2.10 (s, 3H, $OCCH_3$), 4.55-4.76 (m, 3H, H-4', H-5' and H-5"), 5.57 (d, 1H, H-3', $^2J_{3',F}$ 48 Hz), 5.90 (d, 1H, H-2', $^3J_{2',F}$ 16 Hz), 6.21 (d, 1H, H-1'), 7.39 (bs, 2H, NH_2), 7.49-8.12 (m, 5H, Ph), 8.15 (s, 1H, H-2), 8.21 (s, 1H, H-8).

FAB-MS (NBA): 416.20 g/mol (calc. 415.38 g/mol).

9-[3'-deoxy-3'-fluoro-(β-D-xylofuranosyl)] adenine [3.16]

Nucleoside **[3.15]** (2.5g, 6.02mmol) was dissolved in MeOH (100mL) and concentrated ammonium hydroxide (50mL) was added. The solution was stirred overnight and then evaporated to dryness. The nucleoside was either taken to the next step, or purified by absorbing onto silica and performing flash chromatography using chloroform: ethanol (3:1) as eluant (1.33g, 81.9%).

R_f (SiO_2): 0.28 {ethyl acetate: methanol (9:1)}

^{1}H NMR (400 MHz, ppm, DMSO-d_6): 3.66-3.78 (ddd, 2 H, H-5'and H-5''), 4.30 (dm, 1 H, $^3J_{4',F}$ 28.2 Hz, H-4'), 4.74 (distorted triplet, 1 H, $^3J_{2',F}$ 15.6 Hz, H-2'), 5.08 (dm, 1 H, $^2J_{3',F}$ 55.6 Hz, H-3'), 5.93 (d, 1 H, H-1'), 7.36 (br s, 2 H, NH_2), 8.08 (s, 1 H, H-2), 8.15 (d, 1 H, H-8).

^{19}F NMR (400 MHz, ppm, DMSO-d_6): -196.51 (ddd, F-3').

FAB-MS (NBA): 269.80 g/mol (calc. 269.24 g/mol).

9-[N-Benzoyl-3'-deoxy-3'-fluoro-(β-D-xylofuranosyl)] adenine [3.17]

Nucleoside **[3.16]** (1.6g, 5.94mmol) was co-evaporated with pyridine (3 x 15mL) and then suspended in pyridine (40mL). To this trimethylsilyl chloride (6.4mL, 50mmol) was added, the mixture was stirred for 10 minutes followed by addition of benzoyl chloride (5.8mL, 50mmol) at r.t. and stirring continued for 3 hours. The reaction was cooled in an ice bath, water (10mL) added; followed by concentrated ammonium hydroxide (15mL). The reaction was stirred at r.t. for 30 min and evaporated to near dryness. The nucleoside was taken up in water (75mL) and extracted with ethyl acetate

(2 x 25mL). The aqueous layer was separated, allowed to stand and the precipitate formed was collected (1.38g, 62.7%).

R_f (SiO_2): 0.28 {dichloromethane: methanol (9:1)}

^{1}H NMR (400 MHz, ppm, DMSO-d_6): 3.70-3.81 (ddd, 2 H, H-5' and H-5''), 4.36 (dm, 1 H, $^3J_{4',F}$ 29.2 Hz, H-4'), 4.83 (distorted t, 1 H, $^3J_{2',F}$ 14.8 Hz, H-2'), 5.13 (dm, 1 H, $^2J_{3',F}$ 51.6 Hz, H-3'), 6.10 (s, 1 H, H-1'), 7.38-8.41 (m, 7 H, Ph, H-2 and H-8), 8.76 (br s, 1 H, N-H).

CI-MS (MeOH): 374.0 g/mol (373.34g/mol).

^{19}F NMR (400 MHz, ppm, $CDCl_3$): -122.80 (ddd, F-3)

9-[N-Benzoyl-5'-O-(4-monomethoxytrityl)-3'-deoxy-3'-fluoro-(β-D-xylofuranosyl)] adenine [3.18]

Nucleoside **[3.17]** (2.2g, 5.89mmol) was co-evaporated with pyridine (3 x 25mL), followed by addition of 4-monomethoxytrityl chloride (2.2g, 7.07mmol) and DMAP (catalytic). Pyridine (50mL) was added and the solution stirred overnight at r.t. under a N_2 atmosphere. The reaction was quenched by the addition of 5% $NaHCO_3$ (25mL) and evaporated. Extraction was performed using CH_2Cl_2, brine and water. The organic phase was dried (Na_2SO_4), evaporated and purified by flash chromatography using dichloromethane: methanol (with a gradient of 0 → 5%): triethylamine(0.2%) (1.86g, 71.6%).

^{1}H NMR (400 MHz, ppm, DMSO-d_6): 3.55 (dm, 2H, H5' and H5"), 3.79 (s, 3H, O-CH_3), 4.71 (m, 3H, H2' and H4'), 5.13 (ds, 1H, H3', $^2J_{3',F}$ 52 Hz), 6.27 (s, 1H, H1'), 7.2-8.1 (m, 19 H, 3xPh, Ph-OR), 8.06 (s, 1H, H-2), 8.70 (s, 1H, H-8).

R_f (SiO_2): 0.58 {dichloromethane: methanol (9:1)}

APCI-MS: 646.1 g/mol (645.69g/mol).

9-[5'-O-(4-Monomethoxytrityl)-3'-deoxy-3'-fluoro-2'-O-(β–cyanoethyl-N,N-diisopropylphosphoramidite)-β-D-xylofuranosyl] adenine [3.19]

Nucleoside **[3.18]** (0.80g, 1.24mmol) was dissolved in anhydrous THF (10mL) and DIPEA (1.0mL) was added to it. The solution was cooled in an ice bath, kept under a N_2 atmosphere and N,N-Diisopropyl-β-cyanoethylphosphoramidic chloride (0.375mL, 1.68mmol) was added dropwise. The solution was allowed to come to r.t. and stirred for 2 hours. The solution became cloudy indicating salt formation. The reaction was quenched by adding EtOAc (prewashed with 5% $NaHCO_3$) (3mL), further diluting it in EtOAc (30mL) and extracting with brine (2 x 10mL). The organic phase was dried (Na_2SO_4), evaporated and purified by flash chromatography using dichloromethane: hexane: triethylamine (50:45:5) to obtain a white foam (926mg, 88.4%).

R_f (SiO_2): 0.50 & 0.74{dichloromethane: ether(2:1)}

^{31}P NMR (202.3MHz, ppm, acetone-d_6): 152.12, 153.24

1-[5'-O-(4-Monomethoxytrityl)-2'-*tert*-butyldiphenylsilyl-(β-D-xylofuranosyl)}-5-methyluridine [4.2]

To a solution of 1'-{5'-O-(4-monomethoxytrityl) (β-D-xylofuranosyl)}-5-methyl-uridine (0.25g, 0.49mmol), imidazole (0.09g, 1.27mmol) in anhydrous DMF (5mL); *tert*-butyldiphenylsilyl chloride (0.15mL, 0.59mmol) was added and stirred overnight at r.t. The reaction was quenched by the addition of 5% $NaHCO_3$ (2mL). The solution was

evaporated, the residue dissolved in CH_2Cl_2 (10mL) and extracted with brine (5mL) and water (5mL). The organic phase was dried (Na_2SO_4), evaporated and purified by column chromatography using a gradient of dichloromethane: ethyl acetate (from 7:1 to 3:1) (0.405g, Quantitative).

R_f (SiO_2): 0.5 {toluene: ethyl acetate (1:1)}

^1H NMR (500 MHz, ppm, $CDCl_3$): 1.08 (d, 9 H, $C(CH_3)_3$), 1.67 (s, 3 H, C5-CH_3), 3.56 (ddd, 2 H, H-5' and H-5''), 3.58 (d, 1 H, OH-3'), 4.11 (m, 1 H, H-3'), 4.27 (s, 1 H, H-4'), 4.29 (s, 1 H, H-2'), 5.80 (s, 1 H, H-1'), 6.8-8.0 (m, 25 H, 5 x Ph and H-6), 8.20 (bs, 1 H, N-H).

FAB-MS (NBA): 769.10 g/mol (calc. 768.98 g/mol).

1-[5'-O-(4-Monomethoxytrityl)-3'-deoxy-3'-fluoro-2'-*tert*-butyldiphenylsilyl-(β-D-ribofuranosyl)]-5-methyluridine [4.3]

To the nucleoside **[4.2]** (3.4g, 4.73mmol) dissolved in anhydrous dichloromethane (100mL) and cooled to -40°C was added, diethylaminosulfur trifluoride (2.0mL, 14.0mmol). The reaction was allowed to slowly come to r.t. and stirred overnight. The solution was poured into an equal portion of dichloromethane (100mL) and saturated $NaHCO_3$, stirred till bubbling subsided. The organic phase was separated and washed with brine (100mL), dried (Na_2SO_4) and evaporated. The residue was purified by silica gel column chromatography using petroleum ether: ethyl acetate (using a gradient from 5:1 to 3:1) to obtain the white foam (1.98g, 58.1%).

R_f (SiO_2): 0.34 {benzene: ethyl acetate (5: 1)}

^{1}H NMR (400 MHz, ppm, $CDCl_3$): 1.09 (s, 9 H, 3 x CH_3), 1.24 (s, 3 H, CH_3), 3.21 (ddd, 2 H, $^3J_{5',4'}$ 10.8 Hz, H-5' and H-5''), 3.77 (s, 3 H, O-CH_3), 4.25 (dt, 1 H, H-4'), 4.47 (dd, 1 H, $^2J_{3',F}$ 58.6 Hz, $^3J_{3',2'}$ 4.4 Hz, H-3'), 4.50 (ddd, 1 H, H-2'), 6.36 (d, 1 H, $^3J_{1',2'}$ 8 Hz, H-1'), 6.6-7.7 (m, 25 H, 5 x Ph and H-6), 8.17 (s, 1 H, N-H).

^{19}F NMR (400 MHz, ppm, $CDCl_3$): -116.18 (ddd, F-3').

FAB-MS (NBA): 771.0 g/mol (calc. 770.97 g/mol).

1-[5'-O-(4-Monomethoxytrityl)-3'-deoxy-3'-fluoro-(β-D-ribofuranosyl)]-5-methyluridine [4.4]

Nucleoside **[4.3]** (0.9g, 1.16mmol) was dissolved in anhydrous THF (10mL) and TBAF (1M in THF, 2.5mL) was added. The reaction was stirred in a nitrogen atmosphere at r.t. overnight. The solution was then evaporated, dissolved in CH_2Cl_2 (20mL) and extracted with brine (2 x 10mL) and water (2 x 10mL). The organic phase was dried (Na_2SO_4), evaporated and purified by flash chromatography using dichloromethane: methanol (0 → 5% as gradient) (621mg, quant.).

R_f (SiO_2): 0.4 {dichloromethane: methanol (9: 1)}

^{1}H NMR (400 MHz, ppm, $CDCl_3$): 1.43 (s, 3 H, CH_3), 3.41(dd, 2 H, H-5' and H-5''), 3.79 (s, 3 H, O-CH_3), 4.36 (dt, 1 H, H-4'), 4.55 (ddd, , 1 H, H-2'), 5.07 (dd, 1 H, $^2J_{3',F}$ 58.8 Hz, H-3'), 6.24 (d, 1 H, $^3J_{1',2'}$ 8 Hz, H-1'), 6.8-7.6 (m, 15 H, 3 x Ph, H-6 and N-H).

^{19}F NMR (400 MHz, ppm, $CDCl_3$): -116.18 (ddd, F-3').

FAB-MS (NBA): 532.82 g/mol (532.56 g/mol).

1-[5'-O-(4-Monomethoxytrityl)-3'-deoxy-3'-fluoro-2'-O-(β–cyanoethyl-N,N-diisopropylphosphoramidite)-β-D-ribofuranosyl]-5-methyluridine [4.5]

Nucleoside **[4.4]** (0.6g, 1.13mmol) was dissolved in anhydrous THF (20mL) and DIPEA (1.0mL) was added to it. The solution was cooled in an ice bath, kept under a N_2 atmosphere and N,N-Diisopropyl-β-cyanoethyl phosphoramidic chloride (0.375mL, 1.68mmol) was added dropwise. The solution was allowed to come to r.t. and stirred for 2 hours. The solution became cloudy indicating salt formation. The reaction was quenched by adding EtOAc (prewashed with 5% $NaHCO_3$) (5mL), further diluting it in EtOAc (20mL) and extracting with brine (2 x 10mL). The organic phase was dried (Na_2SO_4), evaporated and purified by flash chromatography using dichloromethane: hexane: triethylamine (50:45:5) to obtain a white foam (700mg, 84.7%).

R_f (SiO_2): 0.38 & 0.56{dichloromethane: ether(2:1)}

^{31}P NMR (202.3MHz, ppm, acetone-d_6): 151.60, 152.68

FAB-MS (NBA): 733.17 g/mol (732.79 g/mol).

References:

1) Blackburn, G. M. and Gait, M. J. In *Nucleic Acids in Chemistry and Biology.* Blackburn, G. M. and Gait, M. J. Eds. Oxford University Press: New York, NY, **1990**.
2) Stryer, L. In *Biochemistry.* W. H. Freeman and Company, New York, NY, USA, **1998**.
3) Campbell, M. K. In *Biochemistry.* 2nd Ed. Saunders College Publishing, USA, **1995**.
4) Darnell, J.; Lodish, H. and Baltimore, D. In *Molecular Cell Biology.* W. H. Freeman and Company, New York, NY, USA, **1986**.
5) Sanghvi, Y. S. In *Comprehensive Natural Product Chemistry.* Barton, D. H. R. Ed., Elsevier Science, Oxford, U. K. **1998**.
6) Zamore, P. D.; Tuschl, T.; Sharp, P. A. and Bartel, D. P. *Cell*, **2000**, *101*, 25.
7) Watson, J. D. and Crick, F. H. C. *Nature*, **1953**, *171*, 737.
8) Tyagi, S. and Kramer, F. R. *Nat. Biotechnol.*, **1996**, *14*, 303.
9) a) Bayever, E.; Iversen, P.; Smith, L.; Spinolo, J. and Zon, G. *Antisense Res. Dev.*, **1992**, *2*, 109. b) Roush, W. *Science*, **1997**, *276*, 1192.
10) Gao, X. L.; Mirau, P. and Patel, D. J. *J. Mol. Biol.*, **1992**, *223*, 259.
11) Elghanian, R.; Storhoff, J. J.; Mucic, R. C.; Letsinger, R. L. and Mirkin, C. A. *Science*, **1997**, *277*, 1078.
12) Chen, J. H. and Seeman, N. C. *Nature*, **1991**, *350*, 631.
13) Bock, L. C.; Griffin, L. C.; Latham, J. A.; Vermaas, E. H. and Toole, J. J. *Nature*, **1992**, *355*, 564.
14) a) Bashkin, J. K.; Gard, J. K. and Modak, A. S. *J. Org. Chem.*, **1990**, *55*, 5125. b) Wang, G. and Bergstrom, D. E. *Tetrahedron Lett.* **1993**, *34*, 6721.
15) Adleman, L. M. *Science*, **1994**, *266*, 1021.
16) Saënger, W. In *Principles of Nucleic Acid Structure.* Cantor, C. R. Ed. Springer-Verlag Inc.: New York, NY, USA, **1984**.
17) *Oxford Handbook of Nucleic Acid Structure* Edited by Neidle, S. Oxford University Press, New York, NY, USA, **1999**.
18) Wilkins, M. H. F.; Stokes, A. R. and Wilson H. R. *Nature*, **1953**, *171*, 738.
19) Franklin, R. E. and Gosling, R. G. *Acta Cryst.* **1953**, *6*, 673.
20) Stephenson, M. L. and Zamecnik, P. C. *Proc. Natl. Acad. Sci. U.S.A.*, **1978**, *75*, 285.
21) Zamecnik, P. C. and Stephenson, M. L. *Proc. Natl. Acad. Sci. U.S.A.*, **1978**, *75*, 280.
22) Liebhaber, S. A.; Cash, F. and Eshleman, S. S. *J. Mol Biol.* **1992**, *226*, 609.
23) Summerton, J. and Weller, D. *Antisense Nucleic Acid Drug Dev.* **1997**, *7*, 187.
24) Crooke, S. T.; Lemonidis, K. M.; Neilson, L.; Griffey, R.; Lesnik, E. A. and Monia, B. P. *Biochem. J.* **1995**, *312*, 599.
25) Torrence, P. F.; Maitra, R. K.; Lesiak, K.; Khamnei, S.; Zhou, A. and Silverman, R. H. *Proc. Natl. Acad. Sci. U.S.A.* **1993**, *90*, 1300.
26) Lesiak, K.; Khamnei, S. and Torrence, P. F. *Bioconjugate Chem.* **1993**, *4*, 467.
27) Maran, A.; Maitra, R. K.; Kumar, A.; Dong, B.; Xiao, W.; Li, G.; Williams, B. R. G.; Torrence, P. F. and Silverman, R. H. *Science*, **1994**, *265*, 789.
28) Maitra, R. K.; Li, G.; Xiao,W.; Dong, BB.; Torrence, P. F. and Silverman, R. H. *J. Biol. Chem.* **1995**, *270*,15071.
29) Torrence, P. F.; Xiao, W.; Li, G. and Khamnei, S. *Current Med. Chem.* **1994**, *1*, 176.
30) Torrence, P. F.; Xiao, W.; Li, G.; Lesiak, K.; Khamnei, S.; Maran, A.; Maitra, R.; Dong, B. and Silverman, R. H. In *Carbohydrates: Synthetic Methods and Advances in*

Antisense Therapeutics; Cook, Sanghvi, Eds.; ACS Symposium Series; American Chemical Society: Washington, DC, **1994**, 118-132.
31) Xiao, W.; Player, M. R.; Li, G.; Zhang, W.; Leisak, K. and Torrence, P. F. *Antisense & Nucleic Acid Drug Dev.* **1996**, *6*, 247.
32) Xiao, W.; Li, G.; Maitra, R. K.; Maran, A.; Silverman, R. H. and Torrence, P. F. *J. Med. Chem.* **1997**, *40*, 1195.
33) Ríos, M.; Muñoz, M.; Torrence, P. F. and Spencer, E. *Antiviral Res.* **1995**, *26*, 133.
34) Joklik, W. K. Interferons, In: Fields, B. N. and Knipe, D. M. *et al.* Eds., *Virology*, **1990**, 383-410. Raven Press, New York.
35) Johnston, M. I.; Torrence, P. F. in *Interferon, Mechanisms of Production and Action*, v.3, ed. R. M. Friedman, Elsevier Science, Amsterdam, **1984**, p. 189.
36) Crooke, S. T. and Bennett, C. F. *Annu. Rev. Pharmacol. Toxicol.*, **1996**, *36*, 107.
37) Bennett, M. R. *J. Drug Dev. Clin. Pract.*, **1995**, *7*, 225.
38) Crooke, S. T. *Chem. Ind.*, **1996**, 90.
39) Agrawal, S. and Iyer, R. P. *Cur. Op. Biotech.*, **1995**, *6*, 12.
40) Mesmaeker, A. De; Häner, R.; Martin, P. and Moser, H. *Acc. Chem. Res.* **1995**, *28*, 366.
41) Uhlmann, E. and Peyman, A. *Chem. Rev.* **1990**, *90(4)*, 543.
42) Micklefield, J. *Curr. Med. Chem.* **2001**, *8*, 1157.
43) Crooke, S. T. *Annu. Rev. Pharmacol. Toxicol.* **1992**, *32*, 329.
44) Kumar, M. and Carmichael, G. G. *Microbiol. Mol. Biol. Rev.* **1998**, *62*, 1415.
45) Iyer, R. P.; Roland, A.; Zhou, W. and Ghosh, K. *Curr. Op. Mol. Therap.* **1999**, *1(3)*, 344.
46) Woolf, T. M. *Antisense Res. Dev.*, **1995**, *5(3)*, 227.
47) Crooke, S. T. and Lebleu, B. Eds. In *Antisense Research and Applications*, CRC Press, Boca Raton, FL, **1993**.
48) Agrawal, S. Ed. In *Methods in Molecular Medicine: Antisense Therapeutics*, Humana Press, Totowa, NJ, **1996**.
49) Eckstein, F. and Lilley, D. M. J. Eds. In *Catalytic RNA*, Springer-Verlag, New York, **1996**.
50) Sanghvi, Y. S. and Cook, P. D. Eds. In *Carbohydrate Modification in Antisense Research*, ACS Symposium Series 580, ACS, Washington, DC, **1994**.
51) Hecht, S. M. Ed. In *Bioorganic Chemistry: Nucleic Acids* Oxford University Press, New York, NY, USA, **1998**.
52) Ghosh, P. K.; Kumar, P. and Gupta, K. C. *J. Indian Chem. Soc.* **2000**, *77*, 109.
53) Nielsen, P. E. *Annu. Rev. Biophys. Biomol. Struct.* **1995**, *24*, 167.
54) De Mesmaeker, A.; Altmann, K.-H.; Waldner, A.; Wendeborn, S. *Curr. Opin. Struct. Biol.* **1995**, *5*, 343.
55) a) Wengel, J. *Acc. Chem. Res.* **1999**, *32*, 301. (b) Milligan, J. F.; Matteucci, M. D. and Martin, J. C. *J. Med. Chem.* **1993**, *36(14)*, 1923.
56) Hamilton, S. E.; Simmons, C. G.; Kathiriya, I. S. and Corey, D. R. *Chem. & Biol.* **1999**, *6*, 343.
57) Flanngan, W. M.; Wagner, R. W.; Grant, D.; Lin, K.-Y. and Matteucci, M. D. *Nat. Biotechnol.* **1999**, *17*, 48.
58) Partridge, M.; Vincent, A.; Matthews, P.; Puma, J.; Stein, D. and Summerton, J. *Antisense Nucleic Acid Drug Dev.* **1996**, *6*, 169.

59) Pooga, M.; Soomets, U.; Hällbrink, M.; Valkna, A.; Saar, K.; Rezaei, K.; Kahl, U.; Hao, J.-X.; Xu , X.-J.; Wiesenfeld-Hallin, Z.; Hökfelt, T.; Bartfai, T. and Langel, Ü. *Nat. Biotechnol.* **1998**, *16*, 857.
60) Moulds, C.; Lewis, J. G.; Froehler, B. C.; Grant, D.; Huang, T.; Milligan, J. F. and Matteucci, M. D. *Biochemistry*, **1995**, *34*, 5044.
61) Wagner, R. W. *Science*, **1994**, *372*, 333.
62) Wagner, R. W.; Matteucci, M. D.; Lewis, J. G.; Gutierrez, A. J.; Moulds, C. and Froehler, B. C. *Science*, **1993**, *260(5113)*, 1510.
63) Herdewijn, P. *Liebigs Ann.*, **1996**, 1337.
64) Kool, E. T. *Chem. Rev.* **1997**, *97*, 1473.
65) Schultz, R. G. and Gryaznov, S. M. *Nucleic Acids Res.*, **1996**, *24*, 2966.
66) De Mesmaeker, A.; Lasueur, C.; Bévière, M.-O.; Waldner, A.; Fritsch, V. and Wolf, R. M. *Angew. Chem. Intl. Ed. Engl.*, **1996**, *35*, 2790.
67) Freier, S. M. and Altmann, K.-H. *Nucleic Acids Res.* **1997**, *25*, 4429.
68) Tereshko, V.; Gryaznov, S. M. and Egli, M. *J. Am. Chem. Soc.*, **1998**, *120*, 269.
69) Cailla, H.; LeBorne De Kaouel, C.; Roux, D.; Delage, M. and Marti, J. *Proc. Natl. Acad. Sci. U.S.A.*, **1982**, *79*, 4742.
70) Johnston, M. I. and Torrence, P. F. In *Interferon*, R. M. Friedman Ed., Elsevier, New York, NY, vol. 3, p. 189-298, **1984**.
71) Torrence, P. F.; Maitra, R. K.; Lesiak, K.; Khamnei, S.; Zhou, A. and Silverman, R. H. *Proc. Natl. Acad. Sci. U.S.A.* **1993**, *90*, 1300.
72) Lesiak, K.; Khamnei, S. and Torrence, P. F. *Bioconjugate Chem.* **1993**, *4*, 467.
73) Torrence, P. F.; Xiao, W.; Li, G.; Lesiak, K.; Khamnei, S.; Maran, A.; Maitra, R.; Dong, B. and Silverman, R. H. In *Carbohydrate Modification in Antisense Research*, American Chemical Society Symposium, p. 118-132, **1994**.
74) Sawai, H.; Seki, J. and Ozaki, H. *J. Biomol. Struct. Dyn.* **1996**, *13(6)*, 1043.
75) Eschenmoser, A. *Science*, **1999**, *284*, 2118.
76) Beier, M.; Reck, F.; Wagner, T.; Krishnamurthy, R. and Eschenmoser, A. *Science*, **1999**, *283*, 699.
77) Premraj, B. J.; Raja, S. and Yathindra, N. *Biophys. Chem.* **2002**, *95*, 253.
78) Sawai, H. *J. Am. Chem. Soc.* **1973**, *98*, 7037.
79) Sawai, H. *J. Mol. Evol.* **1988**, *27*, 181.
80) Sawai, H.; Kuroda, K. and Hojo, T. *Bull. Chem. Soc. Soc. Jpn.* **1989**, *62*, 2018.
81) Sawai, H.; Higa, K. and Kuroda, K. *J. Chem. Soc. Perkin Trans 1*, **1992**, 505.
82) Orgel, L. E. and Lohrmann, R. *Acc. Chem. Res.* **1973**, *7*, 368.
83) Ferris, J. P. and Ertem, G. *Science*, **1992**, *257*, 1387.
84) Ferris, J. P. and Ertem, G. *J. Am. Chem. Soc.* **1993**, *115*, 12270.
85) Kawamura, K. and Ferris, J. P. *J. Am. Chem. Soc.* **1994**, *116*, 7564.
86) Dhingra, M. M. and Sarma, R. H. *Nature*, **1978**, *272*, 798.
87) Parthasarathy, R.; Malik, M. and Friday, S. M. *Proc. Natl. Acad. Sci. U.S.A.* **1982**, *79*, 7292.
88) Sarma, R. H. and Dhingra, M. M. In *Conformation in Biology*, Srinicasan, R. and Sarma, R. H. Eds., Adenine Press, NY, p. 259-265, **1982**.
89) Dougherty, J. P.; Rizzo, C. J. and Breslow, R. *J. Am.Chem. Soc.* **1992**, *114*, 6254.
90) Hashimoto, H. and Switzer, C. *J. Am. Chem. Soc.* **1992**, *114*, 6255.
91) Kierzek, R.; He, L. and Turner, D. H. *Nucleic Acids Res.* **1992**, *20*, 1685.

92) Jung, K. E. and Switzer, C. *J. Am. Chem. Soc.* **1994**, *116*, 6059.
93) Lalitha, V. and Yathindra, N. *Curr. Sci.* **1995**, *68*, 68.
94) Premraj, B. J. and Yathindra, N. *J. Biomol. Struct. Dyn.* **1998**, *16*, 313.
95) Robinson, H.; Jung, K.-E.; Switzer, C. and Wang, A. H.-J. *J. Am. Chem. Soc.* **1995**, *117*, 837.
96) Wasner, M.; Arion, D.; Borkow, G.; Noronha, A.; Uddin, A.; Parniak, M. A. and Damha, M. J. *Biochemistry*, **1998**, *37*, 7478.
97) Damha, M. J.: Giannaris, P. A. and Khan, N. *Nucleic Acids Res. Symp. Series*, **1991**, *24*, 290.
98) Giannaris, P. A. and Damha, M. J. *Nucleic Acids Res.* **1993**, *21*, 4742.
99) Alul, R. and Hoke, G. *Antisense Res. Develop.* **1995**, *5*, 3.
100) Prakash, T. P.; Jung, K.-E. and Switzer, C. *J. Chem. Soc. Chem. Commun.* **1996**, 1793.
101) Sheppard, T. L. and Breslow, R. C. *J. Am. Chem. Soc.* **1996**, *118*, 9810.
102) Kandimalla, E. R.; Manning, A.; Zhao, Q.; Shaw, D. R.; Byrn, R. A.; Sasisekharan, V. and Agrawal, S. *Nucleic Acids Res.* **1997**, *25*, 370.
103) Bhan, P.; Bhan, A.; Hong, M.; Hartwell, J. G.; Saunders, J. M. and Hoke, G. D. *Nucleic Acids Res.* **1997**, *25*, 3310.
104) Premraj, B. J.; Patel, P. K.; Kandimalla, E. R.; Agrawal, S.; Hosur, R. V. and Yathindra, N. *Biochem. Biophys. Res. Commun.* **2001**, *283*, 537.
105) Keller, D. In *Circular Dichroism and the Conformational Analysis of Biomolecules*; edited by Gerald D. Fasman, Plenum Press, New York, **1996**, p. 413-431.
106) Johnson, W. C. In *Circular Dichroism: Principles and Applicatinos, Second Edition*, Edited by N. Berova, K. Nakanishi and R. W. Woody, **2000**, p. 703-718.
107) Maurizot, J. C. In *Circular Dichroism: Principles and Applicatinos, Second Edition*, Edited by N. Berova, K. Nakanishi and R. W. Woody, **2000**, p. 719-739.
108) Freifelder, D. In *Physical Biochemistry: Applications to Biochemistry and Molecular Biology*, W. H. Freeman and Company, **1976**, p. 444-474.
109) Glazer, R.; Hartman, K. and Cohen, O. *Biochem. Pharmacol.* **1981**, *30*, 2697.
110) Watanabe, K. A.; Reichman, U.; Chu, C. K.; Hollenberg, D. H. and Fox, J. J. *J. Med. Chem.* **1980**, *23*, 1088.
111) Ellis, D. B. and LePage, G. A. *Mol. Pharmacol.* **1965**, *1*, 231.
112) Ellis, D. B. and LePage, G. A. *Can. J. Biochem.* **1965**, *43*, 617.
113) Cass, C. E.; Selner, M.; Tan, T. H.; Muhs, W. H. and Robins, M. J. *Cancer Treat. Rep.* **1982**, *66*, 317.
114) Roy-Burman, P. *Recent Results Cancer Res.* **1970**, *25*, 1.
115) Harris, B. A. and Plunkett, W. *Cancer Res.* **1981**, *41*, 1039.
116) Nakayama, C. and Saneyoshi, M. *J. Biochem.* **1985**, *97*, 1385.
117) a) De Rudder, J.; Andreeff, F.; Privat de Garilhe, M. C. R. *Hebd. Seances Acad. Sci., Ser. D.* **1967**, *264*, 677. b) Boissier, J. R.; Lepine, P.; De Rudder, J.; Privat de Garilhe, M. French Patent Fr. M. 6, 164. Cl. A 61k, C 07d; *Chem. Abstr.* **1970**, *72*, 44073s.
118) Nakayama, C. and Saneyoshi, M. *J. Biochem.* **1985**, *98*, 417.
119) Johns, D. G.; Adamson, R. H. *Biochem. Pharmacol.* **1976**, *25*, 1441.
120) Adamson, R. H.; Zaharevitz, D. W. and Johns, D. G. *Pharmacology* **1977**, *15*, 84.
121) Peale, A. L. and Glazer, R. I. *Biochem. Pharmacol.* **1978**, *27*, 2543.

122) Garret, C. and Kredich, N. M. *J. Biol. Chem.* **1981**, *256*, 12705.
123) Smith, C. M.; Henderson, J. F. *Can. J. Biochem.* **1976**, *54*, 341.
124) Henderson, J. F.; Smith, C. M.; Snyder, F. F. and Zombor, G. *Ann. N.Y. Acad. Sci.* **1975**, *255*, 489.
125) Glazer, R. I.; Peale, A. L. *Biochem. Pharmacol.* **1979**, *29*, 305.
126) Harris, B. A.; Saunders, P. P.; Plunkett, W. *Mol. Pharmacol.* **1981**, *20*, 200.
127) Harris, B. A.; Plunkett, W. *Biochem. Biophys. Res. Commun.* **1982**, *106*, 500.
128) Glazer, R. I. and Peale, A. L. *Biochem. Biophys. Res. Commun.* **1978**, *81*, 521.
129) Glazer, R. I. and Peale, A. L. *Cancer Lett.* **1979**, *6*, 193.
130) Kredich, N. M. *J. Biol Chem.* **1980**, *255*, 7380.
131) Legraverend, M. and Glazer, R. I. *Mol. Pharmacol.* **1978**, *14*, 1130.
132) Mitsuya, H.; Weinhold, K. J.: Furman, P. A.; St. Clair, M. H.; Lehrman, S. N.; Gallo, R. C.; Bolognesi, D.; Barry, D. W. and Broder, S. *Proc. Natl. Acad. Sci. USA*, **1985**, *82*, 7096.
133) Mustafin, A. G.; Gataullin, R. R.; Abdrakhmanov, I. B.; Spirikhin, L. V. and Tolstikov, G. A. *Russ. Chem. Bull.*, **1998**, *47(10)*, 2007.
134) Hrebanecky, H. and Holy, A. *EP 0301908*: *Chem. Abstrs.*, **1989**, *111*, 78550j.
135) Dyatkina, N. B. and Azhayev, A. V. *Synthesis*, **1984**, 961.
136) Rama Rao, A. V.; Gurjar, M. K. and Lalitha, S. V. S. *J. Chem. Soc., Chem. Commun.* **1994**, 1255.
137) Meguro, H.; Ozui, H. and Fujita, A. *JP 01203399*: *Chem. Abstrs.*, **1990**, *112*, 77872z.
138) Rama Rao, A. V.; Gurjar, M. K. and Lalitha, S. V. S. *Proc. Indian Acad. Sci., (Chem. Sci.)*, **1994**, *106*, 1415.
139) Mustafin, A. G.; Suyundukova, M. V.; Gataullin, R. R.; Spirikhin, L. V.; Abdrakhmanov, I. B.; and Tolstikov, G. A. *Russ. Chem. Bull.* **1997**, *46(7)*, 1362.
140) Ning, J. and Kong, F. *Carbohydrate Res.* **2000**, *326*, 235.
141) Tolstikov, G. A.; Mustafin, A. G.; Gataullin, R. R.; Spirikhin, L. V.; Sultanova, V. S. and Abdrakhmanov, I. B. *Russ. Chem. Bull.* **1993**, *42(6)*, 1095.
142) De Clerq, E. *Antiviral Res.* **1989**, *12*, 1.
143) Lin, T.-S; Schinazi, R. F. and Prusoff, W. H. *Biochem. Pharmacol.* **1987**, *36*, 2713.
144) Balazarini, J.; Kang, G. J.; Dalal, M.; De Clercq, E.; Herdewijin, P.; Broder, S. and Johns, D. G. *Mol. Pharmacol.* **1987**, *32*, 162.
145) Fox, J. J.; Yung, N.; Davoli, J. and Brown, G. B. *J. Am. Chem. Soc.* **1956**, *78*, 2117.
146) Baker, B. R. and Hewson, K. *J. Org. Chem.* **1957**, *22*, 966.
147) Cook, A. F. and Moffatt, J. G. *J. Am. Chem. Soc.* **1967**, *89*, 2697.
148) Hansske, F.; Madej, D. and Robins, M. J. *Tetrahedron* **1984**, *40(1)*, 125.
149) Robins, M. J.; Sarker, S.; Samano, V. and Wnuk, S. F. *Tetrahedron* **1996**, *53(2)*, 447.
150) Robins, M. J.; Fouron, Y. and Mengel, R. *J. Org. Chem.* **1974**, *39(11)*, 1564.
151) Hilbert, G. E. and Johnson, T. B. *J. Am. Chem. Soc.* **1930**, *52*, 4489.
152) Vorbrüggen, H. and Bennua, B. *Tetrahedron Lett.* **1978**, 1339.
153) Vorbrüggen, H.; Krolikiewicz, K. and Bennua, B. *Chem. Ber.* **1981**, *114*, 1234.
154) Vorbrüggen, H. and Höfle, G. *Chem. Ber.* **1981**, *114*, 1256.
155) Vorbrüggen, H. and Bennua, B. *Chem. Ber.* **1981**, *114*, 1279.
156) Lee, W. W.; Martinez, A. P. and Goodman, L. *J. Org. Chem.* **1971**, *36(6)*, 842.

157) Gosselin, G. and Imbach, J.-L. *J. Heterocyclic Chem.* **1982**, *19*, 597.
158) Poopeiko, N. E.; Kvasyuk, E. I. and Mikhailopulo, I. A. *Synthesis*, **1985**, 605.
159) Huss, S.; Gosselin, G.; Pompon, A. and Imbach, J.-L *Nucleosides & Nucleotides*, **1986**, *5(3)*, 275.
160) Gosselin, G.; Bergogne, M.-C.; de Rudder, J.; De Clercq, E. and Imbach, J.-L *J. Med. Chem.* **1986**, *29*, 203.
161) Robins, M. J.; Zuo, R.; Guo, Z. and Wnuk, S. *J. Org. Chem.* **1996**, *61*, 9207.
162) Baker, B. R. " The Ciba Foundation Symposium on Chemistry and Biology of the Purines"; Wolstenholme, G. E. W.; O'Connor, C. M., Eds.; Churchill: London, **1957**; p 120.
163) Lee, W. W.; Martinez, A. P.; Tong, G. L.; Goodman, L. *Chem. Ind.(London)* **1963**, 2007.
164) Ikehara, M.; Nakahara, Y.; Yamada, S. *Chem. Pharm. Bull.* **1971**, *19*, 538.
165) Magnani, A. and Mikuriya, Y. *Carbohydr. Res.***1973**, *28*, 158.
166) Akhrem, A. A.; Adarich, E. K.; Kulinkovich, L. N.; Mikhailopulo, I. A.; Poschastieva, E. B.; Timoshchuk, V. A. *Dokl. Akad. Nauk. SSSR* **1974**, *219*, 99; *Chem. Abstrs* **1975**, *82*, 86532.
167) Paulsen, H.; Brauer, O. *Chem. Ber.* **1977**, *110*, 331.
168) Nakayama, C. and Saneyoshi, M. *Nucleosides & Nucleotides*, **1982**, *1(2)*, 139.
169) Saneyoshi, M. and Satoh, E. *Chem. Pharm. Bull.* **1979**, *27(10)*, 2518.
170) Miyaki, M. and Shimizu, B. *Chem. Pharm. Bull.* **1970**, *18*, 1446.
171) Garner, P. and Ramakanth, S. *J. Org. Chem.* **1988**, *53*, 1294.
172) Zou, R. and Robins, M. J. *Can. J. Chem.* **1987**, *65*, 1436.
173) Gosselin, G. and Imbach, J.-L. *Tetrahedron Lett.* **1981**, *22*, 4699.
174) Torrence, P. F.; Alster, D.; Huss, S.; Gosselin, G. and Imbach, J.-L. *Nucleosides & Nucleotides*, **1987**, *6*, 521.
175) Ginestar, E.; Maury, G.; Chavis, C. and Imbach, J.-L *New J. Chem.* **1987**, *11*, 779.
176) Eppstein, D. A.; Barnett, J. W.; Marsh, Y. V.; Gosselin, G. and Imbach, J.-L. *Nature*, **1983**, *302*, 723.
177) Eppstein, D. A.; Marsh, Y. V.; Schryver, B. B.; Larsen, M. A.; Barnett, J. W.; Verheyden, J. P. H. and Prisbe, E. J. *J. Biol. Chem.* **1982**, *257*, 13390.
178) Schroder, H. C.; Gosselin, G.; Imbach, J.-L and Muller, W. E. G. *Molec. Biol. Rep.* **1984**, *10*, 83.
179) a) Doornbos, J.; Gosselin, G.; Imbach, J.-L and Altona, C. *Nucleic Acids Res.*, **1983**, *11*, 4553. (b) De Leeuw, F.A.A.M and Altona, C. *J. Chem. Soc., Perkin Trans 2*, **1982**, *3*, 375.
180) Ekiel, I. and Shugar, D. *Acta Biochim. Pol.* **1979**, *26(4)*, 435.
181) Klimke, G.; Cuno, I.; Luedemann, H. D.; Mengel, R. and Robins, M. J. *Z. Naturforsch., C: Biosci.* **1980**, *35C(11-12)*, 865.
182) Ekiel, I.; Darzynkiewicz, E.; Dudycz, L. and Shugar, D. *Biochemistry* **1978**, *17*, 1531.
183) Mustafin, A. G.; Petrova, M. A.; Gataullin, R. R.; Spirikhin, L. V.; Faykhov, A. A.; Abdrakhmanov, I. B.; Chertanova, I. F. and Tolstikov, G. A. *Russ. Chem. Bull.*, **1998**, *47(7)*, 1340.
184) Sokolova, N. I.; Dolinnaya, N. G.; Krynetskaya, N. F. and Shabarova, Z. A. *Nucleosides & Nucleotides*, **1990**, *9*, 515.

185) Rosemeyer, H. and Seela, F. *Helv. Chim. Acta* **1991**, *74*, 748.
186) Rosemeyer, H.; Krečmerova, M. and Seela, F. *Helv. Chim. Acta* **1991**, *74*, 2054.
187) Seela, F.; Wörner, K. and Rosemeyer, H. *Helv. Chim. Acta* **1994**, *77*, 883.
188) Seela, F.; Heckel, M. and Rosemeyer, H. *Helv. Chim. Acta* **1996**, *79*, 1451.
189) Rosemeyer, H. and Seela, F. *Nucleosides Nucleotides* **1995**, *14*, 1041.
190) Kaz'mina, E. M.; Stepanenko, B. N. *Tr. 1 [Pervogo] Mosk. Med. Inst.*, **1968**, *61*, 278.
191) Damha, M. J. and Ogilvie, K. K. In *Methods in Molecular Biology- Protocols for Oligonucleotides and Analogues*, Agrawal, S. Ed., Humana Press, Totowa, NJ, vol. 20, **1993**.
192) Johnston, G. A. *Tetrahedron*, **1968**, *24*, 6987.
193) Damha, M. J.; Giannaris, P. A. and Zabarylo, S. V. *Nucleic Aicds Res.* **1990**, *18*, 3813.
194) (a) Pon, R.T. and Yu, S. *Tetrahedron Letters*, **1997**, *38*, 3331. (b) Vargeese, C.; Carter, J.; Yegge, J.; Krivjansky, S.; Settle, A.; Kropp, E.; Peterson, K. and Pieken, W. *Nucleic Acids Res.*, **1998**, *26*, 1046.
195) Lesnik, E. A. and Freier, S. M. *Biochemistry*, **1995**, *34*, 10807.
196) Martin, F. H. and Tinoco, I. J. *Nucleic Acids Res.* **1980**, *8*, 2295.
197) Ratmeyer, L.; Vinayak, R.; Zhong, Y. Y.; Zon, G. and Wilson, W. D. *Biochemistry*, **1994**, *33*, 5298.
198) Hall, K. B. and McLaughin, L. W. *Biochemistry*, **1991**, *30*, 10606.
199) Wang, S. and Kool, E. T. *Biochemistry*, **1995**, *34*, 4125.
200) Steely, H. T.; Gray, D. M. and Ratliff, R. L. *Nucleic Acids Res.* **1986**, *14*, 10071.
201) Ti, G. S.; Gaffney, B. L. and Jones, R. A. *J. Am Chem. Soc.* **1982**, *104*, 1316.
202) Krotz, A. H.; Klopchin, P. G.; Walker, K. L.; Srivasta, G. S.; Cole, D. L. and Ravikumar, V. T. *Tet. Lett.* **1997**, *38(22)*, 3875.
203) (a) Wilds, C. J.; Ph.D. thesis, McGill University, Montreal, **1999** and references therein. (b) Trempe, J. F.; Wilds, C. J.; Danisov, A.; Damha, M. J. and Gehring, K. *J. Am. Chem. Soc.*, **2001**, *123*, 4896. (c) Wilds, C. J. and Damha, M. J. *Nucleic Acids Research*, **2000**, *28*, 3625.
204) Uchiyama, Y.; Inoue, H.; Ohtsuka, E.; Nakai, C.; Kanaya, S.; Ueno, Y. and Ikehara, M. *Bioconjugate Chem.*, **1994**, *5*, 327.
205) Distler, A. M. and Allison, J. *Anal. Chem.* **2001**, *73*, 5000.
206) Noronha, A.; Ph.D. thesis, McGill University, **1999**.
207) Smart, B. E. In *Organofluorine Chemistry: Principles and Commercial Applications*, R. E. Banks Ed., Plenum Press, New York, **1994**.
208) Welch, J. T. In *Selective Fluorination in Organic and Bioorganic Chemistry: ACS Symposium Series 456*, Welch, J. T. Ed., Washington, D.C., American Chemical Society, **1991**.
209) Kalinichenko, E. N.; Podkopaeva, T. L.; Kelve, M.; Saarma, M. and Mikhailopulo, I. A. *Biochem. Biophys. Res. Commun.* **1990**, *167(1)*, 20.
210) a) Howard, J. A. K.; Hoy, V. J.; O'Hagan, D. and Smith, G. T. *Tetrahedron*, **1996**, *52*, 12613. (b) Barbarich, T. J.; Rithner, C. D.; Miller, S. M.; Anderson, O. P. and Strauss, S. H. *J. Am. Chem. Soc.* **1999**, *121*, 4280.
211) Herdewijn, P.; Van Aerschot, A. and Kerremans, L. *Nucleosides & Nucleotides*, **1989**, *8(1)*, 65.

212) Pankiewicz, K. W. *Carbohyd. Res.* **2000**, *327*, 87.
213) Tsuchiya, T. *Adv. Carbohydrate Chem. Biochem.*, **1990**, *48*, 91.
214) Thibaudeau, C.; Nishizono, N.; Sumita, Y.; Matsuda, A. and Chattopadhyaya, J. *Nucleosides & Nucleotides*, **1999**, *18*, 1035.
215) Marquez, V. E.; Lim, B. B.; Barchi, J. J. and Nicklaus, M. C. In *Nucleosides and Nucleotides as Antitumor and Antiviral agents*, Chu, C. K. and Baker, D. C. Eds., Plenum, New York, NY, **1993**, p. 265-284.
216) van den Boogaart, J. E.; Kalinichenko, E. N.; Podkopaeva, T. L.; Mikhailopulo, I. A. and Altona, C. *Eur. J. Biochem.* **1994**, *221*, 759.
217) Yoshitomi, M.; Tomoyuki, A.; Arata, Y. and Keiichi, U. *Jpn. Kokai Tokkyo Koho*, **1989**, 9pp, JP 87-183662.
218) Herdewijn, P.; Ruf, K.; Pfleiderer, W. *Helv. Chim. Acta*, **1991**, *74(1)*, 7.
219) Kalinichenko, E. N.; Podkopaeva, T. L.; Poopeiko, N. E.; Kelve, M.; Saarma, M.; Mikhailopulo, I. A.; van den Boogaart, J. E. and Altona, C. *Recl. Trav. Chim. Pays-Bas*, **1995**, *114(2)*, 43.
220) Kalinichenko, E. N.; Podkopaeva, T. L.; Kelve, M.; Saarma, M. and Mikhailopulo, I. A. *Bioorg. Khim.* **1999**, *25(4)*, 282.
221) Wright, J. A. and Taylor, N. F. *Carbohyd. Res.* **1968**, *6*, 347.
222) Wright, J. A.; Wilson, D. P. and Fox, J. J. *J. Med. Chem.* **1969**, *13*, 269.
223) Koblyinskaya, V. I.; Shalamay, A. S.; Gladkaya, V. A.; Makitruk, V. L. and Kondratyuk, I. V. *Bioorg. Khim.* **1994**, *20(11)*, 1226.
224) Jeong, L. S.; Lim, B. B. and Marquez, V. E. *Carbohyd. Res.* **1994**, *262*, 103.
225) Foster, A. B.; Hems, R. and Webber, J. M. *Carbohyd. Res.* **1967**, *5*, 292.
226) Reichman, U.; Watanabe, K. A. and Fox, J. J. *Carbohyd. Res.* **1975**, *42*, 233.
227) Tewson, T. J. and Welch, M. J. *J. Org. Chem.* **1978**, *43(6)*, 1090.
228) Gosselin, G.; Frédéric, P.; Corinne, G.-D. and Imbach, J.-L. *Carbohyd. Res.* **1993**, *249*, 1.
229) Pitsch, S. *Helv. Chim. Acta* **1997**, *80*, 2286.
230) Pankiewicz, K. W.; Krzeminski, J. and Watanabe, K. A. *J. Org. Chem.* **1992**, *57*, 7315.
231) Etzold, G.; Hintsche, R. and Langen, P. *Chem. Abstr.* **1970**, *73*, 45794k.
232) Etzold, G.; Hintsche, R. and Langen, P. *Chem. Abstr.* **1970**, *73*, 48536p.
233) Etzold, G.; Hintsche, R. and Langen, P. *Chem. Abstr.* **1971**, *75*, 20923e.
234) Etzold, G.; Kowollik, G.; Von Janta-Lipinski, M.; Gaertner, K. and Langen, P. *Chem. Abstr.* **1974**, *81*, 25907m.
235) Kowollik, G.; Langen, P.; Kvasyuk, E. I. and Mikhailopulo, I. A. *Chem. Abstr.* **1983**, *99*, 158785p.
236) Zaitseva, G. V.; Kowollik, G.; Langen, P. and Kvasyuk, E. I. *Chem. Abstr.* **1984**, *101*, 171660y.
237) Ajmera, S.; Bapat, A. R.; Danenberg, K. and Danenberg, P. V. *J. Med. Chem.* **1984**, *27*, 11.
238) Balzarini, J.; Baba, M.; Pauwels, R.; Herdewijn, P. and De Clercq, E. *Biochem. Pharm.* **1988**, *37(14)*, 2847.
239) Neumann, A.; Cech, D. and Schubert, F. *Z. Chem.* **1989**, *29*, 209.
240) Van Aerschot, A.; Herdewijn, P.; Janssen, G.; Cools, M. and De Clercq, E. *Antiviral Res.* **1989**, *12*, 133.

241) Battistini, C.; Giordani, A.; Ermoli, A. and Franceschi, G. *Synthesis*, **1990**, 900.
242) Giordani, A.; Ermoli, A. and Battistini, C. *Nucleosides & Nucleotides*, **1991**, *10(1-3)*, 719.
243) Maruyama, T.; Sato, Y. and Sakamoto, T. *Nucleosides & Nucleotides*, **1998**, *17(1-3)*, 115.
244) Morizawa, Y.; Nakayama, T.; Yasuda, A. and Uchida, K. *Bull. Chem. Soc. Jpn.* **1989**, *62*, 2119.
245) Mikhailopulo, I. A.; Poopeiko, N. E.; Pricota, T. I.; Sivets, G. G.; Kvasyuk, E. I.; Balzarini, J. and De Clercq, E. *J. Med. Chem.* **1991**, *34*, 2195.
246) Kovács, T.; Van Aerschot, A.; Herdewijn, P. and Torrence, P. F. *Nucleosides & Nucleotides*, **1995**, *14(6)*, 1259.
247) Kovács, T.; Pabuccuoglu, A.; Lesiak, K. and Torrence, P. F. *Bioorg. Chem.* **1993**, *21*, 192.